SEISMIC INTERPRETATION OF BASIN-BASEMENT RELATIONSHIPS IN THE EASTERN MIDLAND VALLEY OF SCOTLAND USING QUARRY BLASTS

by

ZAYD A. R. KAMALIDDIN

Thesis submitted for the degree of Master of Science (by research) at the University of Glasgow, Department of Geology, October, 1988.

ProQuest LLC.
789 East Eisenhower Parkway
P.O. Box 1346
Ann Arbor, MI 48106 – 1346

To my parents; thank you

DECLARATION

The material presented in this thesis is the result of research carried out between October 1986 and October 1988 in the Department of Geology, University of Glasgow, under the supervision of Dr J. J. Doody.

This thesis is based on my own independent research and any published or unpublished material used by me has been given full acknowledgement in the text.

Zayd Kamaliddin

J. J. Doody

(Supervisor)

Department of Geology,

University of Glasgow,

Glasgow.

ACKNOWLEDGEMENTS

I would like to express my thanks to the following people to whom this work owes a great deal.

The Iraqi Government for award of my scholarship.

Professor Leake, for allowing me the use of the facilities of the Department of Geology during this research.

Dr. J. J. Doody for his advice and supervision at all stages of the project, and his critical, yet always constructive appraisals of this manuscript.

Dr. Colin Farrow is thanked for his instruction in the use of computers and his forgiveness for the "silly questions" I sometimes ask or for my blaming the computer for "not doing what I wanted it to do".

Dr. M. Dentith for his fruitful discussions and his guidance at the early stages of this project.

I am grateful to the quarry owners and managers of Aberdour, Collace and Newburgh for their assistance and full co-operation.

I would like to express my special thanks to these people: Bob Cumberland for simply everything and for his attempts to learn Arabic in order to teach me things that I do not comprehend in English. Unfortunately these humble attempts turned out to be a disaster for the three of us, me, him, and the Arabic language.

George Gordon for keeping the recorders in a "working" condition. I think he must have learned from my project that his machines sometimes DO NOT work and it is not always "operator's error".

Eddie Speirs who tried to convince me that people in Scotland do not use vehicles but always managed to provide one for my field work.

Kenny Roberts for his help in the field even late on Friday nights.

Emil K. Said for managing "sometimes" to wake up at 5 a.m to help me with my field work.

Fawzi Ahmed for his help in the field.

Mark Wood for reminding me of my elementary maths and physics and teaching me how to measure the length of a straight line when you have a ruler and a straight line!

Roddy Morrison for supplying me with the wrong things that I asked for.

Dogulas Maclean for managing to do all my figures on short notice.

My thanks to the three persons who were the reason behind this work and whose mere presence beside me was the help I needed: Ikbal, Rasha, and Ali. Thank you all.

Finally all my thanks, love, and respect for my parents for teaching and guarding me all their lives. I thank you both again.

Table of Contents

SUMMARY

This project was designed as a reconnaissance study in the Fife region where no previous geophysical projects have been executed. It also allowed the extension of the knowledge obtained by the MAVIS project for the Midland Valley of Scotland towards the north-east.

The project consisted of four refraction lines recorded using quarry blasts. The first profile (line 1) trends N-S across the Fife region, while the second profile (line 2) trends NW-SE crossing the Central Coalfield Syncline and was planned to tie this project with the MAVIS project. The other two lines provided extra information from the area.

Two refractors are recognised defining three crustal layers. The first layer has velocities between 3.3-5.2 km/s and depths between 0.0 and 2.3 km. This layer is interpreted as Carboniferous and Upper Old Red Sandstone rocks and it is exposed along the southern section of line 1 and most of line 2. The second layer was interpreted as Lower Old Red Sandstone and Lower Palaeozoic rocks. It has velocities of 5.3-5.8 km/s and occurs at depths of 2.1-5.2 km in the southern part of the study area and is exposed at the surface, extending down to the basement refractor at 5.2 km depth in the northern section of the study area.

A basement refractor with a velocity of 6.04 km/s occurring at a depth of 5.2 km beneath line 1 was interpreted. This refractor is not completely horizontal since a step north of the Tay is envisaged with an estimated upward displacement of 0.3 km towards the axis of the Strathmore Syncline in the north.

Four major faults are traversed by the profiles, namely, the Ochil Fault, the North Ochil Fault, the South Tay Fault and the North Tay Fault. Only the North Tay Fault was not detected. The estimated throw of the Ochil Fault is 2.2 km near its position of maximum displacement, steeply dipping towards the SE, the North Ochil Fault has a throw of 0.5 km dipping to the south and the South Tay Fault a throw of 0.6 km dipping towards the north.

A flat basement is envisaged where no effect of surface structures on basement was observed. Therefore, the Ochil Fault, the North Ochil Fault and the South Tay Fault are interpreted as of listric nature soleing out either at the layer 1/2 interface (i.e. Middle Devonian unconformity) or within layer 2. This interpretation is consistent with that of the MAVIS project where a listric Ochil Fault was predicted.

INTRODUCTION

The aim of the project was to investigate the upper crustal seismic structure and depositional basins of the Fife region and Clackmannan district using quarry blasts as sources. A particular objective was to gain an understanding of the relationship between Upper Palaeozoic depositional basins and the underlying basement. The work develops the earlier studies in the Midland Valley of Scotland carried out at Glasgow and summarised by Davidson et al. (1984) and Dentith (1987).

The project consists of three main lines and one short profile (see Figure 1.1a for locations). The longest line (Aberdour-Collace) was recorded from quarries at Aberdour, Collace and Newburgh. This line traversed the central part of the Fife region in a N-S direction. The second line (Aberdour-Alva) was recorded from Aberdour and Tillicoultry quarries and it trends in a NNW-SSE direction crossing the Central Coalfield Syncline and Ochil Fault.

A third line was recorded from Tillicoultry quarry trending towards the NE north of Loch Leven. A short profile was recorded from Newburgh quarry towards the west to study the velocity distribution in layer 1 in the area.

The seismic lines cover the mid-western part of the Fife region and cross the northern part of the Central Coalfield Syncline . They were designed to shed light on the depths to the main upper crustal lithologic units in the area and their velocity configuration, namely Carboniferous and Upper Old Red Sandstone (layer 1), Lower Old Red Sandstone (layer 2), and crystalline basement (layer 3). A further goal of this project was to test the proposed model of Dentith (1987) for the Ochil Fault. This fracture, which played an important role in Carboniferous sedimentary basin evolution in the area, crosses the Midland Valley from the Fife coast in the east to west of Stirling in the west separating the Lower Devonian to the north from the Carboniferous to the south (Figure 1.1a). The possible trends which the fault may attain in its extension towards the east were investigated.

Experience attained from previous seismic studies in the region indicated the likely cross over distances to be encountered in this project. The lines were extended as far as the size of charge and

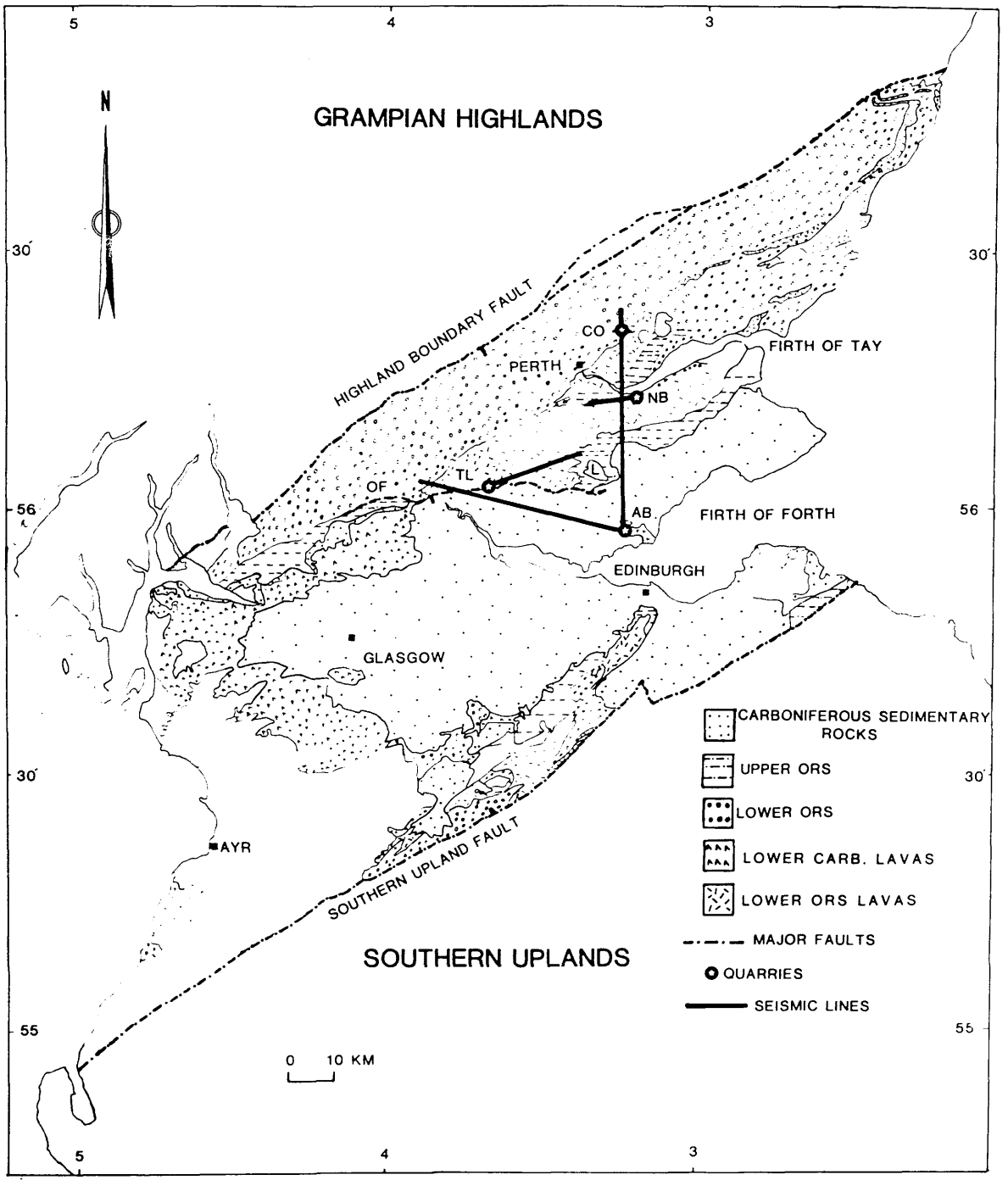

Fig.1.1a Map of the seismic lines of this study and the geological outcrop of the Midland Valley. AB - Aberdour, CO - Collace, L - Loch Leven, NB - Newburgh, OF - Ochil Fault, TL - Tillicoultry.

other conditions (discussed in chapter 2) permitted to be able to reach the target refractors on this basis.

In this project various interpretational methods were used. Wiechert-Herglotz-Bateman (WHB) inversion and the tau-p methods were applied to lines 1 and 2, the planar layer interpretation was applied to all profiles and the Plus-Minus method was used to interpret the Devonian refractor along line 1. Raytracing was undertaken for lines 1 and 2 also.

In the first chapter of this thesis a brief account of the geological and geophysical background of the Midland Valley will be presented with special emphasis on the study area. In chapter two, data acquisition and the methods of digitization will be discussed. Chapter three will deal with interpretational methods and data processing. Chapters four and five will be devoted to the seismic interpretations of the data and their geological and geophysical implications and conclusions.

CHAPTER ONE - REGIONAL GEOLOGY AND GEOPHYSICAL BACKGROUND

1.1. Introduction

The study area is in the NE of the Midland Valley of Scotland (Fig. 1.1a). It extends from Blairgowrie north of the Firth of Tay to the Firth of Forth in the south, and from east of Loch Leven in central Fife to Dunblane in Stirlingshire in the west. The main geological structures traversed are, from the north, the southern limb of the Strathmore Syncline, the Tay Graben, the Ochil Fault and the Kincardine and Clackmannan basins (Fig. 1.1b).

The Midland Valley is flanked to the north by the metamorphic Grampian Highlands, and to the south by the trench sequence (Ordovician to Silurian greywackes) of the Southern Uplands (Fig. 1.1a). The main rock units exposed in the Midland Valley are sedimentary and volcanic rocks of Palaeozoic age.

The history of the Midland Valley remains controversial. Kennedy (1958) and George (1960) interpreted the Midland Valley as a graben receiving detritus from the Grampian Highlands and the Southern Uplands during Devonian times. Dewey (1971) suggested a destructive plate model where the Midland Valley represents a sedimentary wedge region lying between the volcanic front to the north and trench to the south. A similar model was suggested by Leggett (1980). Bluck (1984,1985) interpreted the Midland Valley as a suspect terrane which was juxtapositioned during the Devonian against the Grampian Highlands by strike-slip movement. Hutton (1987) also explained the development of the Midland Valley in terms of sinistral strike-slip movement, assuming the terrane to be derived from the North American margin.

The geological succession and the previous geophysical work of the Midland Valley will be discussed in this chapter highlighting any relevance to the study area.

1.2. Geology

The oldest outcrop in the Midland Valley of Scotland is of Lower Palaeozoic age. The area is mostly covered with sedimentary and igneous rocks of Devonian and Carboniferous age. A brief discussion of the main lithological units in the Midland Valley will be given in this section.

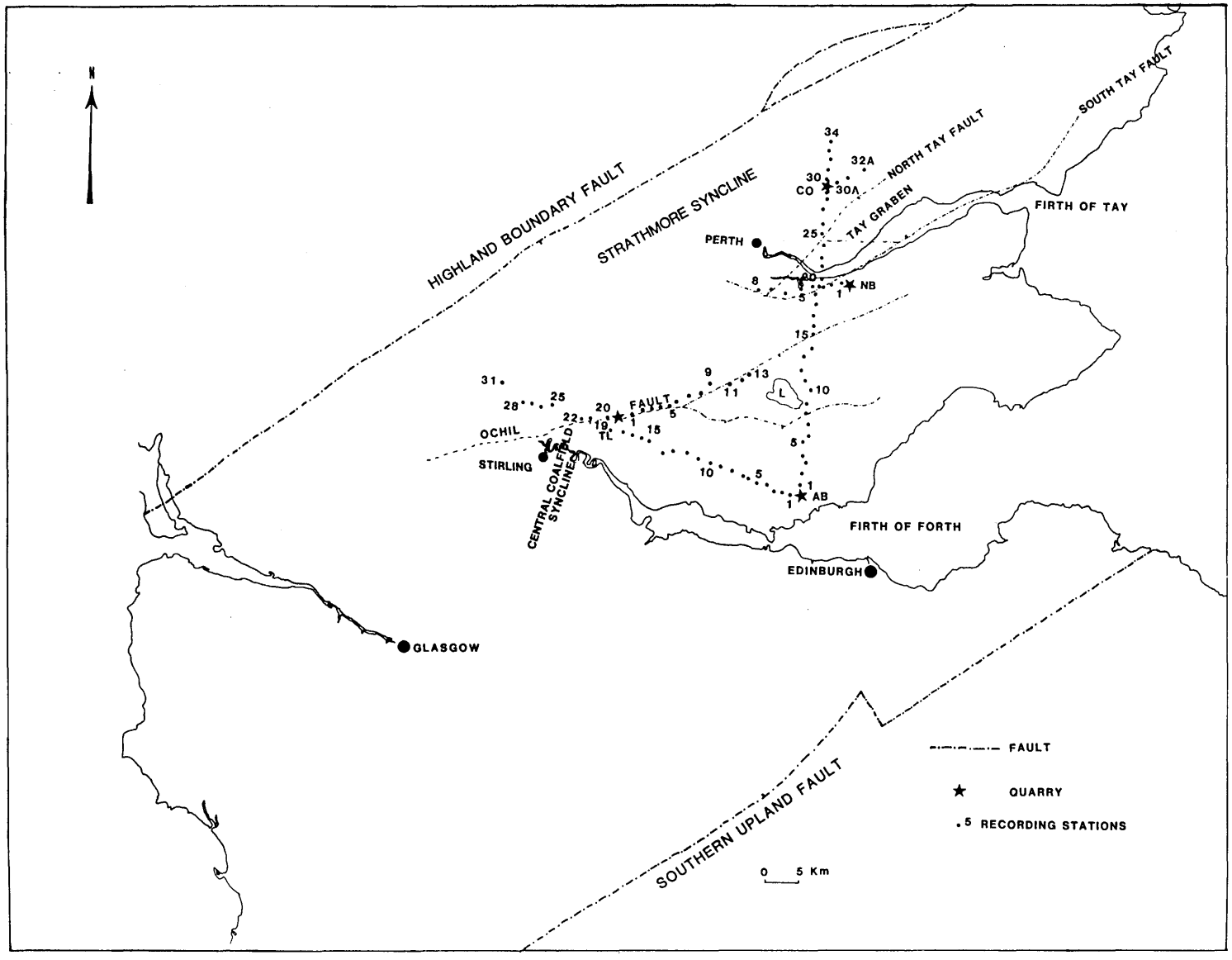

Fig.1.1b Location map of seismic sources and receivers for the project area. Abbreviations as in Fig 1.1a.

1.2.1. Pre-Palaeozoic Basement

Pre-Palaeozoic basement is not exposed in the Midland Valley and different models have been suggested for its nature and evolution, ranging from Dalradian rocks (Yardley et al. 1982) to oceanic crust (Mitchell & McKerrow 1975).

There is, however, indirect evidence for the nature of the basement. Clasts of acidic and intermediate composition present in Lower Palaeozoic conglomerates exposed near Girvan were interpreted by Bluck (1983, 1984) as indicating deposition in a proximal fore-arc setting. Xenoliths associated with Carboniferous volcanism in the Midland Valley were investigated by Upton et al. (1976), who suggested a pre-Palaeozoic basement for the high grade metamorphic granulite facies found. A similar argument was suggested by Graham & Upton (1978), who concluded that quartzo-feldspathic granulites and garnet granulites present in volcanic vents imply the presence of a high grade metamorphic basement and correlated their results with the "pre-Caledonian" layer of 6.4 km/s determined from the LISPB experiment (Bamford et al. 1978). Basic granulitic meta-igneous suites were correlated with the LISPB 7.0 km/s lower crustal layer (Upton et al. 1983).

Aftalion et al. (1984) compiled radiometric data to establish age constraints in the region. They predicted similar compositions for the basement rocks beneath the Midland Valley and the Lewisian complex further north. Further, they argued that isotopic zircon dating from the Midland Valley yielded ages which correspond to those recorded from the NW Highlands.

1.2.2. Lower Palaeozoic

Exposure of Lower Palaeozoic rocks in the Midland Valley are scarce (Fig. 1.2). Lower Ordovician rocks form a narrow discontinuous zone from Stonehaven in the NE to the Isle of Arran in the Clyde estuary along the Highland Boundary Fault ("H" of Fig. 1.2). The other significant area of Ordovician rocks in the Midland Valley is in the Girvan-Ballantrae district and consists of a tectonic assemblage of ultramafic and mafic intrusive rocks, basaltic volcanics and associated sediments.

The Ballantrae ophiolite complex has played an influential role in the moulding of tectonic models for the British Caledonides . Their original tectonic setting has seldom been agreed upon, however, with varying authors invoking ocean island, marginal basin and oceanic ridge settings (c.f. Barrett et al. 1982, Bluck 1982, Lambert & McKerrow 1976). The tectonic setting of the Midland Valley

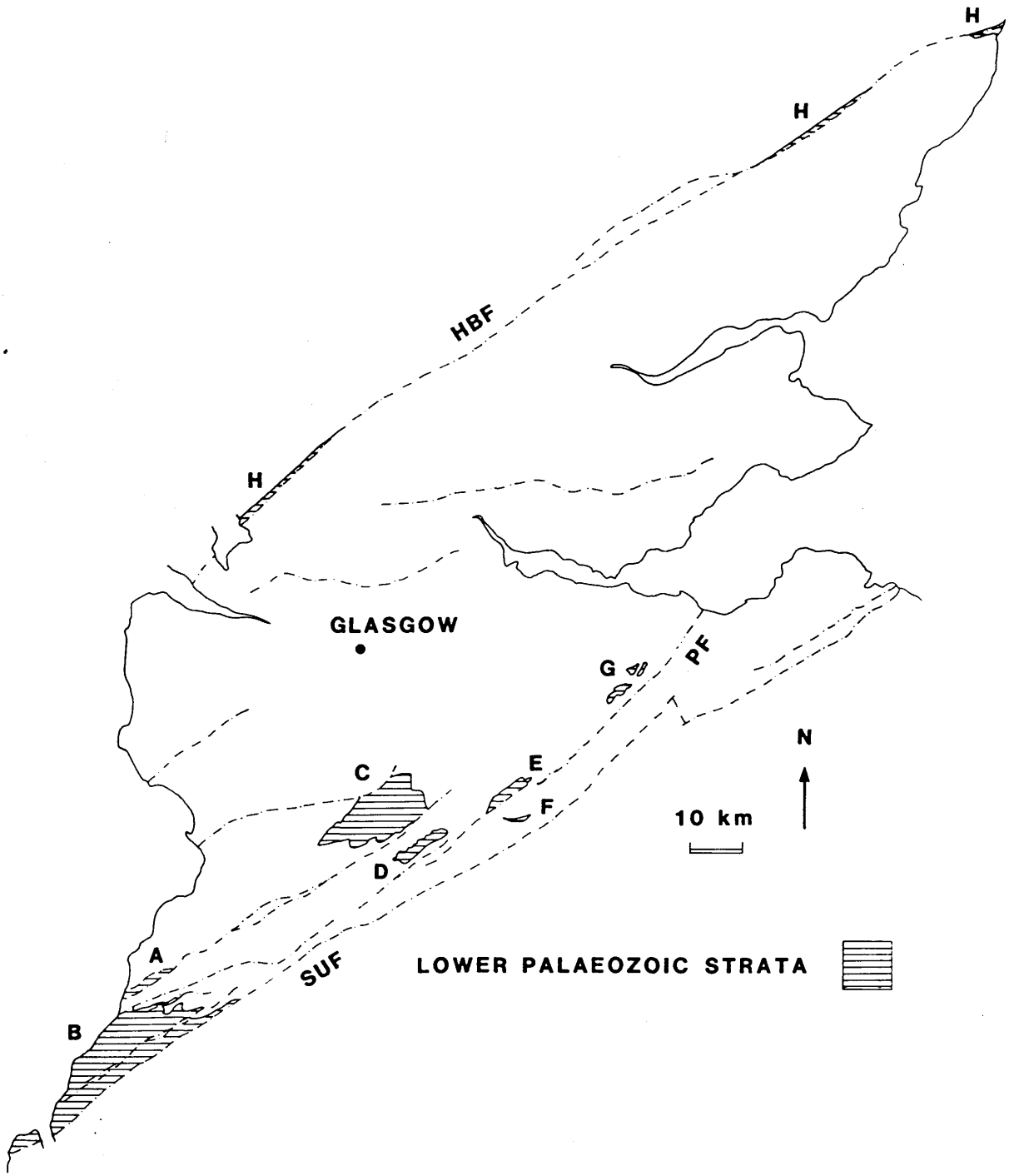

Fig.1.2 Outcrop of Lower Palaeozoic rocks in the Midland Valley of Scotland. A - Craighead, B - Girvan, C - Lesmahagow, D - Hagshaw Hills, H - Highland Border, HBF - Highland Boundary Fault, SUF - Southern Uplands Fault.

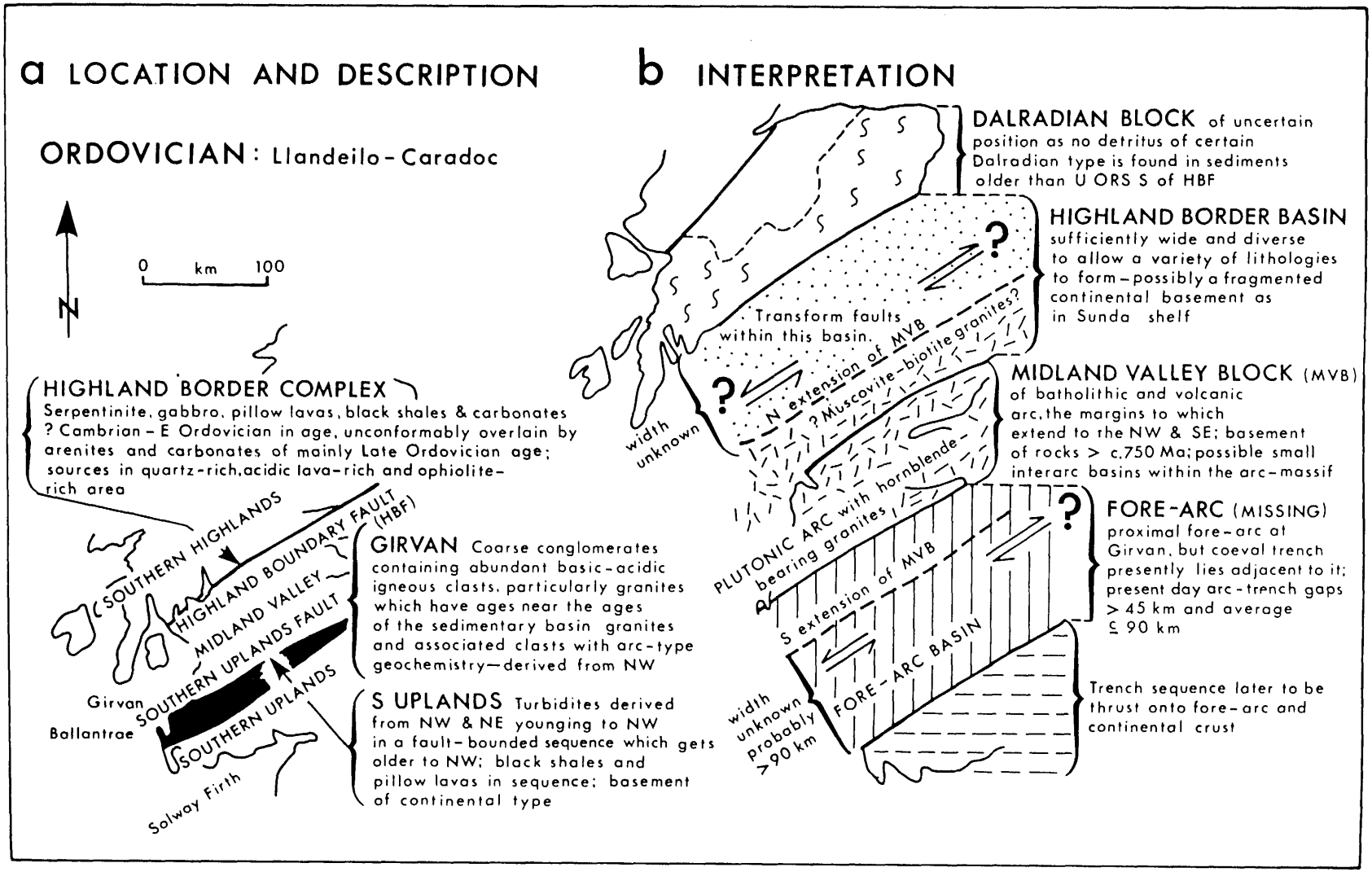

Fig.1.3 Tectonic setting of the Midland Valley of Scotland during the Ordovician (after Bluck 1984)

through the Ordovician is illustrated in Figure 1.3.

Exposure of Silurian strata in the Midland Valley is limited to three main locations: a series of inliers near the Girvan area, along the southern margin of the Midland Valley and in the vicinity of Stonehaven. The tectonic setting of the Midland Valley through the Silurian is illustrated in Figure 1.4. Silurian strata range from Llandovery to Ludlow and show a transition from marine turbidites, shales and conglomerates to terrestrial conglomerates and sandstones. Clast provenance suggests that an igneous basement underlies the Southern Uplands block, and that this basement was the source of the Silurian conglomerates (Bluck 1983).

1.2.3. Devonian

The Devonian rocks of the Midland Valley are usually described by the lithostratigraphic term "Old Red Sandstone" (ORS). The ORS is typically divided into three parts, though the Middle ORS is missing from the Midland Valley . The ORS consists of terrestrial clastic sediments which accumulated in alluvial fans, braided streams and lakes and were deposited on a surface of folded and eroded Lower Palaeozoic sediments. They are described by Mykura (1983) and Cameron & Stephenson (1985).

Lower ORS strata crop out in two main sub-parallel areas within the Midland Valley. The Strathmore Syncline occurs in the north and a discontinuous series of folded and faulted outcrops (Lanark Basin) in the south within a volcanic chain formed of the Lower ORS igneous rocks (calc-alkaline volcanics). Distribution of ORS sedimentary and igneous strata in the Midland Valley is shown in Figure 1.5. Bluck (1983, 1984) used palaeoflow and clast provenance data to describe the tectonic setting of deposition as interarc (Fig. 1.6).

Lower ORS conglomerates, lavas, and sandstones rest unconformably on Silurian strata in the Pentland Hills and near Girvan, though they may have conformable contact at Lesmahagow and in the Hagshow Hills (Rolfe, 1961). In the north of the Midland Valley between Stonehaven and Loch Lomond the sequence attains its maximum thickness of 7500 m, though it is much reduced towards the west (4000 m in the Callander-Dunblane area). The lithology is composed mainly of sandstone, siltstone, mudstone and coarse conglomerates. The strata are folded into the asymmetric Strathmore Syncline and the parallel Ochil-Sidlaw anticline (Fig. 1.5), which are crossed in this project. The axes of the major folds are generally horizontal but in places there is considerable axial plunge, (Armstrong &

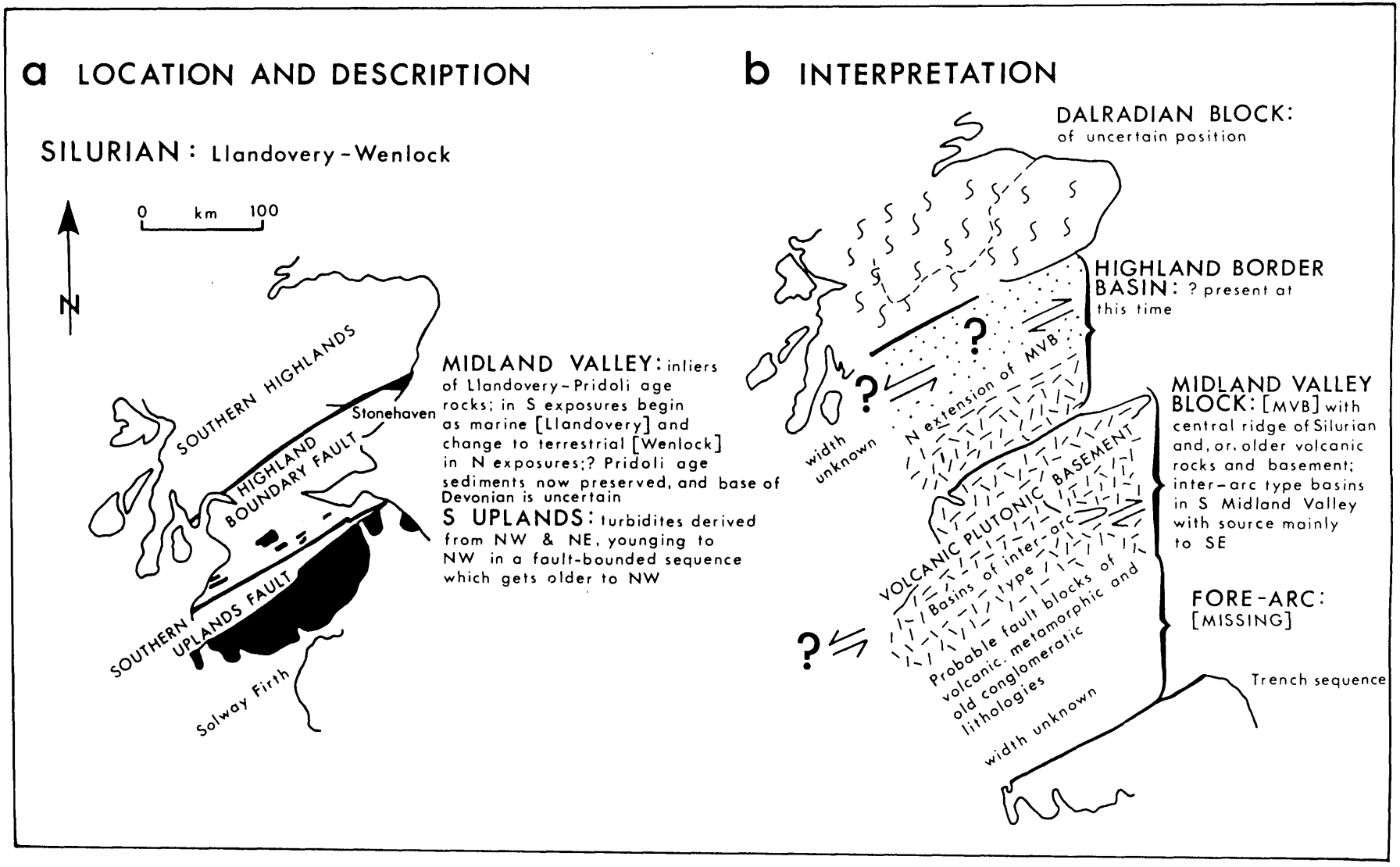

Fig.1.4 Tectonic setting of the Midland Valley of Scotland during the Silurian (after Bluck 1984)

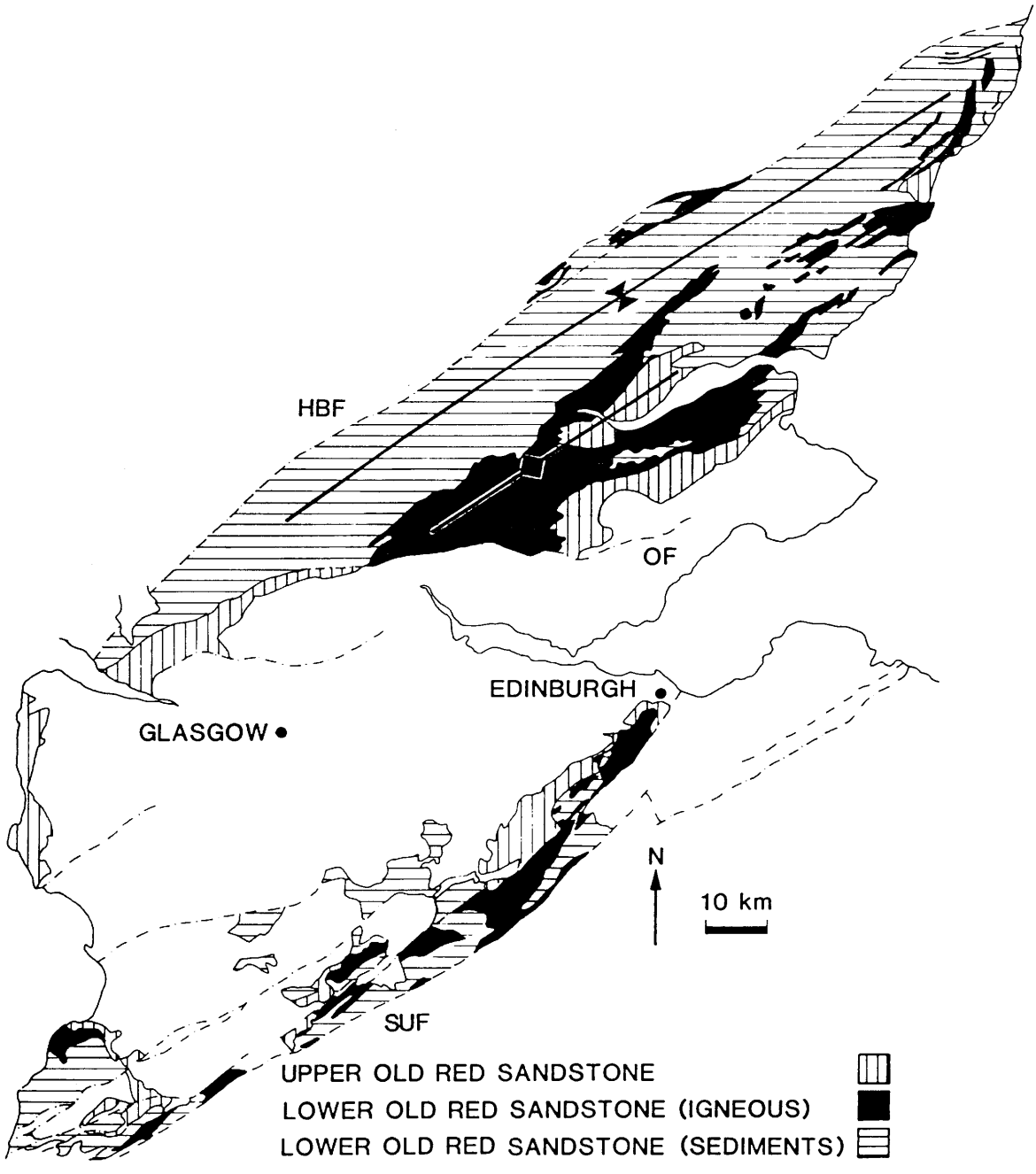

Fig.1.5 Distribution of ORS strata in the Midland Valley of Scotland. HBF - Highland Boundary Fault, OF - Ochil Fault, SUF - Southern Uplands Fault (after Dentith 1987).

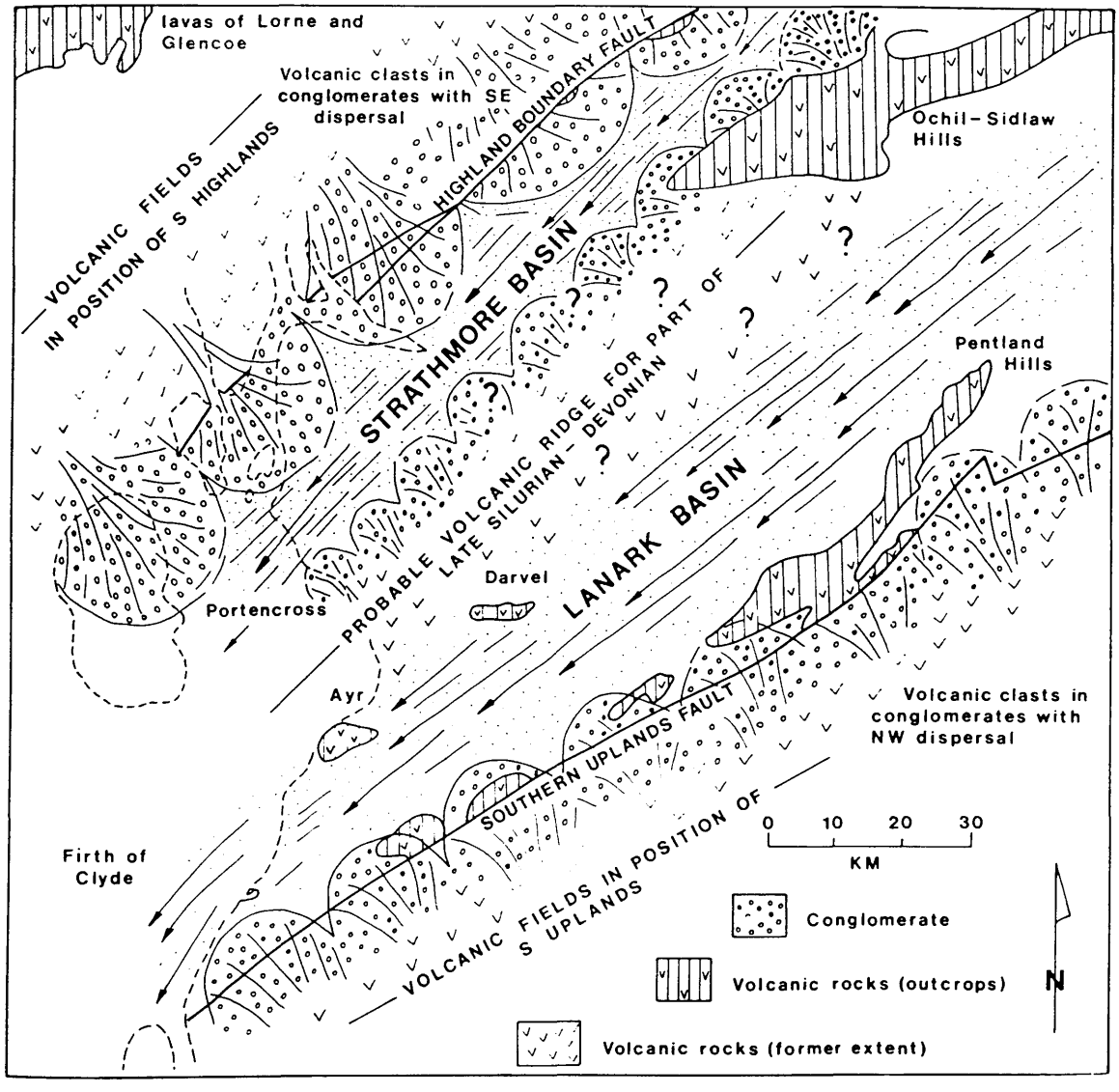

Fig.1.6 Palaeogeography of the Midland Valley during the late Silurian and early Devonian (after Bluck 1983).

Paterson 1970), which is increased in places by faulting (e.g. in the Strathmore Syncline).

In central and west Fife the geological setting and stratigraphy of Lower ORS is described by MacGregor (1968). The Ochil Hills are dominated by volcanic rocks which range in thickness from 1750-2000 m decreasing to the NE , and the sequence crops out in a belt striking SW-NE along the Tay anticline. SW of Perth the lava mass splits into two ranges of hills, the northern range joins the Sidlaw Hills and the southern range forms the North Fife Hills. The lavas are mainly andesites with minor basalts. There is considerable thickness of pyroclastic material and sediments derived from the erosion of the volcanic rocks.

North of the Tay Firth the NE trending Sidlaw Hills lavas are composed of olivine-basalts with minor andesites dipping gently towards the NW beneath younger sediments of Lower ORS age.

Extensive tectonism took place between Lower and Upper ORS times which caused a high rate of erosion. All of the Middle ORS was removed, if it was ever deposited. Consequently, in some places Upper ORS and basal Carboniferous rest on Silurian strata where the Lower and Middle ORS had been completely eroded.

Upper ORS sediments were deposited on the eroded surface of the Lower ORS and therefore the two formations are separated by a major unconformity. The strata crop out in two belts, the northern one is exposed in two major localities: from north Ayrshire and the Firth of Clyde to Stirling in the west and between Kinross and Tayport and in the Tay Graben in the east. The southern belt consists of several small outcrops from south Ayrshire to Lanark and the Pentlands.

Thicknesses of Upper ORS are much less than those of the Lower ORS, ranging between 0.5 km in the SE to 3 km in the NW margin of the Midland Valley . There are no volcanic rocks within the succession. The sediments are mainly fine grained sandstones, siltstones and mudstones and are generally more mature than those of the Lower ORS. Bluck (1978) considers that the sedimentation of Upper ORS was in a series of small, fault controlled basins associated with sinistral movements along the HBF. Most of the Upper Devonian rocks are fluvial in origin (braided, low sinuosity and meandering rivers, alluvial fans, flood plains) but some lacustrine beds occur.

A detailed description of Upper ORS geology in the Tay Graben and Fife region is given by MacGregor (1968), Chisholm & Dean (1974) and Browne (1980) . There is no distinctive boundary between the Upper ORS and Lower Carboniferous in the Firth of Tay. Exposure of Upper ORS in the

area is poor because of drift sediments, but there is evidence that the sequence is of fluviatile origin. Towards the south near Loch Leven the sequence reaches its maximum thickness of 500 m .

1.2.4. Carboniferous

Rocks of Carboniferous age dominate the outcrop of the Midland Valley. A full description of Carboniferous rocks is given by Francis (1983a, 1983b) and Cameron & Stephenson (1985).

A transitional contact between Upper Devonian sediments and Lower Carboniferous strata is common, representing a change in depositional environment from fluviatile and lacustrine conditions to fluvio-deltaic and shallow-marine deposition. Syn-depositional folding, faulting, and volcanism influenced the depositional configuration of the Carboniferous sediments in the Midland Valley, and this is reflected in considerable lateral variation of thickness.

The main factor controlling sedimentation in the west of the Midland Valley during most of the Carboniferous was differential subsidence along basement fractures trending in a NE-SW direction (Fig. 1.7). Their surface expressions are the Dusk Water, Inchgotrick and Kerse Loch faults (Eyles et al. 1949, McLean 1966, 1978). Here and elsewhere, sharp gradients on isopach contours produced for various stratigraphic levels within the Carboniferous sequence indicate their position (Kennedy 1958, Francis 1983 and Browne et al. 1985). Leeder (1982) suggested that lithospheric tensional stretching caused a complicated rift province during Lower Carboniferous times. However, in the east of the Midland Valley deposition was controlled by syn-depositional folding, faulting and volcanism leading to the formation of N-S trending depositional basins (Kincardine-Clackmannan basins).

Dewey (1982) and Dentith (1987) suggested a tectonic regime during Carboniferous times where syn-depositional movements and reactivated structures are related to dextral strike-slip movements. The two largest folds in the Carboniferous of the Midland Valley are the N-S to NE-SW trending Central Coalfield and Fife-Midlothian Synclines. The Ochil Fault which extends east-west across the Midland Valley from the Fife coast to west of Stirling, separates the Lower Old Red Sandstone to the north from the Carboniferous to the south (Fig. 1.1a). The fault has its maximum downthrow in excess of 3 km at Alva (Geikie 1900).

The Carboniferous of the Midland Valley is divided into the following lithological units:

[1] Calciferous Sandstone Measures, CSM:

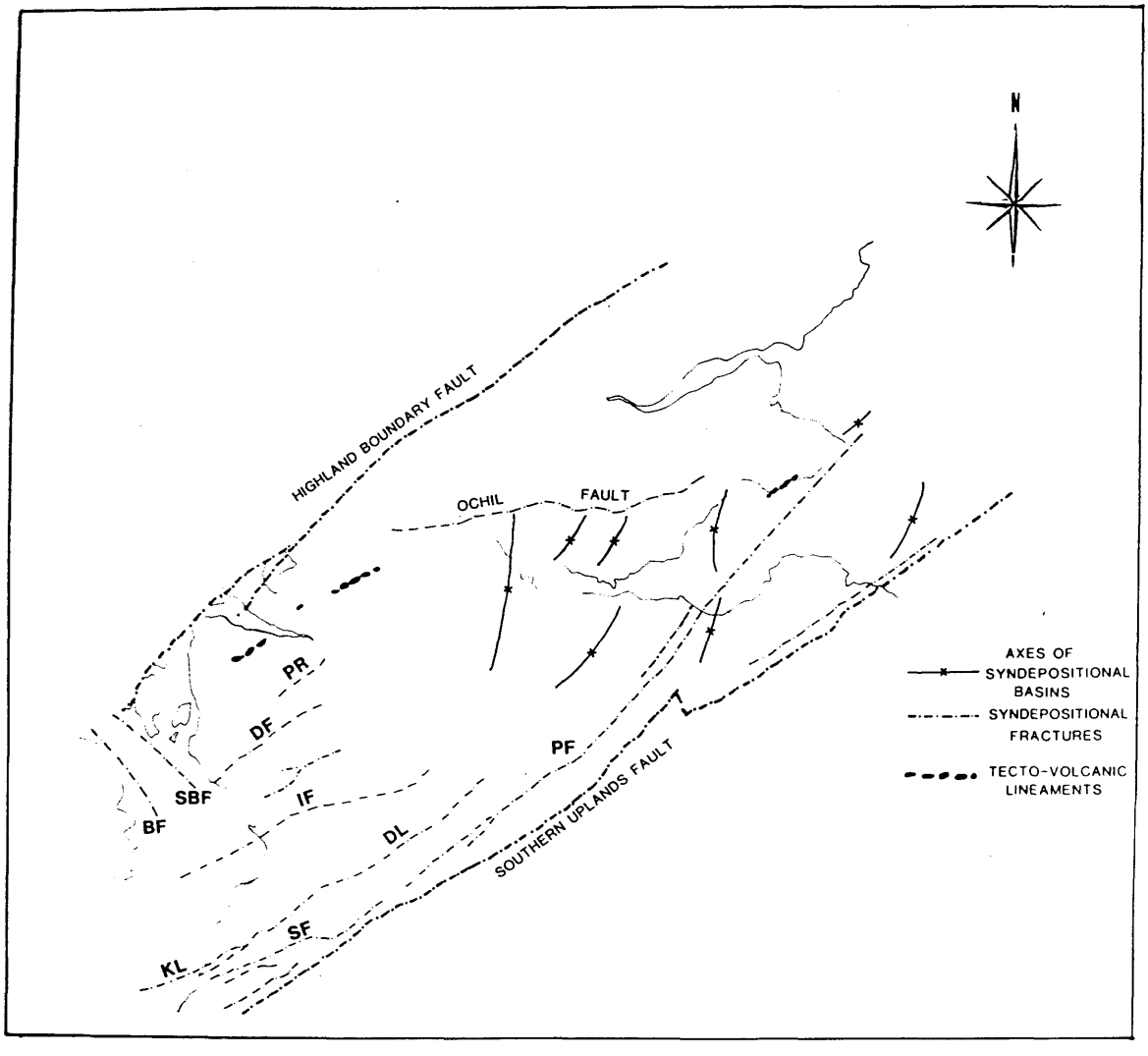

Fig.1.7 Basement control of volcanism and sedimentation during the Carboniferous. BF - Brodick Bay Fault, DF - Dusk Water Fault, DL - Dron Line, IF - Inchgotrick Fault, KL - Kerse Loch Fault, PF Pentland Fault, PR - Paisley Ruck, SF - Straiton Fault, SBF - Sound of Bute Fault.

CSM were deposited under deltaic, swamp and occasionally marine conditions (MacGregor 1968) and are of Dinantian age (Lower Carboniferous). These Measures have a very variable lithology composed of cementstone at the base, oil shales and non-marine limestone. Extreme lateral facies changes occur. There is no clear cut lithologic boundary between this group and the top of the underlying Upper ORS.

In Fife the CSM crop out in three parts of the area 1)south of Loch Leven and at Dron, Bridge of Earn; 2)at Burntisland; 3)in the East Neuk of Fife. They are usually highly reduced in thickness in central Fife but thicken rapidly until they attain their maximum thickness of 2130 m near St. Andrews. The most significant feature in the facies distribution of the CSM is the N-S trending "Lanark Line" (Hall 1971) which separates the dominantly volcanic sequences (Clyde Plateau Volcanic Formation) of western Scotland (up to 1.5 km thick) from the thick sedimentary sequences of Lothian and Fife.

[2] Lower Limestone Group, LLG:

This is the uppermost Dinantian subdivision and has a conformable contact with the underlying CSM. It consists of cyclic sandstones, mudstones, limestones and coals with root beds. Thick beds of marine limestone suggest that they were deposited under marine conditions due to differential subsidence. The sequence attains its maximum thickness of 220 m in the Kincardine Basin.

[3] The Limestone Coal Group, LCG:

This represents the base of the Namurian and consists principally of sandstone, siltstone, mudstone and numerous coals. Thickness varies from 30 to 550 m in the Kincardine Basin. Forested deltaic swamp conditions were predominant during the sedimentation of this group leading to the accumulation of thick coals.

[4] Upper Limestone Group:

This group shows a return to marine conditions, and is lithologically similar to the LLG. It crops out in two main areas in Fife, the Cowdenbeath Syncline and north of Lundin Links. It attains its maximum development of 600 m in the Kincardine Basin.

[5] Passage Group:

The uppermost division of the Namurian. It consists of marine bands interrupted by thick sandstone beds with some coal seams, suggesting deltaic conditions of sedimentation. The group crops out

in two areas of Fife (MacGregor 1968): a small one at Westfield characterised by growth folds (Browne et al. 1985) terminating against the Ochil Fault to the west, and a larger one at Leven. The thickest development of this group occurs in the Kincardine Basin (380 m).

[6] Coal Measures:

These consist of mudstone, sandstone and siltstone with seams of coal and seatclay and represent the Westphalian succession in the Midland Valley. Deposition was in a fluvio-deltaic environment. They are divided into Lower, Middle and Upper Coal Measures. The Lower and Middle Coal Measures are absent north of the Ochil Fault while in the Kincardine Basin the strata are contained in a N-S trending syncline which plunges northwards north of Kincardine and southwards south of Clackmannan. Their maximum thickness (150 m) is at the axial part of the syncline and attenuation is considerable towards the north. Both Measures are found in a small outlier at Westfield with thicknesses of 160m and 200m respectively.

The Upper Coal measures are a sequence of fluvio-deltaic coal bearing cycles and in many places they have been chemically and, to some extent, physically altered by processes of oxidation. Thicknesses of about 270m are present in the Fife region and Central Coalfield.

[7] Carboniferous Igneous Rocks:

The stretching process during Carboniferous times subjected the Midland Valley to considerable igneous activity, it is well described by Francis (1983b) and Upton (1971) and to a lesser extent by MacGregor (1968) and Cameron & Stephenson (1985).

Carboniferous igneous rocks are mostly of alkaline affinity in addition to tholeiitic sills and dykes. Lava plateaux attaining thicknesses of up to 1 km were formed during the Dinantian e.g. in East Lothian and the Clyde area.

Volcanism continued on a reduced scale into the Namurian and Westphalian periods represented by basalt lavas, sills and plugs of alkaline basic rocks. Towards the end of the Carboniferous (Stephanian) changes in the stress-system caused E-W trending faults and dyke emplacement. This was accompanied by abrupt change in the magmatism introducing oversaturated tholeiite magma into the dykes and an extensive sill-complex.

1.3. Previous Geophysical Work

1.3.1. The LOWNET array

A network of permanent radio-linked short period seismometers was positioned in the eastern part of the Midland Valley in 1969 by the Institute of Geological Sciences. Crampin et al. (1970) used this array to study natural events and P-wave arrivals generated from commercial quarry blasts to establish a preliminary upper crustal model for the Midland Valley.

A three layer model was presented (Fig. 1.8). Layers 1 and 2 have velocities of 3 and 5.65 km/s respectively, representing the Palaeozoic sedimentary sequence. The third layer, characterised by a velocity of 6.4 km/s and a depth of 7-8 km, was interpreted as the top of the crystalline basement.

1.3.2. The Lithospheric Seismic Profile Across Britain (LISPB)

The LISPB profile was recorded in 1974. It is a N-S seismic refraction line recorded for 1000 km along Britain. It crosses the Midland Valley near Edinburgh (see Figs. 1.9 and 1.14 for locations). The project is described by Bamford et al. (1976, 1977, 1978), Kaminski et al. (1976) and Assumpcao & Bamford (1979). A brief summary is given by Bamford (1979).

A four layer crustal model for northern Britain was suggested (Fig. 1.10) and the layers were interpreted as:

[1] A poorly constrained superficial layer of upper Palaeozoic and younger sediments with velocity of 4.0-5.0 km/s and thickness of 2-3 km.

[2] A second layer with velocity of 5.8-6.0 km/s was interpreted as a Lower Palaeozoic succession to a depth of 7-8 km. In the Highlands this layer has velocities of 6.1-6.2 km/s and is interpreted as a combination of Caledonian metasediments and intrusions.

[3] A refractor with velocity of 6.4 km/s was inferred as the top of crystalline basement existing at a depth of more than 8 km.

[4] A poorly constrained lower crustal layer with velocity of 7.0 km/s was interpreted south of the Southern Upland Fault. A total crustal thickness of 30 km beneath the Midland Valley was envisaged.

Assumpcao & Bamford (1978) studied shear waves with large amplitudes recorded by three-

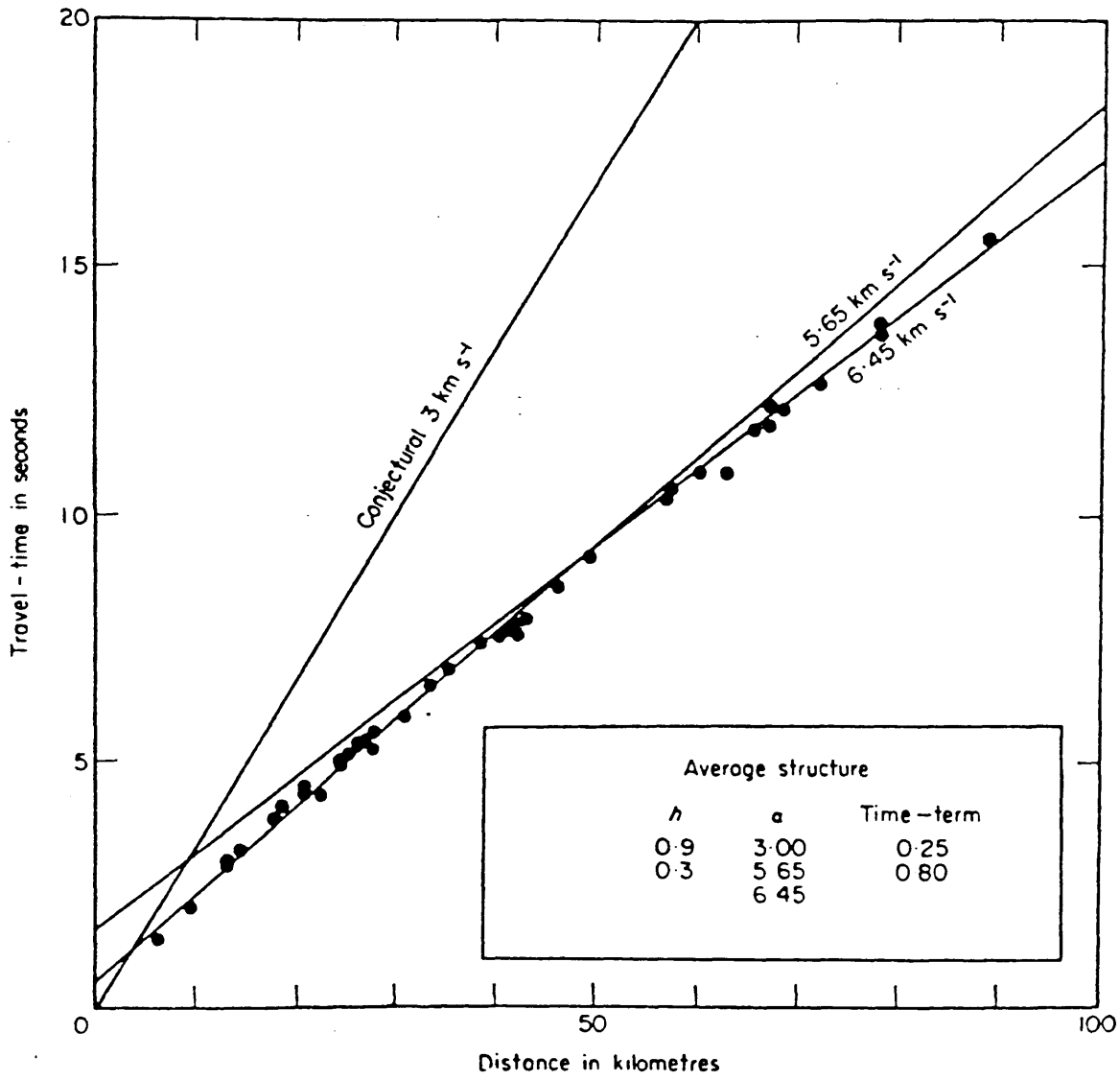

Fig.1.8 LOWNET travel-times and their interpretation (after Crampin et al. 1970).

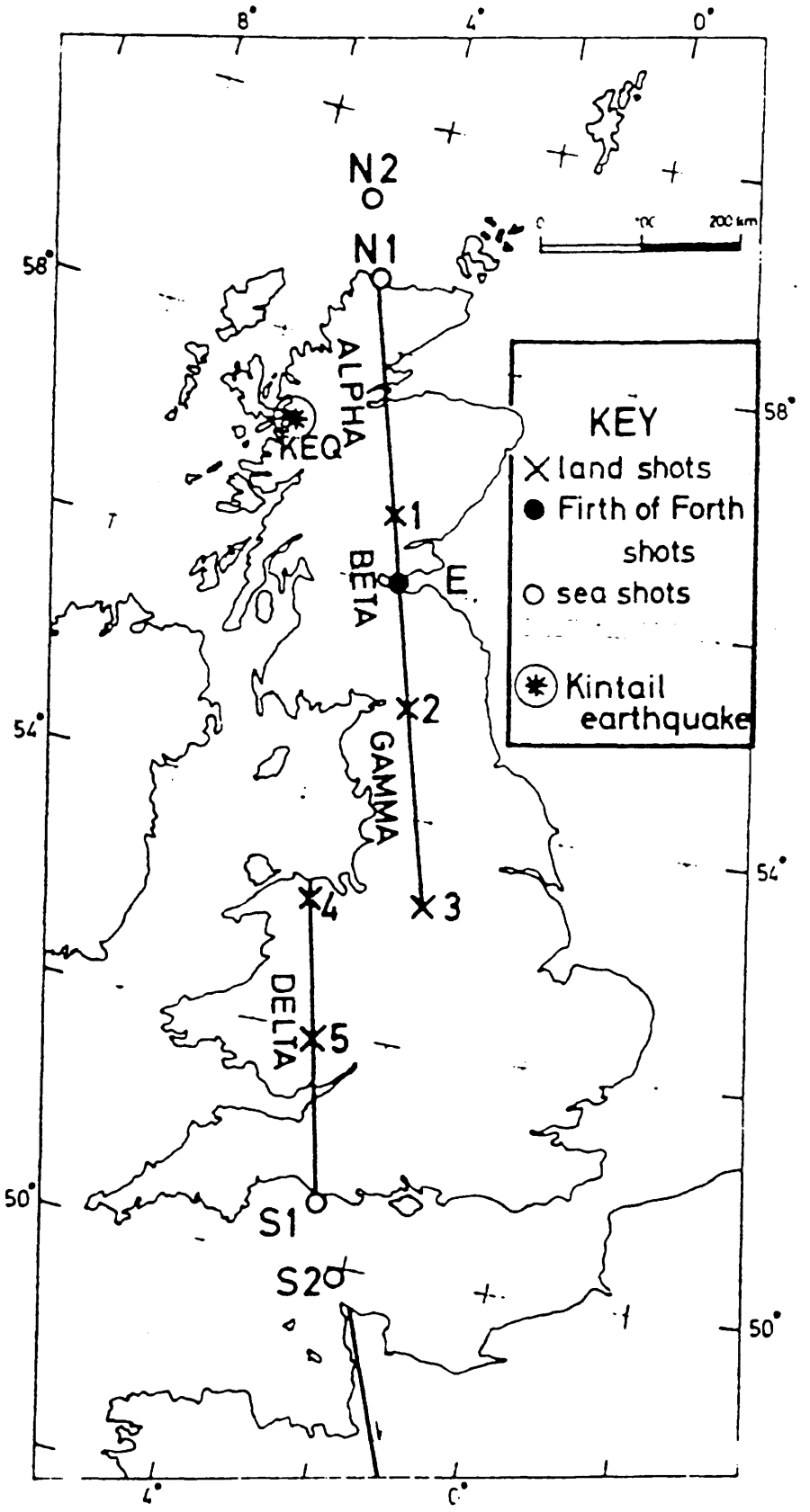

Fig.1.9 Location of the LISPB profile (after Bamford et al. 1976).

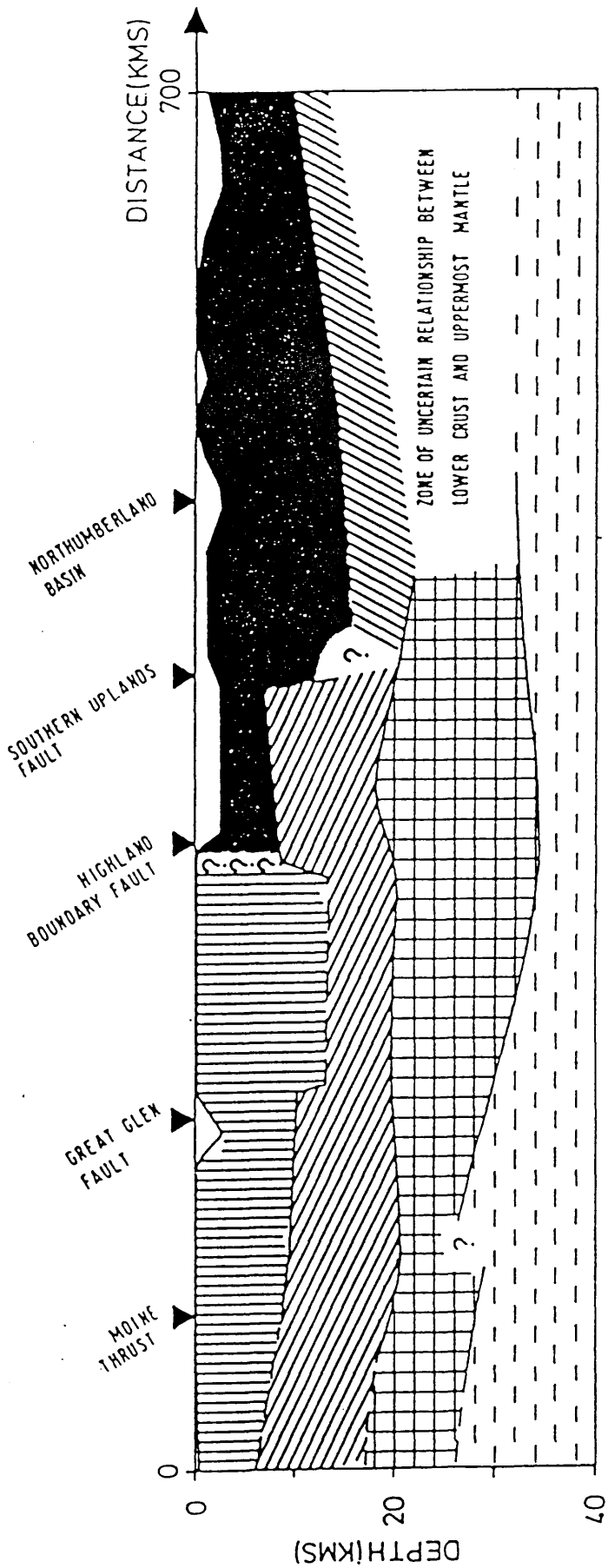

Fig.1.10 Cross-section of the crust and Moho of northern Britain from the LISPB profile (after Bamford 1979).

component stations. They used the compressional and shear waves travel times ratio (ts/tp) to calculate Poisson's ratio which was close to the average crustal value of 0.25, except for layer 1 in the Southern Uplands (0.231) and layer 2 under the Midland Valley (0.224). Their interpretation of these data suggested that the Southern Upland Fault is a major element in the British Caledonides.

Hall et al. (1983) used seismic data from the Southern Uplands Seismic Profile (SUSP) and data recorded at the U.K. Atomic Energy Authority seismic arrays at Eskdalemuir and Broughton to re-interpret the LISPB data. P-wave velocities of 6.0 km/s at a depth of 1 km, increasing to 6.3 km/s at 3-4 km depth were recognised along the SUSP profile which trends nearly at right angles to the LISPB profile. These velocities were confirmed by arrivals recorded at the Broughton array, located at the SUSP line from sources to the NE and SW and from the Midland Valley to the NW. Whilst velocities measured from the south and east were of lower values (5.6-5.8 km/s).

This led to the conclusion that the LISPB high velocity crust beneath the Midland Valley continues south of the Southern Upland Fault, but deepens rapidly to the SE of SUSP and Broughton. This continuation of the basement was later supported by the North Channel deep seismic reflection line (WINCH). Hall et al. (1984) noted that, since no margins to the Midland Valley equivalent to the bounding faults are observed from WINCH data, the basement should be continuous beneath the Midland Valley and Southern Uplands.

1.3.3. Subsequent Refraction Work

The LISPB results initiated a great amount of research work which was aimed either to refine the LISPB data or to acquire new sets of data to be integrated into the LISPB model.

Davidson et al. (1984) and Davidson (1986) interpreted a series of short to medium range seismic lines in the centre and south of the Midland Valley. The LISPB layer 1 was found to be of an average lower velocity (Vp=3.0-3.7 km/s) whereas Lower ORS and Lower Palaeozoic sediments are of a higher velocity (Vp=4.0-5.5 km/s). Dentith (1987) re-interpreted the data and confirmed the velocities for layer 1. Since these two groups of velocities lie within the LISPB layer 1, a subdivision of this layer is suggested (Fig. 1.11). An undulatory refractor with velocities of 6.0-6.1 km/s was seen at a depth of about 3 km which is comparable with the LISPB layer 2. Velocities of this refractor plot within the field for acid-intermediate gneisses strongly suggesting the presence of crystalline basement (Fig. 1.12).

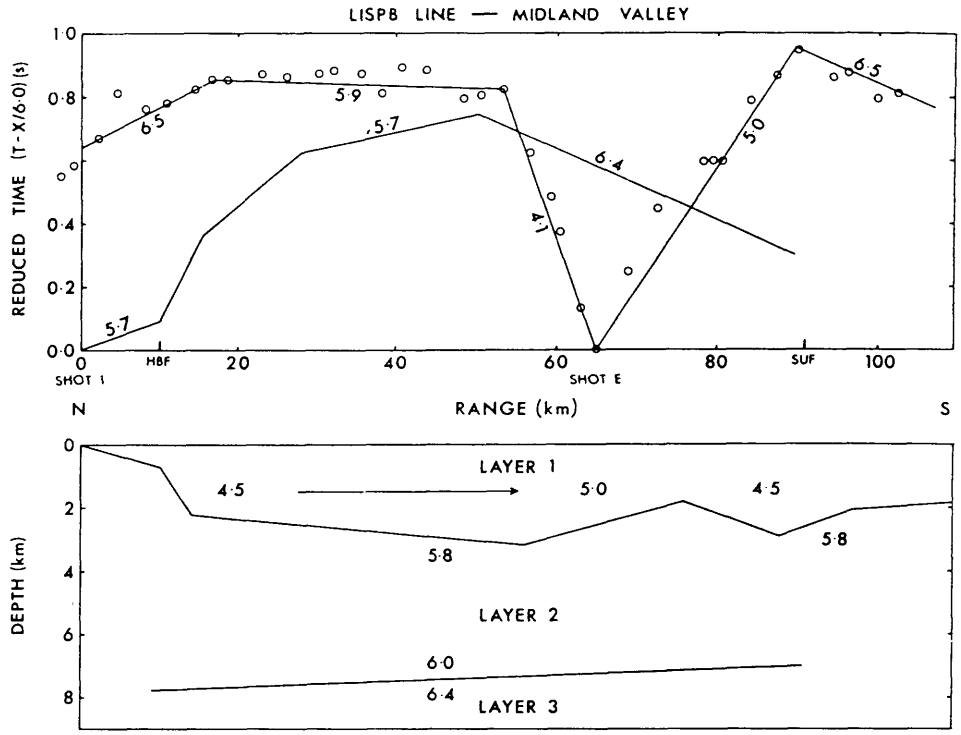

Fig.1.11 The LISPB model and interpretation across the Midland Valley (after Davidson et al. 1984).

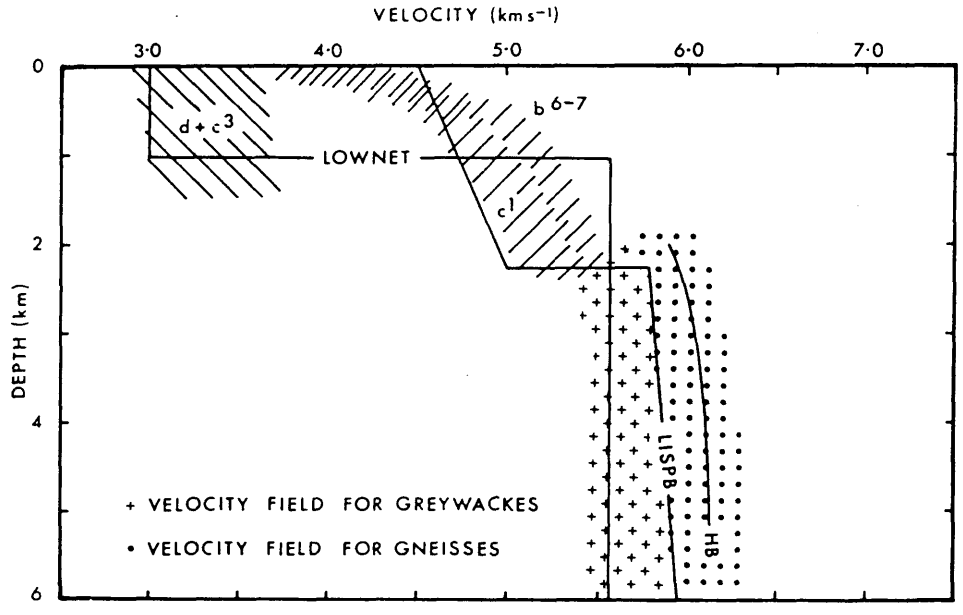

Fig.1.12 Velocity-depth plot for the lithologies of the Midland Valley . The LOWNET model is shown for comparison. d - Carboniferous, c3 - Upper ORS, c1 - Lower ORS, b6-7 - Silurian. HB is the velocity of the basement refractor (after Davidson et al. 1984).

Integration of the data of Davidson et al. with previous work led to a model which consisted of a topmost sedimentary layer of 2-4 km thickness comprising Carboniferous & Upper ORS rocks (Vp=3.2-4.0 km/s), Lower ORS (Vp=4.0-5.2 km/s) together with Silurian and (possibly) Ordovician and Cambrian (Vp=3.5-5.5 km/s). This is underlain by a gneissose crystalline basement (Vp=6.0-6.3 km/s) to a depth of 6-8 km. Below this, and extending to 18-20 km depth, a deeper refractor was envisaged as a layer of granulitic crystalline basement with velocity of Vp=6.4-6.6 km/s. Finally the lower crust was interpreted to be basic pyroxene granulite basement (Vp=7.0 km/s) to a depth of 34-35 km.

Sola (1985) recorded several lines in the central Midland Valley to explain the Bathgate anomaly which is represented by both magnetic and gravity highs centred over the Central Coalfield Basin by integrating seismic data with magnetic and gravity models. The velocity model (Fig. 1.13) is consistent with the model of Davidson (1986), except for layer 2 (Lower ORS and Lower Palaeozoic) where velocities were higher but within the conventional range assigned for the Lower ORS (Vp=5.4-5.8 km/s). These data were re-interpreted by Dentith (1987) (see section 1.3.4).

Al-Mansouri (1986) studied the Ballantrae complex using seismic profiles and high-pressure velocity measurements. The Upper Palaeozoic strata were modelled using velocity values from previous studies whereas for the lower Palaeozoic sequence velocities for only the Lower ORS were interpreted (Vp=5.06-5.57 km/s). A velocity of 6.0 km/s for a shallow basement was assigned increasing rapidly to 6.35-6.4 km/s at a depth of 6 km.

1.3.4. The MAVIS Project

Dentith (1987) interpreted the MAVIS data which were recorded between the years 1984-1986. A preliminary interpretation was published by Conway et al. (1987). The project consists of three parts (see Fig. 1.14 for locations). MAVIS I comprises two E-W sub-parallel lines across the Midland Valley; the MAVIS II is a single N-S profile crossing MAVIS I lines; and the MAVIS III line trends N-S west of Edinburgh across the Firth of Forth. The first two parts used controlled shots while the last part used quarry blasts. Line 1 of this study intersects the MAVIS I north profile SE of Loch Leven while line 2 intersects the MAVIS I north line and the MAVIS II near their intersection point east of Alloa.

In addition to these profiles data from the work of Sola (1985) were used in the interpretation. The MAVIS velocity-depth curve suggests a four layer model (Fig. 1.15).

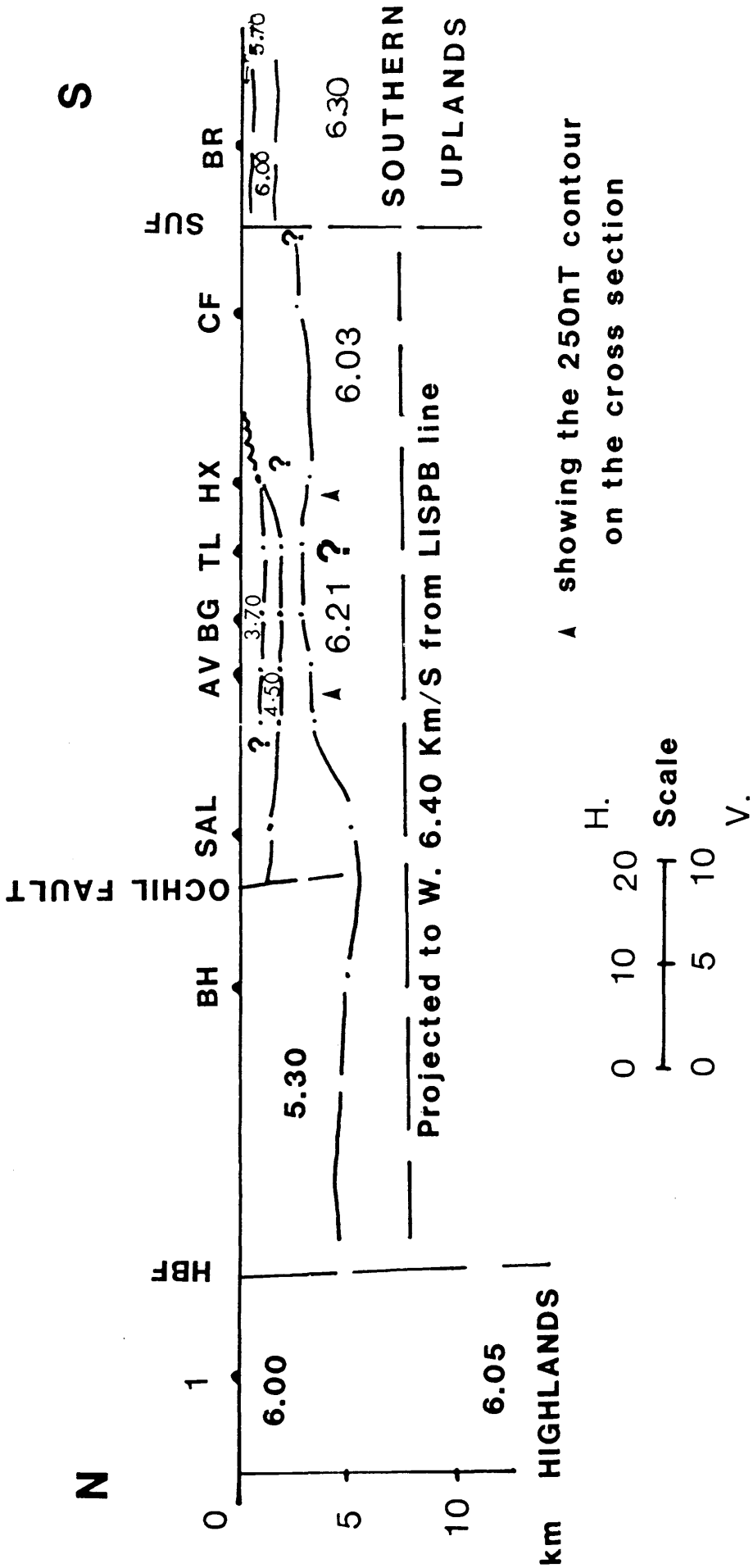

Fig.1.13 Crustal model for the Midland Valley of Scotland (after Sola 1985). AV - Avonbridge shot, BH - Blackhill shot, BR - Broughton array, CF - Caringryffe shot, HBF - Highland Boundary Fault, HX - Headless Cross shot, SAL - Saline shot, SUF - Southern Uplands Fault, TL - Tamsloup shot.

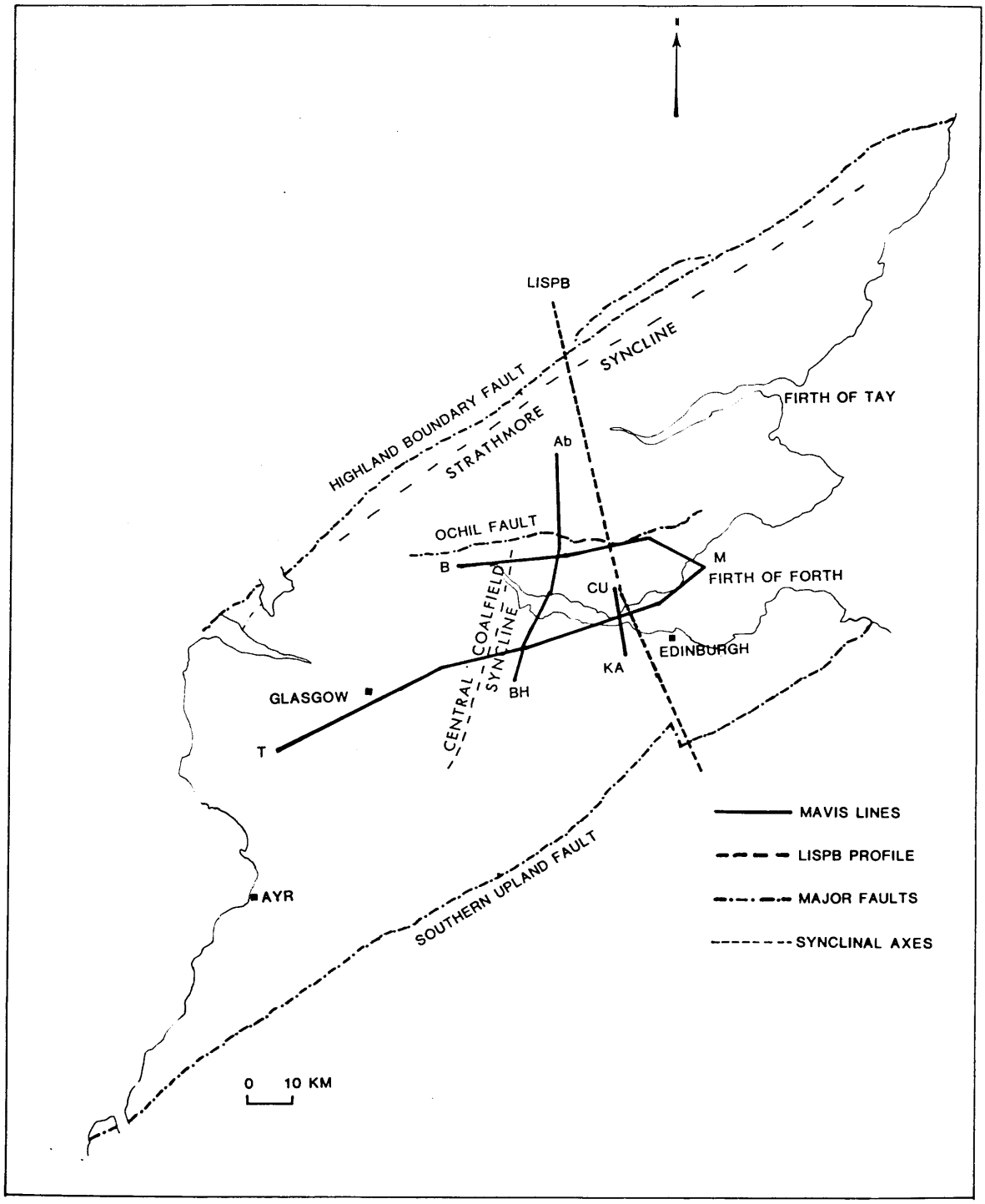

Fig.1.14 Location map for the MAVIS project. B - M: MAVIS I North, T - M: MAVIS I South, Ab - BH: MAVIS II, CU - KA: MAVIS III. Redrawn from Dentith (1987) and Bamford et al. (1976).

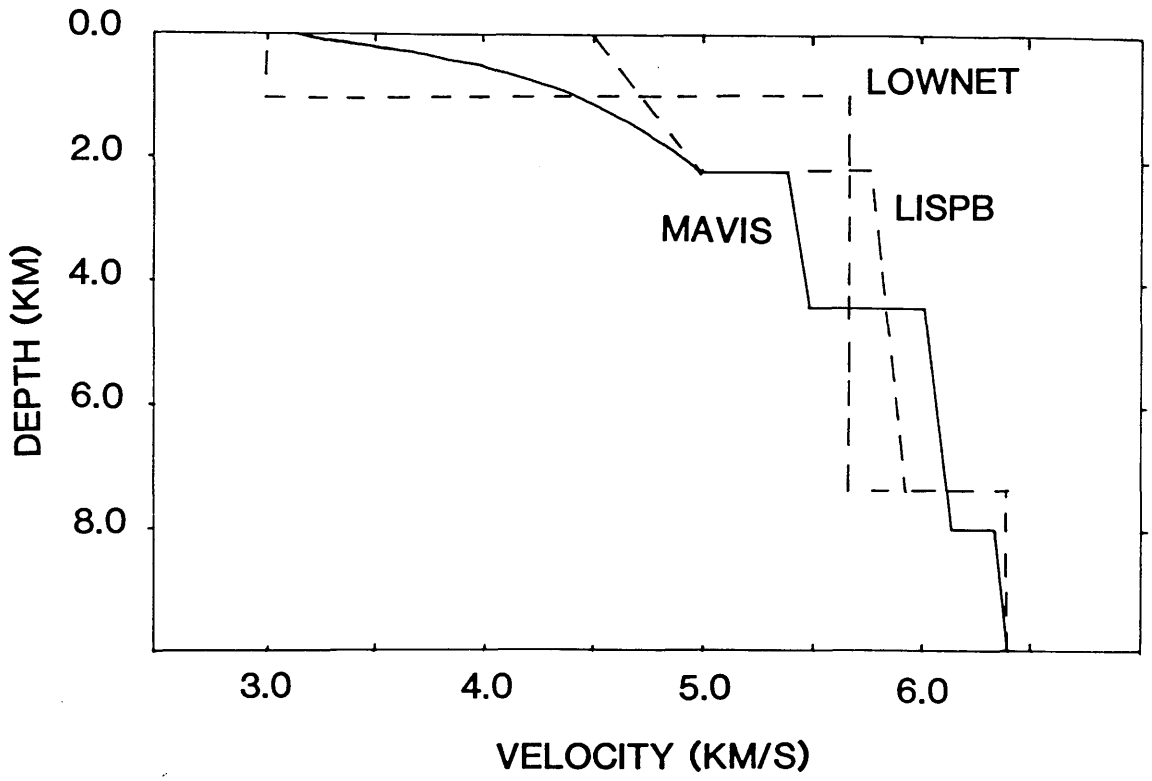

Fig.1.15 Comparison of the velocity depth curves from LOWNET, LISPB and MAVIS (after Dentith 1987).

[1] Layer 1 with P-wave velocity of 3.0-5.0 km/s and thickness of 0-2 km is interpreted as Carboniferous and Upper ORS.

[2] Layer 2 with P-wave velocity of 5.4 km/s and thickness of approximately 2 km, is interpreted as Lower ORS and Lower Palaeozoic.

[3] Layer 3 with P-wave velocity of 6.04 km/s and thickness of approximately 3 km is interpreted as crystalline basement.

[4] Layer 4 with P-wave velocity of 6.43 km/s is interpreted as higher velocity crystalline basement.

The results are in agreement with Davidson (1986) and Sola (1985), especially with reference to the subdivision of the LISPB Layer 1 and the confirmation of its thickness. However, the LISPB layer 2 is subdivided into two layers of about 5.4 and 6.0 km/s respectively. As for layer 3 it was considered to be in an agreement with the LISPB layer 3 both in velocity and depth. The base of the crust is suggested to be about 35 km deep which is the same as the model predicted by the LISPB profile.

An interesting feature observed from the MAVIS model is a postulated basement fracture of Caledonian age towards the northern end of MAVIS II, also seen on the western end of MAVIS I north line. The final interpretation of the MAVIS lines is illustrated in Figures 1.16 to 1.18. The Ochil Fault was interpreted as a listric normal fault dipping to the south. This interpretation will explain the thickening of MAVIS layer 1 south of the fault which was interpreted as a roll-over structure, if the listric fault assumption is correct.

The MAVIS III results were integrated with Sola's south lines to give a model for the structure of the Lothian Oil-Shale Fields south of the Firth of Forth. The larger E-W faults seen at surface were interpreted as being listric and to sole out at shallow depth. They were interpreted to form a flower structure across which a downthrow to the north occurs associated with the Calder-Murieston Fault zone.

The revised crustal model for the Midland Valley of Scotland suggested by Dentith (1987) taking into account all previous data is given in Table 1.1.

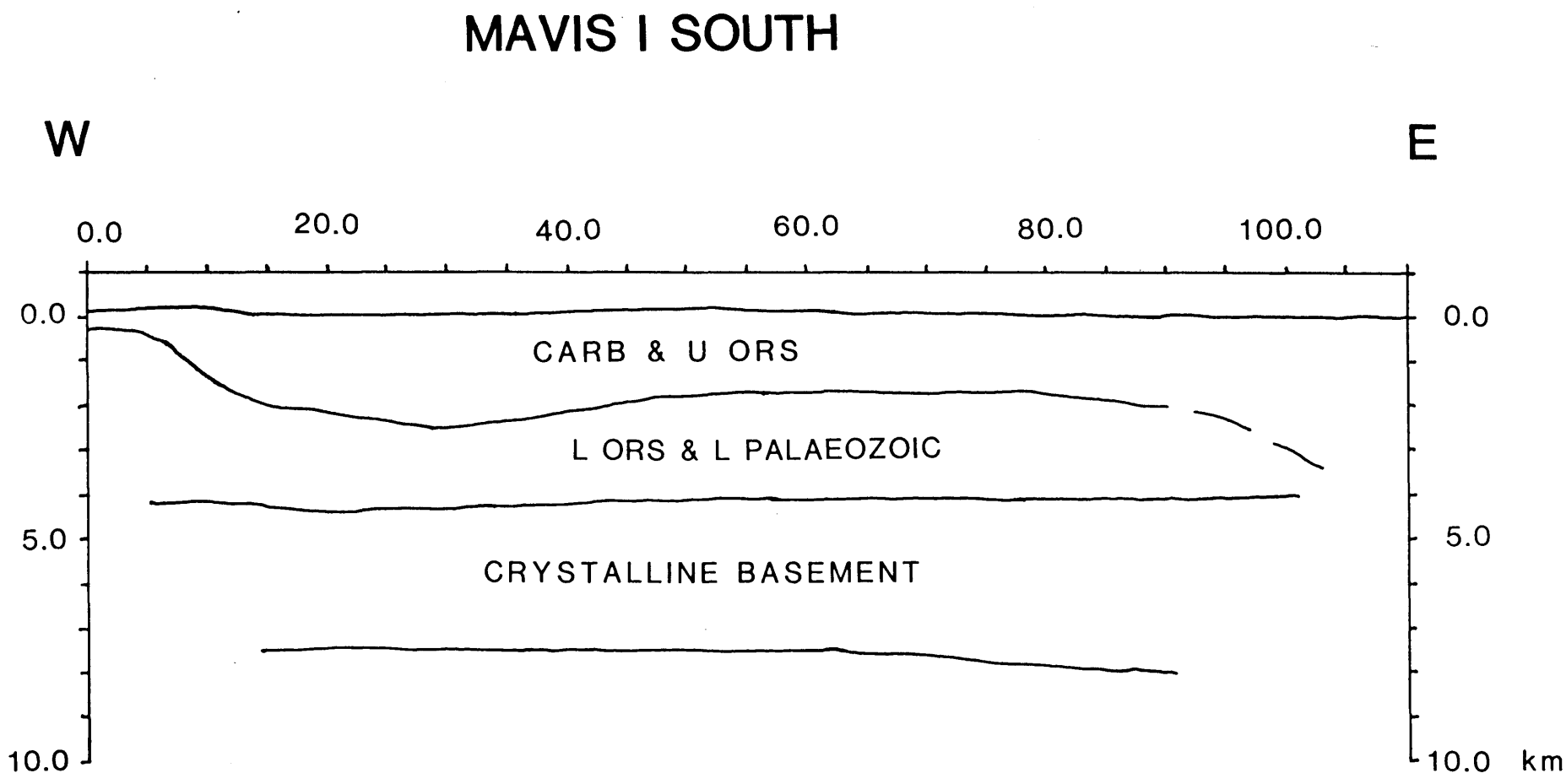

Fig.1.16 Geological interpretation of the MAVIS I south line (after Denlith 1987). Refer to section 1.3.4 for velocity values.

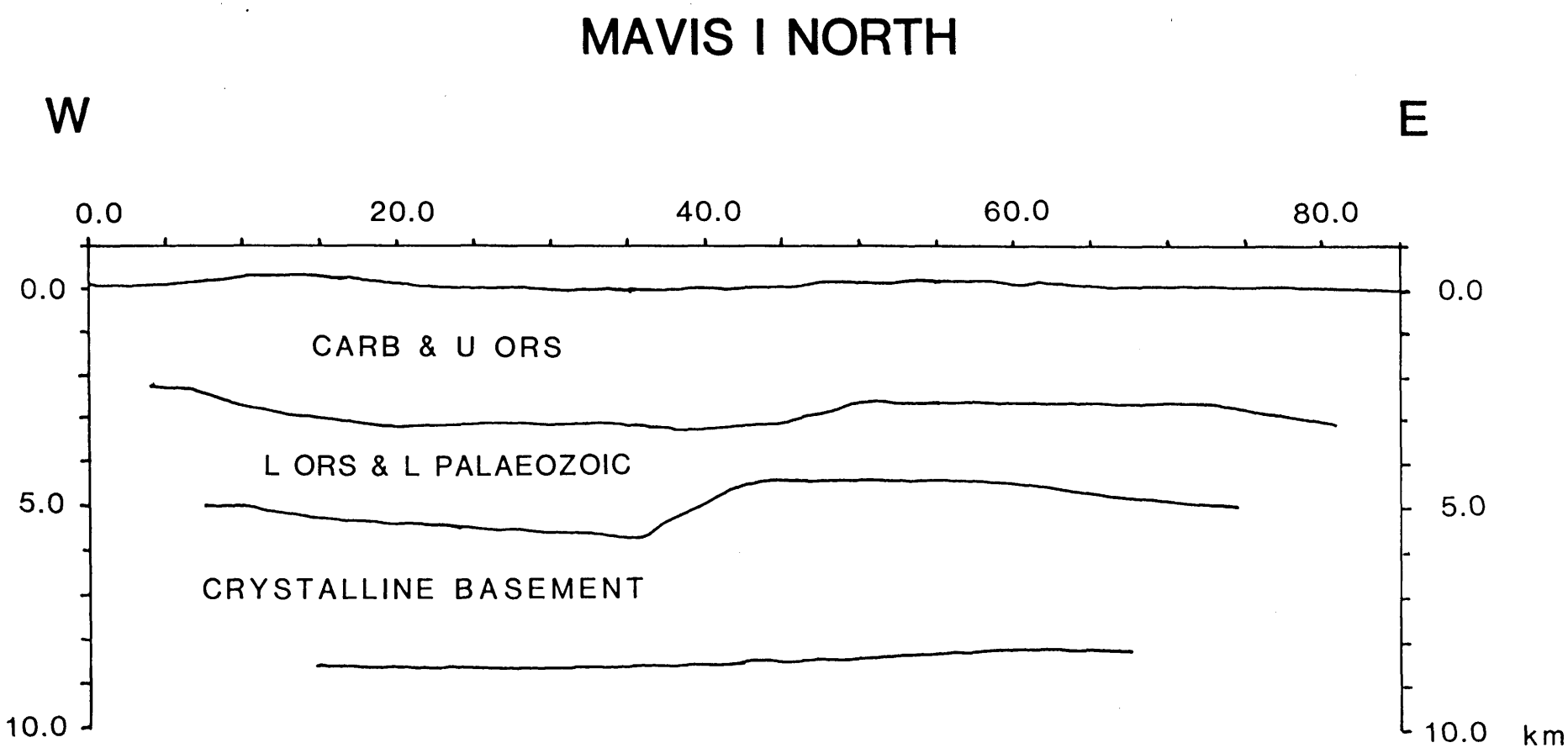

Fig.1.17 The MAVIS I north line interpretation (after Denith 1987). Refer to section 1.3.4 for velocity values.

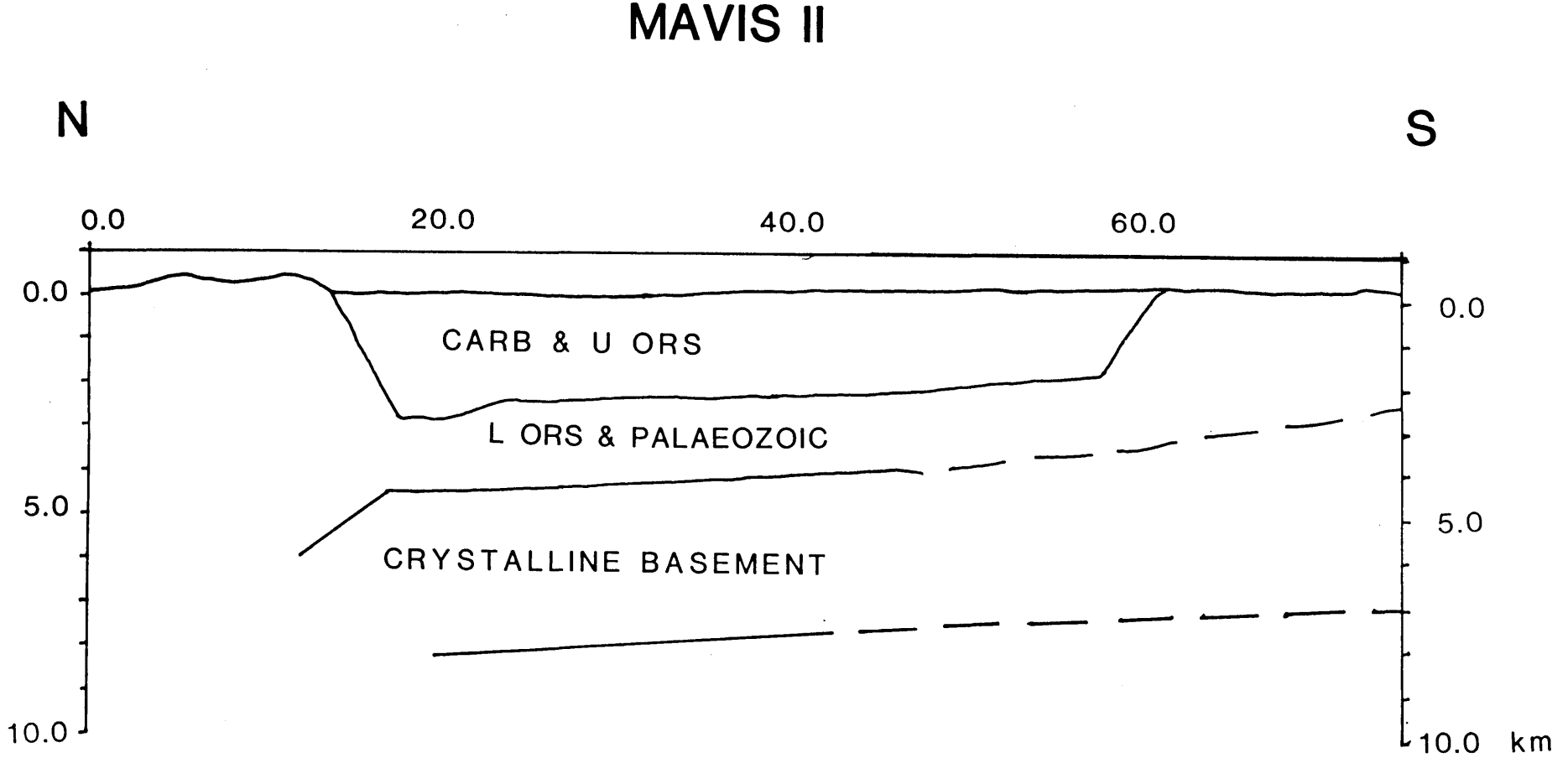

Fig.1.18 The MAVIS II line interpretation (after Dentith 1987). Refer to section 1.3.4 for velocity values.

Table 1.1 Crustal model for the Midland Valley of Scotland (after Dentith, 1987).

Layer	Velocity (km/s)	Approximate Depth(km)	Interpretation
1	2.5-3.5	0-3	Carboniferous and Upper ORS
2	4.0-5.5	3-6	Lower ORS and Lower Palaeozoic
3	5.9-6.2	3-8	Crystalline basement (6.0 km/s)
4	6.4	8-20	Crystalline basement (6.4 km/s)
5	7.0	20-35	Lower crust
6	8.0	>35	Upper mantle

1.3.5. Reflection Studies

No available reflection data could be obtained for the project area and only a brief review will be given here of the previous reflection work done in the Midland Valley.

A number of academic surveys have been undertaken in the Midland Valley and adjacent offshore areas. Hall (1971, 1974) interpreted thicknesses of Carboniferous lavas in the central and western Midland Valley. The Western Isles North Channel (WINCH) profile was recorded by the British Institutions Reflection Profiling Syndicate (BIRPS). It crosses the offshore extensions of the Dalradian, Midland Valley and Southern Uplands terranes (Brewer et al. 1984). The main reflectors interpreted were post-Caledonide shallow structures (e.g. Mesozoic sedimentary basins), top of crystalline basement, top of reflective lower crust, base of the crust (Moho) and a mantle reflector. No conclusive interpretation of the nature of the basement underlying the Midland valley or the bounding faults was given by the WINCH profile.

The Northeast Coast (NEC) profile was also recorded by BIRPS. It ran sub-parallel to the eastern coast of the Midland Valley and the Southern Uplands (Klemperer & Matthews 1987). No upper crustal structure is imaged by the profile but depths of 20 and 30 km were assigned to the top of lower crust and the Moho respectively.

1.4. Regional Gravity and Magnetic Studies

The MAVIS refraction data were used to constrain gravity modelling for the Midland Valley by

Dentith (1987). He suggested that the source of the Bathgate gravity "high" is a body of extrusive and/or intrusive igneous rocks. Gravity modelling of the the Alloa "low" confirmed the offset of the Kincardine Basin to the east from the structural axis of the Central Coalfield Syncline i. e the depositional centre of the Kincardine Basin does not coincide with that of the structure. The southward dip of the Ochil Fault was also corroborated.

Except for the MAVIS study, all other gravity and magnetic research was carried out on a regional scale and contributes little to the present work and so they will be mentioned only briefly.

Qureshi (1970) studied anomalies associated with the HBF. Powell (1978) made a magnetic study along the LISPB seismic profile and inferred that any granulites under the Midland Valley are less magnetic than their counterpart in the NW Highlands. Alomari (1980) modelled the gravity "low" centred around Hamilton, the Bathgate gravity and magnetic "high" were modelled by Hossain (1976). Hipkin & Hussain (1983) describe the regional Bouguer gravity map covering northern Britain.

1.5. Summary

Previous geological and geophysical work provide reasonable regional constraints on the upper crust, but little geophysical work relates directly to the survey area of the present study. The LISPB profile provides a generalised picture of the main refractors and velocities which might be expected in the area, but the results have been refined by later research. The only available data which can be directly correlated with the present work are those derived from the MAVIS project, which covers only the southern half of the study area while to the north of the Ochil Fault an entirely different structural set up is present with no available geophysical data.

CHAPTER TWO - DATA ACQUISITION AND DIGITIZATION

2.1. Introduction

Recording data in the present work started in May 1987 and was finished by the end of August 1988. The project consists of three lines and one supplementary short profile (Newburgh EW). Two of the lines were reversed and the other two were not reversed. The lines cover the central part of the Fife region, the area north of the Tay Graben, the Central Coalfield Syncline and the Ochil Fault (Fig. 1.1a). The total length of lines recorded was approximately 219 km (counting reversed profiles and in-line recording). A total of 136 stations were occupied and an overall total of 136 separate recordings were made, of which 68 have between 2 and 3 duplicate recordings. Re-recording of stations was due either to locating better sites in the immediate vicinity, or to increase signal/noise ratio when weather conditions and other factors were changed.

Quarry blasts were the only seismic sources available for the project, leading to problems in acquiring the data. It is not possible to have complete control of such blasts in terms of fixing the appropriate time window for the shot, amount and configuration of charge and quarry face being removed (see section 2.4). On several occasions important blasts were missed because of unscheduled change of the blasting time.

2.2. Description of Lines

The project is divided into the following profiles:

[1] Line 1: Aberdour-Collace (reversed) is 51 km long and trends N-S. It was recorded using Aberdour and Collace quarries (Fig. 1.1a). Stations 10-32, divided equally north and south of the Firth of Tay, were also recorded from Newburgh quarry which is situated 3.9 km east of the profile (Fig. 1.1b). These extra data were recorded for additional in-line coverage, particularly of the topmost layer. This line covers the main area of the project and was used to study the main lithological units down to the upper basement refractor.

The whole line was recorded from Aberdour to 51 km, some 6 km to the north of Collace. Data quality was good, and coverage down to basement was obtained. Reversal of the profile from Collace was considered successful although some of the stations at the southern end were not recorded. In this

area, from Loch Leven to Aberdour (11 stations) the high noise levels permitted only low gain settings to be used (Fig. 1.1b). Only 5 stations were recorded along this segment, of which 3 are of poor quality. Good constraints on the first two layers were obtained.

[2] Line 2: Aberdour-Alva (reversed) is 45 km long and trends ESE-WNW and was recorded using Aberdour and Tillicoultry quarries (Fig. 1.1a). Reversed coverage was not completed from Tillicoultry quarry because the quarry manager after initially giving his permission for using the quarry, after more than half of the project was completed, made it clear that he does not wish any further work at his quarry to be pursued. However, only 10 km of the reversed section were recorded comprising 7 stations. These later data will be used in the frequency analysis and in interpreting the velocity of layer 1 in the area. The strength of shots at Aberdour permitted recording to a distance of 45 km. Thus coverage from Aberdour extended 16 km beyond Tillicoultry, crossing the Ochil Fault, permitting assessment of its displacement and geometry.

[3] Line 3: Tillicoultry-Leven (unreversed) is 19 km long and was recorded from Tillicoultry quarry toward NNE. It was intended for this line to intersect line 1 north of Loch Leven near its midpoint to act as a "tie" of lines 1 and 2 in addition to that provided by the common shot point at Aberdour. However, for the same reason as for line 2, only half the scheduled length was recorded and will be used in frequency analysis and velocity interpretation of the first layer.

[4] Line 4: Newburgh E-W was recorded from Newburgh quarry. It intersects line 1 south of the Firth of Tay and extends 12 km to the west from the quarry. The data acquired along this line will be integrated with the data obtained towards the north and the south from the same quarry to study the azimuthal change of the velocity of, primarily, layer 2 and to determine if the direction of shooting has any effect on the velocity of this layer.

Tables 2.1 to 2.4 show the dates and numbers of stations recorded to illustrate the progress of the work and the relatively low number of stations recorded per shot due to the factors mentioned above. Blasts which were entirely missed or recorded with no MSF (timing signal) reception are not included. Only the best record of a station recorded more than once is listed (40% of the stations have more than one record).

Table 2.1 Aberdour Quarry Recording Log

Date	Time	Total Charge	No. of	No. of Stations
	hr min sec	kg	Holes	Recorded
11/5/87	12:35:46.46	2972	17	10
29/5/87	12:51:47.54	3675	21	12
1/7/87	14:43:43.04	3500	38	4
18/8/87	15:00:59.83	1900	21	5
7/10/87	12:34:55.41	797	5	3
30/10/87	12:37:56.19	3575	35	5
26/11/87	12:30:20.15	2150	16	5
19/1/88	12:54:01.24	2250	10	2
17/2/88	12:31:02.50	395	23	1
8/3/88	12:32:55.05	2211	18	6
10/3/88	12:44:39.90	5250	48	4
26/4/88	12:33:56.91	3525	28	3
16/6/88	13:00:53.90	2800	28	3

Table 2.2 Newburgh Quarry Recording Log

Date	Time	Total Charge	No. of	No. of Stations
	hr min sec	kg	Holes	Recorded
18/5/87	12:44:51.74	215	8	6
25/5/87	12:45:23.26	140	5	5
8/6/87	12:44:52.93	130	5	5
13/7/87	12:44:27.81	125	4	6
24/8/87	12:44:19.38	220	8	1
8/9/87	12:44:07.73	232	7	8

Table 2.3 Tillicoultry Quarry Recording Log

Date	Time	Total Charge	No. of	No. of Stations
	hr min sec	kg	Holes	Recorded
29/1/88	15:00:04.58	1250	8	4
1/2/88	15:00:40.95	900	9	6
15/3/88	14:59:46.47	1000	14	8
7/7/88	15:11:21.00	600	50	1

Table 2.4 Collace Quarry Recording Log

Date	Time	Total Charge	No. of	No. of Stations
	hr min sec	kg	Holes	Recorded
29/4/88	14:32:11.49	895	32	10
10/8/88	13:15:56.34	1072	7	10
24/8/88	16:13:53.69	1500	71	4

2.3. Site Locations

Choosing recording sites was a serious problem since parts of the lines were in areas of high cultural noise. There were few rock outcrops, especially south of the Firth of Tay and in the Kincardine-Clackmannan region. Locating rock outcrop was important because, in the majority of the cases, the signal to noise ratio was higher at rock sites, provided seismometers were coupled firmly to the rock and shielded from the wind which is a major source of noise.

High levels of noise in some areas (e.g. the middle section of line 2) were unavoidable. However, the frequency spectra of the noise and seismic events were sufficiently different that band-pass filtering could be successfully applied to these traces.

It was noticed that strong noise sources (e.g. factories, roads, small towns etc.) have greater effect on stations located on the same lithologic unit than those situated on another unit at the same distance from the noise source.

A test was carried out to verify this observation. Six stations were recorded at the northern end of line 1 (Fig. 1.1b) where there are several sources of noise (dairy plants, roadworks etc.). Three stations (30-32) were buried in drift, three (30A-32A) were glued to rock (Devonian lava) at nearly equal distances from the noise sources. The stations recorded Aberdour quarry, about 50 km away. Spectral analysis of both arrays showed nearly the same range of noise frequencies (Fig. 2.1), but in drift, where the noise sources are situated, noise levels were higher relative to signal amplitude. Figure 2.2 shows an unfiltered section of both arrays. A comparison of amplitudes and frequencies indicates clearly that recording at rock sites was of a better quality.

Although these results will have no effect on frequency band-pass filtering, they made it possible to locate events using analogue playbacks where isolating events depends to a great extent on amplitude differences.

A good practice in positioning geophones is to place them away from forests, rivers and, even, individual trees to minimize the "root effect" which creates substantial source of noise. Loose soil reduces markedly detectable seismic energy because the low compaction of soil will cause poor coupling of the seismometers and therefore low transmission of energy. In cultivated fields seismometers should be firmly inserted below the ploughed section of soil in the solid earth thus reducing to a great extent noise caused by continuous movement of small fragments of soil in the geophone hole due to

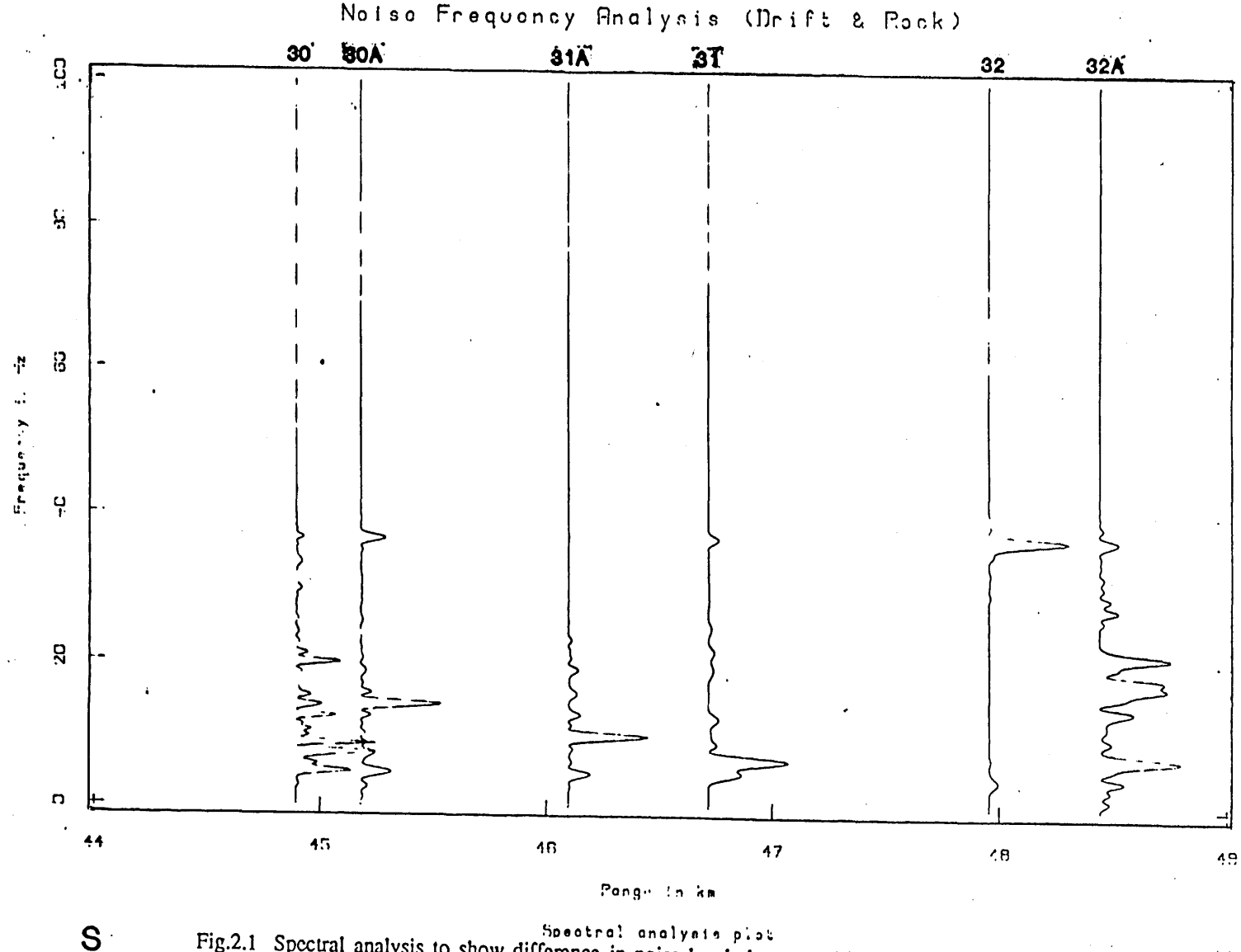

S

Fig.2.1 Spectral analysis to show difference in noise levels between drift and rock sites (subscript **A** = rock site).

N

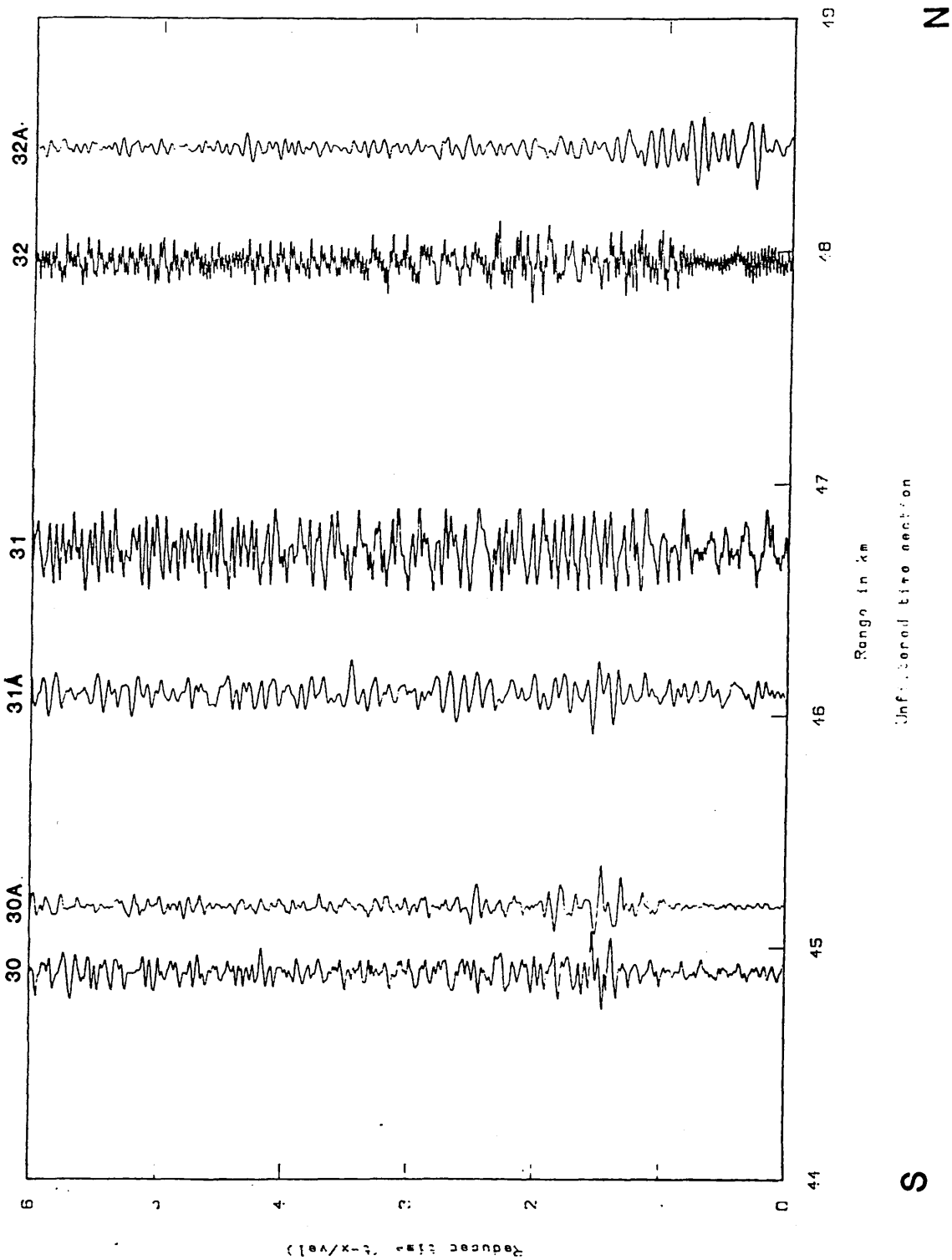

Fig.2.2 Unfiltered section showing difference in signal to noise ratio between drift and rock sites (subscript a = rock site).

improper burial of it and due to rainwater.

Throughout the project station spacing was kept at approximately 1.5 km, but in many cases this distance was highly controlled by the accessibility of sites and locations of noise sources. In some cases stations had to be shifted to either side of the line up to a maximum of 1 km. Along line 2 stations 23 and 24 were not recorded at all because the only accessible road passes through a farm whose owner does not like suspiciously looking geophysicists!

2.4. Gains

Gain setting is a very important factor in determining the amplitudes of data and the range to which it could be recorded. Gain must be high enough to adequately record events at a station at a given distance from a shot of given size, but must be low enough to prevent saturation of the recording system by noise and/or the event. The main factors controlling the gain value at a station in order of importance are:

[1] Weather, especially wind.

[2] Permanent sources e.g. factories, main roads and towns.

[3] Tractors working in the fields especially during spring and summer when quarries work at their maximum capability thus limiting the use of this productive period.

[4] Time of the blast and location of the site. Lower gains should be used at stations near towns if the blasting time is around mid-day when cultural noise increases. High gains can be used on rainy days when movement of people and vehicles is less.

[5] Orientation of the quarry face being removed. High gains should be used if the face being removed is at low angles or facing the direction of the stations being recorded. Lower gains can be used if the face being removed is at right angle to the profile or facing away from it. This is because much of the energy of a blast directed toward a quarry face is consumed in fracturing and moving rock outward. In other directions these processes cause little energy loss, permitting detection of head waves to further distance, with higher signal/noise ratio at a given offset.

A good example of the importance of gain in detecting seismic energy and its relation to the local noise levels is the recording of Collace quarry in the southern part of line 1. Although recording conditions were ideal regarding the charge size, the number of holes, quarry face being removed and weather

conditions, it was impossible to record data along this section (see Fig. 1.1a for locations) due to the high noise levels causing low gains of 2-3 to be used (see Table 2.5) compared to the relatively far distance of the quarry (more than 30 km). In two cases where stations were remote from the noise source (stations 4 and 5), good recording quality was obtained using the same gains as those of stations which were not recorded but much closer to the quarry (stations 6, 7, 9 and 10). The effective factor in this case was that the weak seismic energy was not swamped by the local noise.

During the course of this project several sets of recordings were lost because quarries reduced the charge size substantially on the day of the blast, thus insufficient gains were used and no data were recorded. However this helped in formulating an empirical rule for gain settings (see Table 2.5) which was successfully used and was responsible for much of the good data acquired. The gain scale of the recorders and Table 2.5 is divided into 6 readings corresponding to a range of 88-118 dB i. e. 6 dB per interval.

Table 2.5 Optimum gain values used for an instantaneous charge of 90-150 kg.

Distance in km	Gain
0-5	1
6-10	1-2
11-16	2-3
17-30	3-4
>30	4-6

Quarries divide the total amount of explosive over a large number of holes (typically 21-48) with delays of 17 or 25 ms between each successive charge. Often the holes are arranged in two rows located 4-6 m from the face being blasted and fired in sequence of two holes per delay. So the effective charge for seismic purposes will be the first pair blasted with zero delay which is usually 90-150 kg. Sometimes the holes are arranged in only one row (usually 11-28 holes) and fired with one delay/hole. In both cases the remaining charges will be dissipated as a wave-train of energy causing constructive

and destructive interference. The most effective portion of the total charge on the signal amplitude will be the size of charge fired in the first hole (or group of holes) at zero delay.

Quarries which use small charges (100-500 kg) are inadequate for deep seismic investigations because usually the charge is divided over 10-15 holes with a delay between each hole. This is an average instantaneous charge of 10-40 kg which can be detected to only about 20 km range in ideal conditions and using maximum gains. A quarry of this type (Newburgh) was used to record line 4 and the in-line section of line 1 (see section 2.2). The maximum range reached in this case was approximately 18 km.

Blasts of 2.0-3.5 tonnes divided into 21-35 holes have an instantaneous charge of approximately 100-150 kg. Using the gain settings of Table 2.5 arrivals at a distance of about 51 km along line 1 were received. The furthest seismometers were buried in drift and if rock sites were available further ranges could have been achieved. Comparing gains in Table 2.5 with those suggested by Dentith (1987) it can be shown that higher gains can be used for the same distances provided that noise levels are the same as in the MAVIS project. Davidson (1985) obtained data at 80 km range using Hillhouse quarry but the total charge was 8 tonne divided between 21 holes, that is, an instantaneous charge of 350-400 kg. No instantaneous charge of more than 150 kg was used by quarries throughout this project.

However, from field data obtained during this work and data from one shot obtained by Davidson (1985) a general relationship between total charge used by quarries and maximum ranges of head-waves has been derived. Figure 2.3 suggests this relationship is linear, provided that a low number of holes (i.e high instantaneous charge) is used. This does not imply that arrivals could not be detected at further distances, but significantly high signal to noise ratio is needed to obtain useable data taking into account the wide range of noise spectra typical of heavily populated areas.

The depth at which charges are blasted is another significant factor in determining the range to which head waves can travel. Quarries usually drill holes to depth of 15-30 m to ensure that sufficient energy will be transmitted through the ground. On several occasions holes were drilled to only 3-7 m at Tillicoultry quarry and, although the instantaneous charge was more than 60 kg in two cases, head waves were not received beyond 5 km from the quarry. In this case all the energy was used to remove the overburden i.e. in an upward direction and no significant energy was transmitted downward.

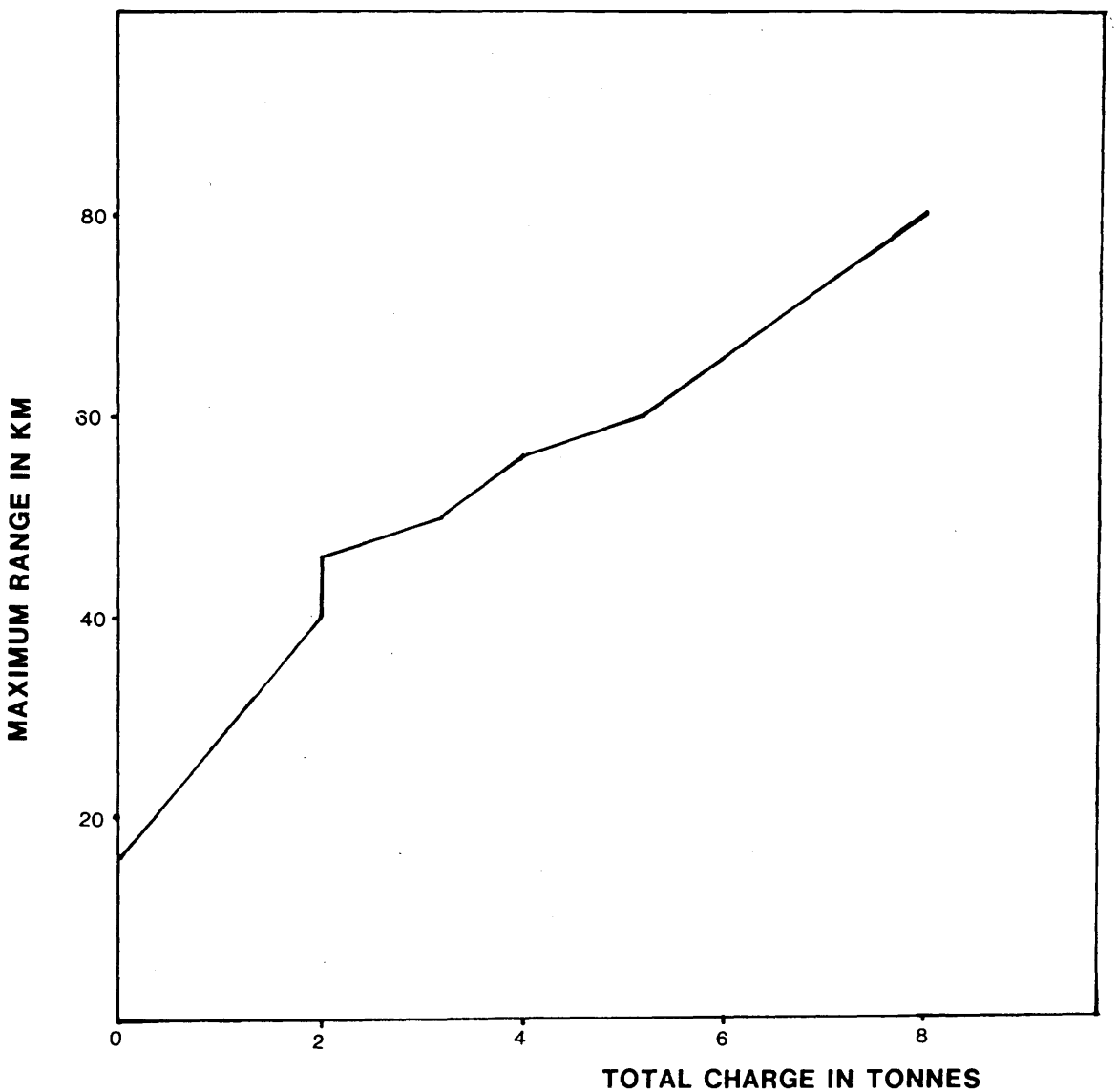

Fig.2.3 Range-charge relationship plot.

Finally it was noticed that at ranges between 35km and 50km, increasing the gain at relatively noisy sites is ineffective as the signal is lost in the noise thus keeping the gains as low as possible at such sites to prevent overloading is recommended. Also in setting the gain a deflection of the amplifier-modulator meter of 20-30% of the full scale is acceptable and even a deflection of 40% could be refined by the deployment of the appropriate filters especially if the noise has constant frequency and amplitude.

2.5. Field Recording Equipment

A vertical 4.5 Hz L15B Mark geophone was used to detect seismic energy. The Glasgow FM "Mark 2" recorder was used to record these data throughout this project. The 50 sets were developed from prototypes designed in 1981 by Dr J. Hall and Mr G. Gordon in the Department of Geology, Glasgow University. The recorders (Fig. 2.4) are based on a standard cassette deck amended to permit simultaneous recording on all four tracks. Therefore the C120 cassette tapes used allow an one hour recording window. Seismic data are pre-amplified and then passed through a band-pass filter of 1.5-60 Hz from which it is passed through an integral amplifier/modulator and recorded on two channels. The first channel covers a gain range of 88-118 dB with selectable 6 dB intervals while the second is fixed at 18 dB down from the selected high gain channel.

The MSF time signal, broadcast from Rugby with 60 KHz frequency, is detected by a tuned radio receiver and is recorded on the third channel. The fourth channel is an auxiliary channel and was not used in this project. The recorders have a remote-start facility and electronic clock allowing deployment up to 24 hours in advance. Recorder geophone specifications are given in Appendix 1.

2.6. Playback and Digitization System

Initially recordings were replayed using an analogue playback facility which comprised a cassette deck mechanism with the tape head wired for replay only. Each seismic channel is then passed through a demodulator and analogue filters which proved to be of great use in refining noisy traces. These filters were usually set to pass frequencies between 3 and 40 Hz, but in traces where noise level is high but of constant frequency the bandpass filter was reduced to 3-21 Hz giving excellent results.

The output of each channel is then amplified and passed to a Bryans 40000 UV oscillograph which has two useful facilities. The first is the ability to adjust the paper speed thus allowing the

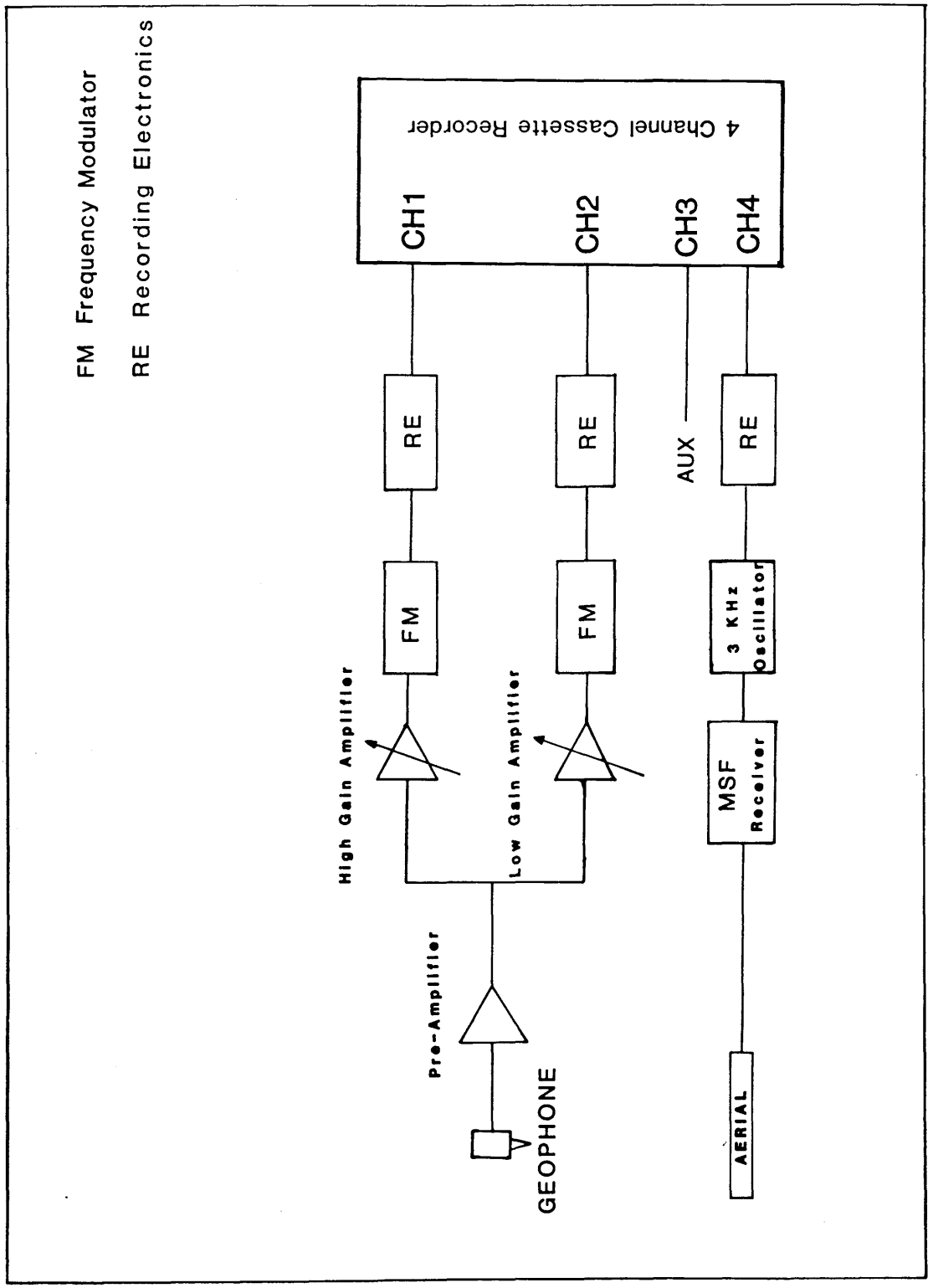

Fig.2.4 Block diagram showing the recording arrangement.

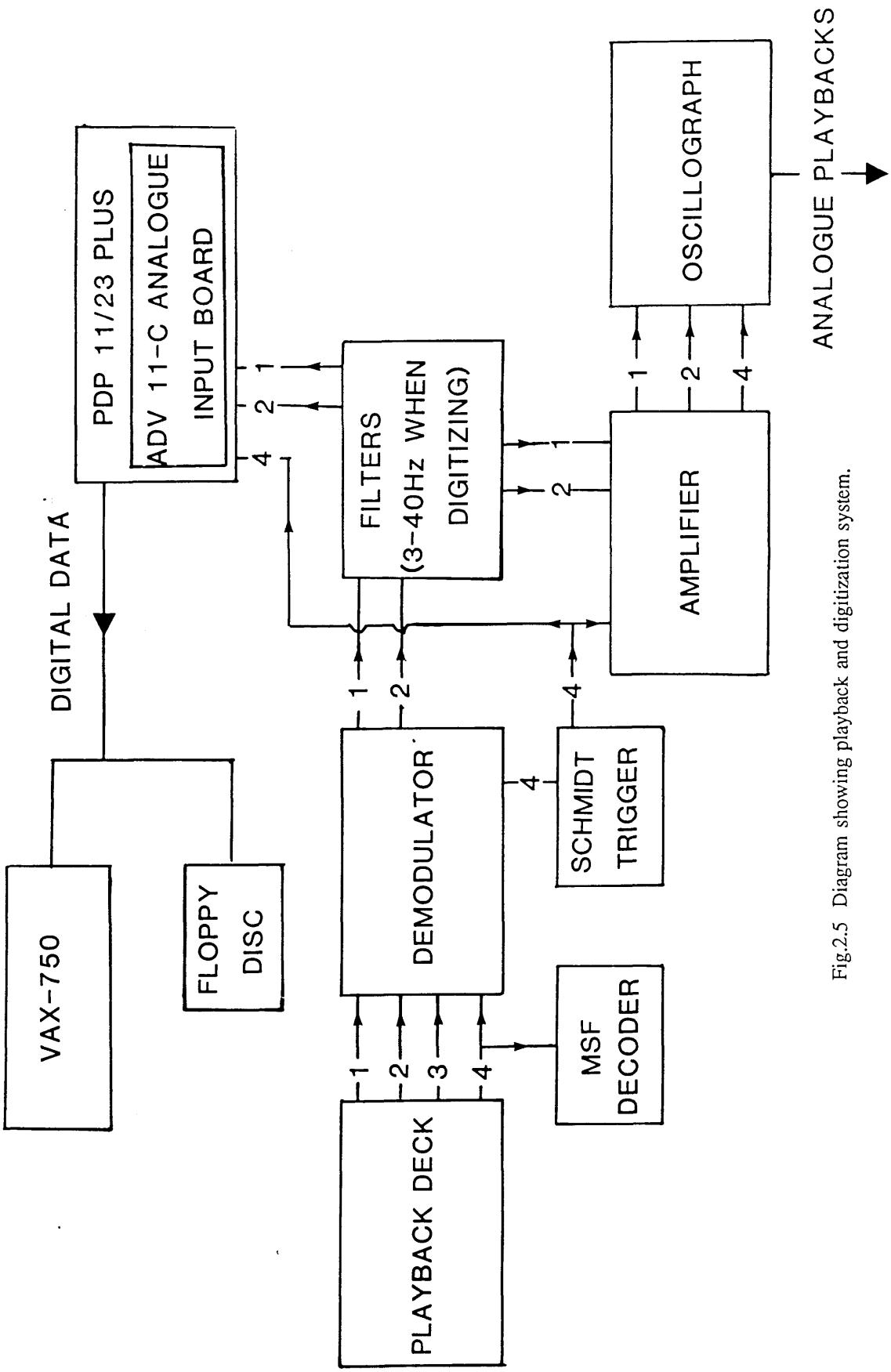

Fig.2.5 Diagram showing playback and digitization system.

separation of the first arrivals from other arrivals (if there is a reasonable frequency and amplitude difference) and the expansion of the onsets over longer time periods permitting onsets to be identified. The second facility is the ability to adjust the amplifier gains allowing weak onset to be magnified.

The MSF channel is also demodulated but passed directly to the oscillograph via an amplifier. A Schmidt trigger is used to enhance the MSF signal to give it a box shape on the analogue playback for easy time correlation. The signal is finally passed to a decoder which displays the time in days, hours, minutes and seconds, allowing quick discovery of the approximate position on the tape of an event. Figure 2.5 summarises the stages involved in producing analogue traces and digitization.

Analogue-to-digital conversion is the technique by which the amplitude of a waveform is expressed in numbers at a specific values of time. The Programmable Data Processor (PDP) 11/23 PLUS microcomputer was used for converting analogue data to digital form. The software was programmed by R.T. Cumberland. The data are passed from the playback system through anti-aliasing analogue filters (3-40 Hz). An ADV11-C analogue-digital conversion board was used which can accept up to sixteen single ended bipolar inputs or 8 differential inputs, either unipolar or bipolar. Data sampling was set at 200 samples/second but varies with recording tape speed.

For traces at less than 20 km offset digitization is carried out for 10 seconds from just prior to the start of event and for traces at 20-60 km range digitization is applied for 15 seconds, thus securing digitization of all useful data. Program MSFPLOT, written by R. Reid, was then used to relate the start of the digitized file to the shot instant for further digital processing and display purposes.

2.7. Summary

This chapter has outlined the data acquisition techniques used in this project, and discussed some of the problems involved. Throughout the project the Glasgow FM system proved to be a reliable way of recording seismic data. Most failures were due to poor reception of MSF signals because of bad transmission from the Rugby station. Only 10% of the failures were due to the sets (e.g. remote start not activated). Although noise limited the range to which onsets could be detected, noise levels were moderate except for certain locations (e.g. the area between Loch Leven and the Firth of Forth and the middle part of line 2 in the Clackmannan region), but with careful choice of locations, gains and filters this problem was overcome. The recorded data quality was good.

CHAPTER THREE - DATA PROCESSING AND INTERPRETATION METHODS

3.1. Introduction

All aspects of data processing and interpretation used in this study are discussed in this chapter. The criteria on which calculation of errors in arrival times are based will be presented. Data quality was good, but bandpass filtering was needed to improve some traces. Spectral analysis gave good estimation of signal and noise peaks in the area which were later utilized in frequency filtering. The principles of frequency analysis and how frequency filtering is applied to the data will be described. A full discussion of the theoretical background associated with the different interpretational methods used in this work from the basic planar layer and the plus-minus methods to the more sophisticated procedures like ray-tracing will be introduced. Finally, the statistical method by which different velocity segments are plotted on the time-distance graphs will be summarised.

3.2. Errors Associated With Arrival Times

A standard error of +/- 0.03 s was calculated for the travel times at all stations. The main components of this error are:

[1] Location errors: Shot positions within a quarry are uncertain due to the movement of the quarry face, which is not updated on Ordnance Survey maps which are used to locate all shots and receivers. The error in locating the exact position of the shot was estimated to be +/- 40 m. The error in locating the position of a receiver was estimated to be +/- 10 m. This will give a total error of +/- 0.01 s assuming an average surface velocity of 5 km/s along the profile.

[2] Onsets on analogue playback records can be read to an accuracy of only +/- 0.01 s. This is due to errors in locating the onset arrivals (especially on noisy traces) and difference in the speed of the playback system when producing analogue output for onset picking which causes a difference in spacing between M.S.F seconds pulses.

[3] Shifts caused by the playback filters giving an estimated error of 0.01 s. This error effects all the traces in the same amount. Therefore it is not included in the calculations and it is mentioned here only for illustration.

[4] When recording shots at the quarry the recorders are usually placed 20 m from the actual position

of the charge. Assuming that the surface velocity at the quarry is 3.00 km/s, this will give a small correction of 0.007 s. This will vary subject to the actual surface velocity.

3.3. Frequency Analysis and Filtering

Program PLOT, written by R. Reid and K. Davidson, was used to process the data. It is designed to handle digital seismic data, either to simply process the data for display, or to undertake spectral analysis, or to frequency filter data based on parameters obtained in the frequency filter design program FWFIR. Graphics were then obtained using the UNIX 'S' plotting package. All the data of this project were processed by these programs.

Spectral analysis for all the lines was carried out to find the dominant frequencies for both first arrivals and noise, thus permitting accurate filtering of the data for onset detection.

The windowing function in program PLOT was used to apply spectral analysis on any desired length of the traces and therefore two windows were chosen to determine the noise and signal frequency spectra. The first window covers the time before the first arrival to give the noise spectrum and the second window was designed to cover 0.5 s after the first window thus giving the onset frequency spectrum. The dominant P-wave frequency range in the area was found to be 8-21 Hz which was used as a guide for filtering purposes. A full discussion of the implications of frequency analysis will be presented in section 4.3 .

Seismic traces are a mixture of signal and noise with frequencies occupying a wide spectrum. They are non-periodic functions, but for the purpose of their analysis they can be treated as periodic waveforms with an infinitely long period. They can be expressed either in the time domain (i.e their amplitude as a function of time) or in the frequency domain (i.e by the amplitude and phase of a finite number of sine waves).

Filters are divided into two main categories: frequency filters and optimum filters. A frequency filter discriminates against predefined unwanted frequencies. It is designed on an arbitrary basis without direct reference to the signal or noise, and without reference to the actual effectiveness of the filter. The optimum filter is designed on the basis of the character of the waveform or on the basis of the actual input and desired output signal (Wiener filtering). Digital processing of seismic data has been described by many authors (e.g. Robinson & Treitel 1964, 1980; Hatton et al. 1986).

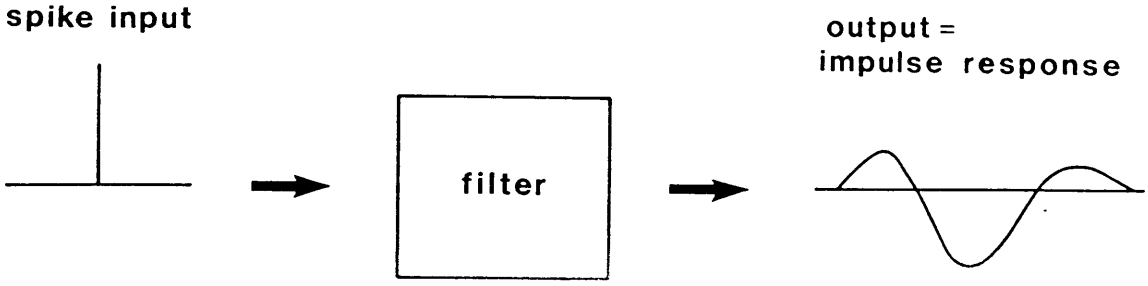

Fig.3.1 The impulse response of a filter (after Kearey & Brooks 1984).

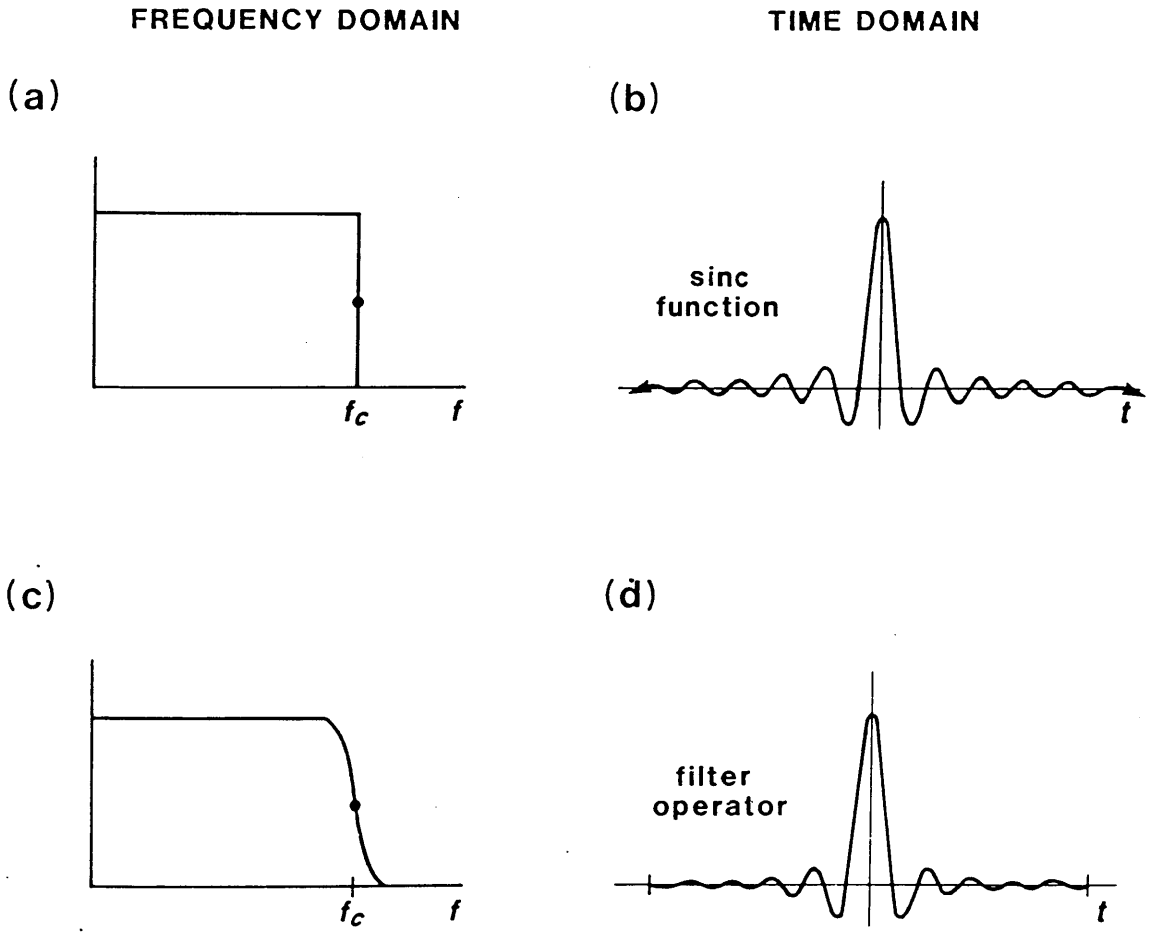

Fig.3.2 Design of a low-pass filter (after Kearey & Brooks 1984).

The main effect of a filter is defined by its impulse response which is the output of the filter when a spike function is input (Fig. 3.1) and is sometimes called the operator. It is the impulse response which is mathematically convolved with the input signal to give the filtered trace.

In order to carry out frequency filtering Fourier transformation is used to convert the signal from the time domain to the frequency domain and vice versa. This is done by converting a time function, g(t), into its amplitude, A(f), and phase spectra, θ(f), or into the frequency spectrum G(f) such that

$$G(f) = A(f)e^{i\theta(f)} \tag{3.1}$$

g(t) and G(f), the time and frequency domain representation of the waveform, are known as a Fourier pair and are interchangeable.

Digital frequency filtering was used in processing the data according to the results obtained from frequency analysis. Program FWFIR provides several options of filters to be used and these are low-pass, high-pass, band-pass and band-stop filters with rectangular, triangular, Hamming, generalized Hamming, Hanning, Kaiser(10-sinh) and Chebyshev windows. They may be of minimum or zero phase and of variable length. This program produces the coefficients of the desired filter, which are stored for use by the filter option in program PLOT.

To design a filter, a transfer function is specified in the frequency domain which is then used to design an impulse response of finite length in the time domain. To illustrate this consider a low-pass filter whose cut-off frequency is fc. The ideal output of the filter is represented by the amplitude spectrum shown in Figure 3.2a. Frequencies greater than fc have zero amplitude and below fc have constant unit amplitude. This is the transfer function of the ideal low-pass filter which is then converted into the time domain by Fourier transformation giving the impulse response shown in Figure 3.2b. This filter will only pass frequencies between 0 and fc.

The impulse response of this filter is a sinc function and therefore it is infinitely long and must be truncated to produce a realisable filter operator (Fig. 3.2c). This operator when convolved with an input waveform will result in gradual cut-off low-pass filtering (Fig. 3.2d). Several window functions are used to control the truncation of the operator. The Hamming window consists of one cycle of a cosine wave with its trough raised slightly greater than zero. This window is then multiplied by the infinitely long operator to produce an operator of specific length and amplitude spectrum.

A band-pass filter may be thought of as a set of cosine waves of equal amplitude which are in phase and which are restricted to frequencies within the frequency band that is to be passed. The output of the filter process will only contain cosine waves that are common to both the input trace and the filter. Filters are not ideal. They cannot reject everything below and above the pass band desired. There is a ramp-off of the pass band at both ends, so increasing the rate of cut off frequencies will decrease the side lobe levels at the expense of a softer reject slope.

Despite the fact that zero phase filters result in a phase shift in the time domain of half the filter length used, they were used because of their memory and ability to anticipate future waveforms thus resulting in more of the data being affected during each convolution operation. In contrast minimum phase filters cause no phase shift but can operate only on the present and past of the waveform thus less data being convolved.

From results obtained by Dentith (1987) and tests carried out through this work a combination of filter type and length (using the Hamming window) was applied to process the data. As expected noise and signal frequency spectra partially overlap in many sections of the profiles. Tests to determine the best filter were undertaken and a band-pass filter of 10-25 Hz was applied to all the data (see section 4.3). The impulse and frequency response of the 10-25 Hz band-pass filter used is shown in Figure 3.3. Altering the high-cut frequency by +/- 5 Hz did not improve the signal while changing the low-cut frequency by the same amount distorted the signal, indicating that signal and noise co-exist at these frequencies which prevented the use of high-pass filter with a low cut of 5 Hz because of signal attenuation.

Both signal and noise frequencies have different spectra but in many locations they coexist at a frequency range of 4-8 Hz which made it necessary to use a sharp cut-off window. The Hamming window with its comparatively sharp cut-off frequency response was chosen, enabling better discrimination against noise frequencies. However apart from the rectangular window (which has gradual cut-off frequency response), all the other windows have broadly similar effects. The filters used were quite adequate, though in general the good quality of the data acquired meant that their usage did not result in improvement of the data, except for a few stations.

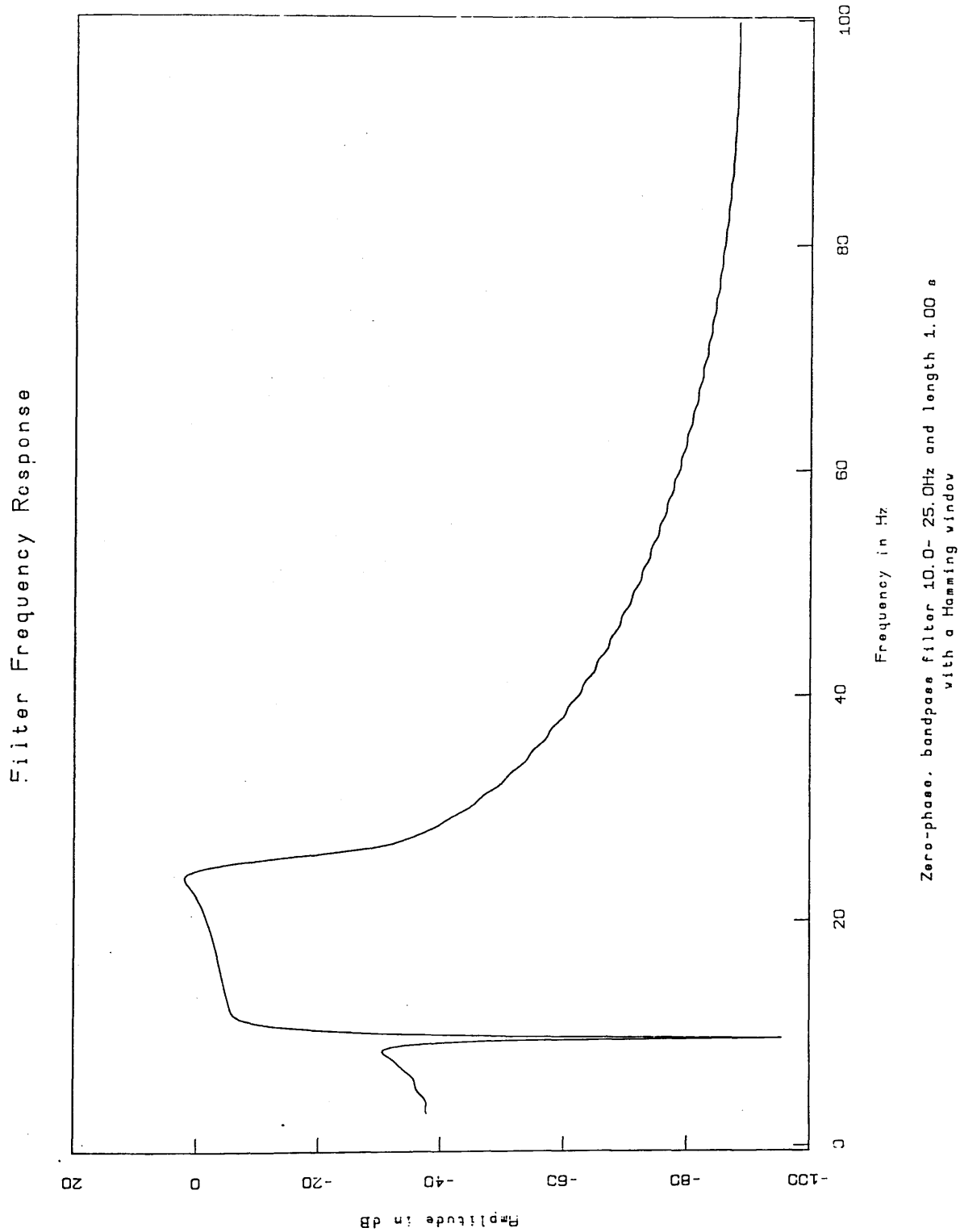

Fig.3.3a Frequency response of a band-pass filter (10 - 25 Hz) with a Hamming window.

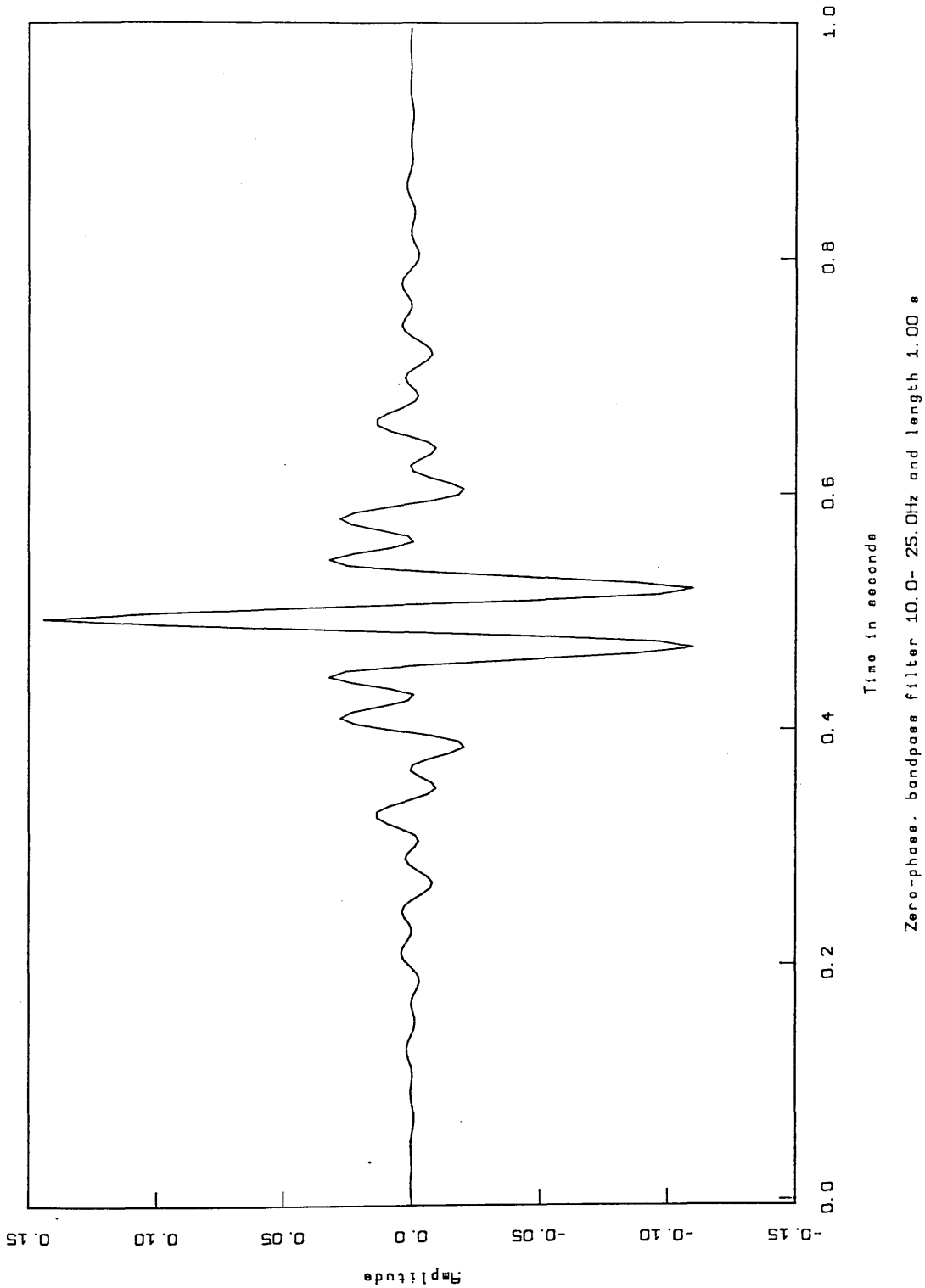

Fig.3.3b Impulse response of a band-pass filter (10-25 Hz) with a Hamming window.

3.4. Interpretation Methods

3.4.1. Principles of the Refraction Method

The principles of refraction are discussed in detail by, for example, Dobrin (1960) and Kearey & Brooks (1984). Consider a seismic ray incident on an interface between two layers of different velocity. The transmitted ray will obey Snell's Law and will be refracted according to the following equation:

$$\frac{\sin i}{\sin r} = \frac{V1}{V2} \tag{3.2}$$

where

i = angle of incidence relative to the normal

r = angle of transmission relative to the normal

V1= velocity in the first layer

V2= velocity in the second layer

Figure 3.4 shows an ideal case of the raypaths refracted at a horizontal interface and travelling through layers of constant velocity. The direct ray travels horizontally through layer 1 at a velocity V1. The resulting travel-time curve is a straight line of slope 1/V1 and zero intercept. The angle θ is such that the ray AB is critically refracted, i. e. the ray is refracted so that it is transmitted along the interface between the two layers. Therefore, sin r is equal to 1. Consider the path of the ray ABCD critically refracted at the interface between layers 1 and 2. The travel time, T(AD), along this path is

$$T(AD) = T(AB) + T(BC) + T(CD) \tag{3.3}$$

$$= \frac{Z1}{V1\cos\theta} + \frac{X - 2Z1\tan\theta}{V2} + \frac{Z}{V1\cos\theta} \tag{3.4}$$

since $\sin r = 90^{o}$

$$\sin\theta = \frac{V1}{V2} \ (snell's\ Law) \tag{3.5}$$

$$\cos\theta = \left[1 - \frac{V1^2}{V2^2}\right]^{1/2} \tag{3.6}$$

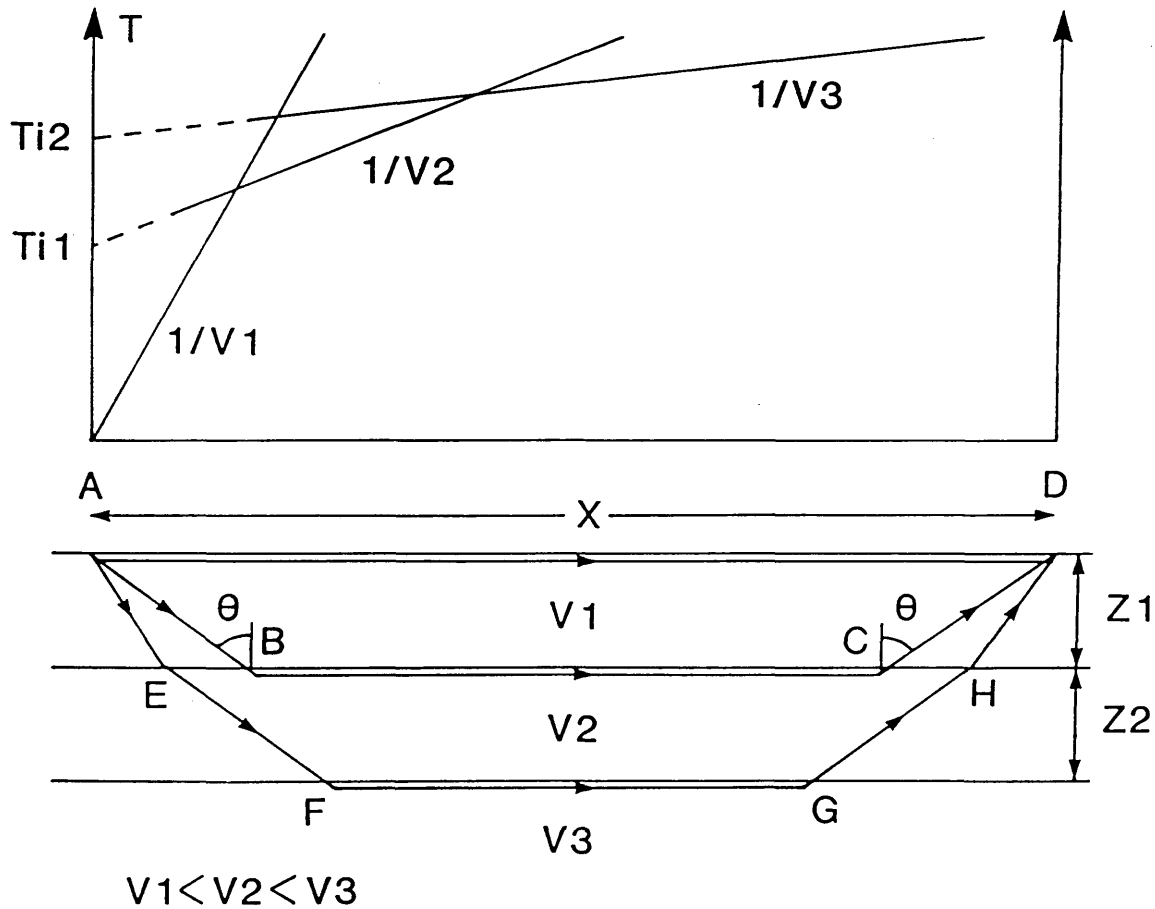

Fig.3.4 Principles of the refraction method.

equation 3.4 may be rewritten as

$$T(AD) = \frac{X}{V2} + \frac{2Z\ (V2^2 - V1^2)^{½}}{V1\ V2} \tag{3.7}$$

From the time-distance plot the intercept time (Ti1) on the time axis is given by

$$Ti1 = \frac{2Z\ (V2^2 - V1^2)^{½}}{V1\ V2} \tag{3.8}$$

and therefore

$$Z1 = \frac{Ti1\ V1\ V2}{2\ (V2^2 - V1^2)^{½}} \tag{3.9}$$

Thus, the depth to layer 2 can be determined by the use of the intercept time if V1 and V2 are known. Similarly depth to layer 3 can also be determined if V3 is known.

$$Z2 = 0.5 \left[Ti2 - 2\ Z1\ \frac{(V3^2 - V1^2)^{½}}{V3\ V1} \right] \frac{V3\ V2}{(V3^2 - V2^2)^{½}} \tag{3.10}$$

In reality refractors cannot be treated as perfectly horizontal or planar, so the time-distance plot does not give the true refractor velocity but another quantity called apparent velocity which is a function of the true velocity of the refracting layer and its structure along the recording profile recording.

In the presence of dipping refractors reverse shooting becomes essential to determine the dip of the refractor along the profile. The gradients and intercept times for the forward and reverse curves are different (Fig. 3.5). Derivations of the equations for the dipping interface are given in Dobrin (1960) and Kearey & Brooks (1984). Only the main equations will be presented here.

The angle of dip can be determined by the relation

$$\alpha = \frac{1}{2}(\sin^{-1}V_1 m_d - \sin^{-1}V_1 m_u) \tag{3.11}$$

where

α = *refractor dip along the profile*
m_d = *slope of the downdip segment*
m_u = *slope of the updip segment*

The perpendicular distance Zu in an updip direction to the interface can be calculated from the intercept time, Tiu.

$$Tiu = \frac{2Zu\cos i_c}{V_0} \tag{3.12}$$

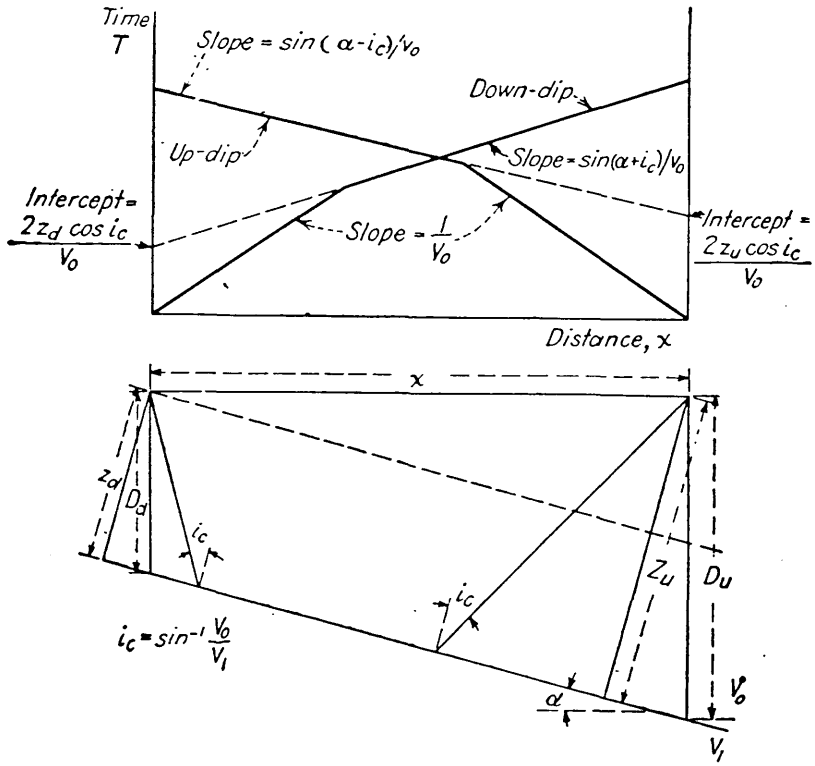

Fig.3.5 Refraction at a dipping interface (after Dobrin 1960).

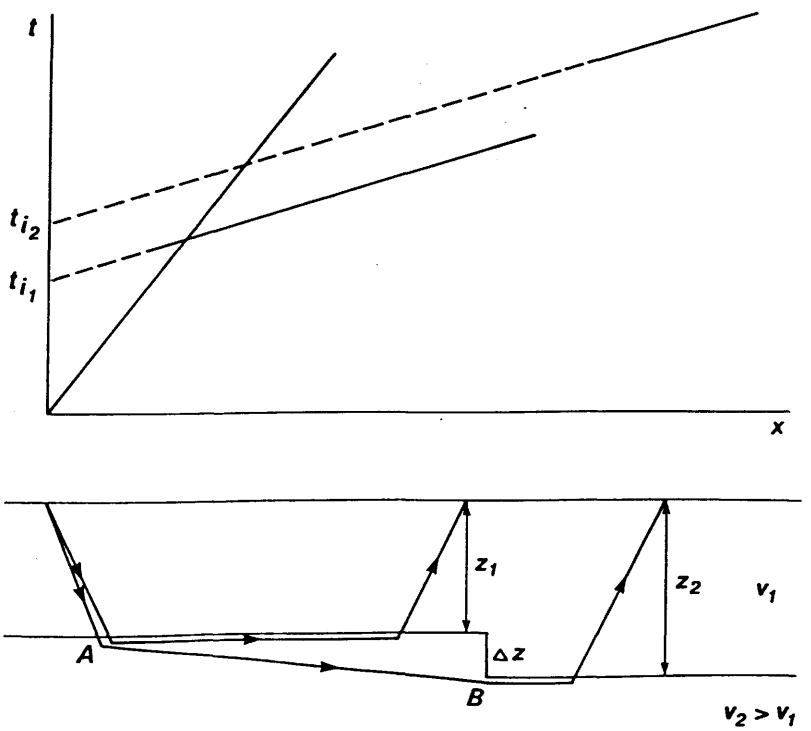

Fig.3.6 Effect of a fault on refracted rays (after Kearey & Brooks 1984).

therefore

$$Zu = \frac{V_0 Tiu}{2\cos i_c} \tag{3.13}$$

i_c = *the angle which the incident ray makes with normal*

The perpendicular distance Zd in the downdip direction can be derived in a similar way.

The actual depth Du at the up dip direction shot is

$$Du = \frac{Zu}{\cos\alpha} \tag{3.14}$$

and at the down dip shot point:

$$Dd = \frac{Zd}{\cos\alpha} \tag{3.15}$$

Faults may offset the refractor arrival velocity segments of the travel-time curve observed from opposite sides of the fault (Fig. 3.6). Therefore two intercept times will be present Ti1 and Ti2. The difference between them will be the measure of the throw of the fault. The equation for determining the throw of the fault is

$$\delta Z = \frac{\delta T V1 V2}{(V2^2 - V1^2)^{1/2}} \tag{3.16}$$

where

δZ *is the throw of the fault*

δT *is the difference between the time intercepts*

The above equations are valid only if the fault throw is much less than the depth to the refractor.

3.4.2. Plus-Minus Method

The assumption of planar refracting interfaces would often lead to unacceptable imprecision in the interpretation of refraction data. Hagedoorn (1959) introduced the plus - minus method which is based on the calculation for each receiver of a "plus time", analogous to an intercept time, for conversion to refractor depth and a "minus time" for the estimation of refractor velocity. Dips of refractor topography are assumed to be less than 5 degrees and reversed coverage is essential for the application of this method. Figure 3.7 illustrates the geometry of an undulatory refractor where the plus time is the

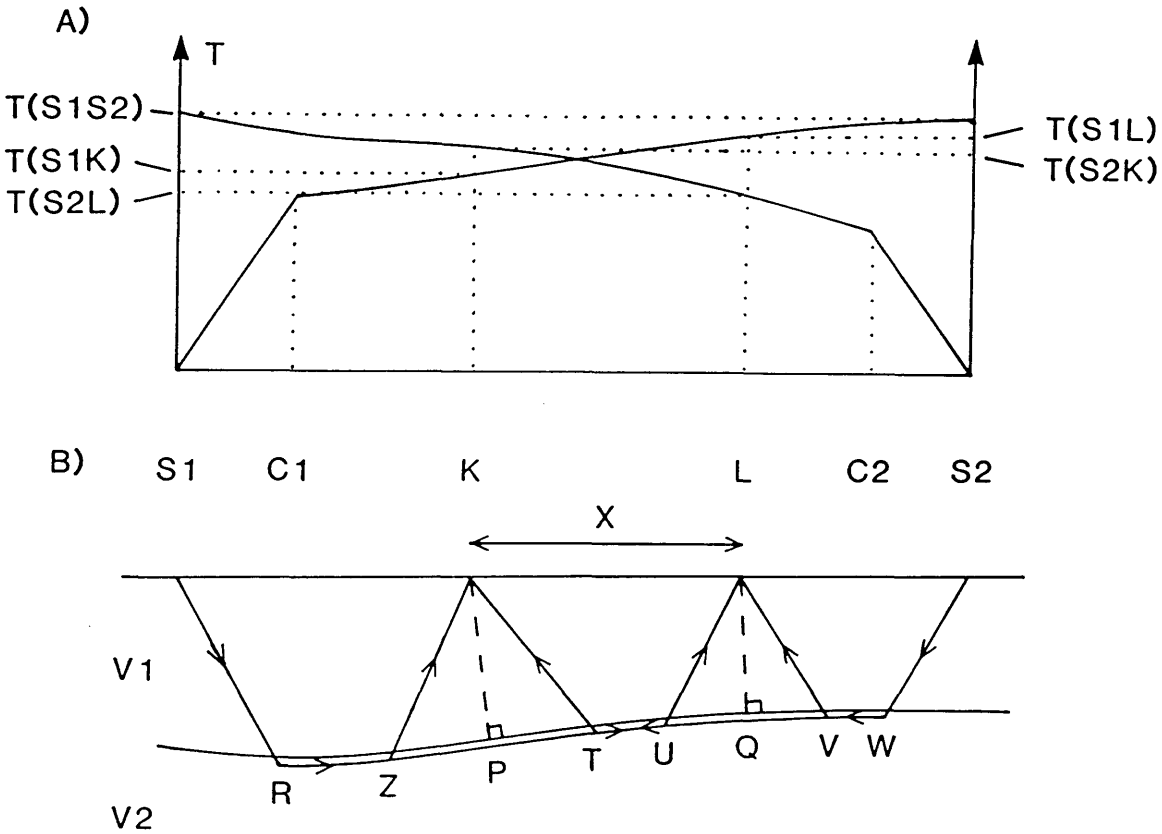

Fig.3.7 The plus-minus method of refraction interpretation; A), travel-time curves B), ray-paths from end shots (S1, S2) to intermediate receivers (K, L). (after Dentith 1987).

sum of the travel-times to a receiver from the two sources, S1 and S2 (T(S1S2)). For a receiver K

$$Tplus(K) = T(S1K) + T(S2K) - T(S1S2) \tag{3.17}$$

$$= (T(S1R) + T(RZ) + T(ZK)) + (T(S2W) + T(WT) + T(TK)) - (T(S1R) + T(RW) + T(S2W)) \tag{3.18}$$

$$= T(ZK) + T(TK) + T(RK) + T(WT) - T(RW) \tag{3.19}$$

$$= T(ZK) + T(TK) - T(ZT) \tag{3.20}$$

This is the same as the intercept time (Tint) for a shot fired at K. Therefore the refractor depth below K, Z(K), is given by

$$Z(K) = \frac{Tplus(K)\ V2\ V1}{2\ (V2^2 - V1^2)^{1/2}} \tag{3.21}$$

The minus time is defined as the difference in travel-times between arrivals from sources S1 and S2 arriving at a receiver K. V2 is obtained from the minus times.

$$Tminus(K) = T(S1K) - T(S2K) \tag{3.22}$$

$$= (T(S1R) + T(RZ) + T(ZK)) - (T(S2W) + T(WT) + T(TK)) \tag{3.23}$$

Since refractor relief is assumed to be negligible between Z and T

$$\angle KPZ = \angle KPT = 90^\circ$$

$$KZ = KT$$

therefore

$$Tminus(K) = (T(S1R) + T(RZ)) - (T(S2W) + T(WT)) \tag{3.24}$$

similarly

$$Tminus(L) = (T(S1R) + T(RU)) - (T(S2W) + T(WV)) \tag{3.25}$$

A straight line is obtained when plotting the minus time against the receiver position with a gradient equal to half the refractor velocity.

$$Gradient = \frac{X}{Tminus(L) - Tminus(K)} \tag{3.26}$$

$$= \frac{X}{T(S1R)+T(RU)-T(S2W)-T(WV)-T(S1R)-T(RZ)+T(S2W)+T(WT)} \tag{3.27}$$

$$= \frac{X}{T(RU) - T(WV) - T(RZ) + T(WT)} \tag{3.28}$$

$$= \frac{X}{T(ZU) + T(VT)} \tag{3.29}$$

For low relief $ZU = VT = KL = X$

and therefore

$$T(ZU) + T(VT) = \frac{2X}{V2} \tag{3.30}$$

and hence the gradient of a minus time graph can be expressed as

$$Gradient = \frac{V2}{2} \tag{3.31}$$

3.4.3. The Wiechert-Herglotz-Bateman (WHB) Method

Davidson (1986) and Dentith (1987) noticed that in the Midland Valley the first segment of the time-distance graphs (corresponding to the direct waves from the first layer) are always curved, indicating rapid increase of apparent velocity with range due to vertical and lateral variation of velocity. This was also the case in the present work, thus the data were suitable for inversion to a velocity-depth model using a solution to the WHB integral (e.g. Grant & West 1965).

$$Z(V) = \frac{1}{\pi} \int_{x=0}^{x=X} \cosh^{-1}(V\ dt/dx)\ dx \tag{3.32}$$

where

$V = (dx/dt)_{x=X}$

This represents the velocity V, at a depth Z, Z being the turning point of a ray arriving at the surface at a range X from the source. The method assumes that velocity always increases downwards without lateral velocity variation.

3.4.4. Tau-P Method

Diebold & Stoffa (1981) suggested that travel time can be represented by the horizontal (p) and vertical (q) components of wave slowness.

$$\Delta T = p\Delta X + q\Delta Z \tag{3.33}$$

where

$$p = \frac{\sin i}{V} \quad \text{and} \quad q = \frac{\cos i}{V}$$

V = velocity of medium

i = direction of ray path relative to the vertical.

Wave slowness, u, is given by

$$u = \frac{1}{V} = (p^2 + q^2)^{1/2} \tag{3.34}$$

For a series of horizontal homogeneous layers a refracted ray has travel time

$$T = pX + 2 \sum_{j=1}^{n} qj \; Zj \tag{3.35}$$

(Note that as p is a constant for horizontal layers only the single term px is required).

The above equation defines a straight line tangential to the time-distance curve at the point (T, X) with a gradient p and an intercept on the time axis of tau. Thus the time-distance curve is represented by a series of straight lines which are inverted to velocity-depth data using the solution to the planar layer equations for intercept time from which depth is calculated.

When the source-receiver offset is small, u1 (the slowness in the topmost layer) can be taken as equal to p1 and hence

$$u1 = \frac{1}{Vapp\,1} \tag{3.36}$$

Assuming a series of planar layers

$$Z1 = \frac{\gamma\,(p2)/2}{(u1^2 - p1^2)^{1/2}} \tag{3.37}$$

where γ = time intercept

allowing for use of the expression

$$Zk = \frac{\gamma\,(pk+1)/2 - \sum_{j=1}^{k-1} Zj\;(uj^2 - pk{+}1^2)^{1/2}}{(uk^2 - pk{+}1^2)^{1/2}} \tag{3.38}$$

for inversion of the tau-p data to the velocity depth plane

3.4.5. Raytracing Method

The Midland Valley is characterized by its geological complexity which involves substantial vertical and lateral variation of lithology with a consequently complex seismic velocity distribution. In such circumstances the velocities and depths determined by the above methods, which contain simplifying assumptions, are of limited value. A more sophisticated method for modelling is necessary. The raytracing method traces rays through two-dimensional laterally inhomogeneous media and can handle curved interfaces, block structure, vanishing layers and isolated bodies. This proved to be an adequate interpretive method for modelling the data.

The SEIS83 raytracing package is a slightly modified version of the SEIS81 (Cerveny & Psencik 1981) and consists of the raytracing program SEIS83, the program RAYPLOT to plot the rays, and the programs SYNTPL and SEISPL which, respectively, calculate and plot synthetic seismograms based on the output of SEIS83. The program is a two-point raytracing program which uses the "modified shooting" method of initiating a ray where a ray-path is defined and travel times computed from the source to a specified receiver geometry with rays leaving the source between predetermined angles. The dynamic raytracing system is used to determine the geometrical spreading of the generated rays by solving a system of two linear ordinary differential equations by a modified Euler's method.

Raytracing is an iterative process, where a trial ray is generated and is traced through the model back to the surface. When successive rays terminate at the surface on either side of a receiver, the difference between the positions of the ray termination at the surface and the intended receiver point is calculated and a new initial ray angle chosen. This process is repeated a specified number of times, or until the ray terminates within a pre-selected distance of the receiver.

A grid of velocity values which may vary laterally and vertically is input for each layer. A continuous velocity function is obtained by using one of the following methods: fitting bicubic splines to these data, linear interpolation between grid points, or by piece-wise bilinear interpolation.

3.5. Statistical Determination of Time-Distance Segments

The onsets which define a velocity segment on a time-distance plot are invariably scattered about the "best-fit" line for this segment. The scatter can be due to a variety of causes (e.g. refractor topography, near surface layers). Linear regression analysis was undertaken to determine best-fit gradients and,

thus, velocities and time intercepts.

Linear regression software forms part of the UNIX 'S' package. In this method the best fit line to the data is determined by considering two variables, one independent (distance in this case) and the other dependent (time), and minimizing the deviation of the points from the line. The equation of the best fit line is

$$y_i = mx_i + c + e \tag{3.39}$$

where

y_i =*estimate of y deviation.*

m = slope

c = intercept

e = error

The best fit line is one which satisfies the condition

$$\sum_{i=1}^{n}(\delta y_i - y_i)^2 \text{ is a minimun} \tag{3.40}$$

where

n = number of observations

y_i = *travel−time of the i−th observation of the arrival*

The sum of the squares of the vertical deviations about the line is a minimum. Error is considered negligible on x values while the dependent variable y has random-error term (e).

The regression function was used to determine all the velocity values obtained from the time-distance graphs (except the first curved velocity segments where the WHB velocities were used) together with the time intercepts and the errors associated with these values. The error values were calculated by adding and subtracting the reciprocal of the standard error derived from the function to the reciprocal of the gradient to obtain the minimun and maximum velocity variation respectively.

CHAPTER FOUR - DATA ANALYSIS AND INTERPRETATION

4.1. Introduction

This chapter will deal with the presentation, analysis and interpretation of the data gathered for this project. In seismic interpretation, obtaining good estimates of velocity values for the different lithological units is an important tool by which depths and structural variations are modelled. In this work, apart from the MAVIS project, no other sources of velocity-depth data were available. Some boreholes have been drilled in the area. However, the Glenrothes borehole, which is situated to the east of line 1, did not reach sufficient depth to give useful data, while reports concerning other boreholes are confidential.

Refractor depths and their interpretation were obtained using the velocities deduced along the profiles. The results were integrated with the MAVIS lines which intersect the profiles south of the Ochil Hills. Where data are well constrained, depths and velocities are correlated with the local geology, though a detailed discussion of the geological implications of the data is deferred to chapter 5.

The number of quarries used in this project, the large number of shots recorded and the varied lithologies crossed by the profiles made it feasible to study the relationship of P-wave frequencies to lithology and quarry engineering practices. This will be discussed in detail. The large amount of data recorded were suitable for modelling the variation in seismic velocity with depth through the topmost crustal layers. The application of the different interpretational methods discussed in the previous chapter to the data and a comparison of velocity values derived by these methods and their significance will be presented.

4.2. Data Presentation

The set of data presented in this thesis comprises several wide-angle seismic lines which cover the western part of the Fife region and the Clackmannan district (Fig. 1.1b). Tables of shot times, locations and arrival times are listed in Appendix 2. Figures 4.1 to 4.14 show the unfiltered and filtered seismic sections for each profile successively. Figures are arranged in pairs. The first figure shows the unfiltered data from a shotpoint: figure "a" shows the unfiltered data and figure "b" shows the same data with first arrival picks. The second figure of a pair shows the same data but uninterpreted and frequency

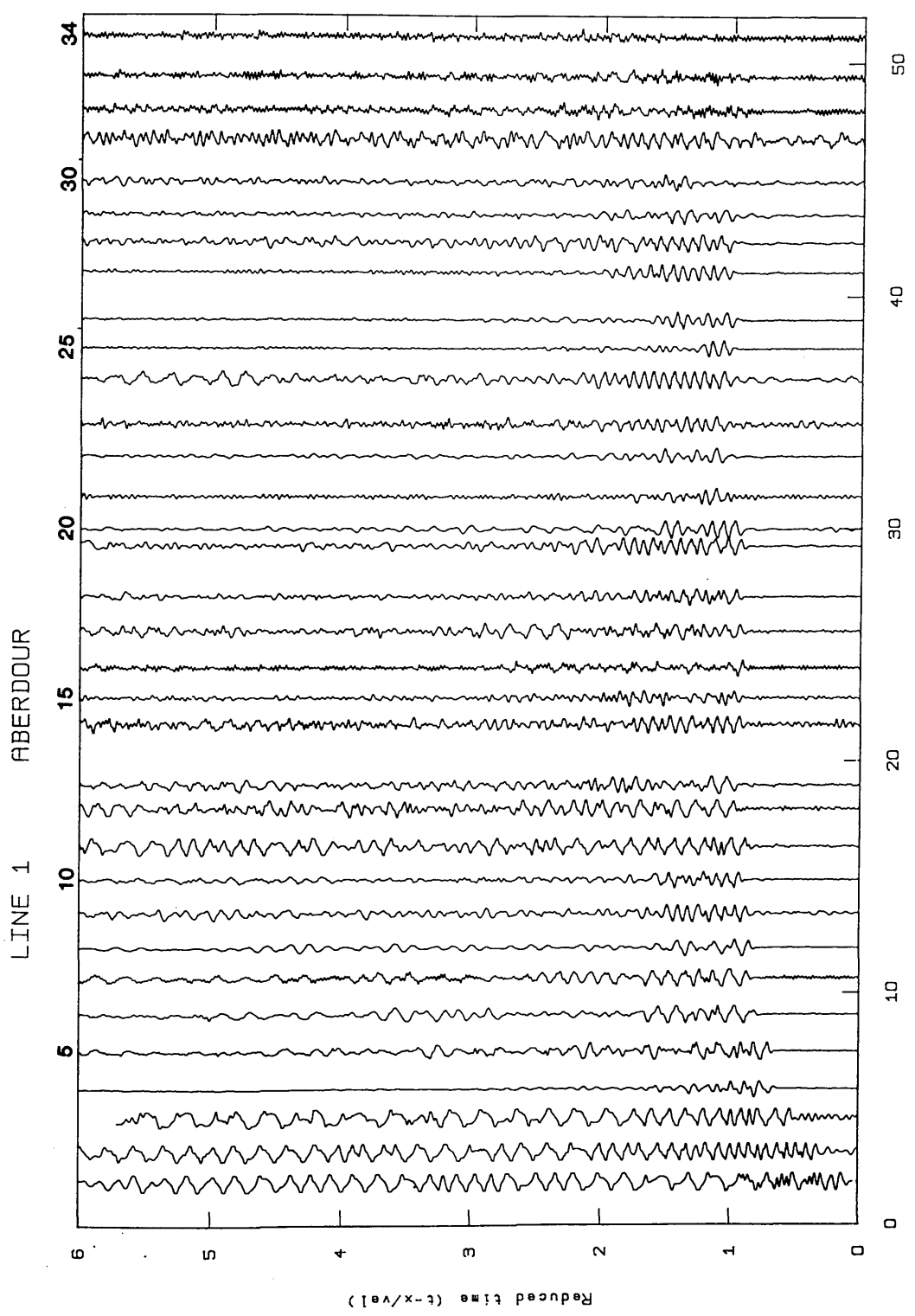

Fig.4.1a Unfiltered section for line 1 (Aberdour shot).

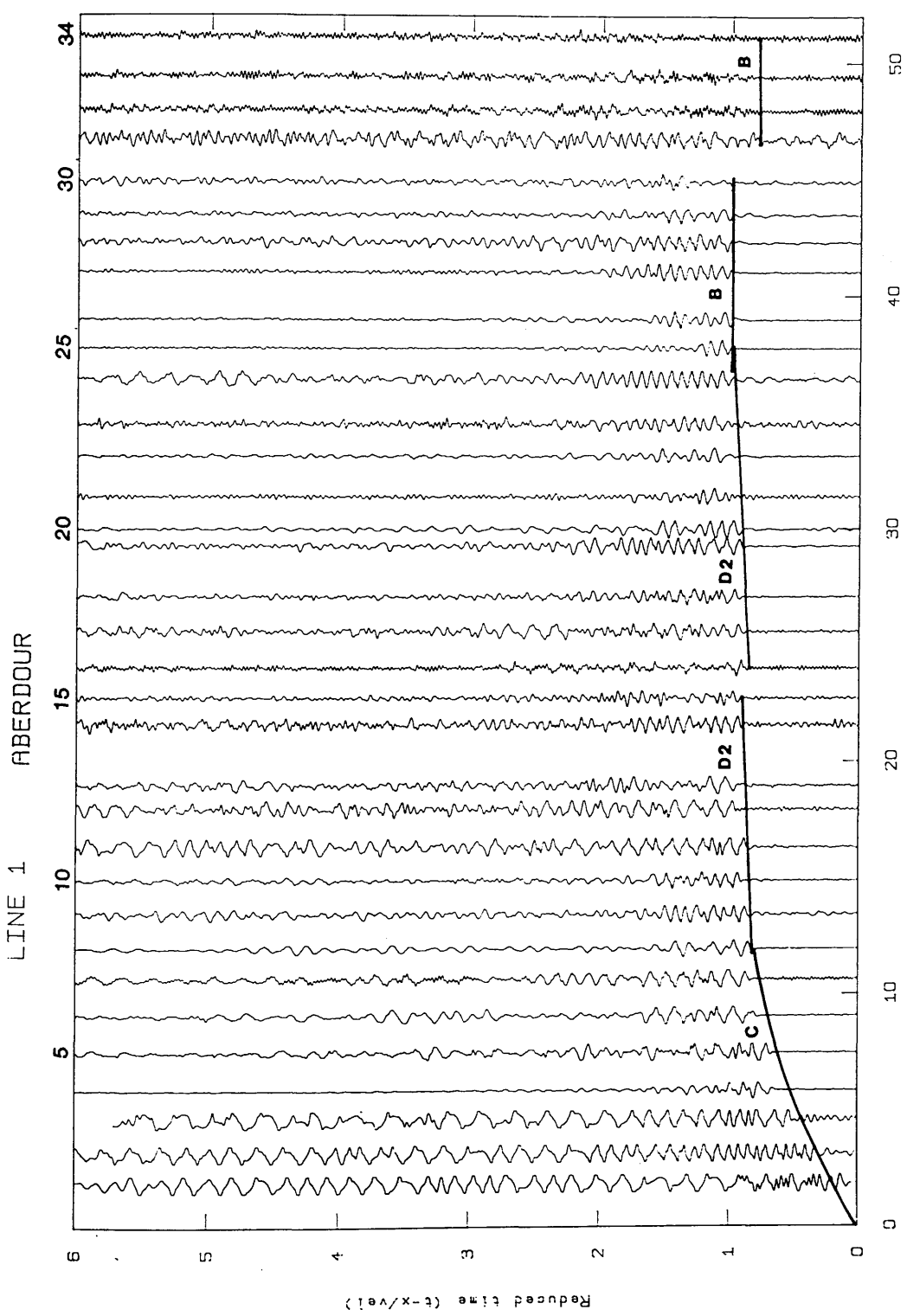

Fig.4.1b Unfiltered section for line 1 (Aberdour shot), interpreted.

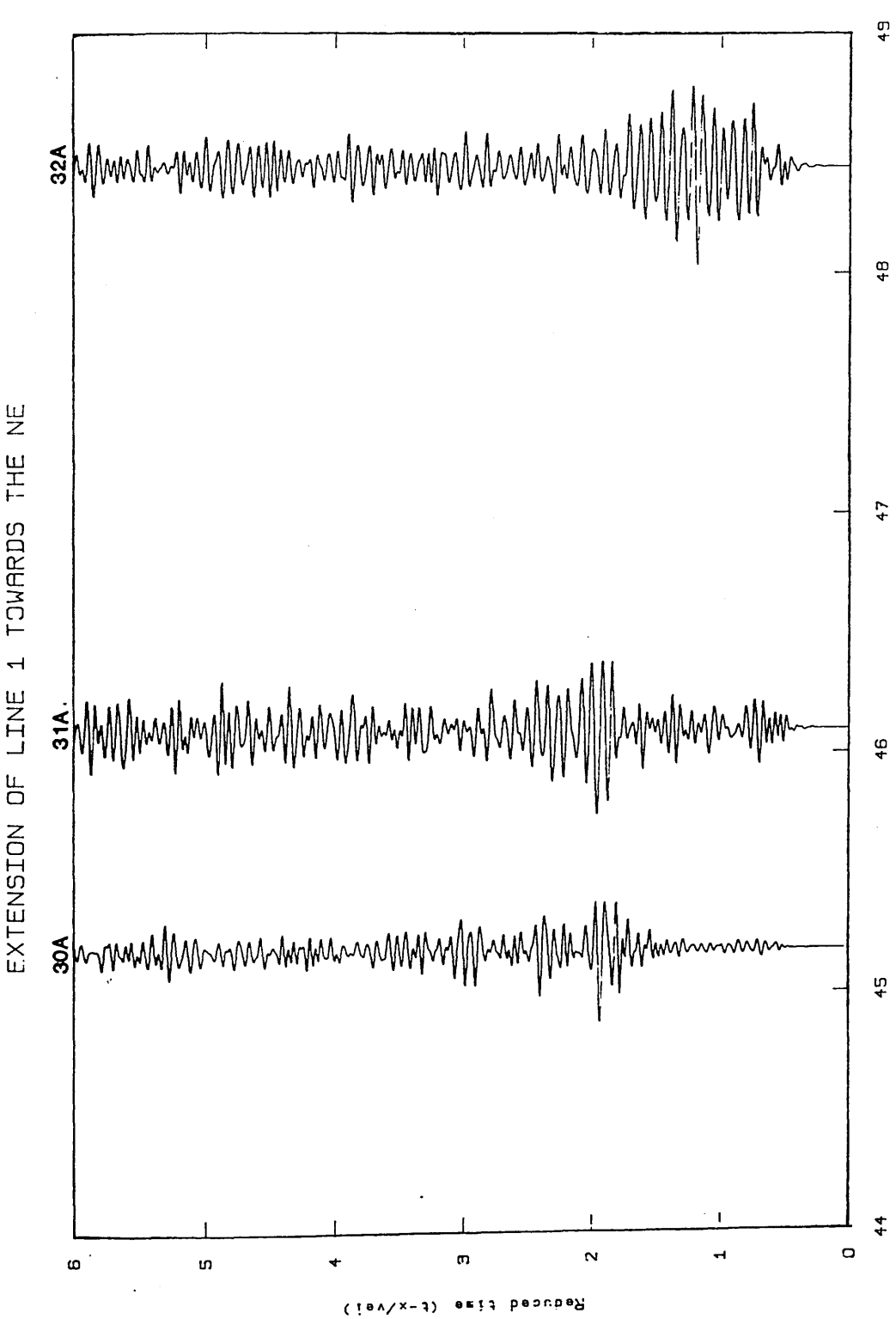

Fig.4.1c Filtered section for stations 30A-32A of line 1.

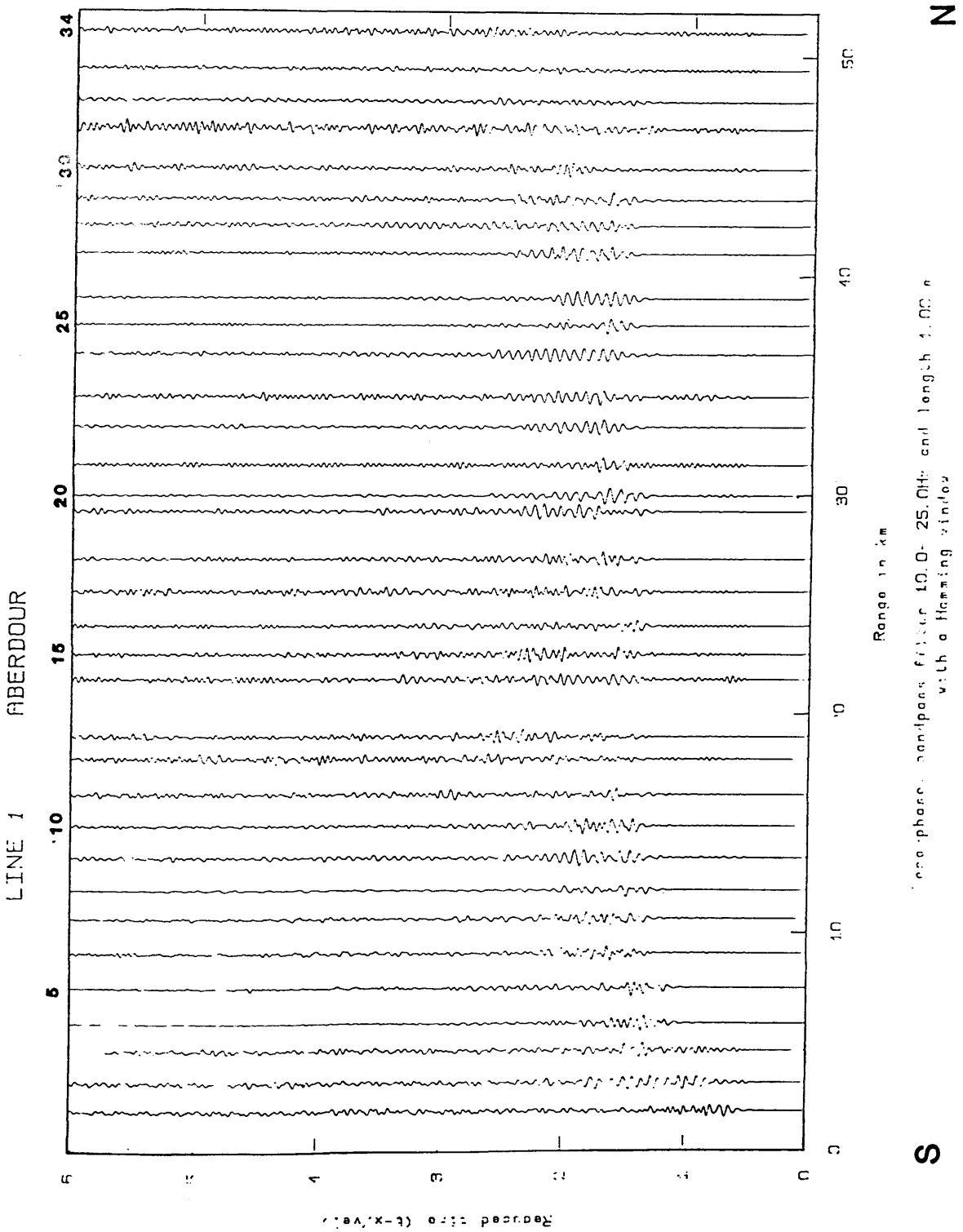

Fig.4.2 Filtered section line 1 (Aberdour shot).

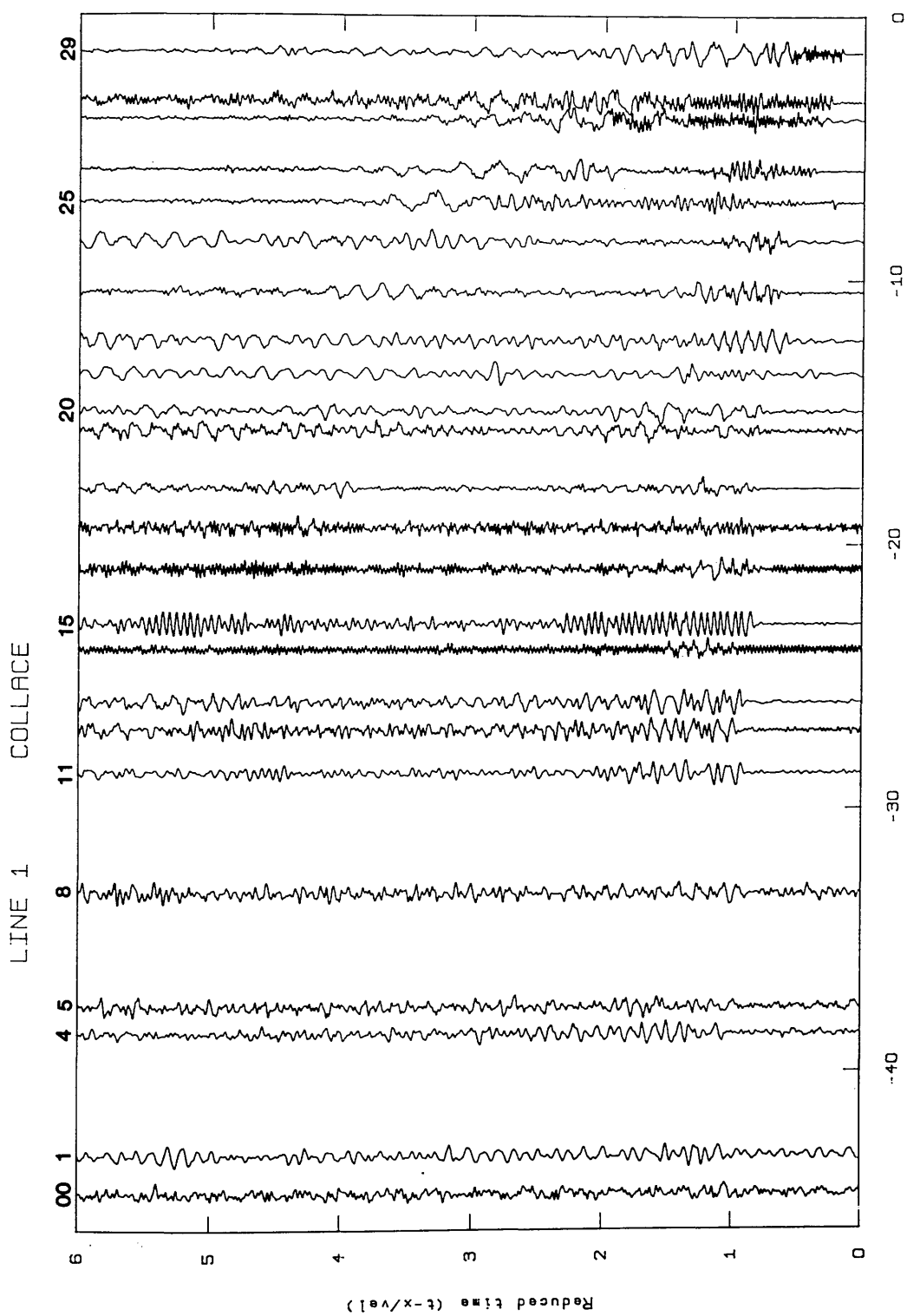

Fig.4.3a Unfiltered section line 1 (Collace shot).

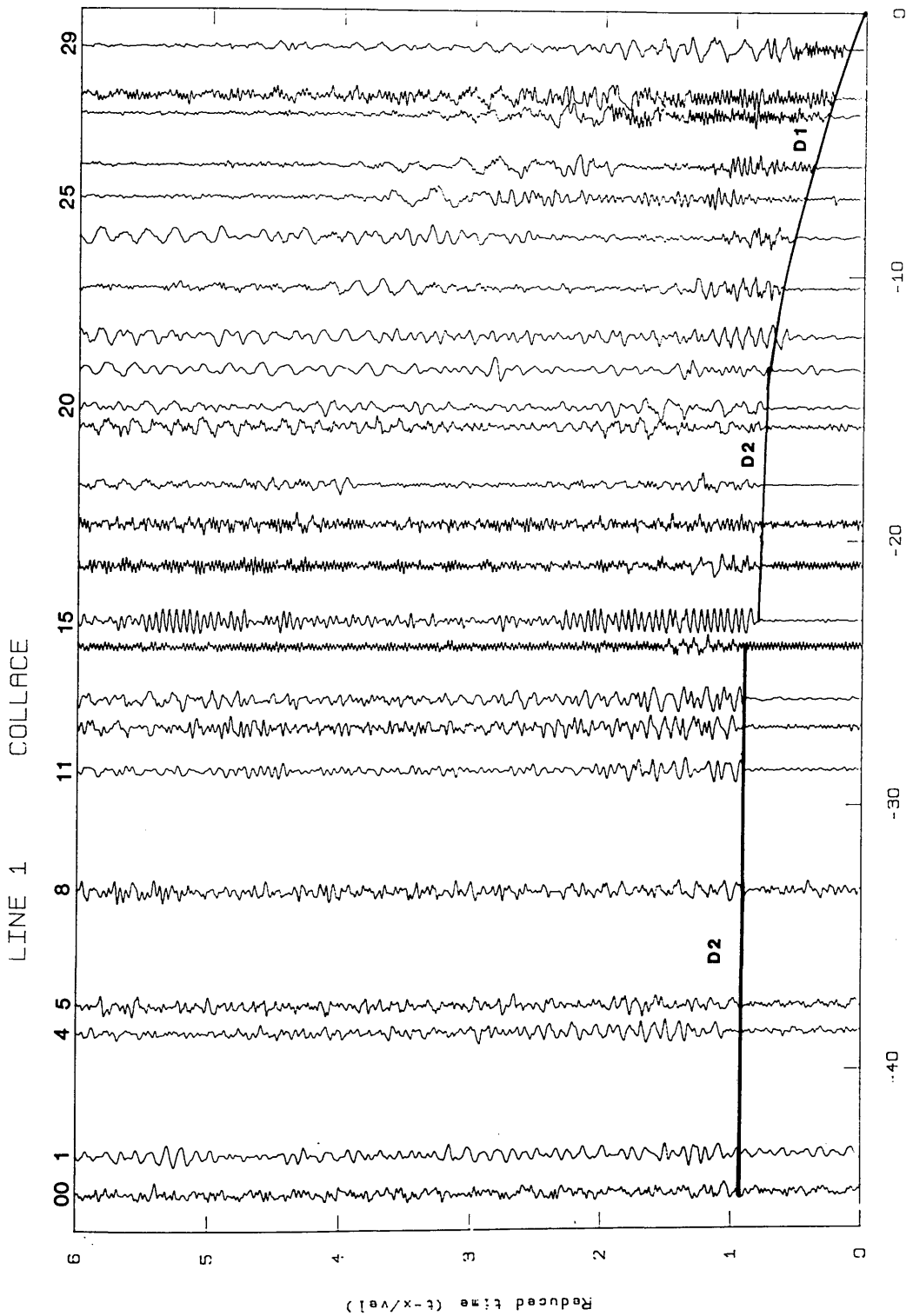

Fig 4.3b Unfiltered section line 1 (Collace shot), interpreted.

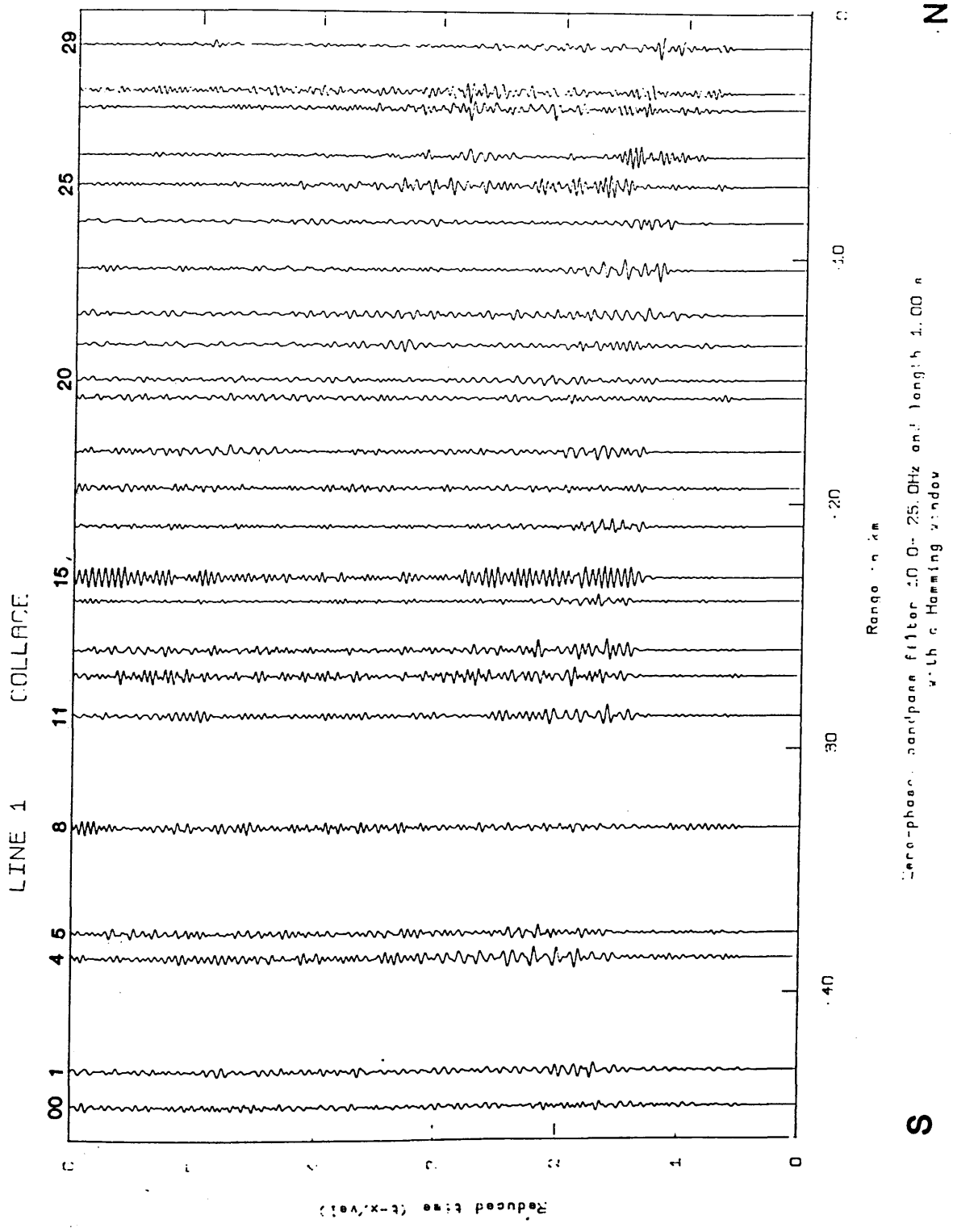

Fig.4.4 Filtered section line 1 (Collace shot).

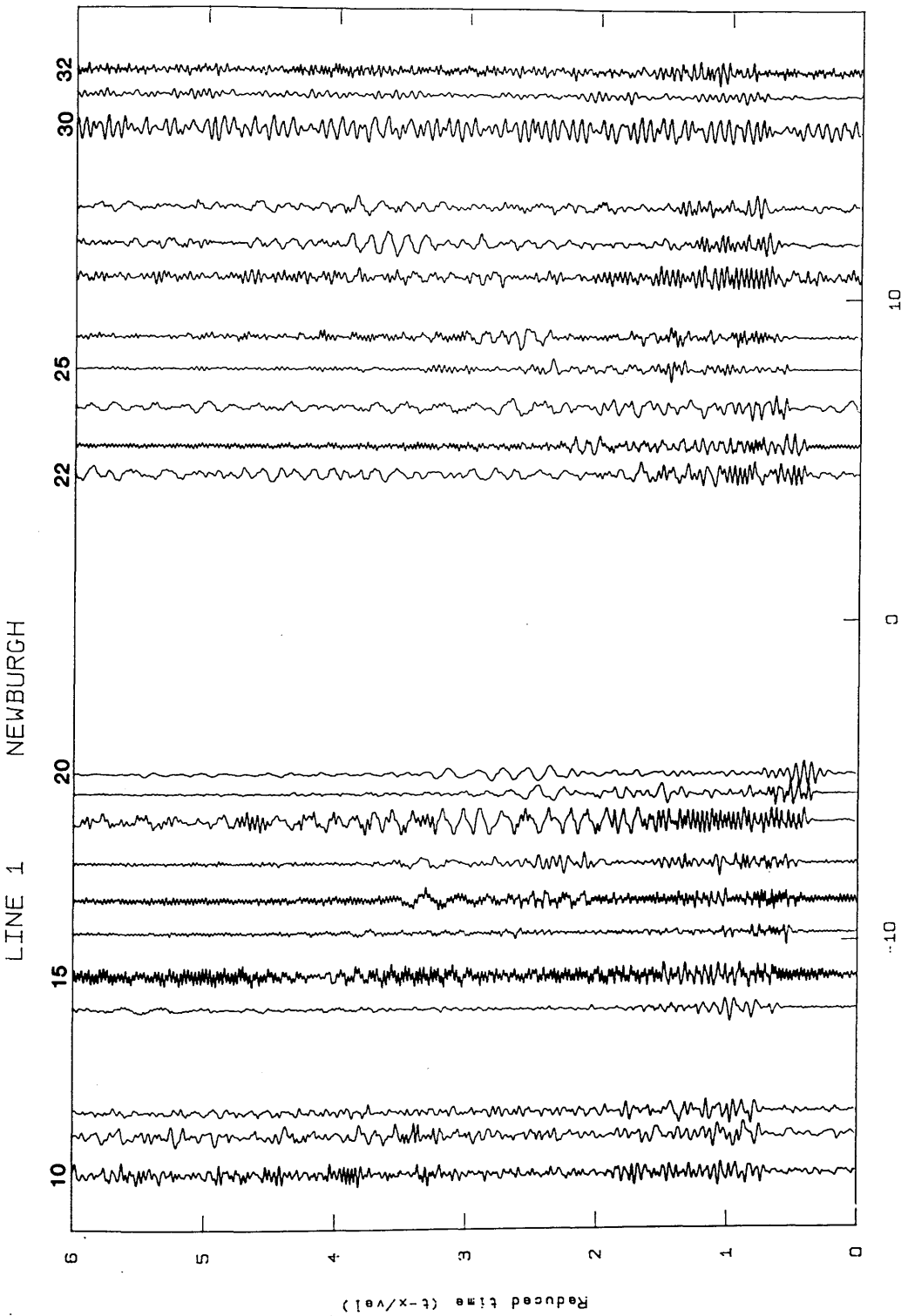

Fig.4.5a Unfiltered section line 1 (Newburgh shot).

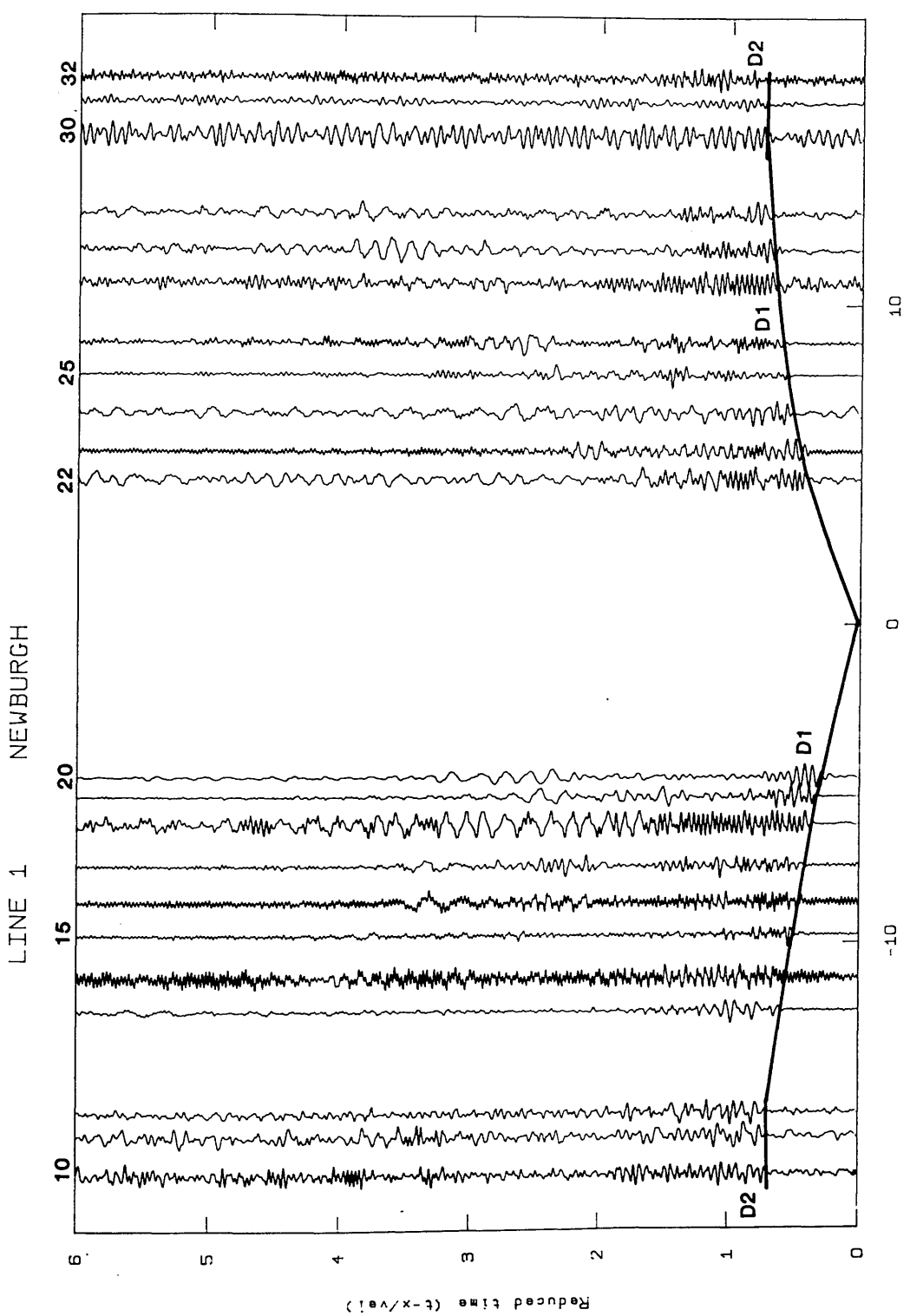

Fig.4.5b Unfiltered section line 1 (Newburgh shot), interpreted. sp2

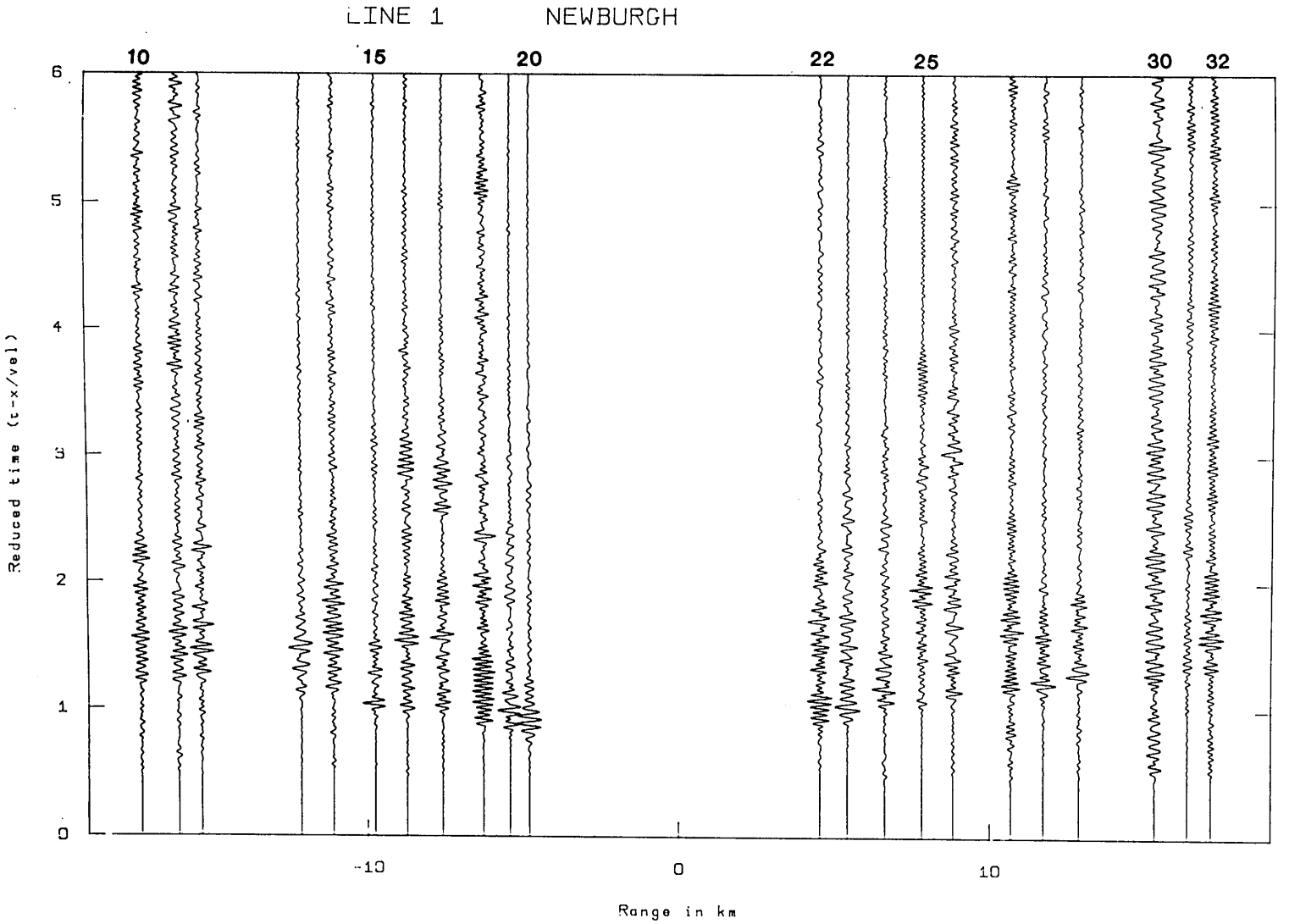

Fig.4.6 Filtered section line 1 (Newburgh shot).

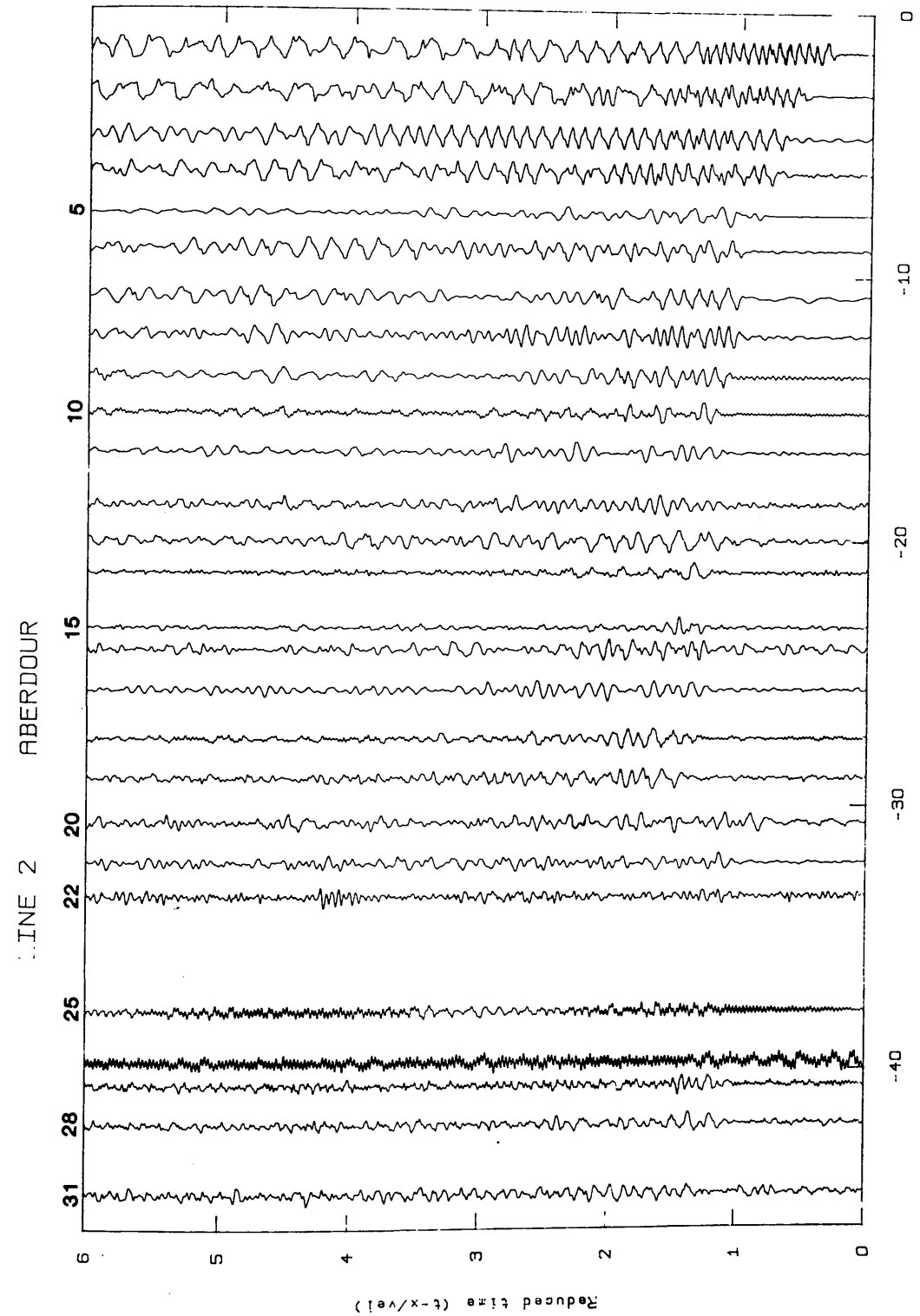

Fig.4.7a Unfiltered section line 2 (Aberdour shot).

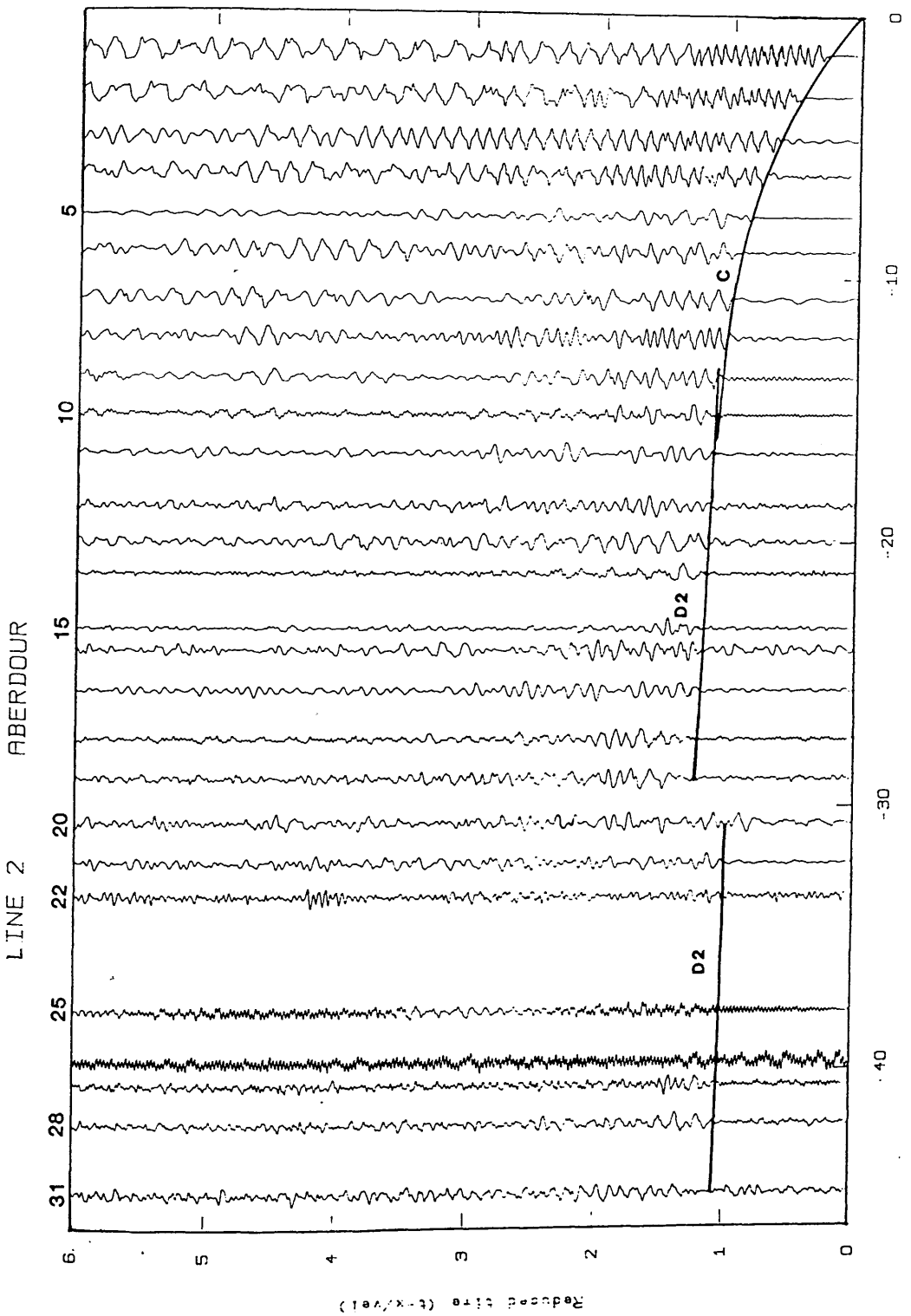

Fig.4.7b Unfiltered section line 2 (Aberdour shot), interpreted.

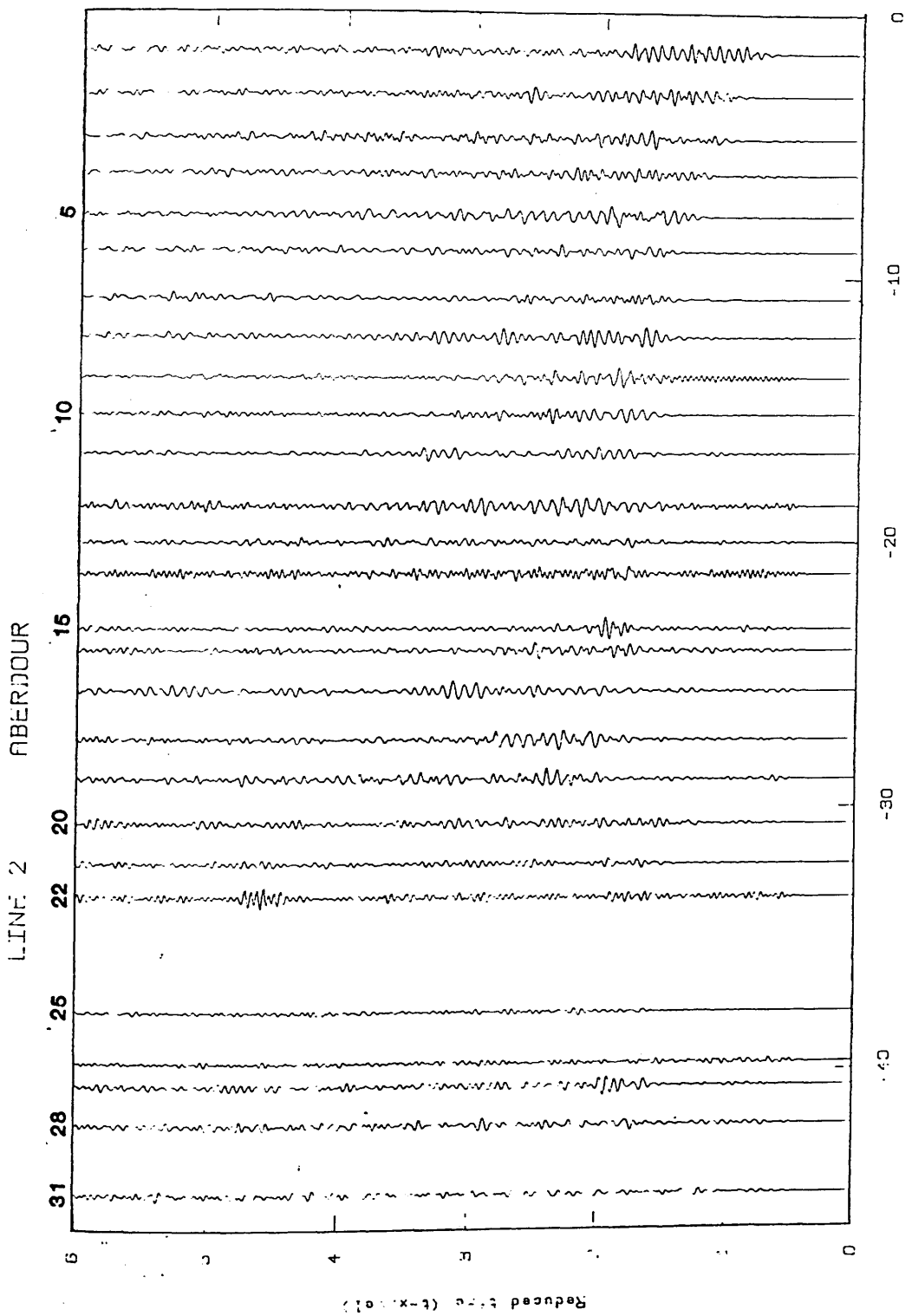

Fig.4.8 Filtered section line 2 (Aberdour shot).

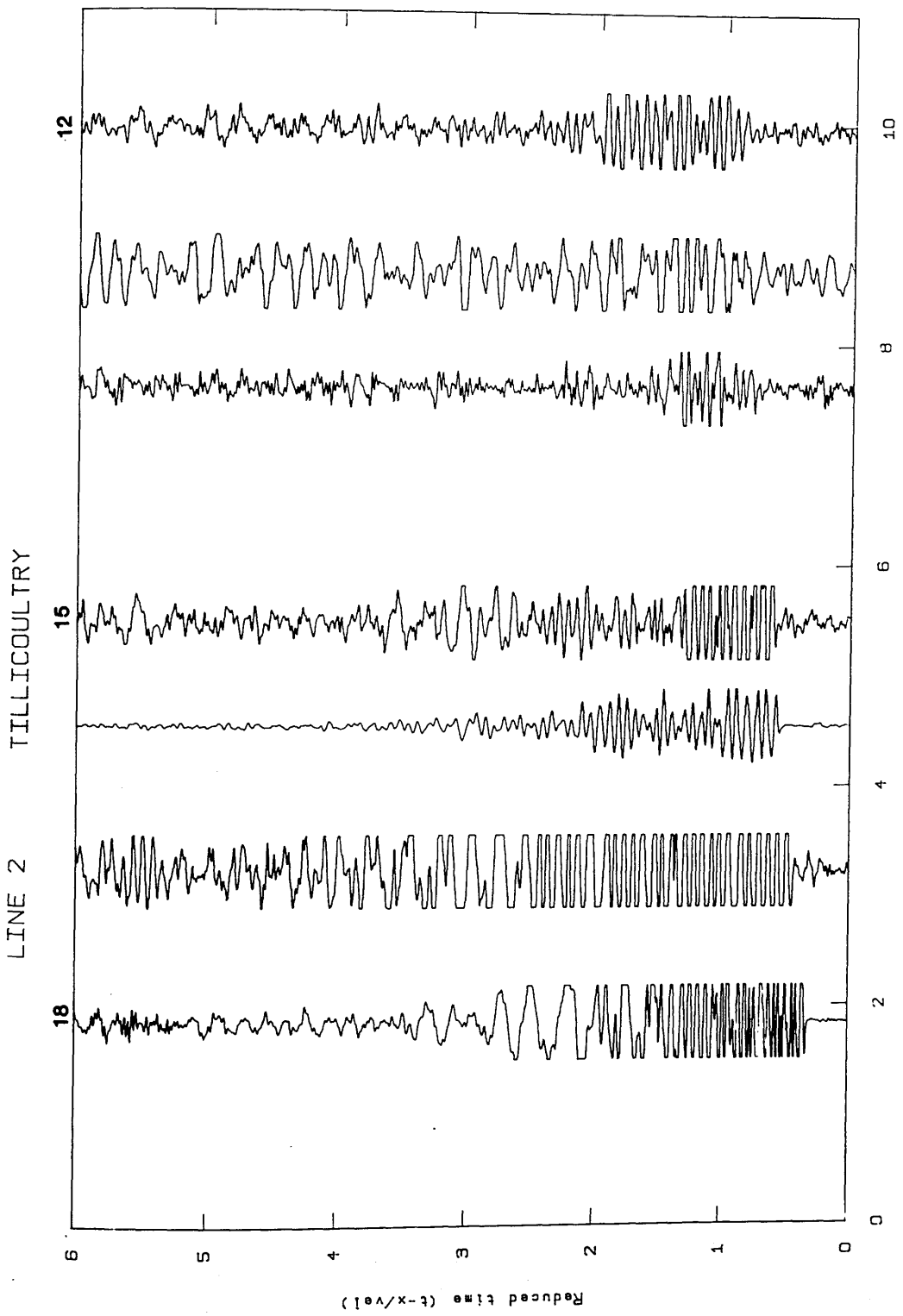

Fig.4.9a Unfiltered section line 2 (Tillicoultry shot).

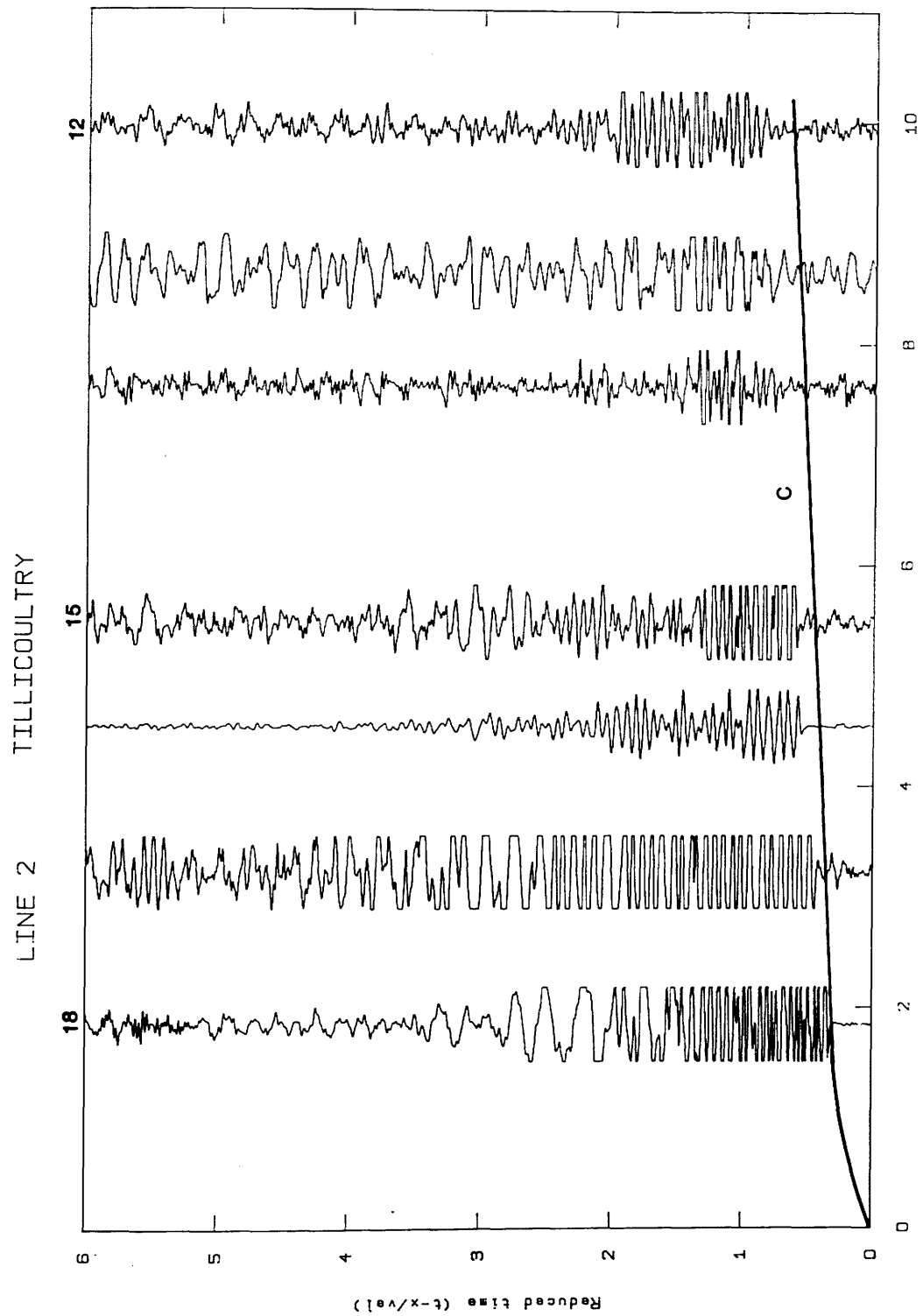

Fig.4.9b Unfiltered section line 2 (Tillicoultry shot), interpreted.

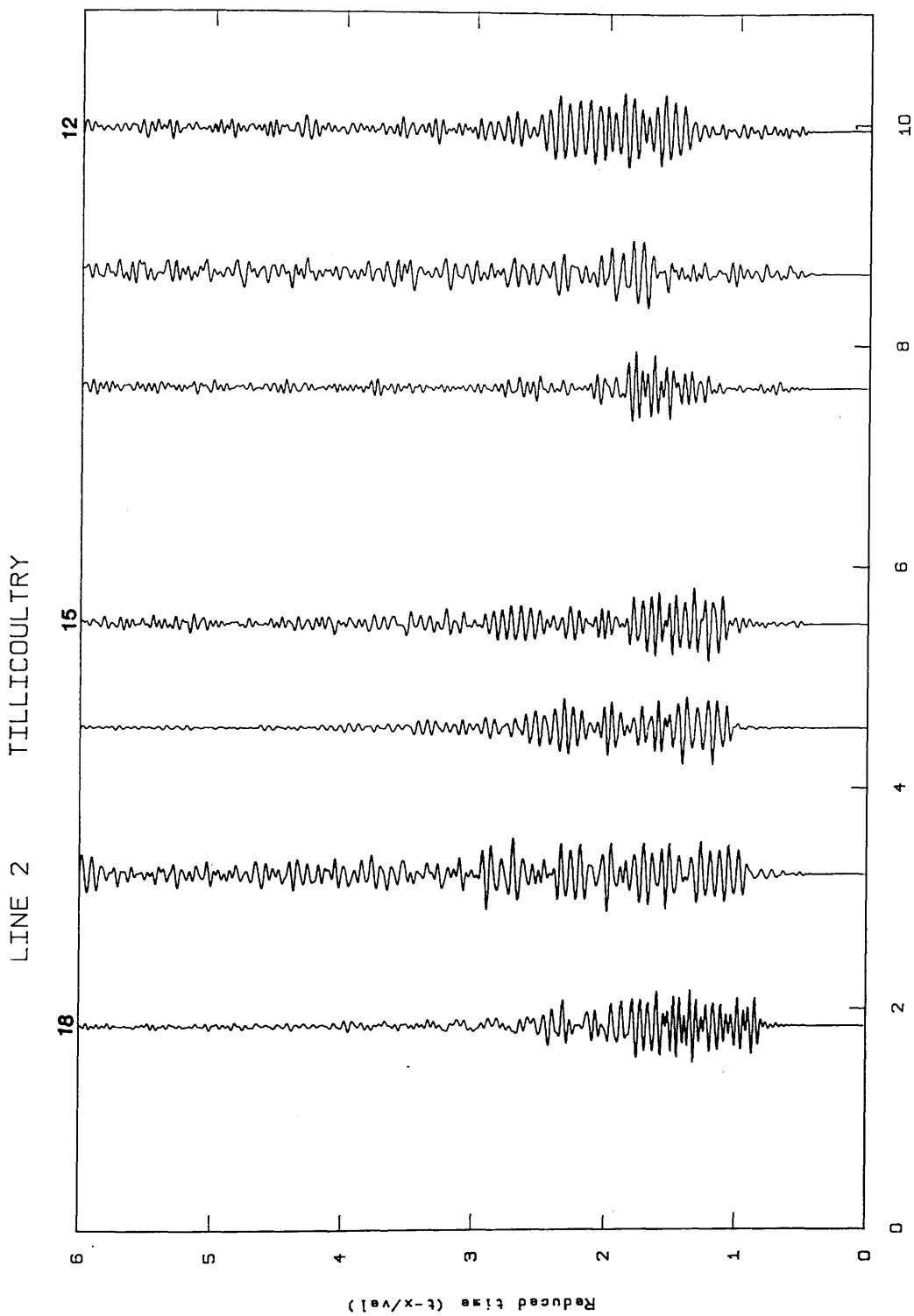

Fig.4.10 Filtered section line 2 (Tillicoultry shot).

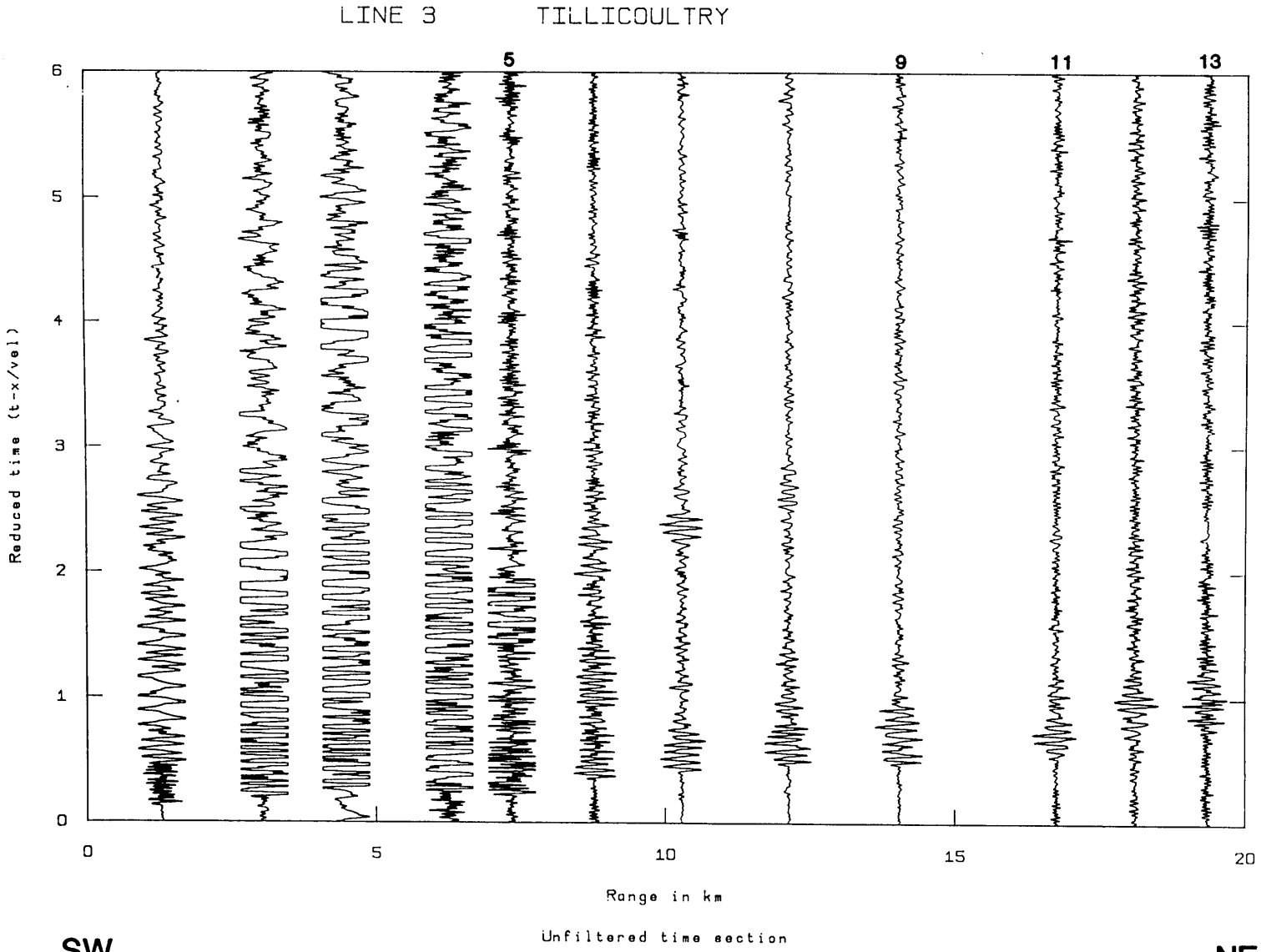

Fig.4.11a Unfiltered section line 3 (Tillicoultry shot).

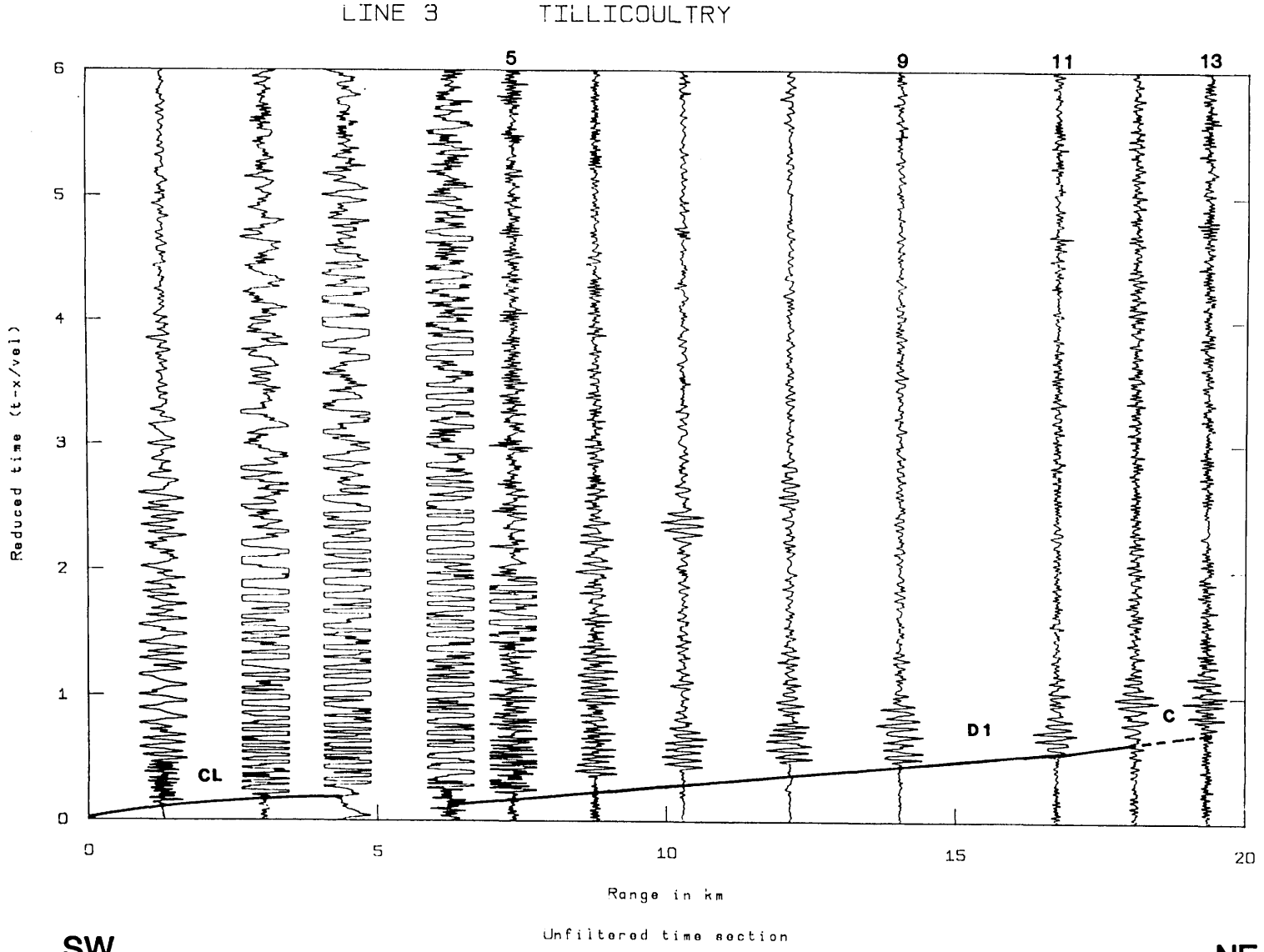

Fig.411b Unfiltered section line 3 (Tillicoultry shot), interpreted.

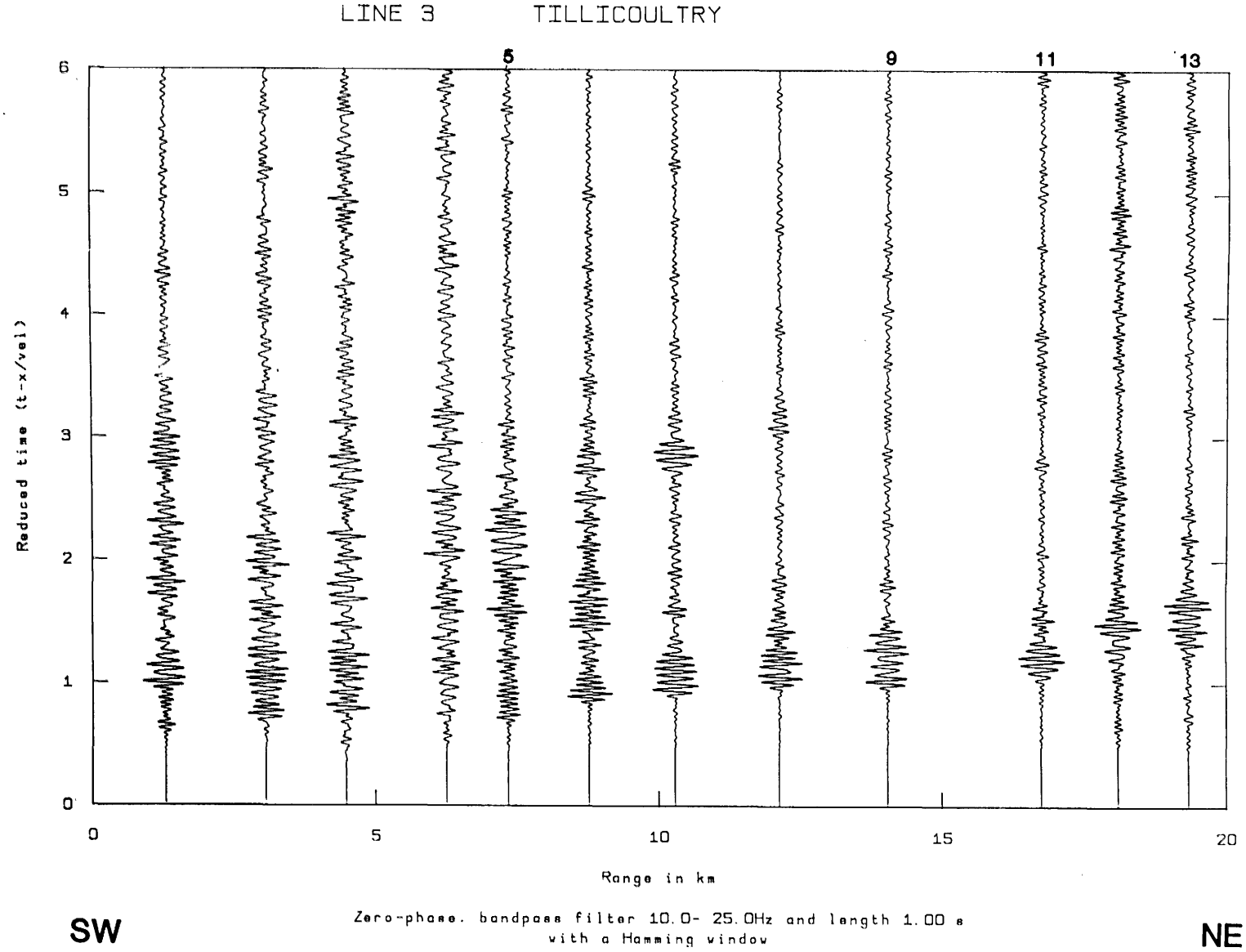

Fig.4.12 Filtered section line 3 (Tillicoultry shot).

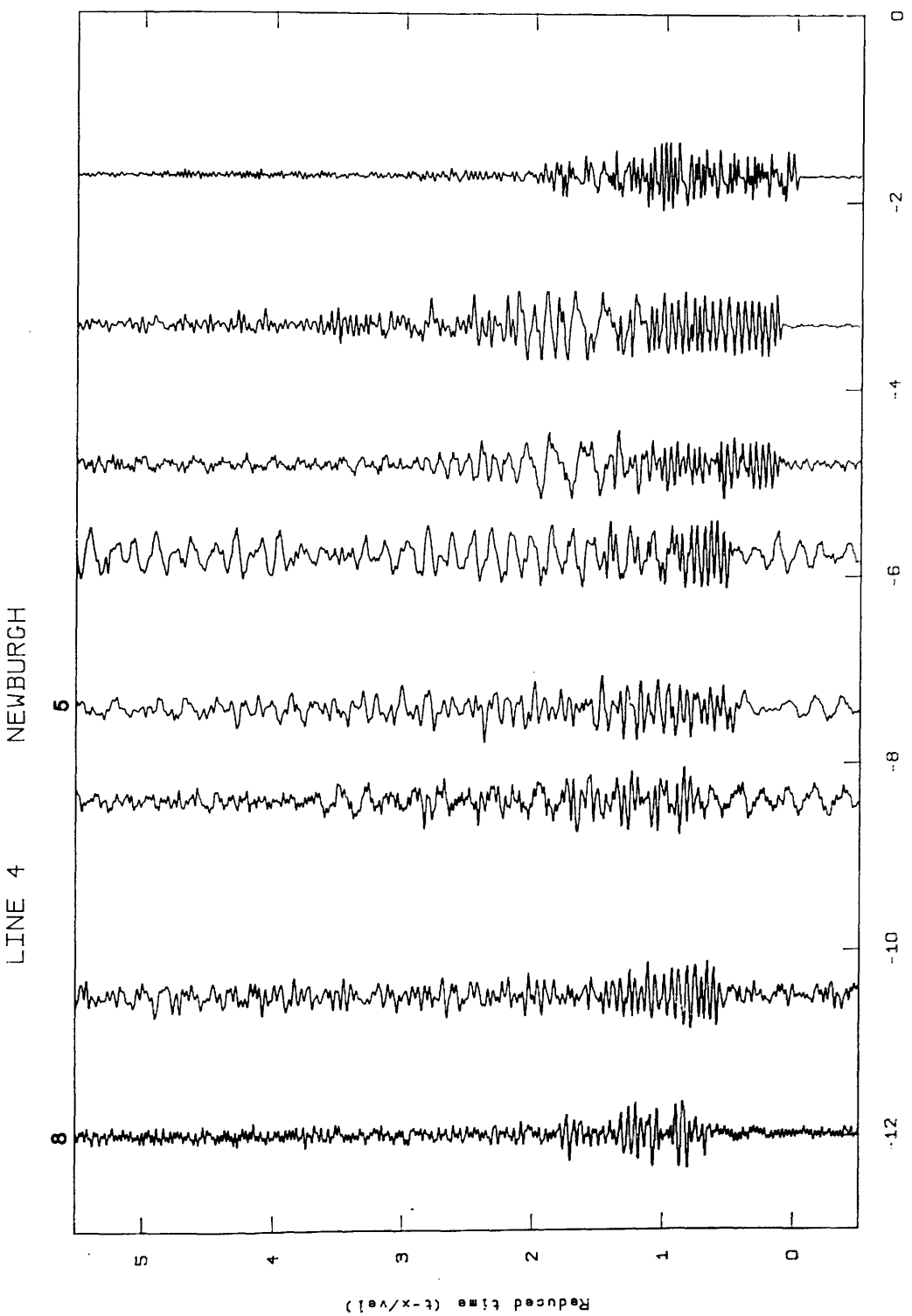

Fig.4.13a Unfiltered section line 4 (Newburgh shot).

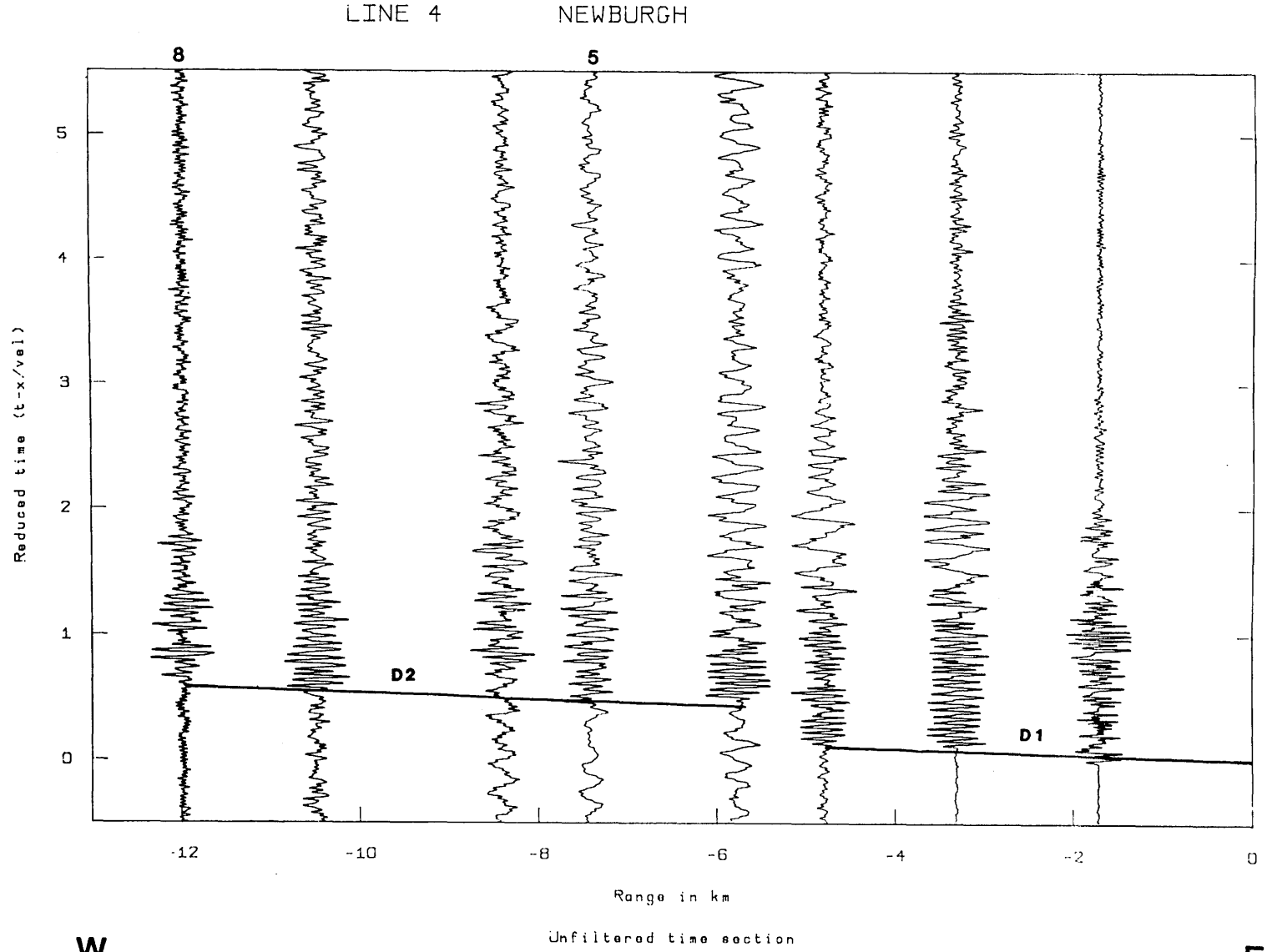

Fig.4.13b Unfiltered section line 4 (Newburgh shot), interpreted.

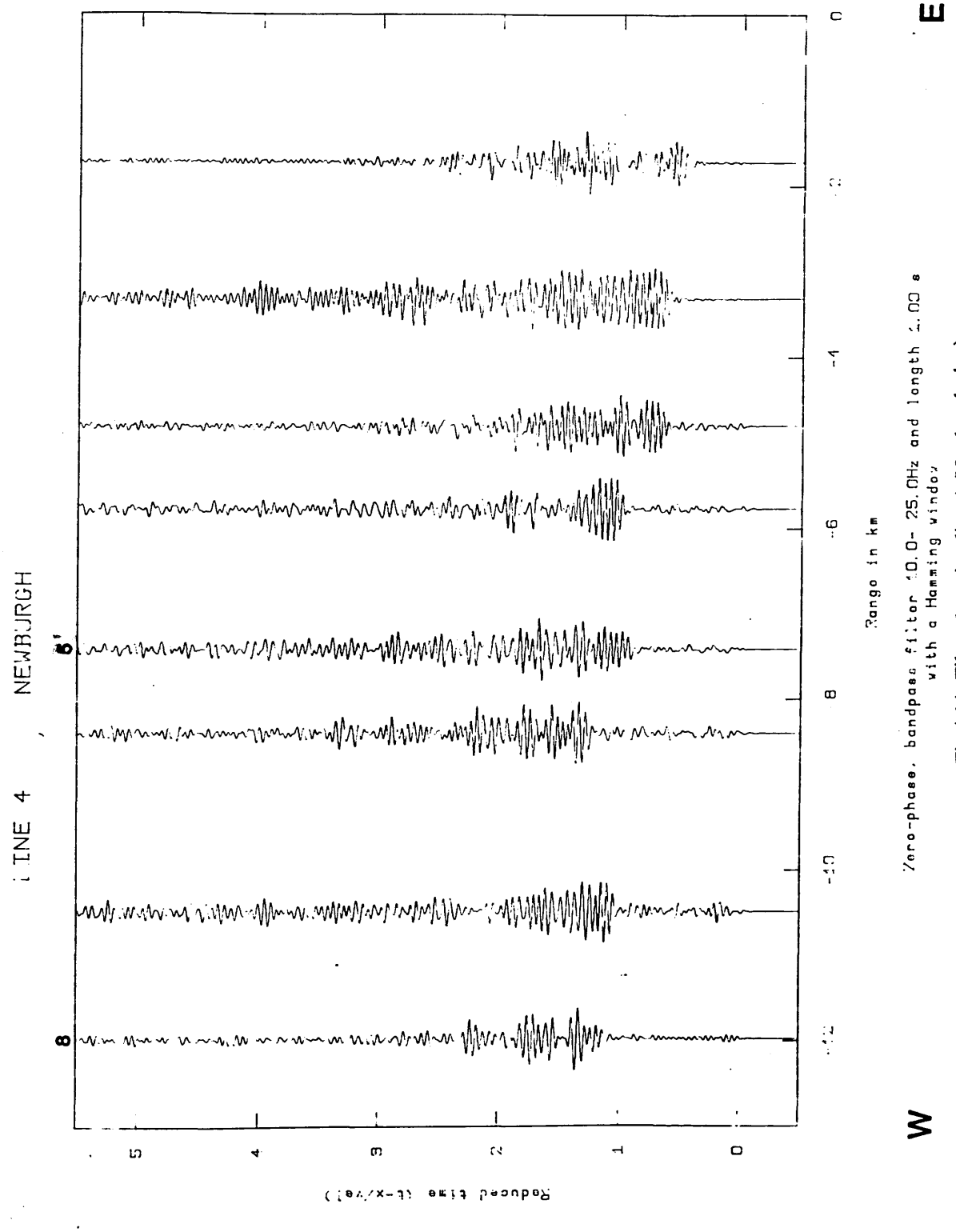

Fig.4.14 Filtered section line 4 (Newburgh shot).

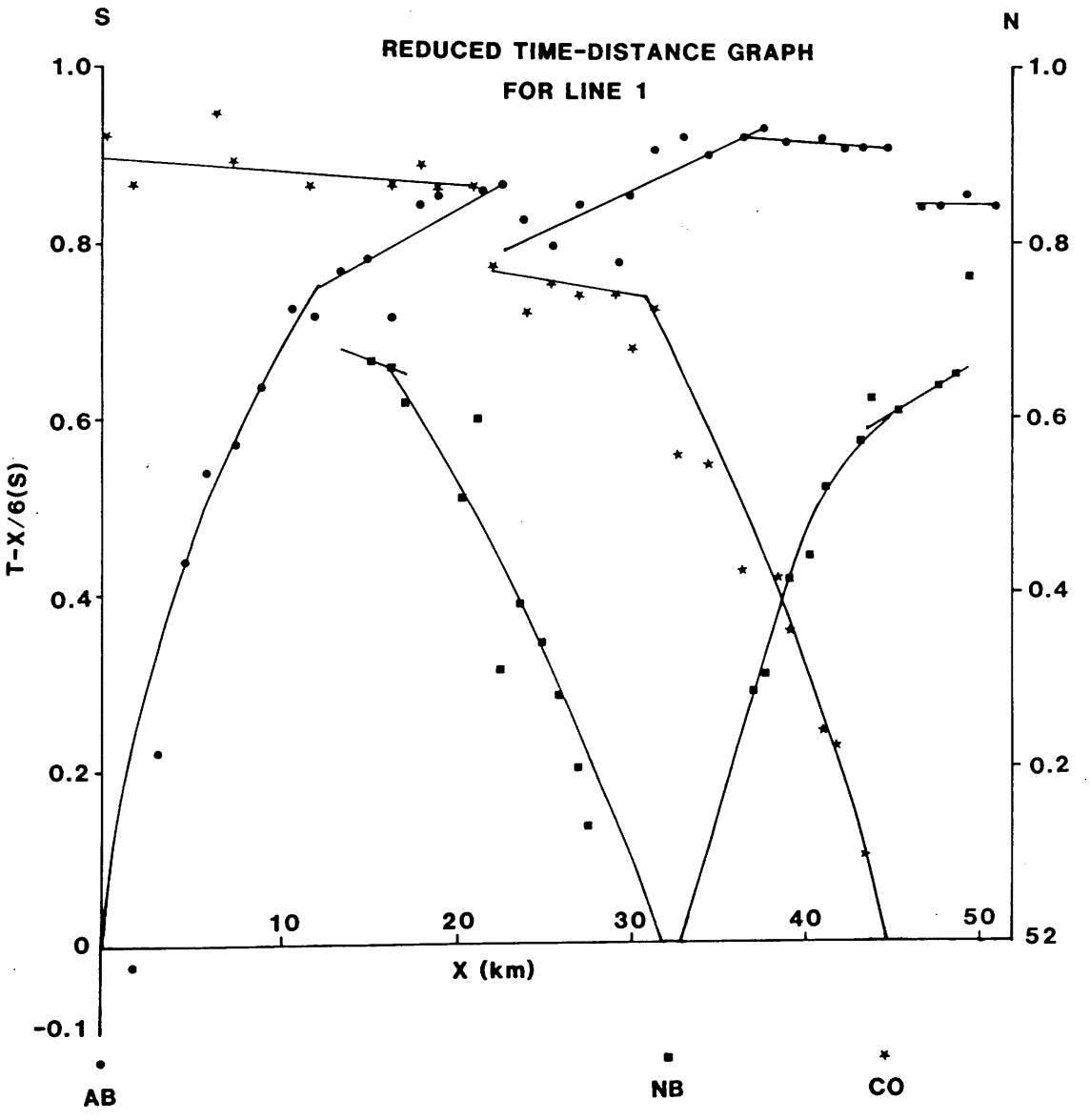

Fig.4.15 Reduced time-distance graph for line 1. AB - Aberdour, CO - Collace, NB - Newburgh.

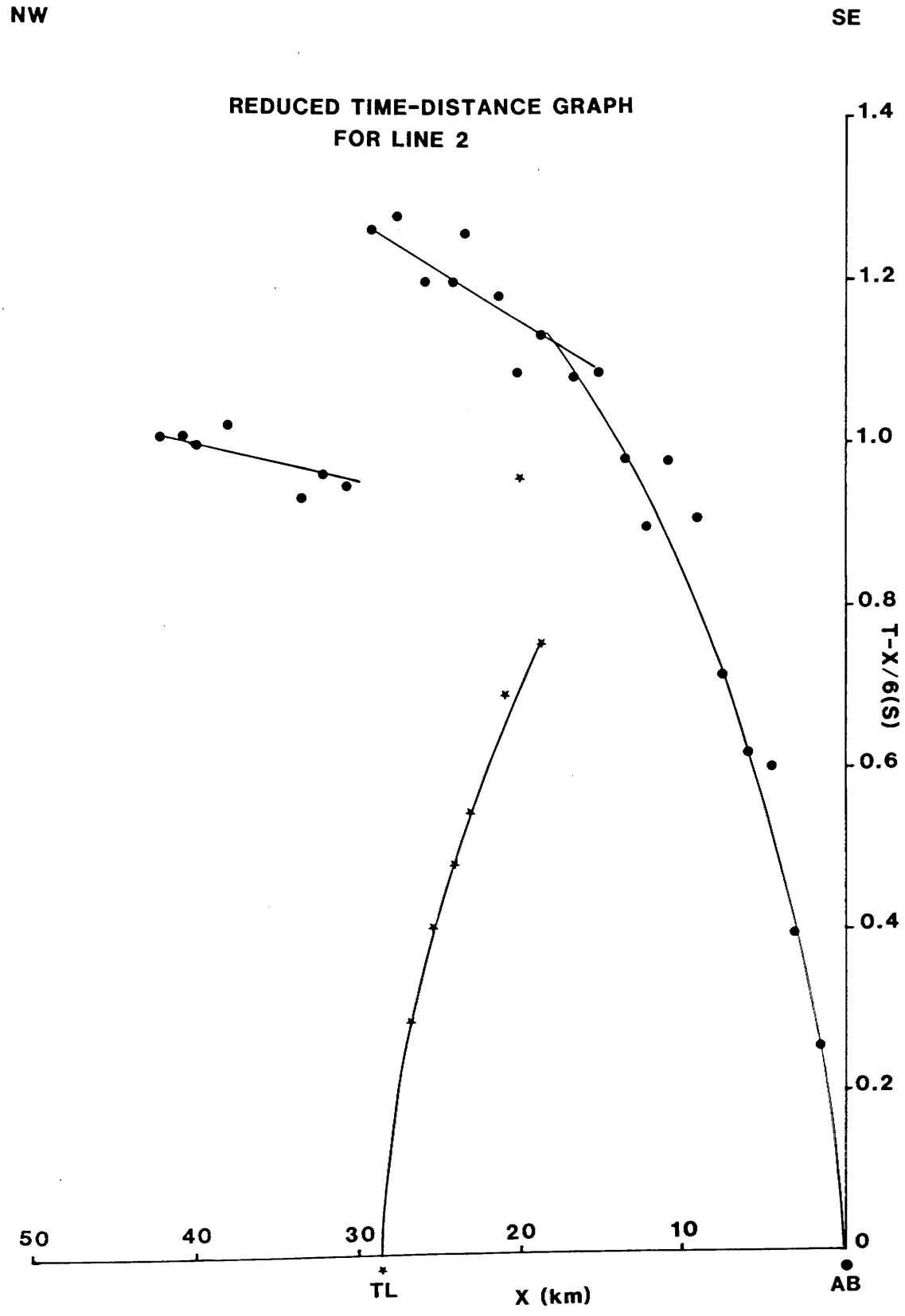

Fig.4.16 Reduced time-distance graph for line 2. AB - Aberdour, TL - Tillicoultry.

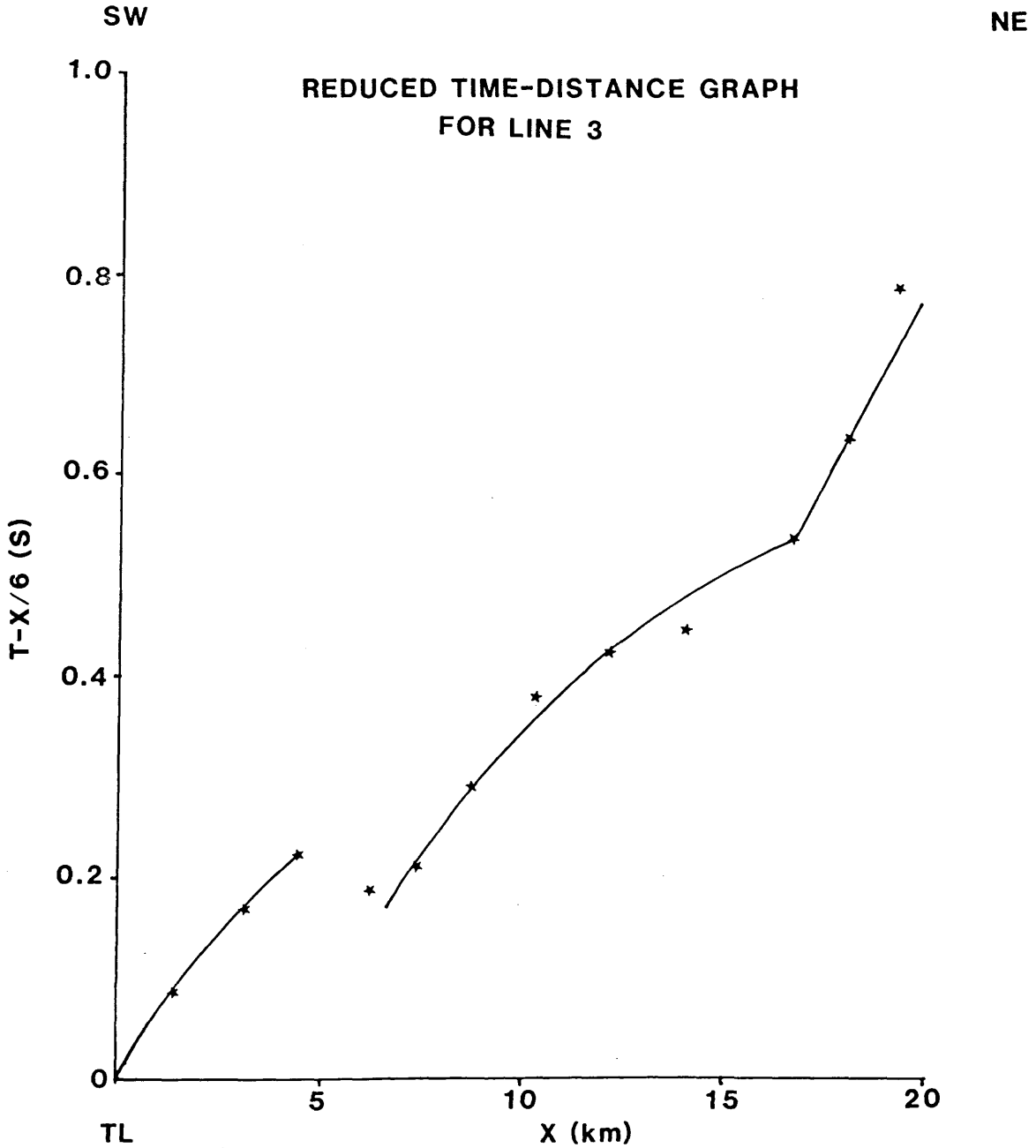

Fig.4.17 Reduced time-distance graph for line 3. TL - Tillicoultry.

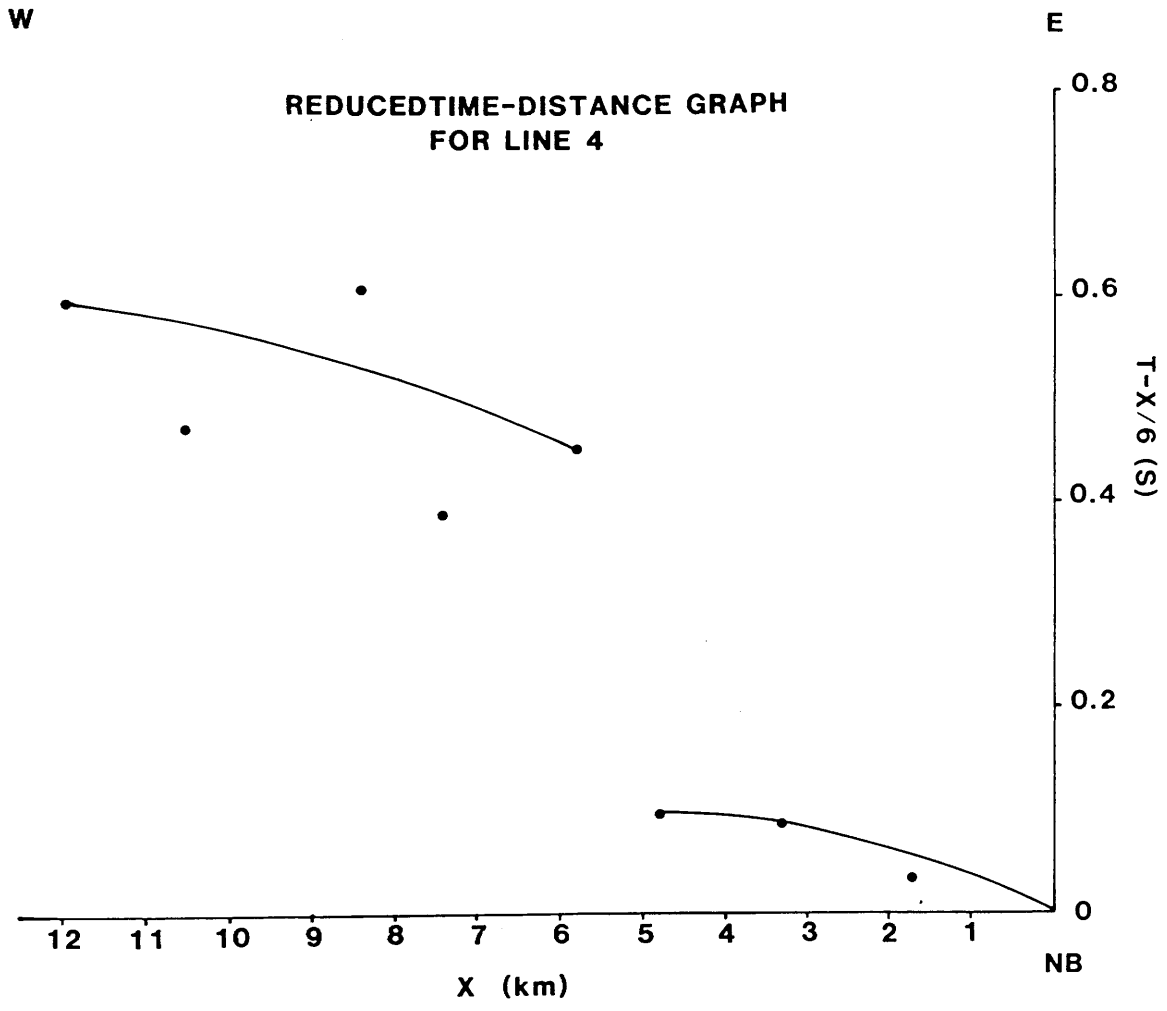

Fig.4.18 Reduced time-distance graph for line 4. NB - Newburgh.

filtered. Figure 4.1c shows a filtered section of the NE extension of line 1. The arrivals are labelled as follows: layer 1 (Carboniferous and Upper Devonian) is C; layer 2 (Lower Devonian) is D1 or D2, corresponding to near surface (low velocity) or deeper arrivals from this layer respectively; and arrivals from the basement will be denoted by B.

Traces on the digital sections are usually numbered in every fifth case only. Each trace is normalised with respect to its maximum amplitude. In examining the filtered digital sections a time shift of 0.5 s (half the filter length) is present between them and the unfiltered sections due to use of the zero-phase filter. The effect of clipping can be seen on most of the profiles for the first three or four traces. Time-distance graphs of the P-wave first arrival picks are plotted at a reduction velocity of 6.0 km/s in Figures 4.15 to 4.18.

Frequency filtering to enhance first arrivals made little difference to the data which were generally of good quality, except for a few noisy stations. Filtering was especially useful if the source of noise generates constant frequency (e.g. pumping station and similar machines) where the deployment of the appropriate filter eliminated such noise which was usually of higher frequency than the high cut used (25 Hz). This effect can be seen on stations 14 and 16 of line 1 (recording from Newburgh quarry) and station 25 of line 2 (Figs. 4.5, 4.6, 4.7 and 4.8 respectively).

Good quality second arrivals (reflected and shear waves) were obtained, at some stations (Figures 4.4 and 4.6), when frequency filtering was applied. Lack of time meant no attempt was made to interpret these data.

On the reduced time-distance graphs first arrivals from stations at 1-5 km from some quarries (e.g. Aberdour and Newburgh) show higher velocities than more distant stations. It is suggested that the direct waves to these stations travel mostly in the igneous rocks in which all quarries are situated. This caused some problems in applying the WHB method because the program does not accept any velocity inversion and the time-distance curve at such stations had to be smoothed (see section 4.4).

4.3. Implications of Spectral Analysis

Frequency analysis was carried out to find the dominant P-wave frequencies in the area for filtering purposes (Fig. 4.19). Results obtained from this process were satisfactory and discrimination between noise and signal frequencies was successfully obtained for use in the filtering process.

Spectral analysis of arrivals from Aberdour quarry along line 1 showed a dominant P-wave frequency in the range of 5-18 Hz (Fig. 4.19a) with peaks at about 14 Hz. Frequency peaks are consistent for traces up to 47 km, beyond which a substantial attenuation of the dominant frequencies occurs. A possible explanation for this lack of attenuation of energy is that blasts from Aberdour quarry generate only a narrow band of low frequency energy which is better preserved with range than high frequency energy which suffers rapid decay with distance. Dentith (1987) obtained the same results when analyzing frequency peaks along the MAVIS I north line with data recorded from the Methil shot where no noticeable energy attenuation was observed. This effect was only detected along this line when it was recorded from the Methil shot.

At the last three stations of line 1 from Aberdour quarry high frequency peaks of 38 Hz are present, which might be attributed to second arrivals (wide angle reflections) from a lower interface arriving nearly at the same time as the first arrival. Analysis of data from Aberdour quarry along line 2 (Fig. 4.19b) yielded identical results regarding the frequency spectrum (5-18 Hz), the relatively low frequencies produced and the consistency of energy for long distance. Therefore, although both lines cross different lithologies, data recorded from the same quarry (Aberdour) yielded identical results.

Davidson (1985), who recorded similar sources in the Ayrshire area, explains the presence of low frequencies by the occurrence of layered crystalline igneous rocks at a relatively shallow depth. The likely absence of such a layer in the Fife region makes this explanation unlikely here. However, he further argued that P-wave frequencies are dependent on the engineering practices and lithology of the shot point.

Spectral analysis for Collace quarry (Fig. 4.19c) produced a frequency range of 5-14 Hz. This range bears some similarity to the peaks derived from the reversed section from Aberdour (Fig. 4.19a). Both quarries use gelatine explosive, which may be the cause for such similarity.

Frequency analysis of data recorded from Tillicoultry quarry along line 2 (Fig. 4.19d) showed different frequency peaks (10-18 Hz) although the same sites were used as those recorded from Aberdour quarry (i.e. the same lithology). Using the same quarry (Tillicoultry) to record line 3, frequency analysis (Fig. 4.19e) gave very similar results (10-20 Hz), although the profile crosses entirely different lithologies. These results suggest clearly that, over the ranges used (up to 40 km), the ffect of lithology on frequency along a profile is insignificant and the main factors relate to the quarry.

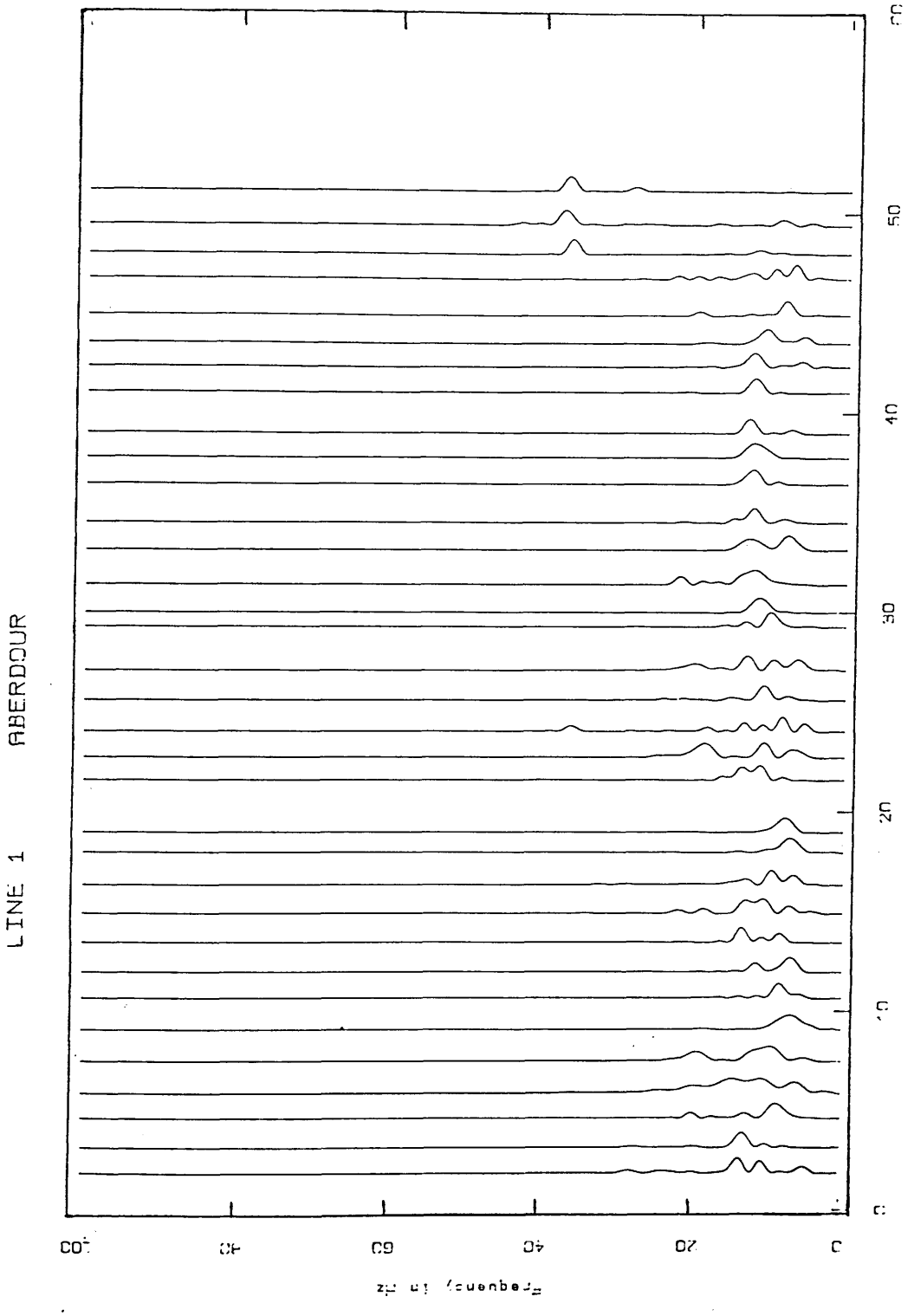

Fig.4.19a Spectral analysis for line 1 (Aberdour shot).

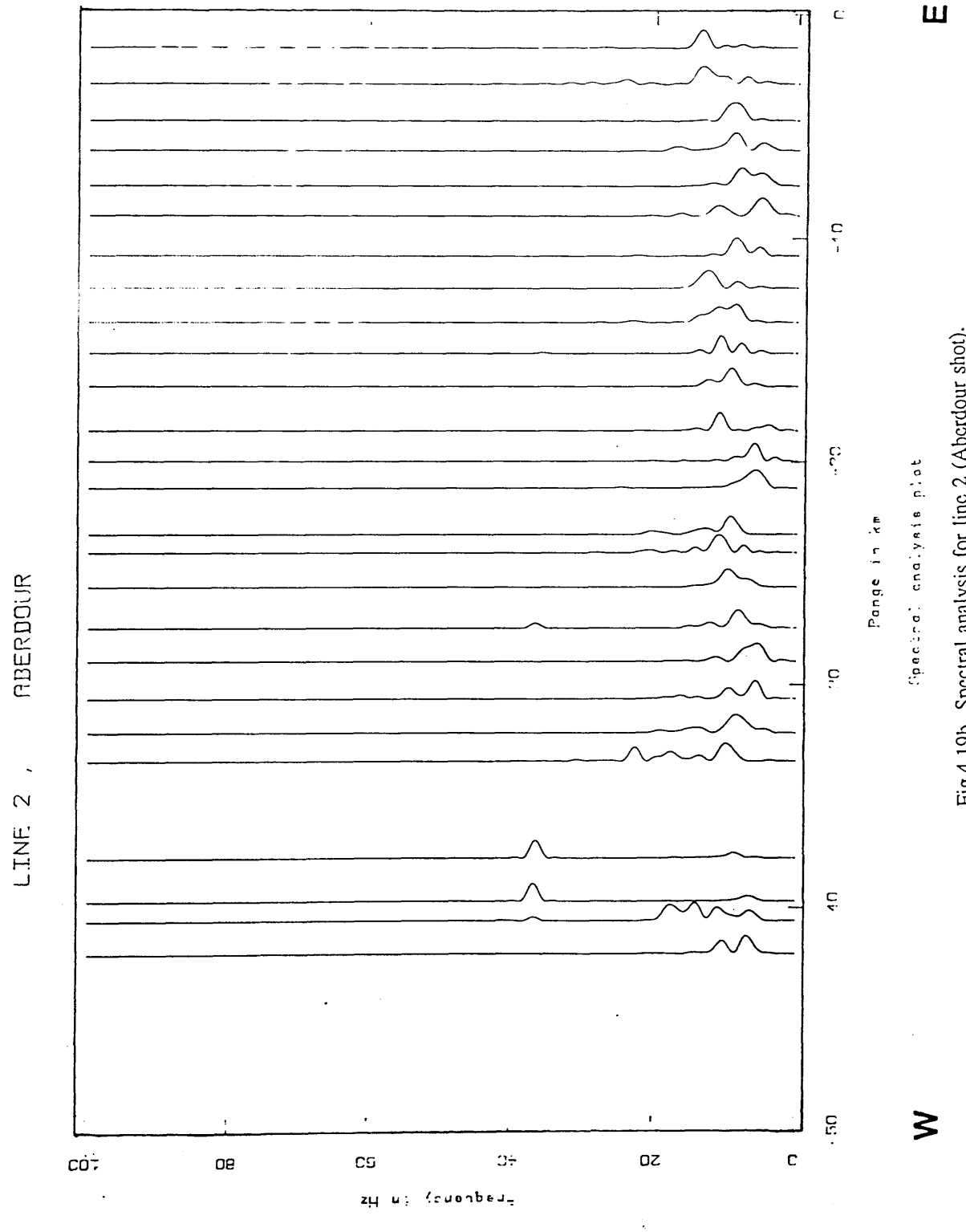

Fig.4.19b Spectral analysis for line 2 (Aberdour shot).

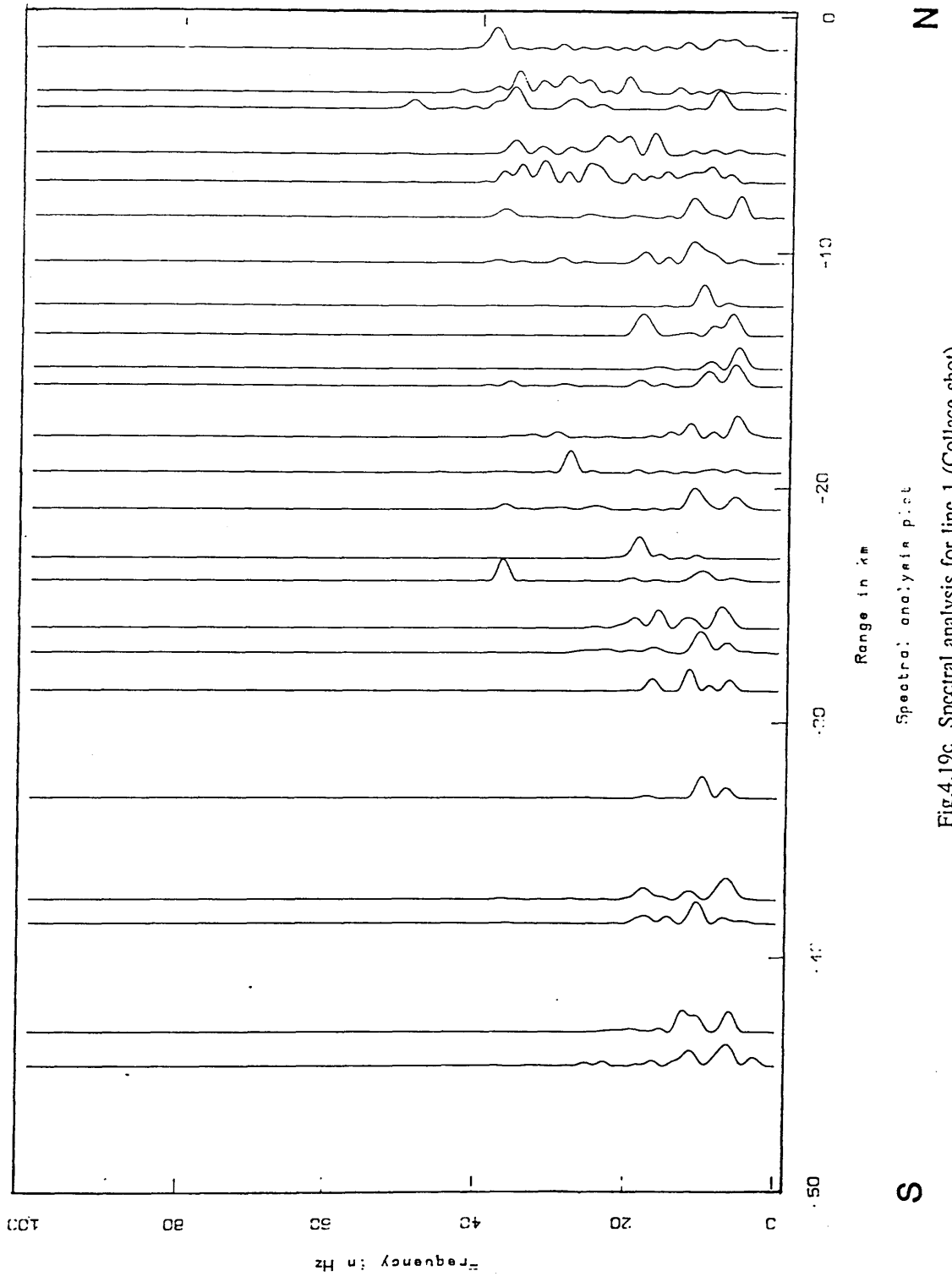

Fig.4.19c Spectral analysis for line 1 (Collace shot).

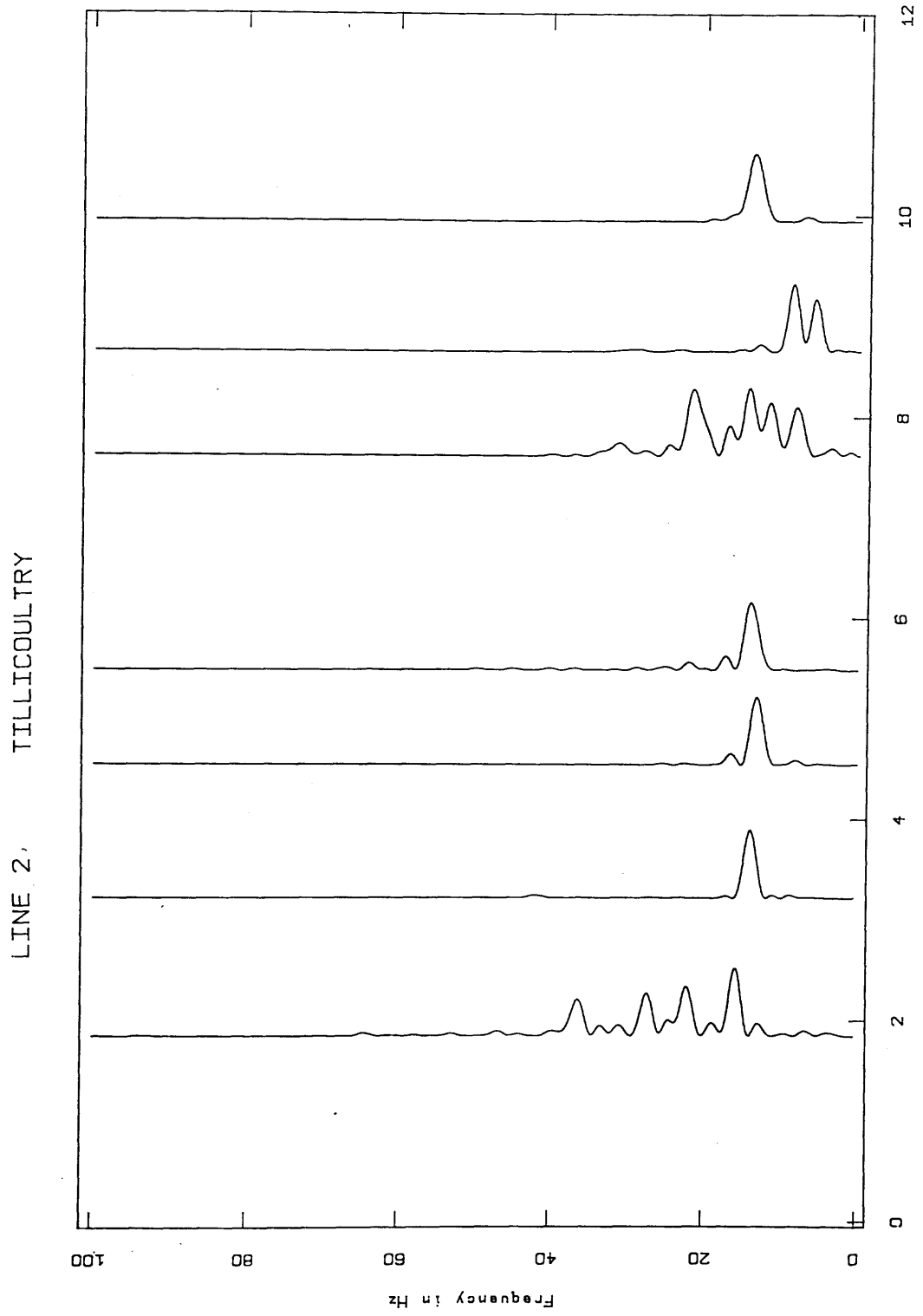

Fig.4.19d Spectral analysis for line 2 (Tillicoultry shot).

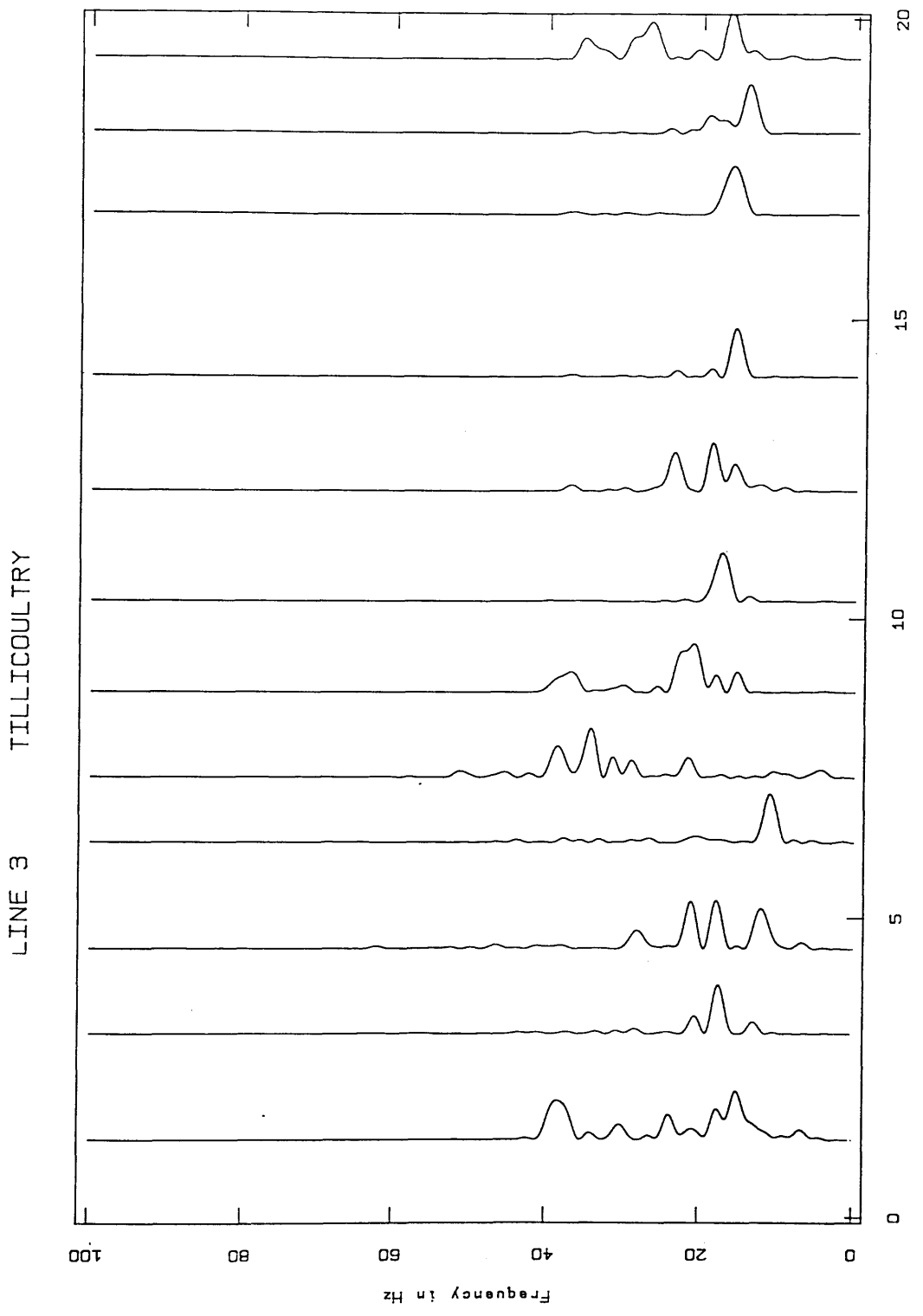

Fig.4.19e Spectral analysis for line 3 (Tillicoultry shot).

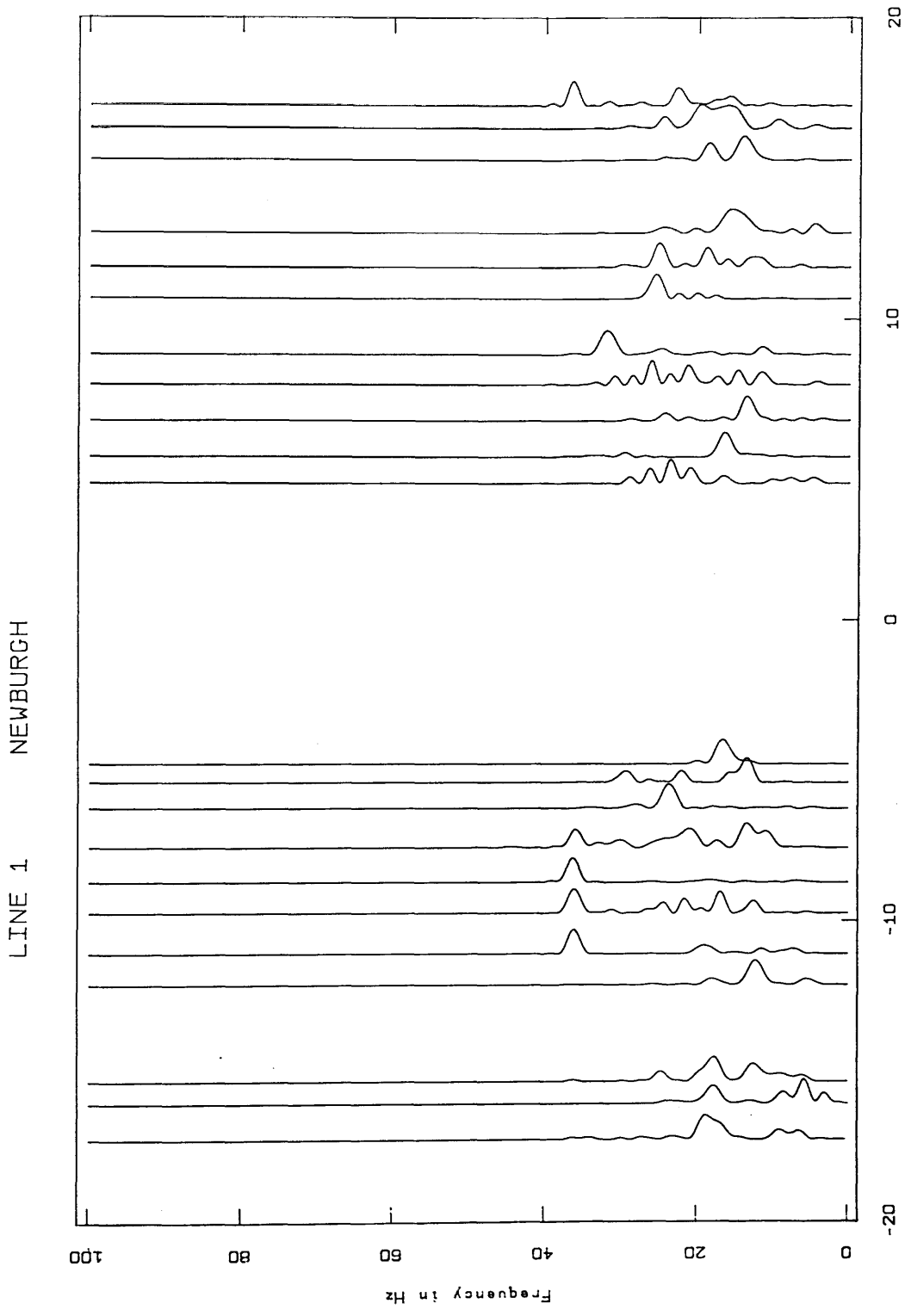

Fig.4.19f Spectral analysis for line 1 (Newburgh shot).

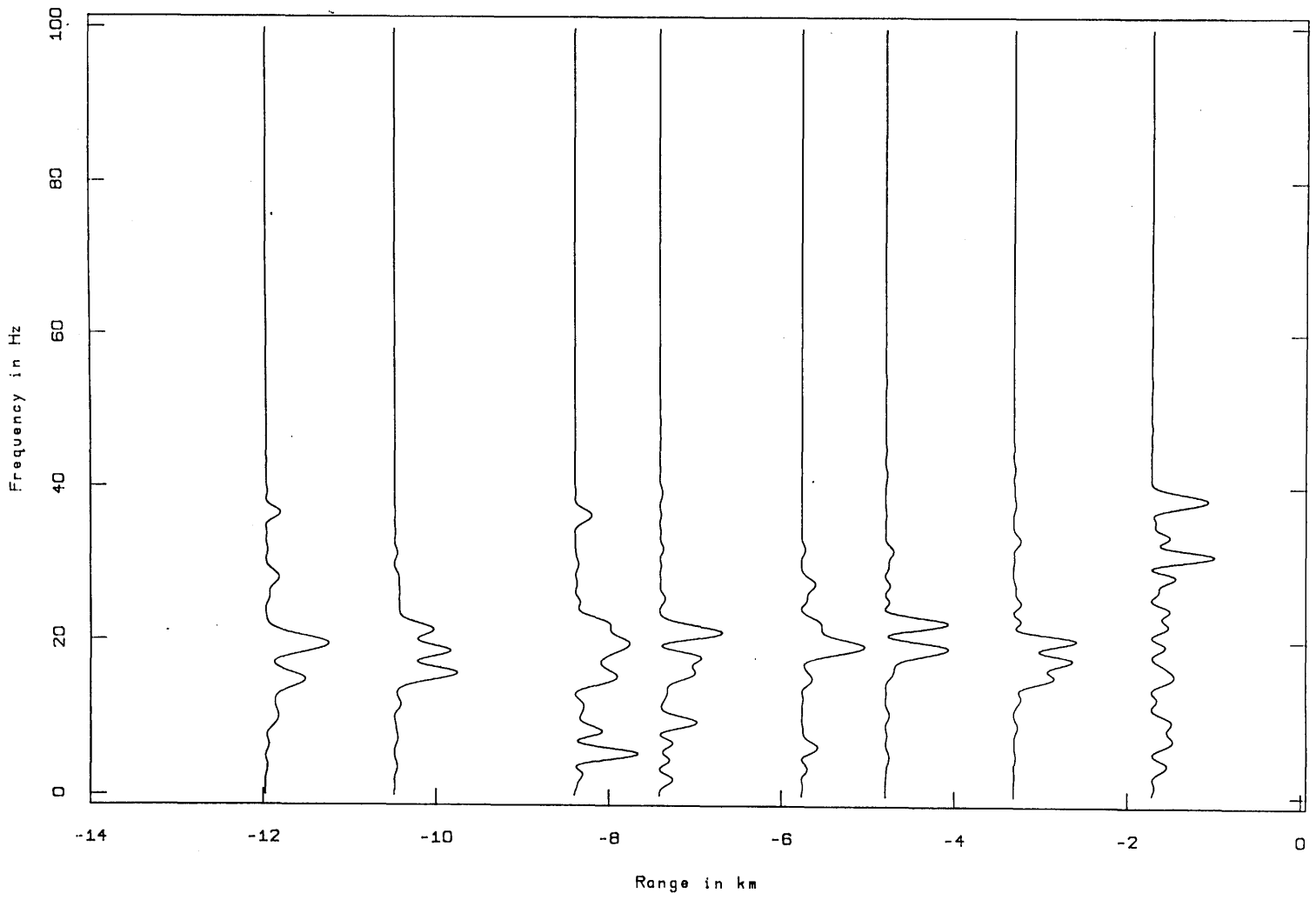

Fig.4.19g Spectral analysis for line 4 (Newburgh shot).

A higher range of P-wave frequencies (Fig. 4.19f) was obtained from Newburgh quarry(12-22 Hz). This represents a change of frequencies compared to data recorded from other quarries along the same profile. This quarry also uses gelatine explosive, but the higher band of frequency peaks derived may be due to the way each hole is fired. The charge in each hole is divided into three portions: the largest (about 60%) at the bottom, a smaller charge midway and the smallest about 1 m from the top. The three portions are separated by packed sand and delays are placed between them. This may have caused the wider frequency band. This method is only applied in this quarry so this hypothesis cannot be confirmed by data from other quarries.

The same frequency peaks were obtained along line 4 from Newburgh (Fig. 4.19g), recorded in an E-W direction (Fig. 1.1a). This line crosses different lithology than the middle section of line 1 (also recorded from Newburgh), but gave the same results.

Therefore engineering practices at quarries may have some effect on frequencies but this cannot be confirmed using the present data set. However, data recorded from Newburgh quarry suggest that further studies should be made to analyse such affect.

Newburgh and Collace quarries are both situated on the same type of rock (andesite) but frequency peaks obtained from both quarries are different. This suggests that the type of rock at the quarry has little effect. The role of the local lithology at the quarry acting as a "filter" permitting only certain frequency bands to be transmitted cannot be disregarded, although the above example suggests otherwise.

The only parameter common to all quarries is the type of explosive used (plaster gelatine). This might be the reason for the general similarity in frequency peaks. Small differences in frequency content might be attributed to the proportions in which explosives are mixed. A mixture of plaster gelatine and ammonium nitrate is sometimes used to cut costs. This may explain the difference in P-wave frequency ranges derived along line 2 since at Aberdour quarry only plaster gelatine is used, while at Tillicoultry quarry a mixture of high explosive and fertilizer is employed. However, the possibility of the effect of the other factors mentioned above should be considered.

No discrimination between lithological units on the bases of frequency studies in the area was made because of the preservation of energy for long distances and thus no change in wave properties across different rock units was observed. Also, cross-over distances could not be resolved using

frequency changes because of the above reasons.

In conclusion, frequency analysis was used to determine the P-wave peaks characteristic of each quarry and they were later used to design the appropriate band-pass filters. It illustrated the affect of lithology and quarries on the P-wave frequencies, suggesting that the type of explosive, and perhaps, engineering practices at the quarry are the major factors affecting these frequencies.

4.4. Application of the Inversion Methods

The WHB and tau-p methods were used to determine the velocities of the topmost layers along the profiles. Both techniques were contained in a program written by J. Hall and modified by K. Davidson and M. Dentith. The program can read data at irregular intervals where the time-distance segments are well constrained. Five curves were fitted to the data representing the best fit curve, the straightest, the most curved, the maximum and minimum fit to the error bars respectively. The program was applied to all "direct arrivals" since these displayed curved arrival segments indicative of vertical and/or horizontal velocity changes in the near surface layer.

However, the two methods suffer a serious limitation when applied to data from the Midland Valley. The program assumes only vertical velocity variation to be present, but steep dips, rapid lateral facies changes, heavy faulting and the presence of igneous bodies will lead to significant lateral changes of velocity.

The necessity to know the surface velocity (V0) for tau-p comprised another problem. Since all lines were recorded using quarries in igneous rock, on which the first few receivers were also situated. The remaining stations, corresponding to the main direct arrival segments, were located on sedimentary rocks in most cases. Since the igneous rocks were sometimes associated with a higher velocity, the curves had to be smoothed at such stations, omitting such close receivers in order to obtain the necessary curves. No smoothing was applied if this affect is observed for more than two stations. This process was undertaken for both techniques.

The assumption that u1=1/Vappl (section 3.4.4) is often invalid since short offset receivers are frequently absent, or are on atypical igneous rock. The program allows a parameter V0 to be input, but this can often only be estimated since the necessary data are not available. When applying the tau-p method underestimation of V0 causes overestimation of velocity at a given depth and overestimation of

V0 distorts the shape of the velocity-depth curve near the surface.

Dentith (1987) suggests that a surface velocity of 3.0 km/s produces the best results in the Midland Valley. This value could not be applied to data derived at the northern section of line 1 due to the abundance of large thicknesses of lava with surface velocity higher than 3.0 km/s. However, this velocity was applied where appropriate.

Error bars (discussed in section 3.2) of 0.03 s were applied to all arrival times to obtain the five smoothed curves fitted to the data. Figure 4.20 shows the velocity-depth data with the corresponding time-distance curves obtained along line 1 from Aberdour using WHB. A velocity range of 4.2-4.9 km/s corresponding to direct arrivals from Carboniferous and Upper Devonian rocks is seen with the maximum velocity being at a depth of 1.3 km. Studying tau-p results for the same data (Fig. 4.21), the effect of overestimation of the surface velocity can be observed where no results are obtained at shallow depths. Figure 4.22 show the WHB and tau-p results on the same plot for comparison.

Application of the WHB inversion for data recorded from Collace is shown in Figure 4.23. Direct arrivals detected along this line correspond to Lower Devonian rocks with a velocity range of 4.4-4.7 km/s and a maximum depth of 0.8 km. Dentith (1987) obtained similar results along the MAVIS I north line to the south of the Tay Graben (4.5 km/s at 0.8 km depth). Tau-p results of this shot are shown in Figure 4.24, assuming a surface velocity of 3.0 km/s while Figure 4.25 illustrates the effect when V0 is increased to 4.0 km/s. Comparison of the two figures show how the results are affected when the surface velocity is underestimated.

WHB results from Newburgh, recording to the north and the south, are shown in Figures 4.26 and 4.27 respectively. A velocity range of 4.4-4.9 km/s corresponding to Upper Devonian rocks in the Tay Graben is obtained towards the north with a depth range of 0.4-1.3 km, while towards the south, traversing Lower Devonian lava, a higher velocity range of 4.7-4.9 km/s with a depth range of 0.4-0.7 km is seen. The tau-p results for the northern and southern sections of this shot are shown in Figures 4.28 and 4.29 where a V0 value of 3.0 km/s is applied to the northern section to compensate for the effect of layer 1 which gave better results, while to the south, where the profile traverses Devonian lava, a surface velocity of 4.0 km/s was used. Similarities in velocities and corresponding depths between the Newburgh north and Collace data suggest a uniform velocity profile in the top 1 km between these shotpoints. Figures 4.30 and 4.31 show a comparison between the two inversion methods for the two

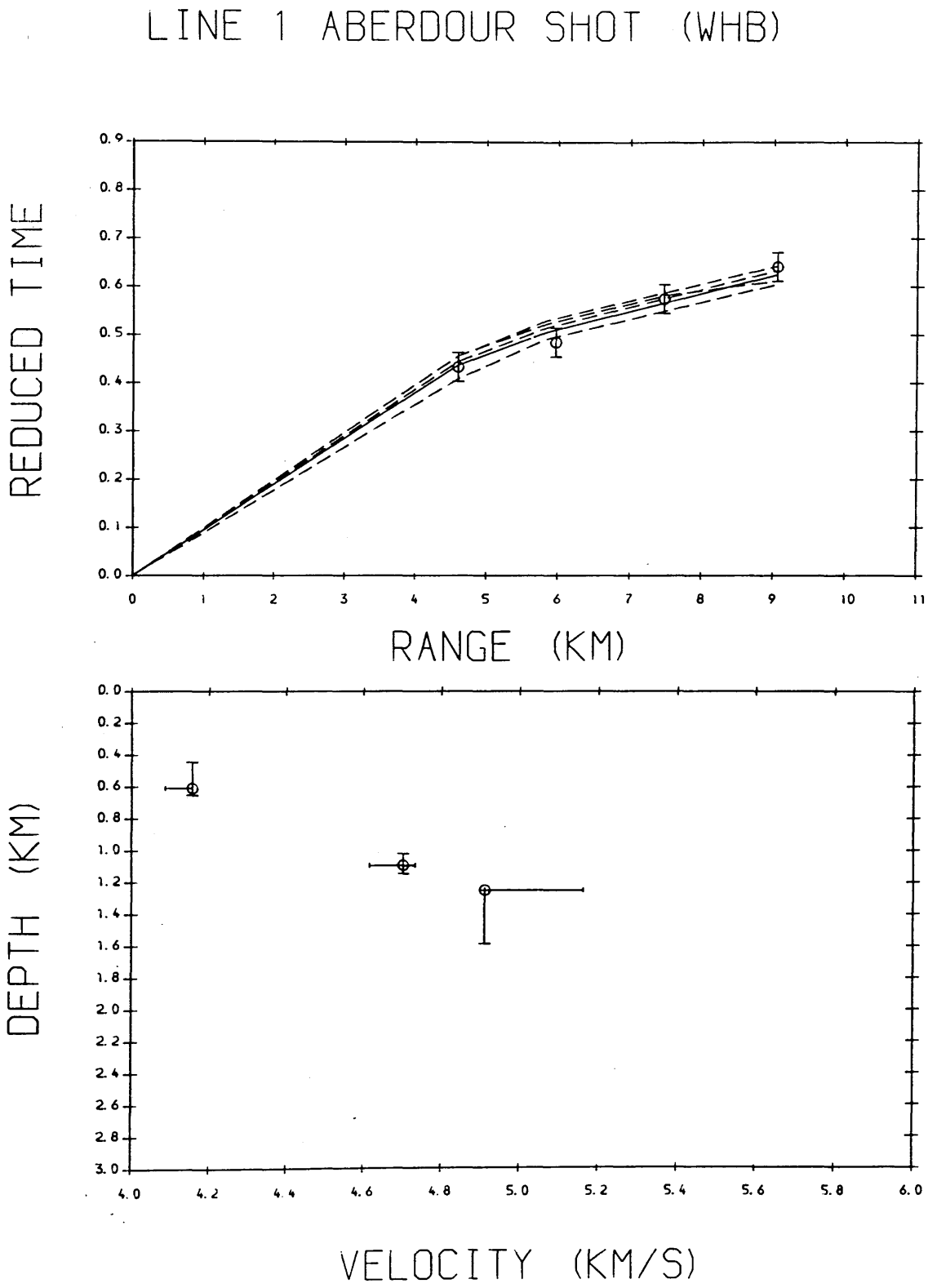

Fig.4.20 Time-distance and velocity-depth data from WHB inversion; line 1 (Aberdour shot). Reduction velocity is 6.0 km/s. Surface velocity is 3.0 km/s.

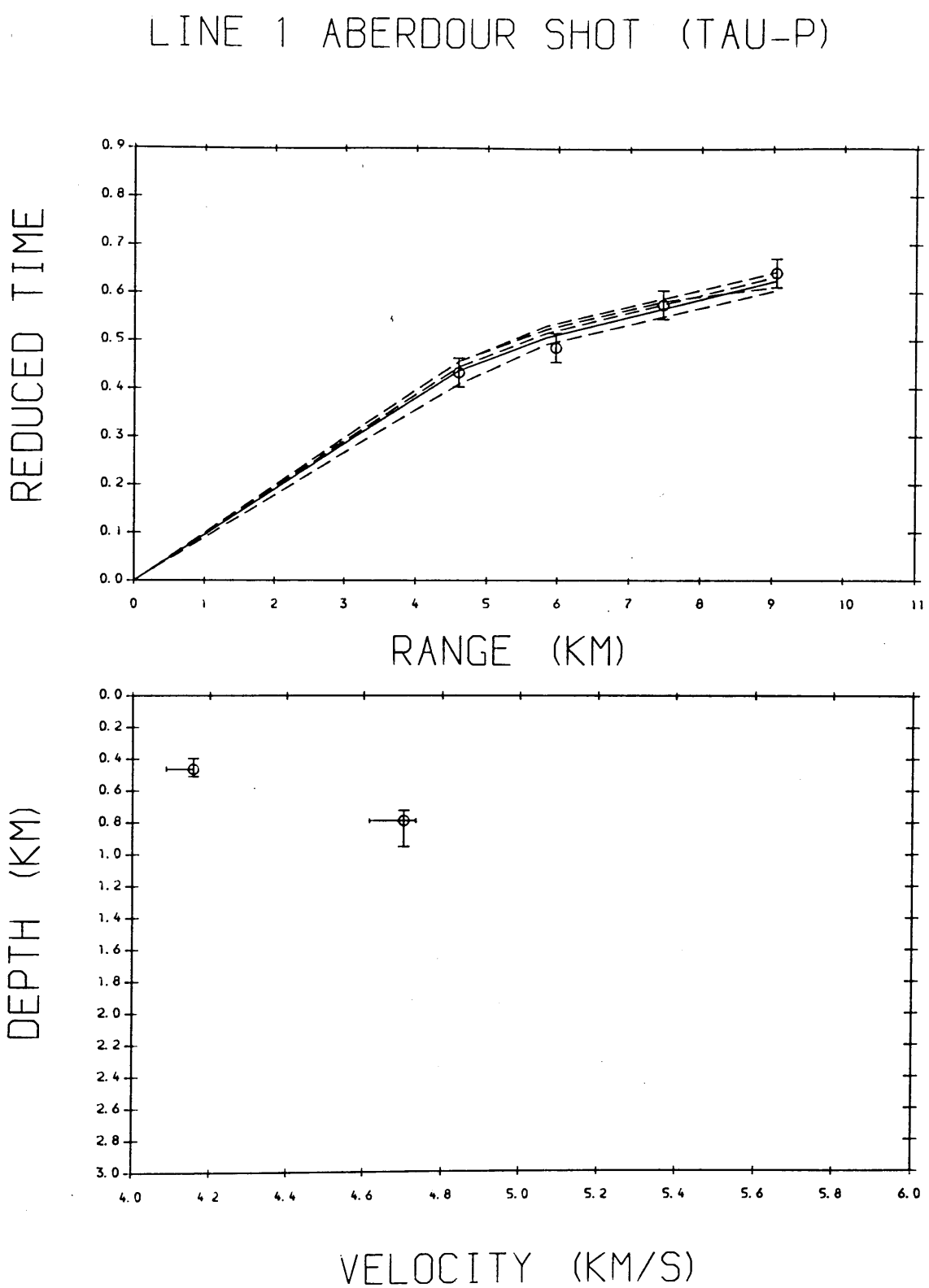

Fig.4.21 Time-distance and velocity-depth data from tau-p inversion; line 1 (Aberdour shot). Reduction velocity is 6.0 km/s. Surface velocity is 3.0 km/s.

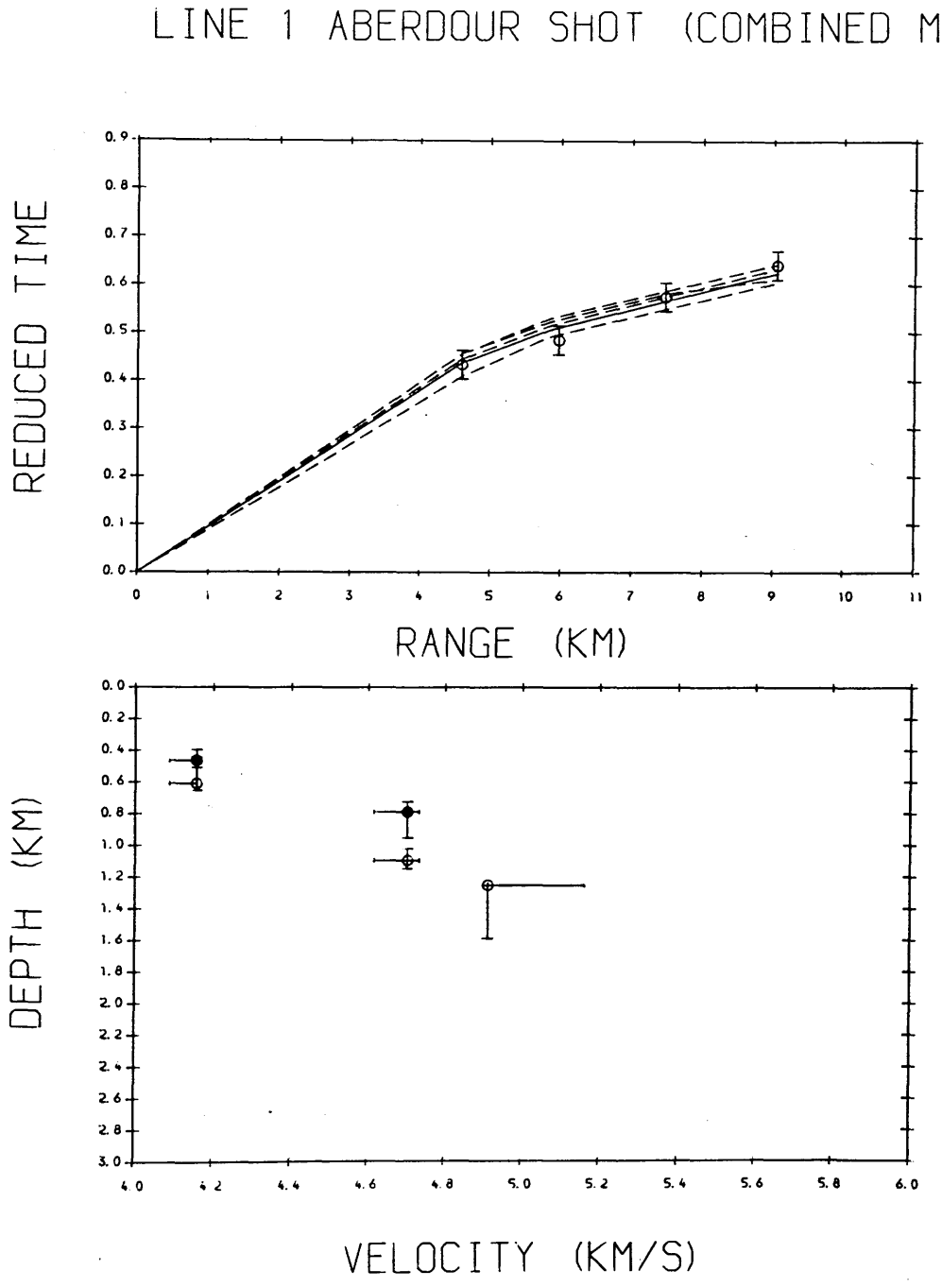

Fig.4.22 Comparison of WHB and tau-p data. WHB open circles, tau-p data solid circles. Data along line 1 (Aberdour shot). Reduction velocity is 6.0 km/s. Surface velocity is 3.0 km/s.

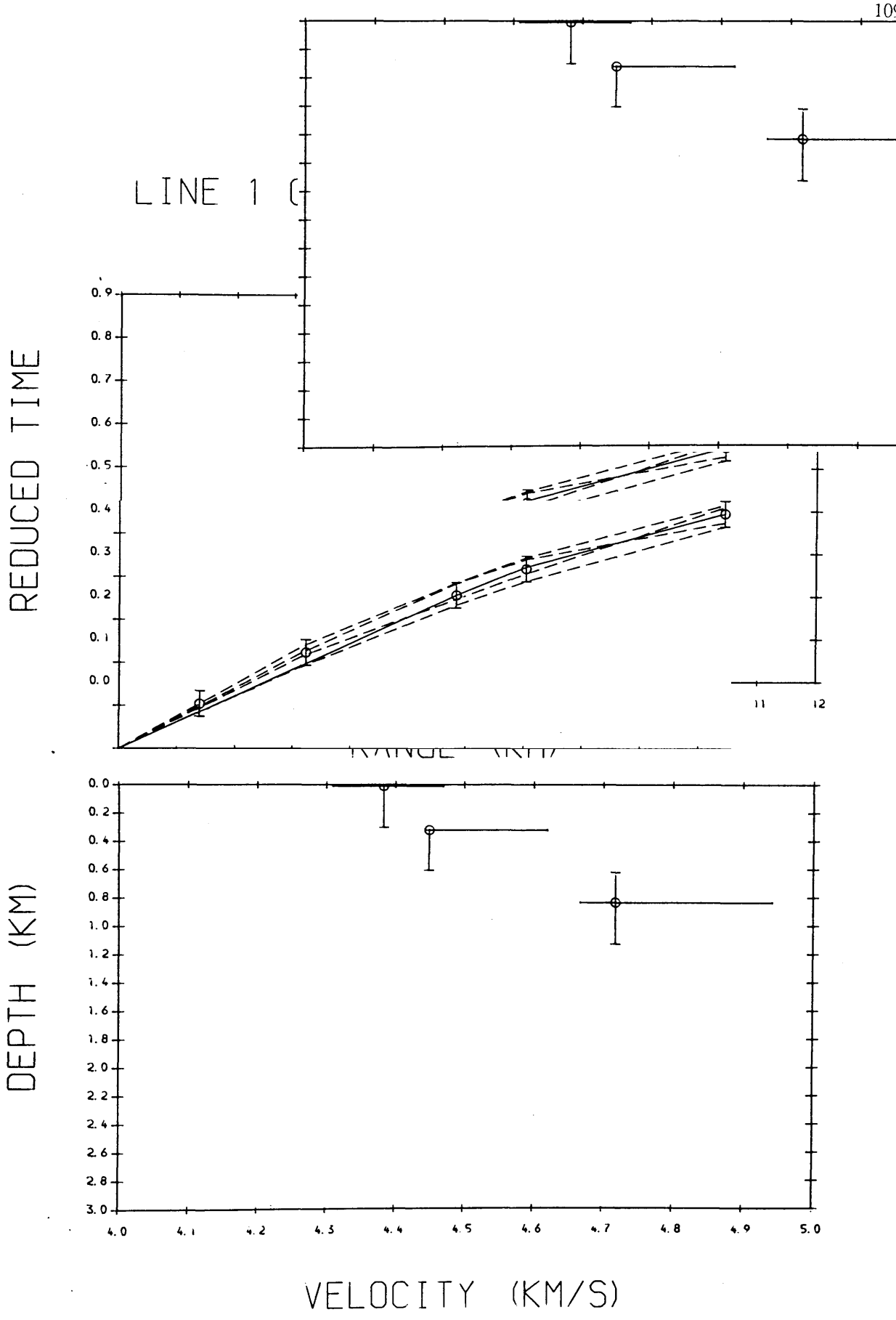

Fig.4.23 Time-distance and velocity-depth data from WHB inversion; line 1 (Collace shot). Reduction velocity is 6.0 km/s. Surface velocity is 4.0 km/s.

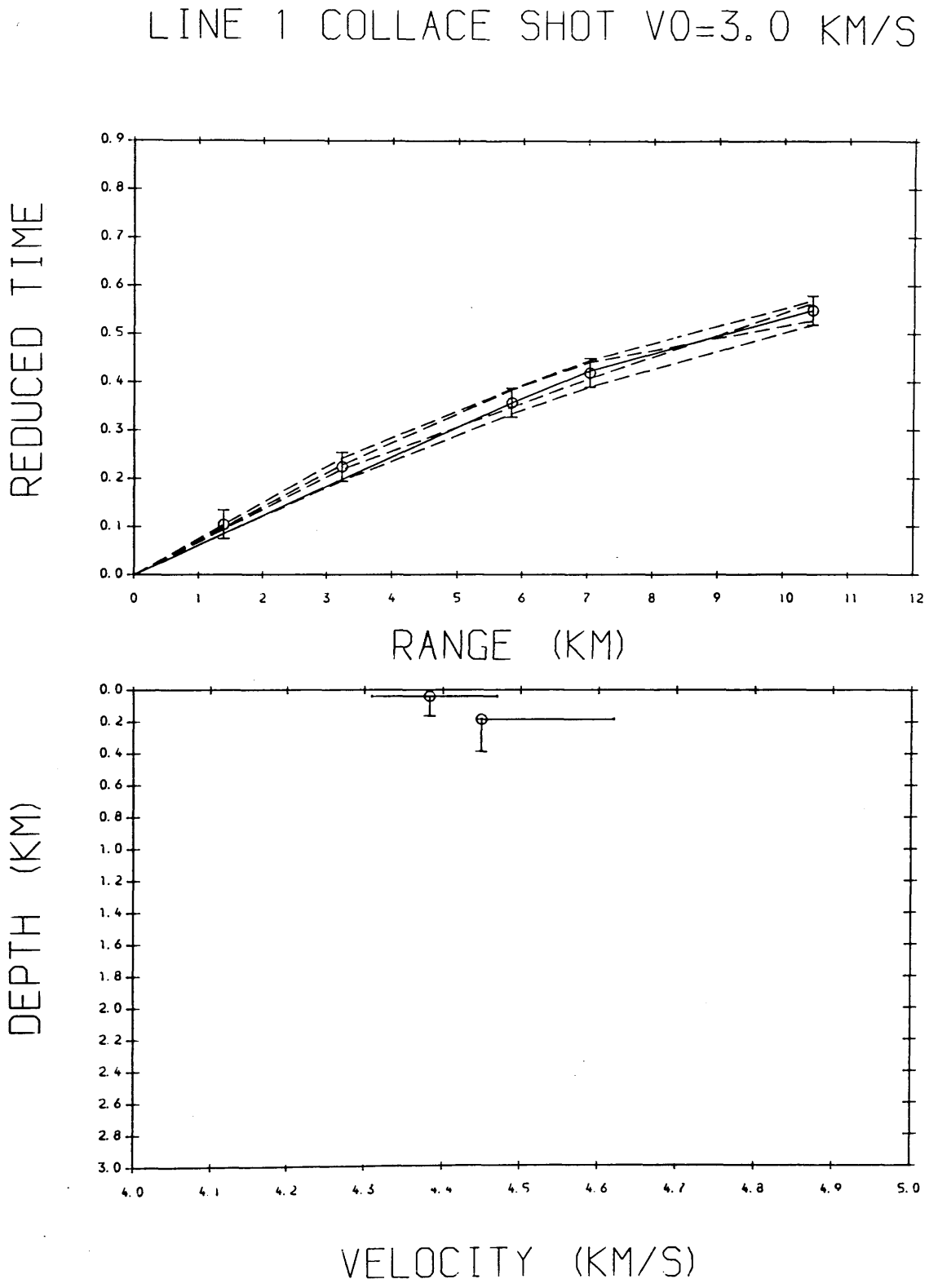

Fig.4.24 Time-distance and velocity-depth data from tau-p inversion; line 1 (Collace shot). Reduction velocity is 6.0 km/s. Surface velocity is 3.0 km/s.

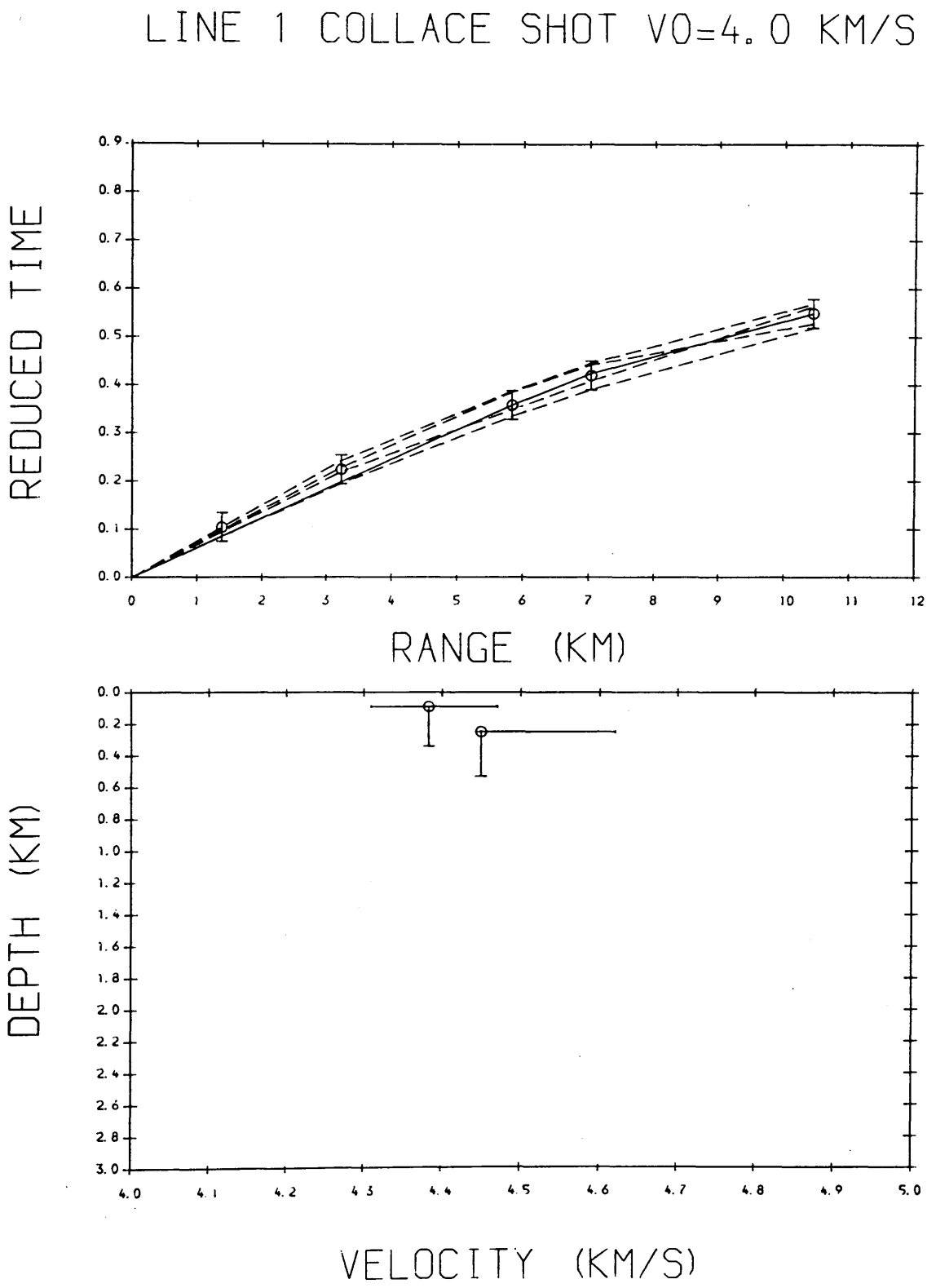

Fig.4.25 Time-distance and velocity-depth data from tau-p inversion; line 1 (Collace shot). Reduction velocity is 6.0 km/s. Surface velocity is 4.0 km/s.

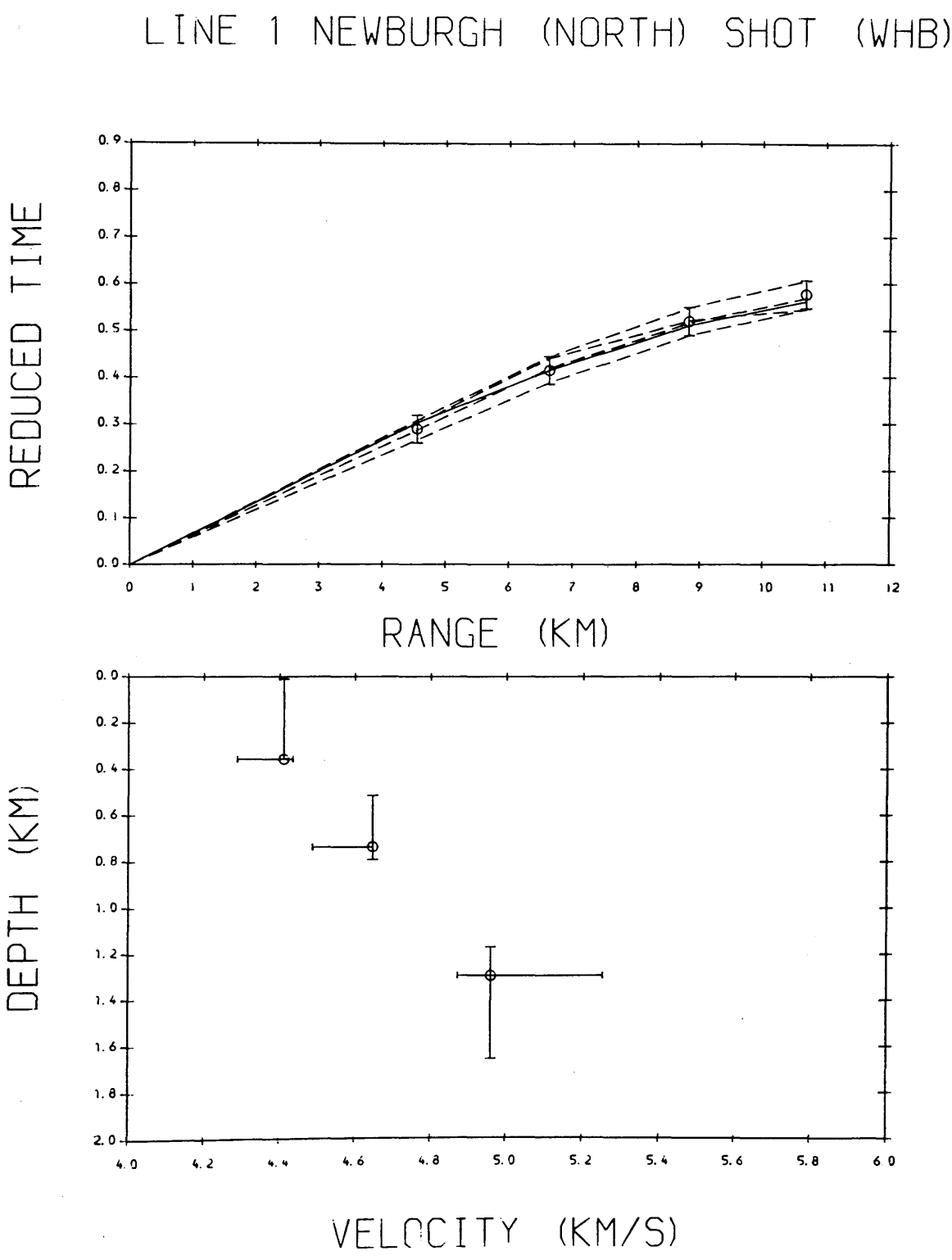

Fig.4.26 Time-distance and velocity-depth data from WHB inversion; line 1 (Newburgh north shot). Reduction velocity is 6.0 km/s. Surface velocity is 4.0 km/s.

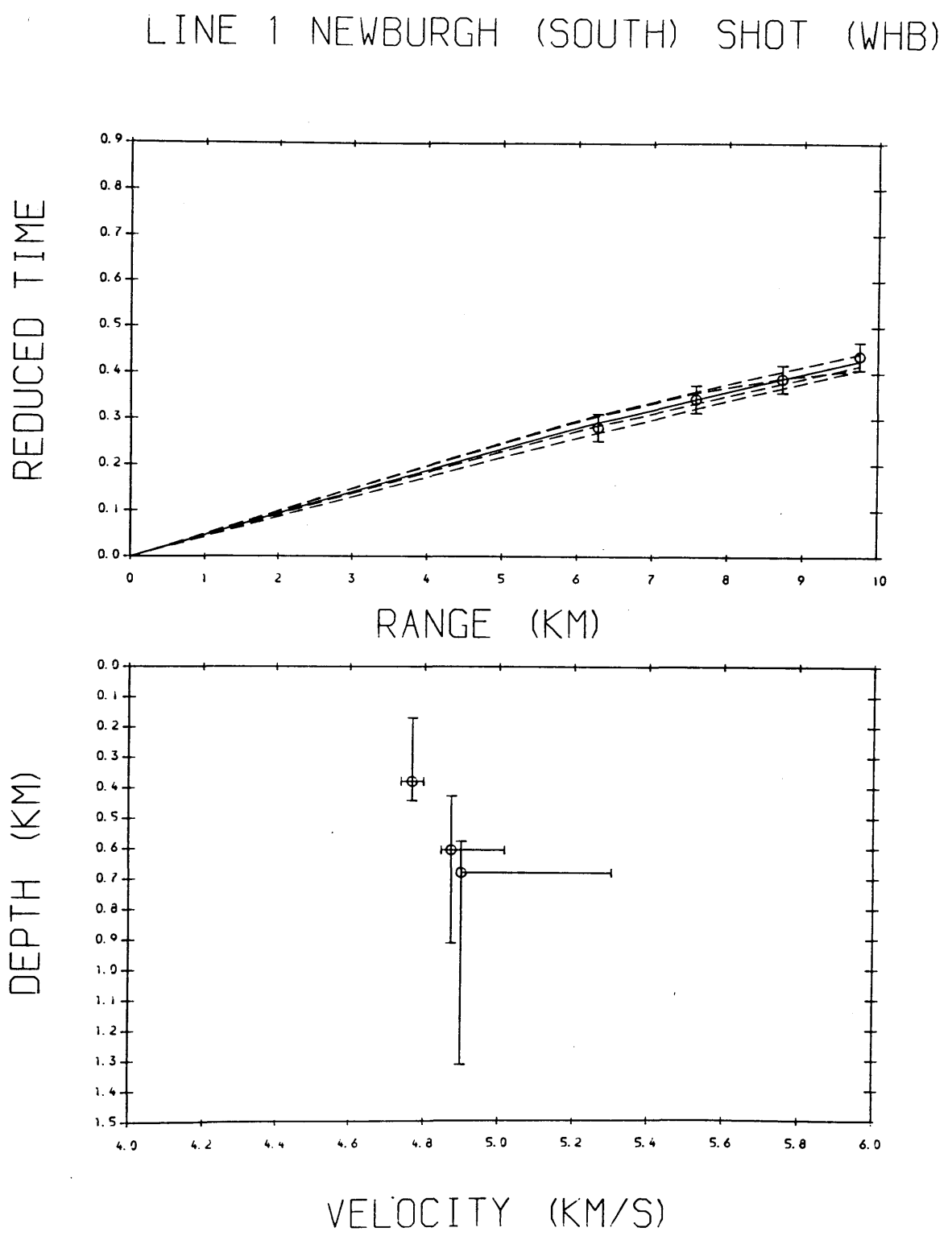

Fig.4.27 Time-distance and velocity-depth data from WHB inversion; line 1 (Newburgh south shot). Reduction velocity is 6.0 km/s. Surface velocity is 4.0 km/s.

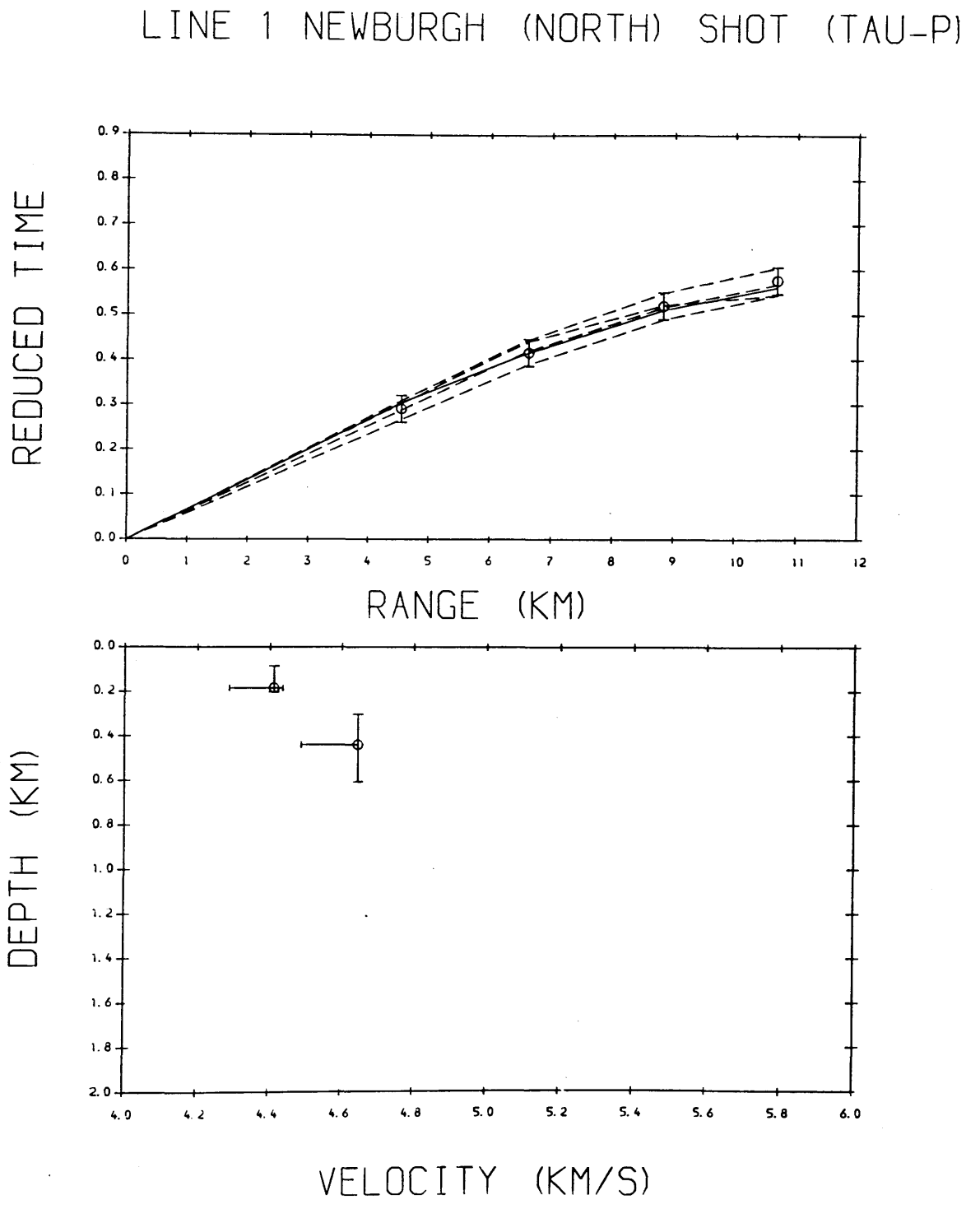

Fig.4.28 Time-distance and velocity-depth data from tau-p inversion; line 1 (Newburgh north shot) Reduction velocity is 6.0 km/s. Surface velocity is 3.0 km/s.

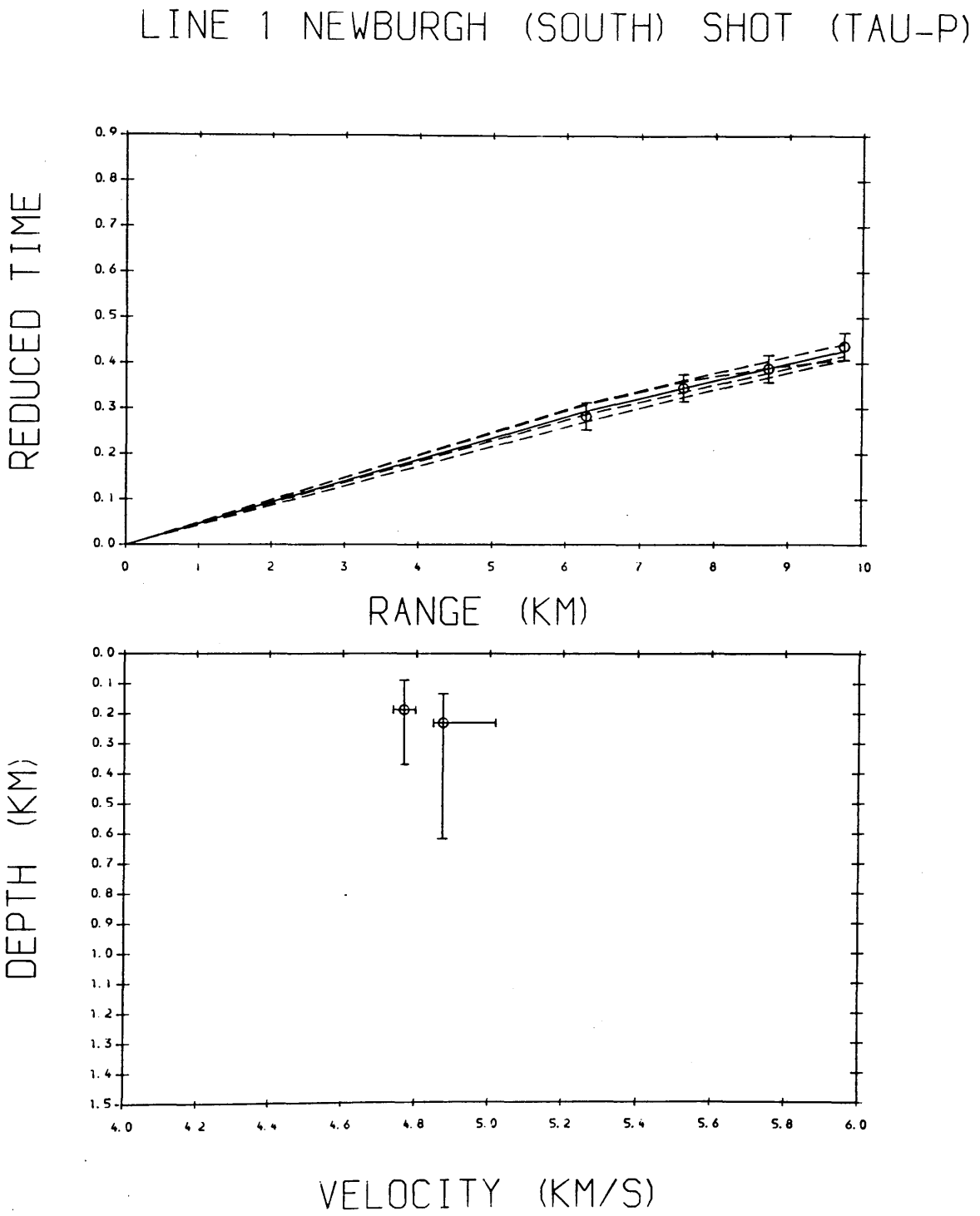

Fig.4.29 Time-distance and velocity-depth data from tau-p inversion; line 1 (Newburgh south shot). Reduction velocity is 6.0 km/s. Surface velocity is 4.0 km/s.

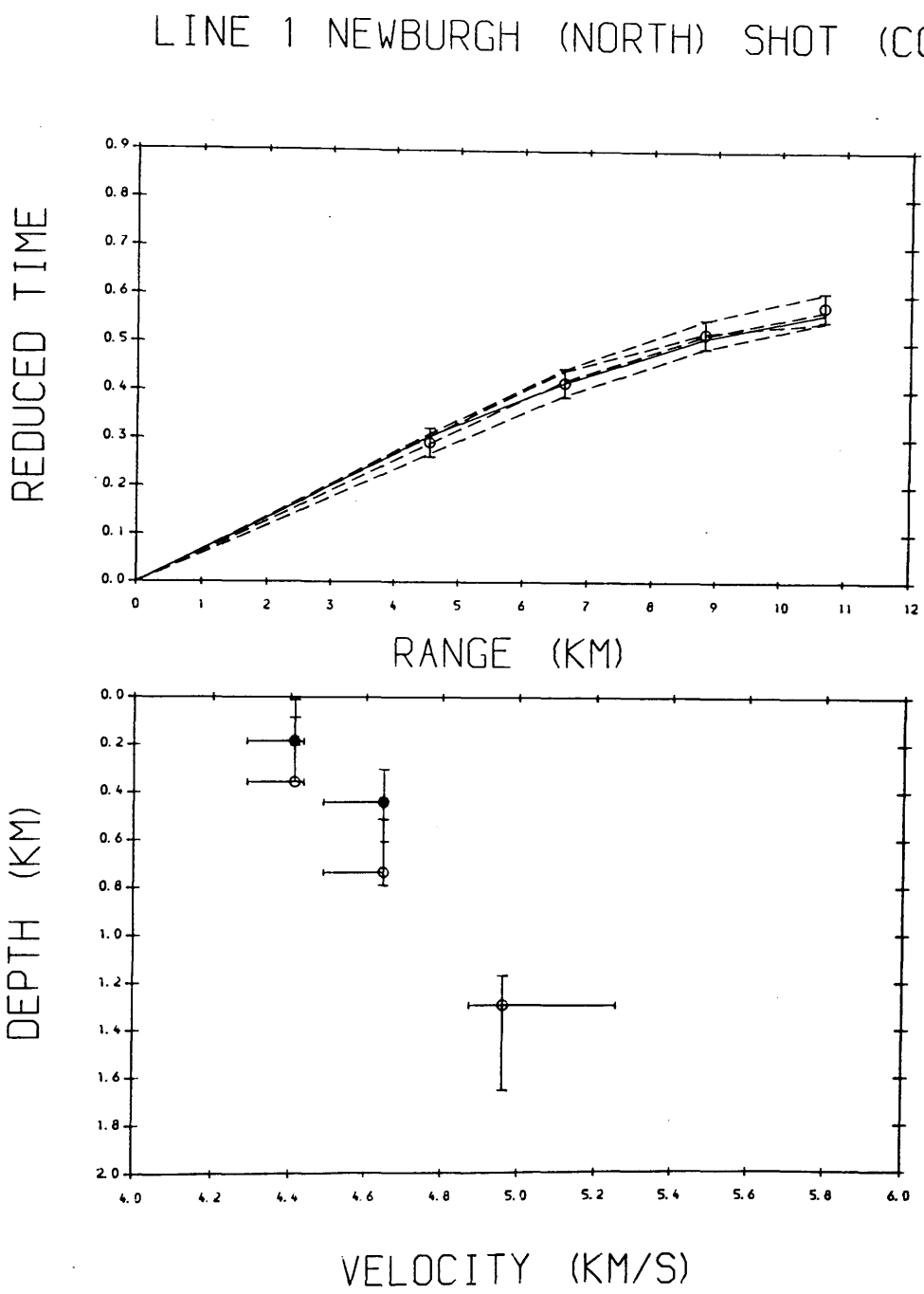

Fig.4.30 Comparison of WHB and tau-p data. WHB data open circles, tau-p solid circles. Data along line 1 (Newburgh north shot). Reduction velocity is 6.0 km/s. Surface velocity is 4.0 km/s.

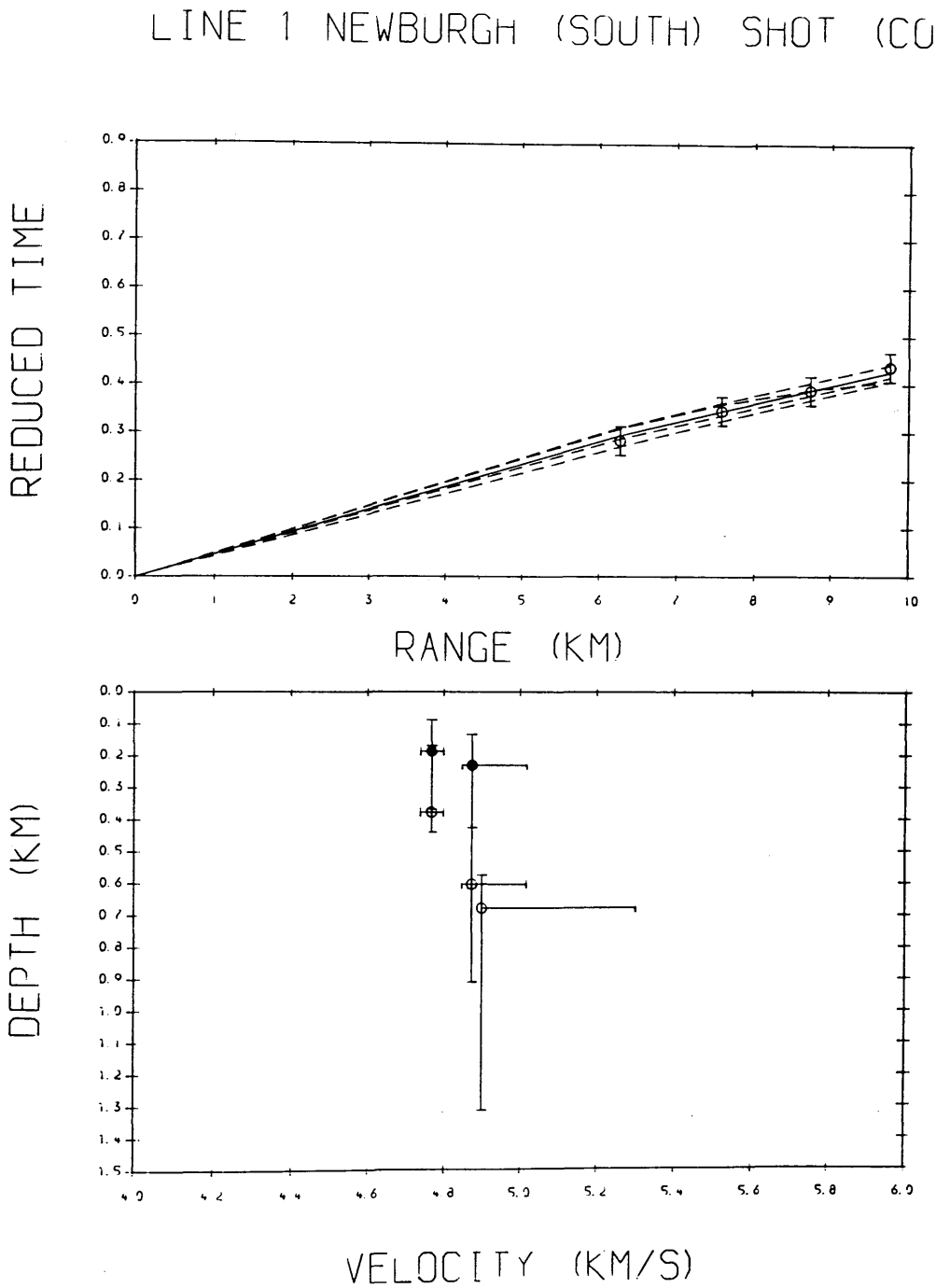

Fig.4.31 Comparison of WHB and tau-p data. WHB data open circles, tau-p solid cicles. Data along line 1 (Newburgh south shot). Reduction velocity is 6.0 km/s. Surface velocity is 4.0 km/s.

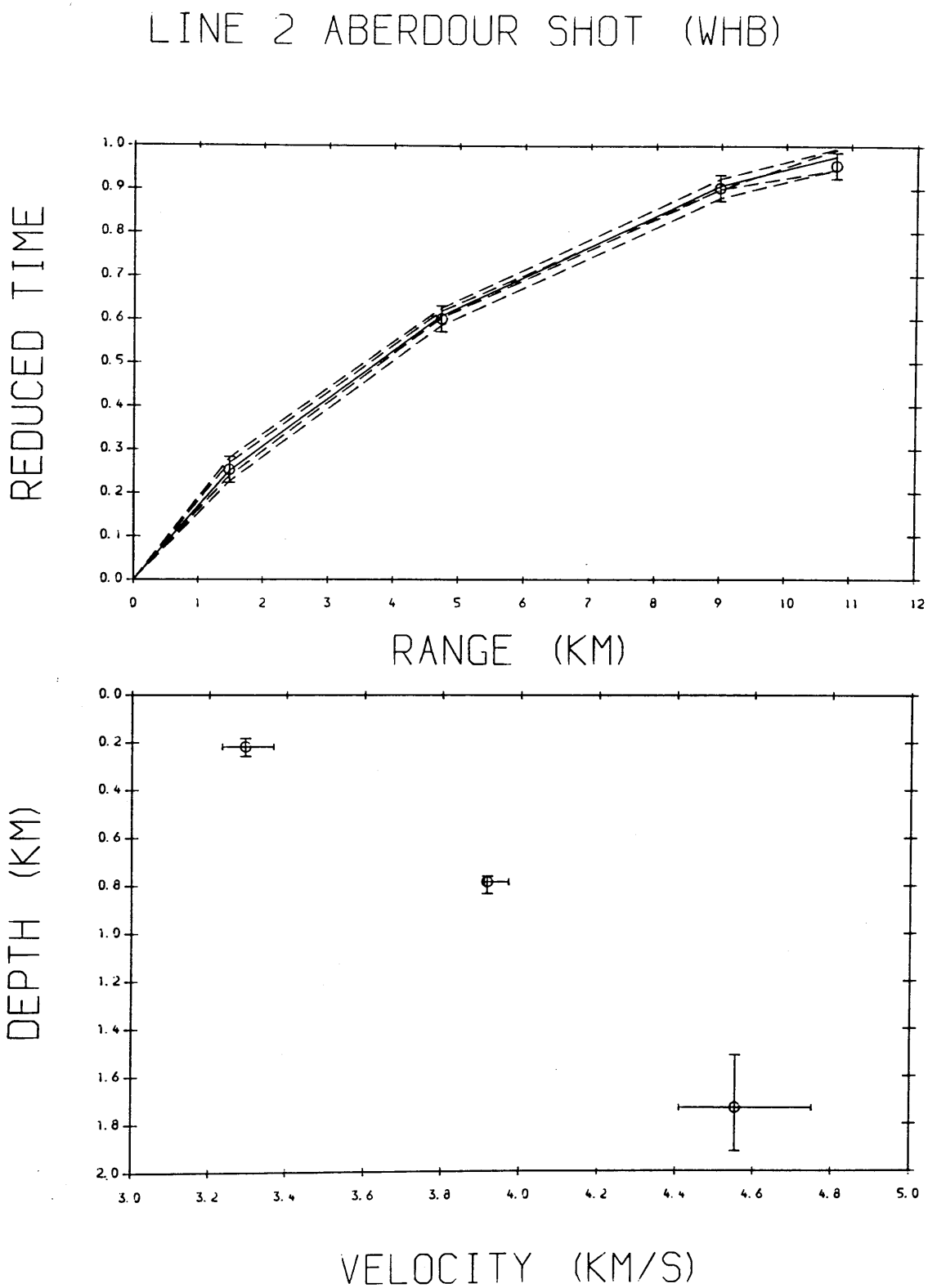

Fig.4.32 Time-distance and velocity-depth data from WHB inversion; line 2 (Aberdour shot). Reduction velocity 6.0 km/s. Surface velocity 3.0 km/s.

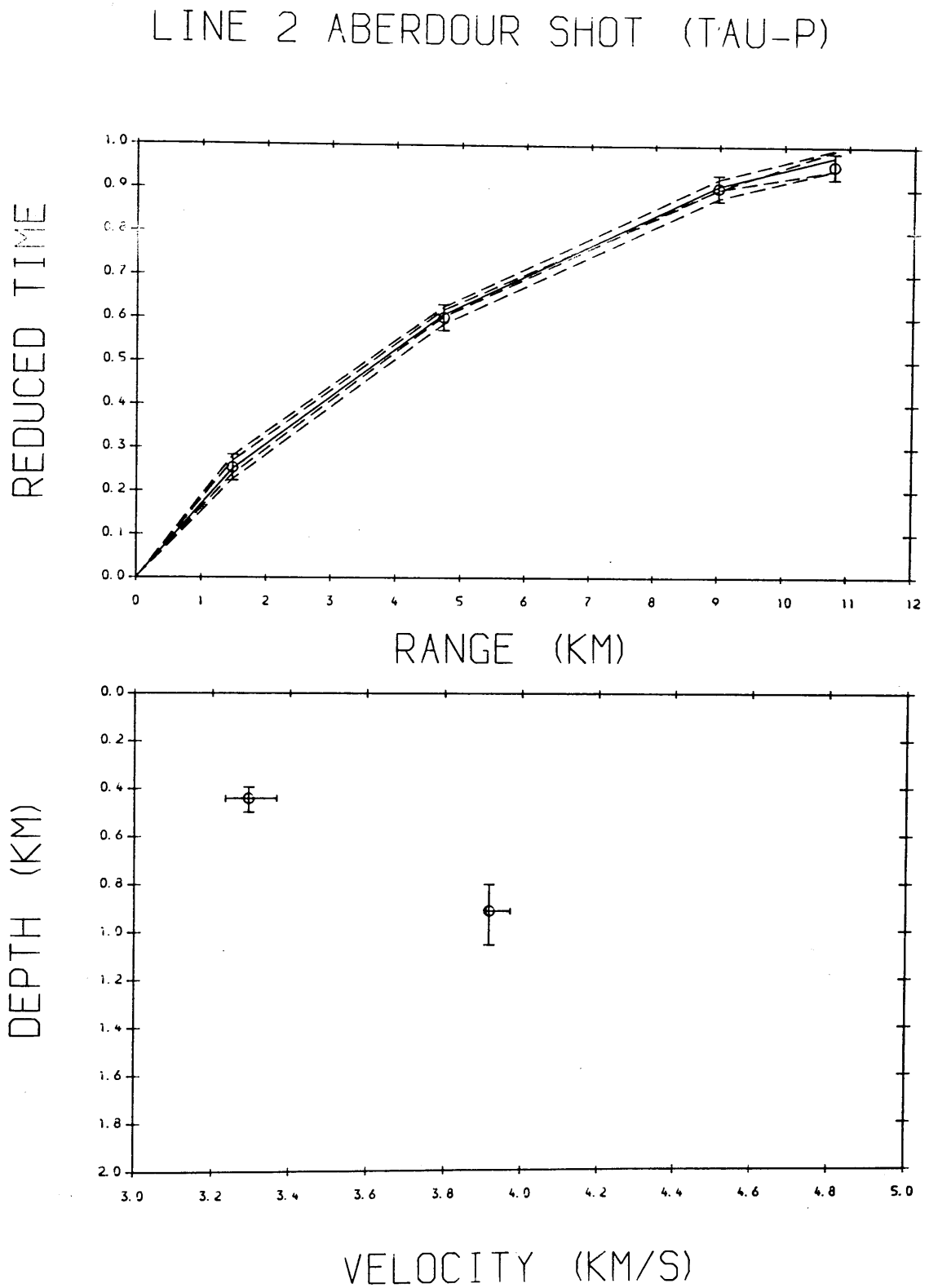

Fig.4.33 Time-distance and velocity-depth data from tau-p inversion; line 2 (Aberdour shot). Reduction velocity is 6.0 km/s. Surface velocity is 3.0 km/s.

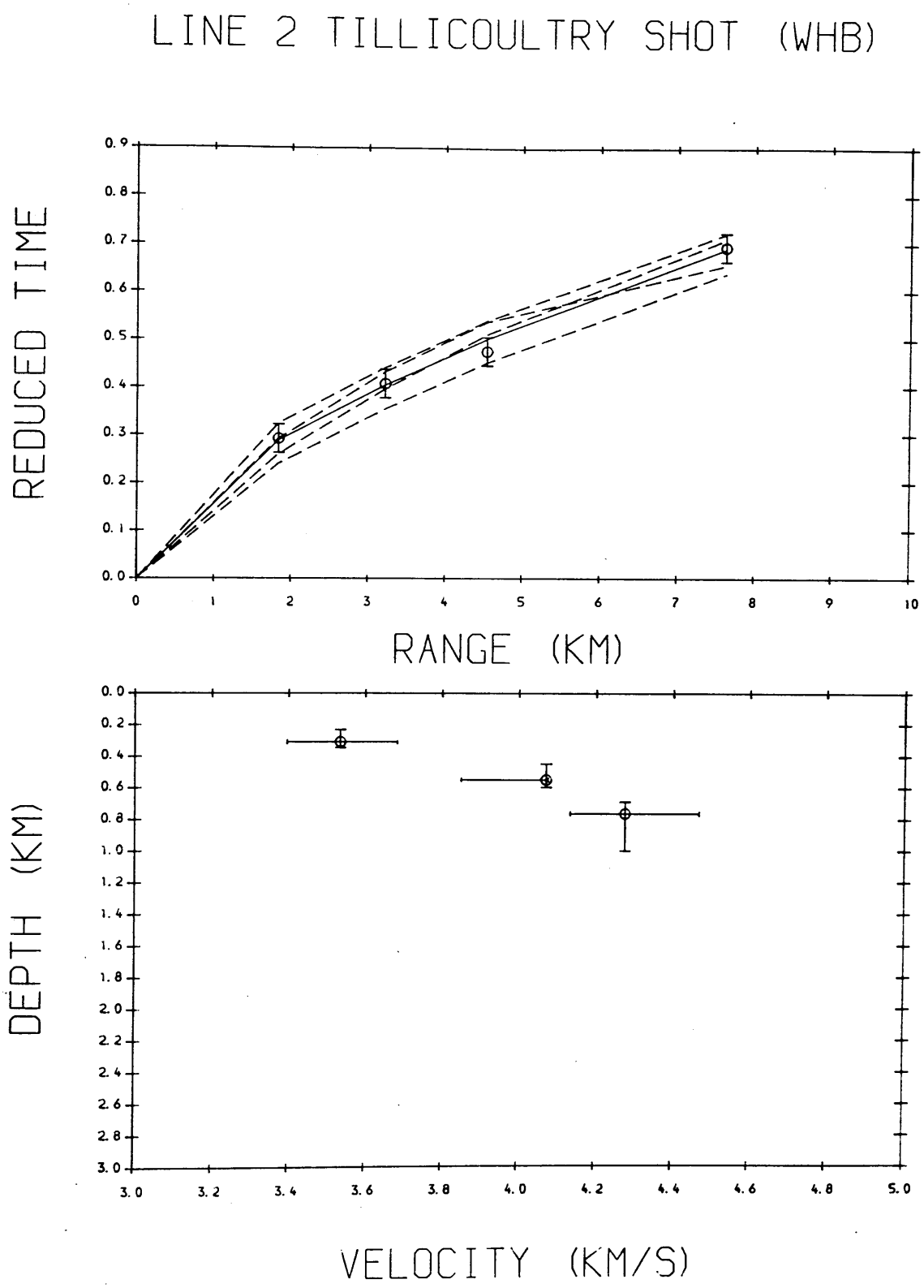

Fig.4.34 Time-distance and velocity-depth data from WHB inversion; line 2 (Tillicoultry shot). Reduction velocity is 6.0 km/s. Surface velocity is 3.0 km/s.

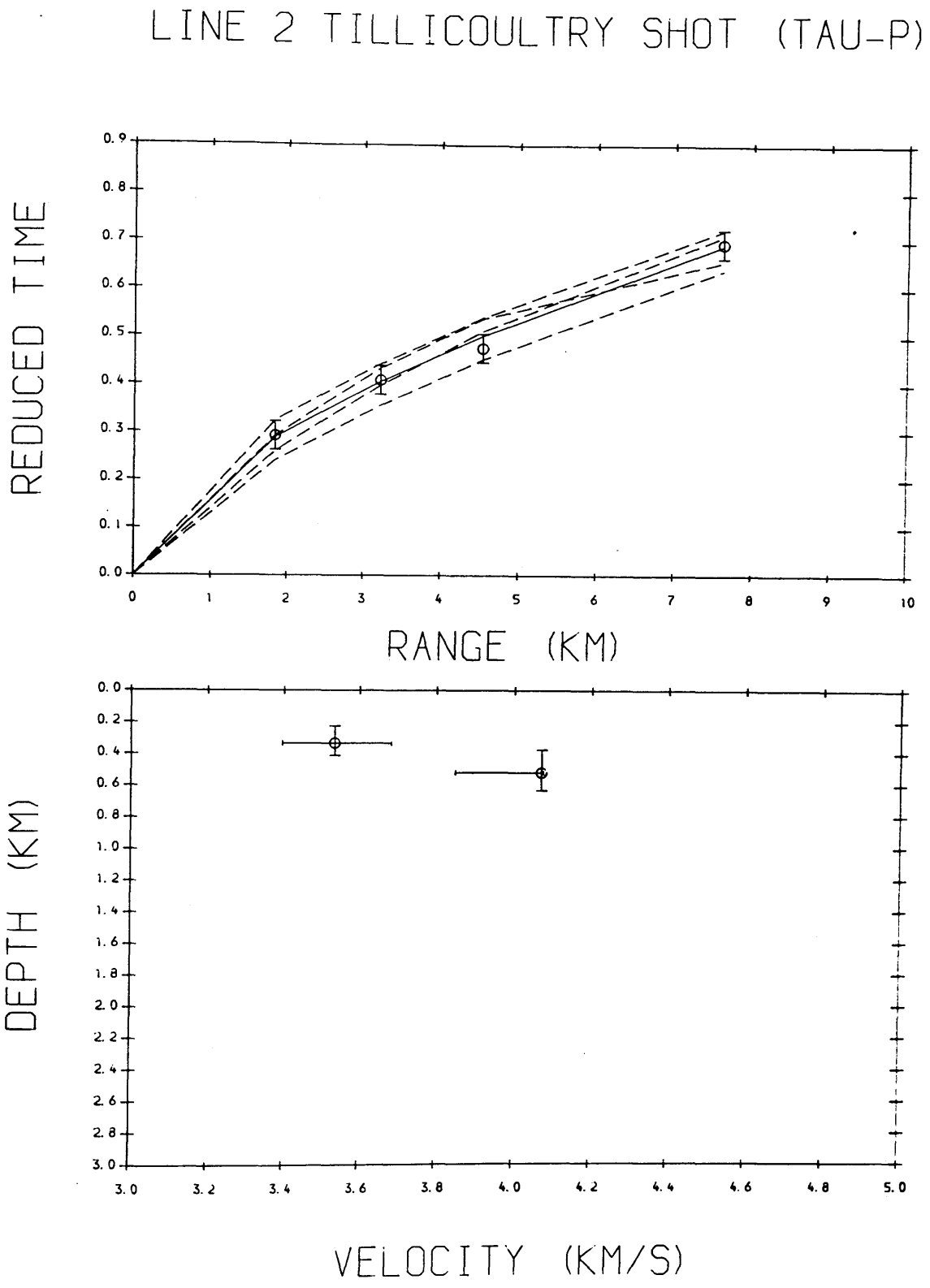

Fig.4.35 Time-distance and velocity-depth data from tau-p inversion; line 2 (Tillicoultry shot). Reduction velocity is 6.0 km/s. Surface velocity is 3.0 km/s.

profiles.

The presence of the Carboniferous and Upper Devonian layer 1 outcrop at much of line 2 with its substantial thickness is reflected in the WHB and tau-p results along this line. Figure 4.32 shows the WHB results derived from Aberdour (with surface velocity of 3.0 km/s). A velocity range of 3.3-4.6 km/s with the maximum velocity being at a depth of 1.7 km is obtained. The tau-p results for this line are shown in Figure 4.33 where another example of the necessity of knowing the surface velocity is evident.

Figures 4.34 and 4.35 show the WHB and tau-p results for the reversed section of this profile from Tillicoultry. A velocity range of 3.5-4.3 km/s is obtained with the maximum velocity at a depth of 0.8 km. Notice the increase of velocity compared to that recorded from Aberdour along the same profile at the same depths. Comparison of Figures 4.20 and 4.32 for the WHB results obtained from Aberdour along lines 1 and 2 gives an indication of the variation in velocity and thickness of layer 1 in the area. In the NE higher velocities occur at a given depth compared to further SW. This appears to be linked to a thickening of layer 1 toward the SW.

The inversion methods were not applied to lines 3 and 4 because of the presence of delayed velocity segments where no smooth curves can be drawn.

It was noticed that the presence of a quarry on igneous rock affected the velocities observed at the closest stations in many cases. A possible explanation is that part of the igneous rock in which the quarry and near receivers are located may have been less influenced by weathering with a consequent smaller reduction of its velocity . Seismic waves travelling in such rock would give velocities near the quarry that are higher than those derived for the rest of the direct arrival segments which would be less due to passage through the mix of sedimentary and igneous rocks that comprise layers 1 and 2 (see section 1.2). Table 4.1 compares the velocities calculated for the first two stations, where curves had to be smoothed with the general velocity of the local topmost layer derived from the WHB at the further stations.

Table 4.1 Comparison between near quarry and topmost layer velocities.

Quarry	Near Quarry Velocity in km/s	Topmost Layer Velocity in km/s
Aberdour	4.3	4.1
Newburgh (N)	4.4	4.3
Newburgh (S)	5.0	4.7

4.5. Planar Layer Interpretation

In section 3.4 the principles of the refraction method were discussed with all the relevant assumptions. In this section initial interpretation of all lines will be carried out using the assumptions of the planar layer method where possible. These simple interpretations served as a guide for modelling by raytracing.

The regression function, which was used to determine all velocity values derived from the time-distance graphs, could not be applied in the case of the first (direct) velocity segments. However, the WHB results were used to determine the velocities of the first layer by correlating the change in velocity with depth and averaging the results. For consistency, all the terminology used in describing the different layers and interfaces by previous projects will be used in all interpretations (see section 1.3). Refer to Figure 1.1b for location of stations mentioned in this section.

4.5.1. Line 1

Figure 4.15 shows the time-distance graph of all the first arrivals derived along this line. Data recorded from Aberdour quarry show 4 distinctive time-distance segments corresponding to layer 1 (observed at an offset of 0-11 km), layer 2 with a crossover distance of 11 km, layer 3 with a crossover distance of 36-37 km. Two groups of arrivals are detected from layer 2 with a forward time difference of 0.05 s between them occurring at a distance of 23 km. Another step forward in time (0.05 s) occurs within the basement arrivals at a distance of 46 km from Aberdour quarry.

The step in layer 2 arrivals is inferred to be due to a major fault trending NE along the SE boundary of the Ochil Hills, intersecting the profile at station 15, and upthrowing to the NW. This fault seems to be the major fracture in the region and its presence is confirmed by the reversed coverage

from Collace. Layer 2 comes to the surface to the north of the fault. Layer 1 is absent on this side, except for a thin sequence in the Tay Graben. East of Dollar, the Ochil Fault branches eastward into two faults, the southern of the two is considered to be the W-E continuation of the fault; the northern extension will be termed the North Ochil Fault (NOF) in this work and is the structure discussed here.

Geological evidence suggests that the Ochil Fault extends towards the east intersecting line 1 at 12 km from Aberdour quarry. Data obtained along line 1 does not show its effect within the range of direct arrivals from Aberdour. Assuming that the continuation of the fault is present at depth, head-waves from Collace should be affected by it. However, no change in arrival times was observed at stations south of its surface expression.

Interpretation of the direct arrivals from Aberdour quarry yielded an average velocity of 4.60 km/s corresponding to layer 1. The location of the quarry on a thin sill affected the arrival times for at least the first two stations where station 1 has a negative reduced time value. Using equation 3.9 and the time intercept of the first time-distance segment of layer 2, a thickness of 2.3 +/- 0.3 km was assigned for layer 1.

South of the NOF the velocity of layer 2 is calculated to be 5.55 +/- 0.20 km/s, while to the north of the fault the velocity value is 5.65 +/- 0.08 km/s. This difference in velocity values is possibly due to an increased presence of volcanic rocks north of the fault. Using equation 3.10, the thickness of layer 2 was calculated to be 2.5 +/- 0.3 km. The velocities of layers 1 and 3 (4.60 and 6.04 km/s respectively) were used in obtaining this value. The value of V2 used in this equation was obtained by averaging the two velocity segments corresponding to this layer north and south of the NOF and the intercept of the first layer 3 velocity segment was used for the value of Ti. Adding the thickness of layer 2 to that of layer 1, the depth to the basement refractor was calculated to be 4.76 km.

The NOF offsets layer 2 resulting in two different velocity segments with overlapping time intercepts, it was not possible to measure the exact difference in time intercepts so the difference in arrival times for the stations on either side of the fault was assumed to correspond to the difference in time intercepts and thus the throw of the fault was calculated to be 0.38 km +/-42 m.

Two early arrivals are detected at stations 19 and 20, located to the south and north of the South Tay Fault, when recording from Aberdour and Collace quarries respectively (Fig. 4.15). These two arrivals cannot be correlated with the presence of the fault because they are both early arrivals while

the fault should affect opposite travelling rays in different ways. Therefore the presence of such arrivals must be due to other unknown factors, such as the presence of high velocity body at a shallow depth near the location of the fault.

Starting from station 25, arrivals from crystalline basement (layer 3) are detected with a velocity of 6.04 +/- 0.03 km/s. At station 31 another velocity segment with a velocity of 5.98 +/- 0.10 km/s is detected up to the end of the profile. A time difference of 0.05 s is present between the two basement segments at a distance of 45 km (station 31) indicating a step up to the north of the basement. The difference in the basement velocities is probably due to the poor quality of the last four traces (see Fig. 4.1a), which is indicated by the larger error.

This step is also seen in the noise test data discussed in section 2.3 and recorded at the northern end of line 1. The last trace of this data set (trace 32A, Fig. 4.1c) shows an early arrival relative to the rest of the traces, indicating that this basement step extends at least 4 km NE of line 1. Correlation with the point of observance on line 1 suggests that the basement step runs parallel to the axis of the Strathmore syncline (for location see Figure 1.1b).

Equation 3.16 was applied in calculating the fault displacements, which requires that the observed velocities on either side of the fault are similar (Fig. 3.6), so that the difference in the time intercepts can be used. Assumptions made in calculating the throw of the NOF were used in calculating the basement step displacement which gave a value of 0.73 +/- 0.03 km. The two calculated throws are only tentative estimations of the real throws because the assumptions made were not precise.

Studying data obtained from the reversal of the profile from Collace quarry (Fig. 4.15), the first 3 time-distance segments are consistent with those obtained from the Aberdour shot, but arrivals from layer 3 were not detected due to lack of coverage. The direct arrivals do not represent layer 1, which is absent at outcrop north of the NOF, except for the Tay Graben. An average velocity of 4.70 km/s is assigned to the direct arrival segment observed across the Lower Devonian lavas south of the quarry. Equation 3.9 was used to calculate the thickness of this layer which yielded a value of 2.50 +/- 0.3 km. The weathering of the topmost section of this layer and the presence of cracks are probably reasons for the relatively low velocity of this part of layer 2, but this effect is usually observed only to a depth of typically 1 km.

Delayed arrivals corresponding to the NOF are seen starting from station 14 to the end of the profile. The velocity of the upthrown (north) side of layer 2 at the NOF is 5.81 +/- 0.10 km/s while the velocity of the downthrow segment is 5.94 +/- 0.04 km/s. Within the error values these two velocities are equivalent and represent the same layer but the slightly higher velocity value for the southern segment is probably because of the poor constraints on the this segment and the possibility of including some of the basement arrivals when regression was applied. The throw of the NOF was determined to be 0.70 km +/- 74 m. Part of the difference in the throw values when calculated from the opposite directions is due to the different velocities used in the computations, but the different velocities used cannot be the sole factor since the difference of throw is more than double.

Part of the profile was recorded from Newburgh quarry to constrain the topmost layer in the middle of the line (layer 2). Figure 4.15 shows the time-distance curves for this shot with arrival times representing mostly the direct waves, except for the last few stations where refracted arrivals were observed and used in the calculations of the depths of the top of layer 2. Recording toward Collace quarry an average velocity of 4.70 km/s was obtained from direct arrivals which is the same velocity value recorded from Collace quarry in the north.

A velocity of 5.78 +/- 0.31 km/s was obtained using the last 4 stations of this segment where the refracted rays were detected, which is very close to the value obtained when recording from Collace. A depth of 2.2 +/- 0.2 km was calculated representing the upper portion of layer 2, which is slightly lower than the thickness obtained from the Collace data.

Interpretation of data recorded towards the south resulted in velocities of 4.81 km/s and 5.27 +/- 0.31 km/s for layer 2, representing the average near surface and deeper parts of this layer respectively. These values are lower than those obtained when recording from the south (Aberdour). The depth to which rays from each direction travel is possibly factor in these different velocity values. Using the time intercept obtained from the time-distance graph a depth of 1.62 +/- 0.2 km was calculated.

The availability of the reversed coverage for this line permitted the use of equations 3.11 to 3.15 to determine the velocity and dip of layer 2 and the depth to the Devonian interface under Aberdour quarry. This also permitted the calculation of the depth and dip of an observed "low velocity zone" (discussed in section 4.5.5) within layer 2 under Collace quarry. For this purpose the line was divided into 2 parts: south and north of the NOF. Apparent velocities in each section gave the dips and true

velocities, which were combined with the time-intercept at the reversed end shotpoint to determine depths to layer 2.

Velocities of 5.73 km/s at the south and 5.74 km/s at the north were computed for layer 2, while the respective dips were 3 and 1 degrees in a north direction. The vertical depths under Aberdour and Collace quarries were 2.25 and 2.62 km respectively. The last figure does not represent the Devonian interface under Collace shot, since layer 1 is absent in the region, but it represents a continuation of this interface within layer 2 towards the north separating the two velocity zones within this layer.

Thickness values obtained for layer 1 using the above equations and values calculated using the horizontal interface equations are nearly identical indicating that the dip of this layer is negligible in the south, while at the north of line 1, a flat base to the low velocity zone of layer 2 is indicated.

Variations in velocity values for layer 2 along this profile were expected given the complicated structural and lithological distribution of the Midland Valley. The velocity for layer 2 actually ranged between 5.6 and 5.8 km/s, except in two cases. When measured from Collace quarry the velocity was computed to be 5.94 km/s, the segment corresponding is poorly defined and arrivals from the basement might be included in the calculation. In the second case, recording from Newburgh towards the south, the velocity is only 5.27 +/- 0.31 km/s. In calculating this velocity, however, arrivals at only three stations were used.

4.5.2. Line 2

Figure 4.16 illustrates the interpreted arrival times along this profile. Two time-distance segments are detected from Aberdour corresponding to layers 1 and 2. The first time-distance segment is present at an offset of 0-17km and represents layer 1 direct wave arrivals. The second segment starts at a cross-over distance of 17km and is interpreted as head waves refracted from layer 2. At a distance of 30.5 km from the shot, this segment is subdivided into two groups of arrival times with a time difference of 0.31 s, where the second group is forward in time. This was interpreted as due to the presence of the Ochil Fault which juxtaposes Carboniferous and Upper Devonian (layer 1) against Lower Devonian (layer 2) at this location. A velocity of 4.0 km/s was estimated for layer 1 along this line. Using equation 3.9 a thickness of 2.4 km for layer 1 was calculated.

The profile intersects the Ochil Fault at station 20 (Fig. 4.16). The velocity of the southern down-

thrown layer 2 was calculated to be 5.50 +/- 0.10 km/s while the velocity of the footwall layer 2 is 5.79 +/- 0.07 km/s. Both values are in agreement with the values obtained for line 1. Again it is clear that the difference between the two velocities is consistent with a more substantial presence of lavas north of the fault. Equation 3.9 was used to calculate the throw of the fault where V2 was assumed to be the average of the layer 2 velocities on either side. In determining the difference in Ti, the same assumptions were made as those made in calculating the throw of the NOF. The throw of the Ochil Fault here was determined to be 1.8 +/- 0.2 km. A noisy trace was obtained at the last station along this line (station 31) but no onset can be determined (Fig. 4.7a).

Reversal of this line from Tillicoultry was incomplete and only 7 stations were recorded. This permitted the estimation of the velocity of layer 1 only, which was determined to be an average of 4.1 km/s. Minor differences in velocity values obtained along this line and values obtained along line 1 are attributed to errors caused by the high level of noise along line 2, resulting in a larger scatter of arrival times. The difference in the distribution of lava along both lines should also be considered.

4.5.3. Line 3

Figure 4.17 shows the interpreted arrival times for this profile. The WHB inversion was not applied to this line because of the early arrivals starting at station 4 where no smooth curves can be drawn. Therefore, the regression function was used to determine the velocity of the different time-distance segments.

Only 12 stations were recorded from Tillicoultry, which can be divided into 3 groups of arrivals. The first three receivers were situated on intermediate and basic intrusive rocks of Carboniferous age which yielded a velocity of 4.75 +/- 0.04 km/s. The next 7 receivers were located on Lower Devonian lava with a velocity of 4.94 +/- 0.05 km/s. This is a relatively high velocity for the top of layer 2 compared to values obtained from Collace and Newburgh. A sharp reduction in velocity occurs at the last two stations which were positioned on the Upper Old Red Sandstone (layer 1) with a value of 3.81. This velocity is in an agreement with the MAVIS I north line which trends to the south of this profile and the MAVIS II line where it intersects the line north of Dollar. Since only direct waves were detected along this profile, the velocities obtained for the lava are considered to be from the weathered section of this lava.

4.5.4. Line 4

For the same reasons discussed in the previous section, the WHB method was not applied to this profile also. Examining Figure 4.18, two segments are observed along the time-distance curve with a delay of approximately 0.35 s between them. The first segment includes stations 1, 2, and 3 which are on Lower Devonian lavas (layer 2). The remaining stations form the second segment and are located on Upper Devonian rocks (layer 1). The two segments give velocity values of 5.31 +/- 0.22 km/s and 5.38 +/- 0.50 km/s respectively. Both values are consistent with arrivals from Lower Devonian rocks, presumably lava, of layer 2. Therefore the delay between the segments is attributed to the South Tay Fault which intersects the line between stations 3 and 4, the second segment being head-waves from the graben base.

The throw of the South Tay Fault was calculated to be 2.1 +/- 0.3 km using the above data. Two assumptions were made in calculating this value. Firstly, that the velocity of layer 1 (which is not available from these data) is 4.00 km/s and, secondly, that the time difference between the stations on either side of the fault corresponds to the difference in the time intercepts. The velocity derived from the second segment was used as the actual V2, since it probably represents a truer estimate of the layer 2 velocity.

4.5.5. Velocity Study of North Fife/Tay Graben

Data were recorded from Newburgh quarry in three directions nearly perpendicular to each other (line 1 to north and south, line 4 to the west). These and the reversed profile recorded from Collace quarry allow the study of velocity variation within layer 2 in this area. Table 4.1 summarises the velocity and depth values obtained along these profiles. For convenience the velocity of layer 2 is subdivided into upper V2 and lower V2 corresponding, to the two velocity groups derived from this layer.

Table 4.2 Velocity and depth values obtained in the northern half of the study area.

Profile	Upper V2 km/s	Lower V2 km/s	Thickness of upper V2, km
Newburgh South	4.81	5.28	1.62
Newburgh West	-	5.38	0.00
Newburgh North	4.70	5.80	2.20
Collace	4.70	5.81	2.50

Studying these values, a substantial reduction in the thickness of the upper "lower velocity" portion of layer 2 occurs towards the south of Newburgh accompanied by a velocity increase. Velocity values obtained along the Newburgh North profile and the reversed profile from Collace quarry are remarkably similar, while thickness values along the same section suggest that there is a gradual decrease in thickness of the layer 2 low velocity zone towards the south. This zone presumably terminates at the NOF and is being thickest at the northern end of line 1. The slightly lower velocity values obtained north of Newburgh are probably because of the presence of layer 1 in the Tay Graben, while direct waves travelling toward the south pass only through the higher velocity Lower Devonian lava. Along the Newburgh West profile no direct arrivals were obtained indicating the absence of the low velocity zone in this direction.

The differences in velocities obtained along the profiles recorded at Newburgh quarry may indicate the presence of an additional factor controlling such variations. Weatherby et al. (1934) suggested that, in stratified rocks, the velocity parallel to bedding differs from that perpendicular to bedding, being higher by 10-15% in the former case and they related that to the effect of the anisotropic nature of rocks. A detailed study of the role of anisotropy is beyond the scope of this project but it is a factor which should be considered since velocity variations lie within close ranges and rays travelling from Newburgh quarry across the Tay Graben traverse rocks dipping in different directions.

4.5.6. Summary

The following points arise from the planar layer interpretation. From the data obtained along line 1 a generalized velocity-depth model can be visualized for this profile (Fig. 4.36). To the south of the

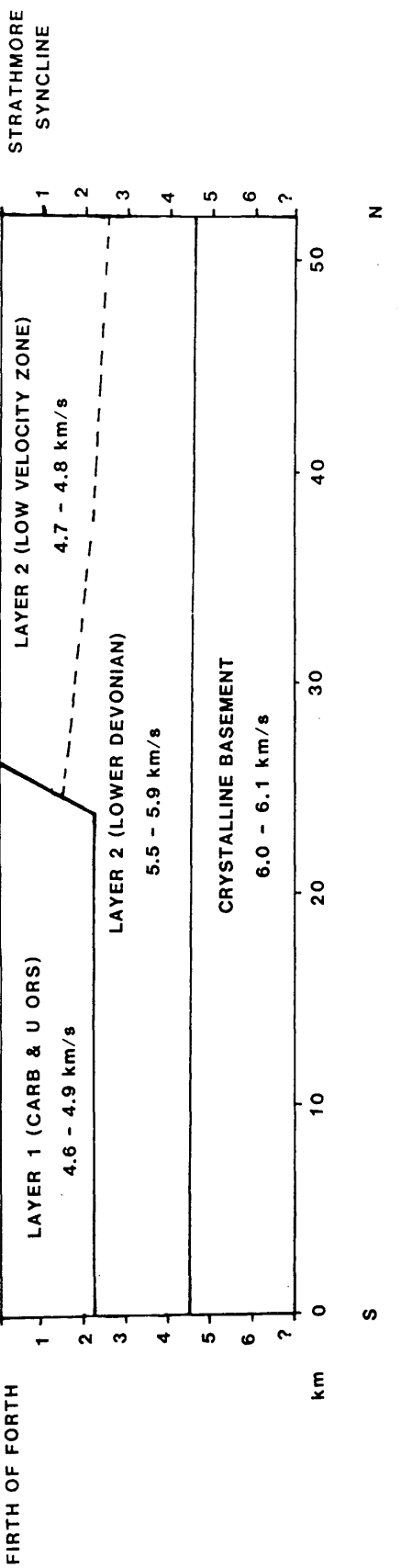

Fig.4.36 Planar layer interpretation of line 1.

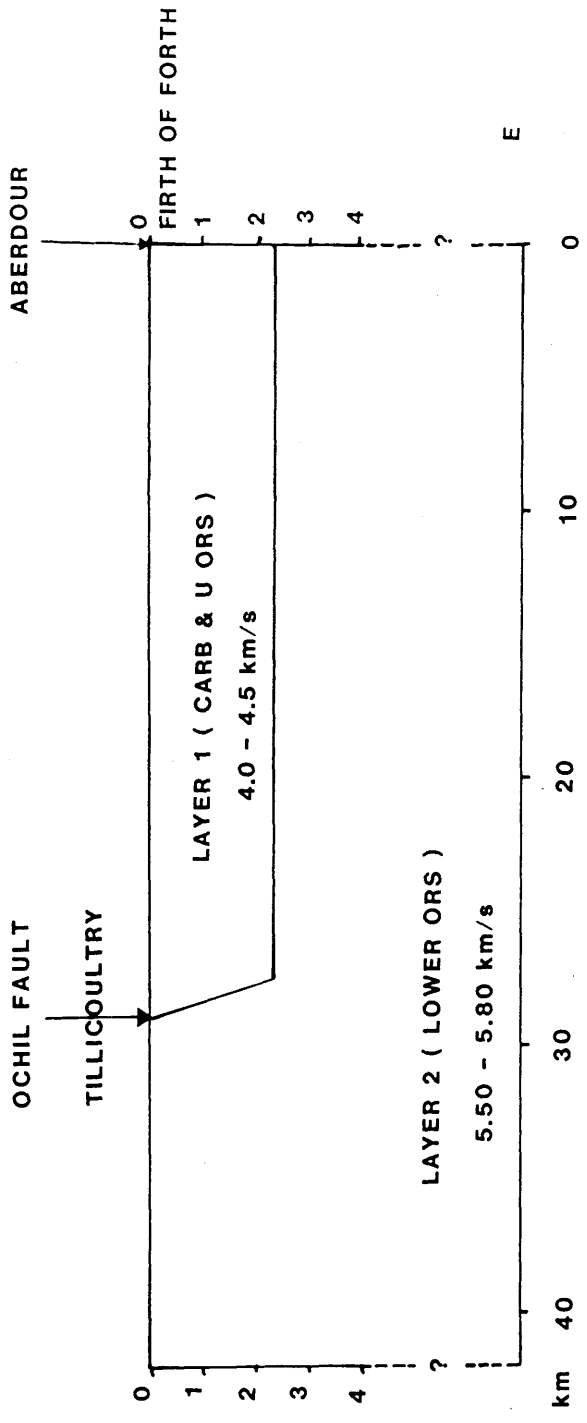

VELOCITY - DEPTH SECTION LINE 2

Fig.4.37 Planar layer interpretation of line 2.

NOF, layer 1 crops out with a velocity of 4.6 km/s and thickness of approximately 2.3 km. Its absence north of the NOF indicates a minimum vertical throw of 2.3 km for the fault on this basis. Layer 2 which crops out north of the NOF can be divided on the basis of its velocity distribution into two "zones", an upper zone of 4.7-4.8 km/s and a lower zone of 5.5-5.9 km/s. The thickness of this layer is 2.4 km in the south and 4.8 km in the north of line 1 respectively. Layer 3 (upper crystalline basement) occurs at a depth of 4.8 km with a step up of 0.7 km towards the north.

Figure 4.37 shows the planar layer interpretation along line 2. A velocity of 4.0 km/s is assigned for layer 1 with a thickness of 2.4 km. Layer 2 has an observed velocity of 5.5-5.8 km/s which is within the range of the values derived for this layer along line 1. The throw of the Ochil Fault was determined to be at least 1.8 km.

4.6. Application of the Plus-minus Method

The application of the plus-minus method to the data derived along line 1 was based on the recognition of a consistent reversed recording from layer 2 (Fig. 4.15). A refractor velocity of 5.69 +/- 0.3 km/s was obtained for layer 2, which is in good agreement with the velocities derived in section 4.5. Extrapolation of the time-distance branch of layer 2 was done to determine the reciprocal time corresponding to this layer and was used to calculate the plus times. Layer 1 is absent north of station 15, so averaging the velocities obtained for the first observed time-distance segments yielded a value of 4.65 km/s for the layer above the refractor. Curve A of Figure 4.38b shows the depth to the layer 2 refractor determined using this velocity and that obtained from the minus times. However, a more realistic approach is to use an average layer 1 velocity (4.6 km/s) south of the NOF, and the average "upper" layer 2 value (4.7 km/s) further north. This resulted in interface B of Figure 4.38b, and is preferred.

Effects of the NOF and the North Tay Fault can be seen at distances of 23 and 34 km respectively. The minus time plot is shown in Figure 4.38a. The plus times and minus times are listed in Appendix 3.

4.7. Raytracing

The raytracing method is described in section 3.4.5. An initial velocity model was produced for lines 1 and 2 from the methods described in sections 4.3-4.5 (see Figures 4.36 and 4.37) and used as

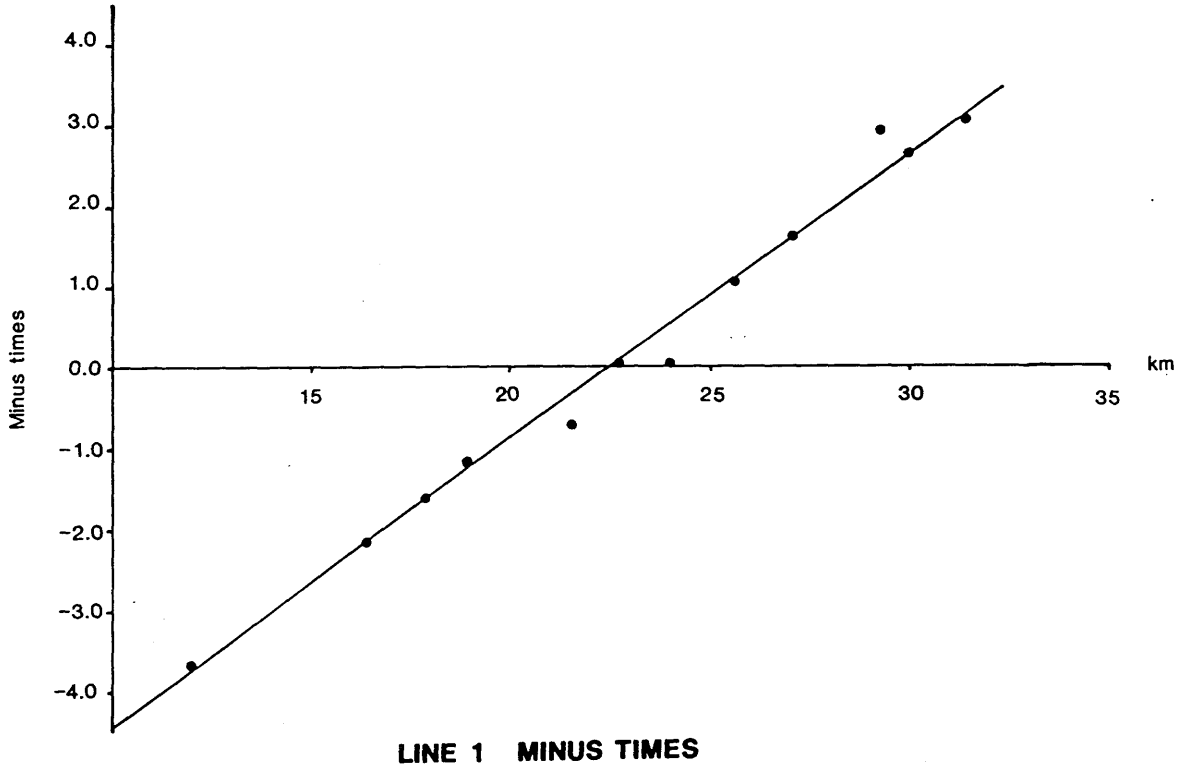

Fig.4.38a Plot of minus times versus distance.

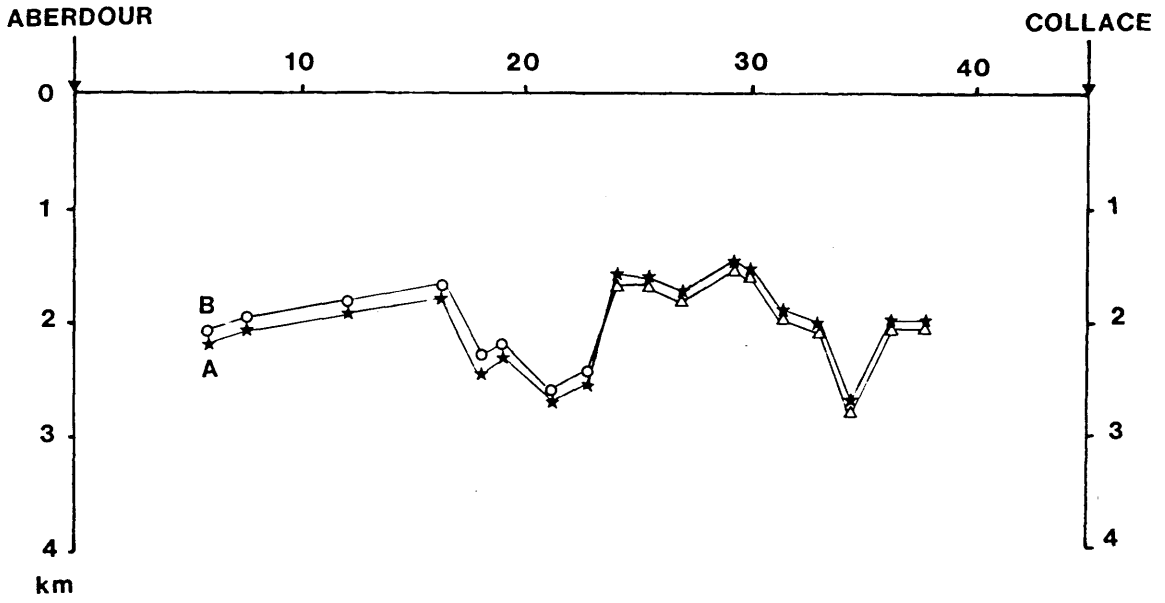

Fig.4.38b Plus-minus interpretation of line 1.

"raw models" for raytracing modelling. A discrepancy of +/- 0.03 s was considered to be an acceptable agreement between computed and observed travel times. Discrepancies in the calculated times at the ray-traced stations are listed in Appendix 4.

Raytracing on line 1 was controlled as follows:

[1] Velocities of 4.2-4.9 km/s for the Carboniferous and Upper Devonian were taken from the WHB results obtained at both end-shotpoints, which are in agreement with velocities obtained from the MAVIS I north line at their intersection point (see section 4.4). The thickness of this layer used was obtained from the planar layer interpretation (section 4.5) and by correlation with the MAVIS I north line.

[2] Velocities of rocks of Lower Devonian and Lower Palaeozoic age (layer 2) were derived from the planar layer interpretation and a range of 5.3-5.9 km/s was used. The WHB velocity of 4.7 km/s was used in controlling the velocity of the upper part of layer 2 at the northern section of line 1 where this layer 2 is at the surface.

[3] Basement refractor velocities were derived from those obtained by this project and from published geophysical literature (see chapter 1).

Raytracing on line 2 was controlled as follows:

[1] Velocities for layer 1 were obtained from the WHB results with a range of 3.3-4.6 km/s. These velocities were later re-adjusted due to problems encountered in raytracing, which are discussed later.

[2] Layer 2 velocities used for raytracing along this line were derived from the planar layer interpretation and correlation with the MAVIS results, since two MAVIS profiles intersect the line. A range of 4.8-5.8 km/s was used.

The resulting ray models are shown in Figures 4.39 and 4.40; the velocity models are shown in Figures 4.41 and 4.42. The raytracing confirms the existence of a surface layer 1 in the south of line 1 with no lateral velocity variation and uniform vertical velocity change while, in the north (where layer 2 is the main outcrop) there is a notable vertical change in velocity. A velocity range of 4.3-4.9 km/s was obtained for layer 1 in the south while layer 2 velocities were 4.7-5.8 km/s being at the higher limits in the north. Along line 2, the velocity distribution for layers 1 and 2 is more uniform where layer 1

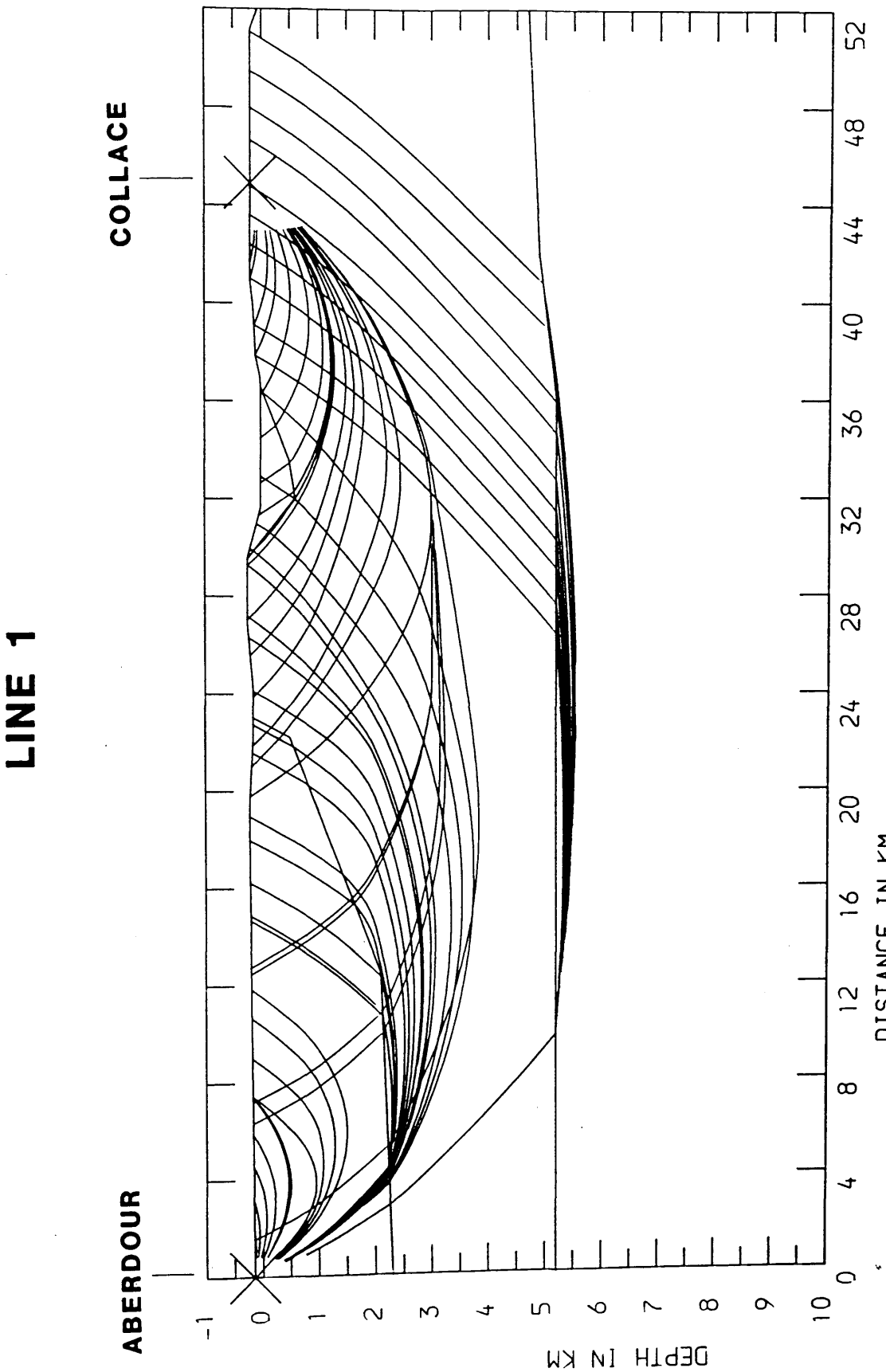

Fig.4.39 Ray-paths used in the calculation of travel-times along line 1. Shotpoint is denoted by (X).

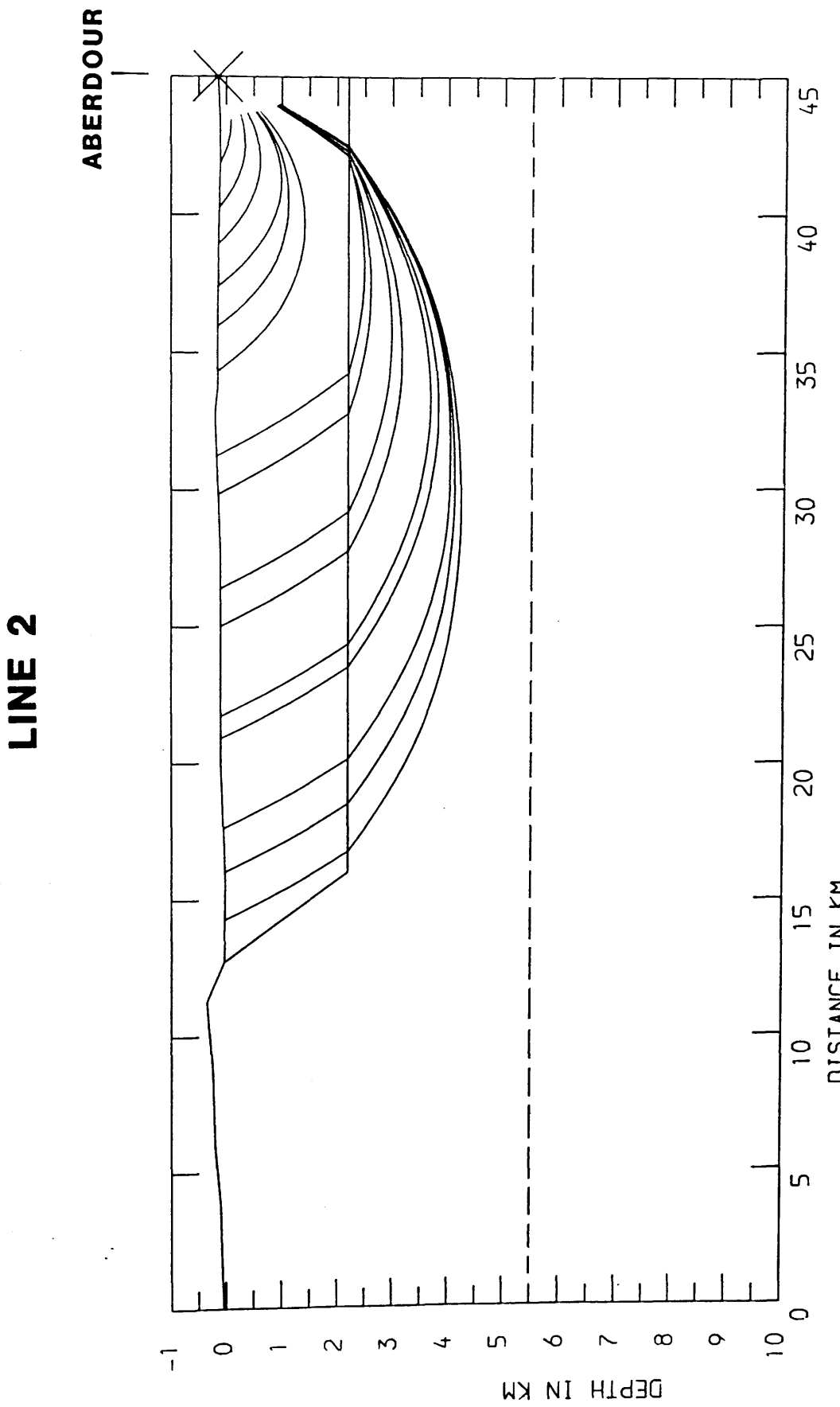

Fig.4.40 Ray-paths used in the calculation of travel-times along line 2. Shotpoint is denoted by (X).

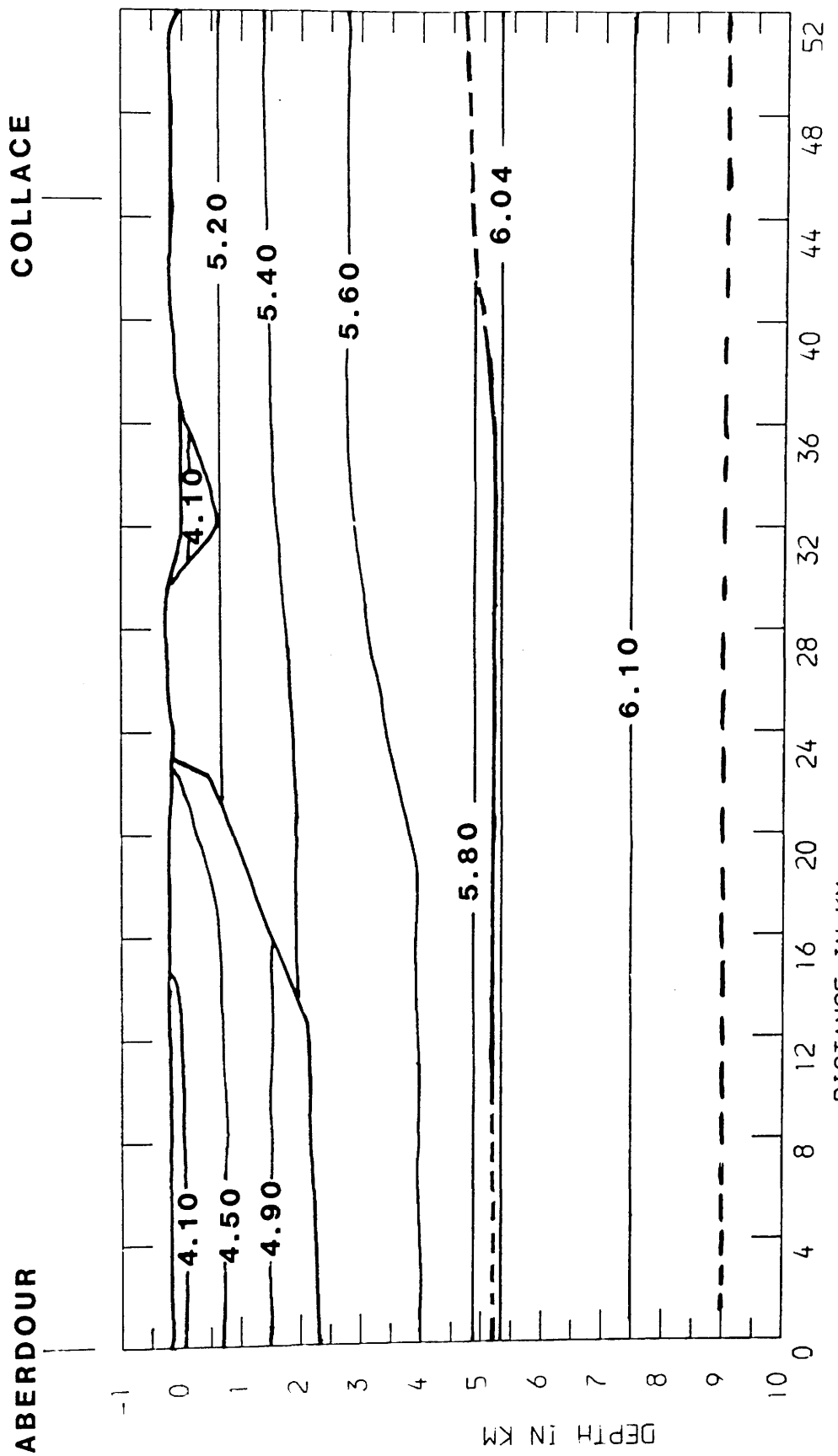

Fig.4.41 Ray-traced model of line 1. Interfaces shown by thick lines, seismic velocity contours, in km/s, by thin lines.

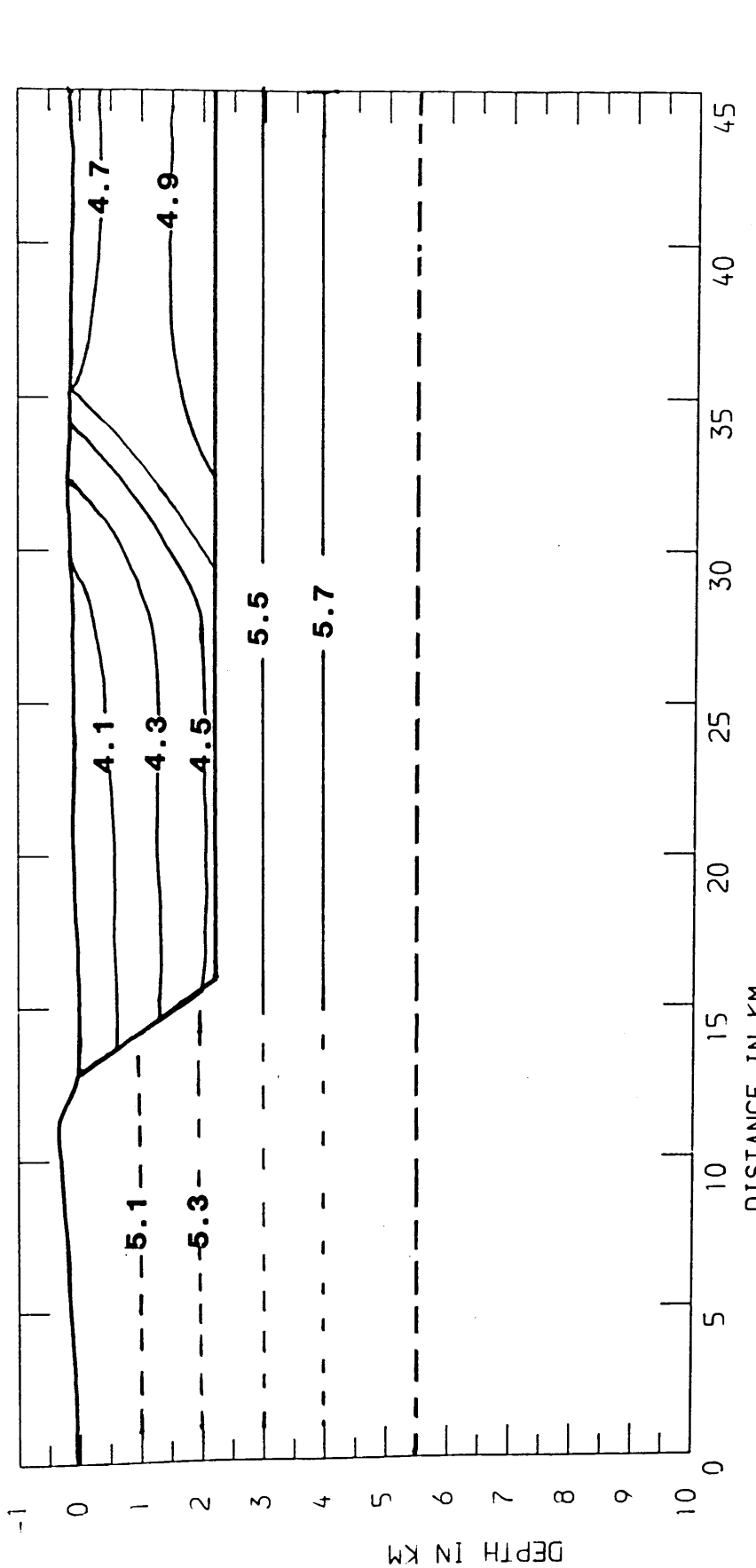

Fig.4.42 Ray-traced model of line 2. Interfaces shown by thick lines, seismic velocity contours, in km/s, by thin lines.

velocity range is 3.8-4.9 km/s and layer 2 range is 5.1-5.7 km/s.

Several problems were encountered in raytracing the data recorded at both lines. Dentith (1987) argues that velocity gradients must be kept as smooth as possible in order to satisfy the data, but along line 1 this was not possible due to the lateral and vertical variations within each layer, in addition to the presence of several faults and the abundance of Carboniferous sills which cause abrupt changes in observed arrival times. The overall data required a closely spaced velocity grid with large velocity variations especially along the northern section of line 1. This type of velocity grid affected successful raytracing of the direct arrival rays and this was especially observed from Collace. Here discrepancies between the observed and calculated times were determined, frequently exceeding the "acceptable" timing error.

Raytracing of data obtained from Newburgh required a dense velocity grid with low velocities, changing rapidly to higher values at short distances across the faults to the north and south of the quarry. Similar changes are required once more across the NOF. This affected the general model for line 1 to a great extent and, since modelling the Tay Graben was not the main objective of this work, raytracing of line 1 was undertaken without the Newburgh data. Furthermore, the velocities of the topmost layer in the region are constrained by the direct arrivals which do not agree with such variations. The possible presence of the low velocity zone discussed in section 4.5 might have attributed to such velocity inversions, a matter which should be considered in any future work in the area.

Modelling of line 2 was hindered by another problem at stations beyond the Ochil Fault from Aberdour. Headwaves from layer 2 to these stations begin their upward path south of the Ochil Fault. This path requires them to pass through the steep part of the Ochil Fault (i.e. to re-enter layer 2). This proved to be beyond the iteration capabilities of the program where modelling such rays caused the program to terminate. Another attempt was made to raytrace the line using the same parameters as those used in the MAVIS interpretation (which did not sample the fault from the same angle as line 2), but with no success.

However, geological evidence suggests that the Devonian interface dips to the NW along this profile being shallower near the shotpoint in the SE. When modelling such dipping interface the same problem was faced again where the rays had to pass through the same path discussed above causing the program to either sample only few stations, or to terminate when a large angle was used and the

original situation is faced again. Therefore, modelling this line was carried out assuming no dip to be present and the velocity model is in good agreement with that of the MAVIS profiles, but the final geological model for line 2 is considered to be conjectural.

A final attempt was made to model the further stations by using a grid of relatively low velocities for layer 2 to estimate the velocities required for the rays to curve around the fault to reach these stations. A very low velocity grid was needed which is not even within the extreme low limits of layer 2 and this attempt was abandoned.

However, raytracing successfully modelled most of the structures and lithologies interpreted using the methods discussed earlier. It gave reasonable estimates of the throws of the faults traversed by the profiles and values of 2.3, 0.5 and 0.6 km were assigned for the throws of the Ochil Fault, North Ochil Fault and the South Tay Fault respectively. It defined the velocities of the different layers with good control and velocity ranges of 4.3-5.1 km/s and 5.3-5.8 km/s were estimated for layers 1 and 2 respectively. These velocities are in agreement with those derived by the MAVIS in the same area. A value of 5.2 km was obtained for the depth to the basement refractor and a throw of 0.3 km is assigned for a low angled basement step. The velocity of the top basement refractor was determined to be 6.04 km/s which agrees with value obtained by Dentith (1987).

CHAPTER FIVE - GEOLOGICAL IMPLICATIONS AND CONCLUSIONS

5.1. Introduction

This study has provided more information on the range and distribution of P-wave velocities in the Carboniferous and Devonian sedimentary sequence of the eastern Midland Valley of Scotland together with data on the basement refractor. Seismic studies in this part of the Midland Valley can be divided into two areas. The first, which is covered by the MAVIS project (Dentith 1987) and this work, extends from the Firth of Forth, in the south, to the Ochil Fault and its eastern extension. The second part is covered by this project only and extends from the Ochil Fault into the Strathmore Syncline in the north. In this chapter a discussion of the geological implications of the seismic structure in the project area will be presented along with a comparison of results obtained by this and previous projects. The final geological models for the two profiles are shown in Figures 5.1 and 5.2.

5.2. Seismic Velocities

Two sets of P-wave velocities for layers 1 and 2 are obtained along line 1. The first covers the area south of the NOF and the second covers the area to the north. Table 5.1 shows a comparison between P-wave velocities obtained by the MAVIS project and the present data set. A limited amount of information was derived for layer 3.

Table 5.1 Comparison between Velocities of the MAVIS and Eastern Fife Projects.

Project	V1	V2	V3
	km/s	km/s	km/s
MAVIS	3.0 - 5.0	5.4	6.0 - 6.1
Eastern Fife	4.2 - 4.9	5.4	6.04

5.2.1. Layer 1

The MAVIS project provides data south of the NOF where the MAVIS I north line intersects line 1 at a distance of approximately 13 km north of Aberdour quarry (station 9, Fig. 1.1b) and line 2 east

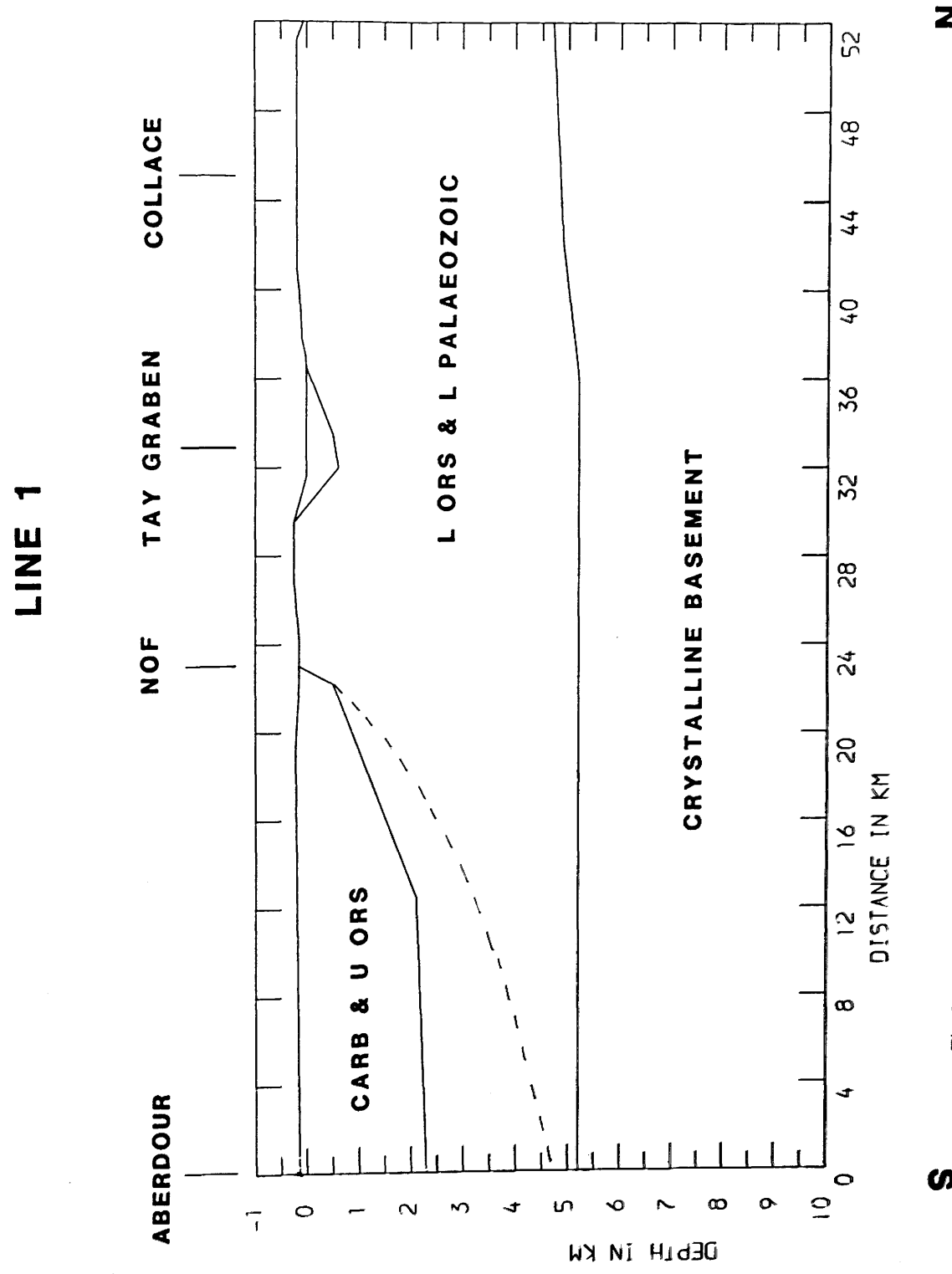

Fig.5.1 Final interpretation of line 1. Dashed line show the conjectural extension of the North Ochil Fault.

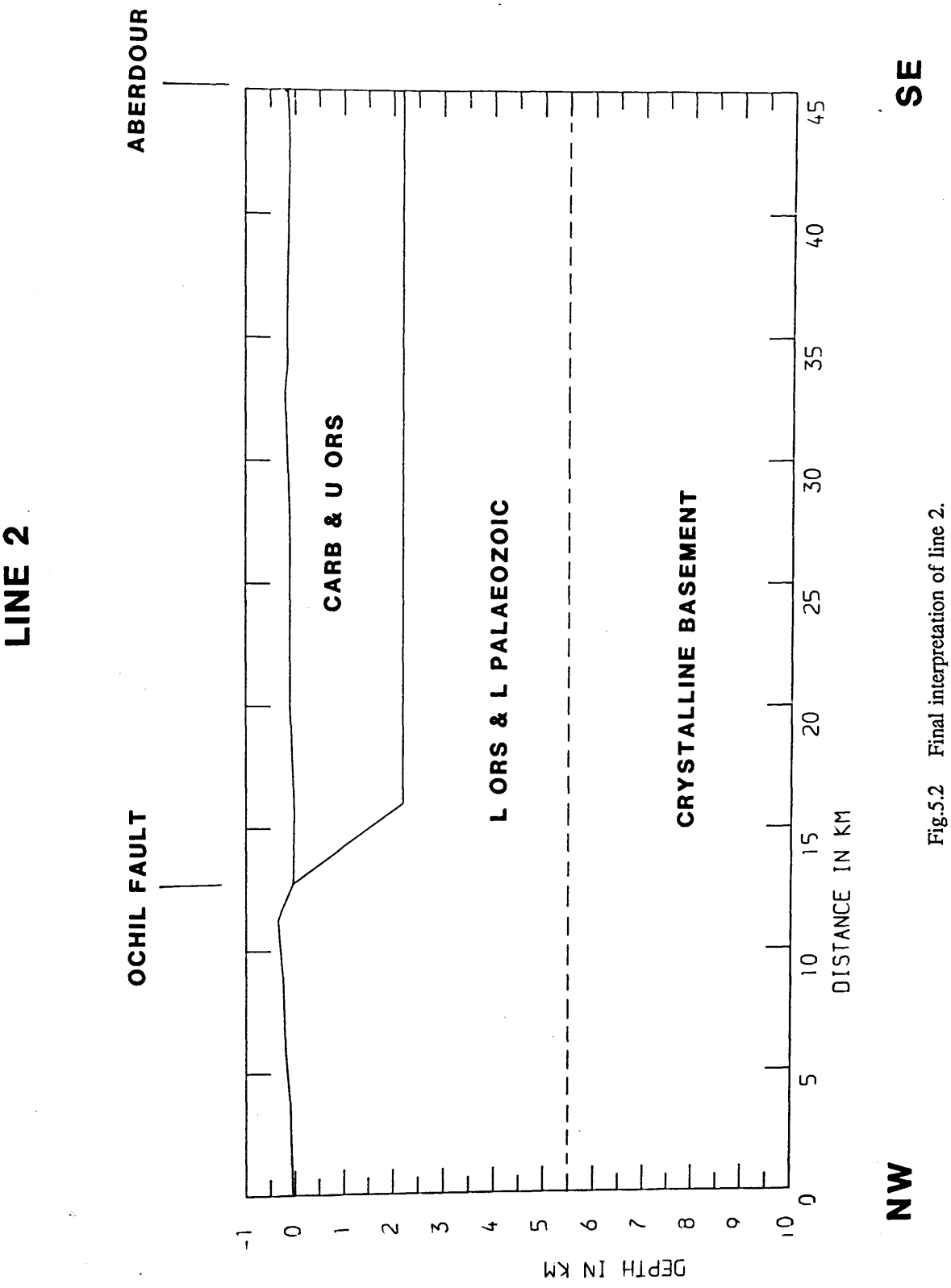

Fig.5.2 Final interpretation of line 2.

of Alva (station 14, Fig. 1.1b), while the MAVIS II profile intersects line 2 nearly at the same location as the other MAVIS profile.

Velocities assigned by both projects for the Carboniferous and Upper Devonian deltaic and clastic sediments of layer 1 are obtained from the WHB inversions. In this project the WHB results from Aberdour quarry along line 1 were used and a velocity range of 4.2-4.9 km/s was estimated. Along the MAVIS I north line, five shots were recorded with the Cattlemoss shot being near the axis of the Clackmannan syncline where layer 1 is nearly at its maximum thickness. Therefore lower velocities for layer 1 were obtained along this segment of the MAVIS I north line, increasing the range of velocities obtained for this layer. This explains the discrepancy in the minimum velocity values obtained by the present work along this line. However, layer 1 velocities along line 2 are in good agreement with the MAVIS results where a range of 3.3-4.6 km/s is obtained (see Table 5.1 for the MAVIS values).

5.2.2. Layer 2

Generally velocities obtained for the Lower Palaeozoic layer 2 are in good agreement with the MAVIS results. However, north of the NOF the velocity configuration is different. Here, layer 1 is absent from outcrop, except for a limited outcrop at the Tay Graben. The main stratigraphic unit exposed is of Lower Devonian age (layer 2), and consists of clastic sediments and an abundance of lavas.

Along line 1, a velocity range of 5.3-5.8 km/s is obtained which is comparable with the interpreted velocities of the MAVIS I north line, 9 km to the south (Fig. 1.14), but at equivalent depths the velocities obtained for this layer are slightly lower than those of the MAVIS. Velocities obtained along line 2 with a range of 5.1-5.7 km/s, in the Central Coalfield Syncline, are again in agreement with the MAVIS results in this area.

Using the planar layer method to interpret the profiles recorded in the area of the Tay Graben, a subdivision of layer 2 into two velocity zones was suggested (section 4.5.5), but raytracing (Fig. 4.41) does not support the presence of such subdivision. Rather, the velocity configuration and thicknesses obtained by this technique lie within the ranges obtained by previous projects. The lateral increase in the velocity of layer 2 (Fig. 4.41) towards the north is expected since there is an excessive abundance of Lower Devonian lava north of the NOF.

5.2.3. Layer 3

The data of line 1 indicate the presence of the top basement refractor at a depth of 5.2 km with a velocity of 6.04 km/s (Fig. 5.1). Basement headwaves were not observed along other lines. Considering the available data and the presence of no reversed coverage from the north, this depth is considered in reasonable agreement with that obtained by the MAVIS experiment in the same area, although it is deeper by 0.7 km.

5.3. Structure

The acquired data allowed the interpretation of the main structural features in central Fife and a general correlation with the structures interpreted by the MAVIS project in the Clackmannan Syncline. The main structures which are intersected by the profiles are the Ochil Fault, the North Ochil Fault, the Tay Graben and the basement step at the northern end of line 1.

5.3.1. The Ochil Fault

The Ochil Fault occurs as a single fracture or a zone of faults to the south of the Strathmore Syncline offsetting Lower ORS to the north against the Carboniferous to the south (Fig. 1.1a). It trends in an E-W direction from the Fife coast to west of Stirling dipping to the south with an estimated throw of 3 km at Alva (Geikie 1900). No conclusive evidence for the amount of dip of the fault is present, though a steep dip is envisaged by Dentith (1987) and supported by this work. A large number of E-W trending faults traverse the Carboniferous sequence to the south of the fault, while faults present in the north at the southern limb of the Strathmore Syncline assume a SSW-NNE direction.

The MAVIS interpretation of the Ochil Fault suggested that the fault dips to the south and soles out in, or at the base of, the MAVIS layer 2 (i.e. at 2-4 km depth) since no effect on crystalline basement (layer 3) is seen. A thickening of the Carboniferous and Palaeozoic sequence (layers 1 and 2) immediately south of the fault suggested a roll-over structure associated with a listric Ochil Fault. Dentith (1987) argued that this was caused by a N-S oriented Carboniferous extensional stress field affecting the basement resulting in a listric fault in the cover. The fault terminates abruptly to the west near Stirling, and extension is assumed to decrease E and W from a maximum at Alva.

At Alva, along line 2, an estimated throw of 2.2 km for the Ochil Fault was obtained by raytracing, which is, less than the value obtained by the MAVIS project (2.8 km). The data along line 2 are

poorly constrained and this may explain such a discrepancy. However, the two values are not so different given all the above mentioned uncertainties.

5.3.2. The North Ochil Fault

East of Dollar, the Ochil Fault branches into two major faults. The southern branch trends south of Loch Leven and is generally considered to be the main extension of the Ochil Fault and a northern branch, which intersects line 1 22.5 km north of Aberdour. Data obtained along line 1 in this work found no evidence for the presence of the assumed eastern extension of the fault in the Fife region although the surface expression of this fault lies within the zone of direct arrivals from Aberdour at 10 km from the quarry and headwaves detected along the reversed profile from Collace did not prove the presence of the fault at depth (i.e. within layer 2). This will support the interpretation made by Dentith (1987) for an E-W spoon shaped listric fault dying out in both directions.

However, results obtained along line 1 suggest the presence of a fault dipping steeply to the south with a throw of approximately 500 m occurs at the same location as the northern branch of the Ochil Fault. The behaviour of this fault bears great similarities to the interpretation of the Ochil Fault made by Dentith (1987), except for its much smaller throw and its northerly position. To the east of line 1 there are no geophysical data on the manner of this fault but a possible interpretation for its presence is that this fault is the true extension of the Ochil Fault and was caused by the same N-S extensional forces which activated the Ochil Fault. In the light of this evidence, the theory of a spoon shaped Ochil Fault appears to be conjectural. If this fault proves to be of listric nature, it will sole out at the Devonian refractor or within layer 2. However, the possibility of the fault soleing out at the boundary between layers 2 and 3 also exists.

Another possibility for the presence of the NOF is that it is a result of a reactivated Ochil Fault during Carboniferous times where fractures started at weaker zones assuming new directions of faulting and, therefore, extending the Ochil Fault in an easterly direction. However, the absence of Carboniferous deposits on the downthrownside of the fault (only Upper Devonian rocks) does not give this hypothesis much support and may indicate an earlier age for the NOF than the Ochil Fault, which would imply that the two faults are not related to each other.

5.3.3. The Tay Graben

The Tay Graben is a post-Carboniferous structure trending E-W and is 5.1 km wide where line 1 intersects it. The two main faults are the South Tay Fault and the North Tay Fault. They attain their maximum separation in the NE at Dundee (10.2 km) and meet south of Perth. Data obtained by the present project indicate that the main fault of the graben is the South Tay Fault which dips towards the north with an estimated throw of 600 m.

However, the fault offsets layer 1 against layer 2 where Lower Carboniferous and Upper Devonian are present at the surface. Browne (1980), using data obtained from boreholes drilled in the graben area reports a minimum thickness of 600 m for the Upper Devonian (Clashbenny Formation). This broadly agrees with the estimated throw of the fault derived along line 1.

5.3.4. Basement Step

Along line 1, a basement step occurs at 36 km (station 24 Fig. 1.1b) north of Aberdour quarry with a throw of 0.3 km shallowing towards the Highland Boundary Fault in the north. The presence of such a step is supported by the additional short profile recorded at the northern end of line 1 (section 2.3) and suggests that this step trends NE-SW parallel to the trend of the Strathmore Syncline. The observation of a step indicates that the basement refractor is of undulatory nature, or stepped by faults. In the south where line 1 intersects the MAVIS I north line, Dentith (1987) interpreted a flat basement with little relief. The lack of reversed coverage in the southern part of line 1 cannot give evidence as to the nature of the upper basement refractor in the area.

5.4. Conclusion

The project successfully mapped the upper crustal layers of the Fife region and obtained good correlations with results obtained by Davidson et al. (1985) and Dentith (1987). The thickness of the Carboniferous and Upper ORS layer varied between 0-2.3 km. The Lower ORS and Lower Palaeozoic layer extends from 0-5.2 km in the northern section of the study area and 2.1-5.2 km deep in the southern section of the study area. The basement refractor occurs at a depth of 5.2 km in the south of the study area while, in the north, where the step is located, it is 4.9 km deep. The velocities obtained are in good agreement with previous results. As for layer 2 in the north, higher velocities are predicted by the MAVIS and this projects probably due to the presence of larger amounts of lava.

The estimated throws of the Ochil Fault, the North Ochil Fault, and the South Tay Fault are 2.2, 0.5 and 0.6 km respectively at the points crossed, while a basement step with a throw of 0.3 km is envisaged in the extreme north of the study area. All velocities and depths corresponding to the various lithological units mapped are presented in Table 5.2.

The project was designed to study basin-basement relationships using quarry blasts, but the limited power of the sources available prevented a detailed study of these relationships since the data detected from the basement were limited. However, the data permitted a detailed study of the shallower structures and lithologies. The data obtained from the basement suggest that it is nearly flat and the surface structures at the surface are not observed in the basement. This supports the conclusion put forward by Dentith (1987) in this matter.

Table 5.2 Final interpretation of the Eastern Fife Project.

Rock unit	Depth in km	Velocity in km/s
Carb. and U. Devonian	0 - 2.3	3.3 - 5.1
Lower Devonian	0 - 5.2	5.3 - 5.9
Basement	>5.2	6.1

5.5. Recommendations for Further Work

[1] The presence of dependable quarries along line 1, especially Aberdour and Newburgh, permits a further study of the velocity distribution and lithology in the Tay Graben.

[2] Using Newburgh and Collace quarries, a grid of refraction lines across the Tay Graben, and extending for longer distances, can give a positive answer to the nature and distribution of the low velocity zone detected along line 1 in this area which may support the subdivision of layer 2 in

the region.

[3] Several refraction profiles to the east of line 1 to detect the lateral variations of layers 1 and 2 in east Fife will provide good constraints on these layers and indicate any basement control on deposition. Such profiles can shed light on the extension of the Ochil Fault especially if supplemented by one or more profiles between lines 1 and 2.

[4] The presence of Collace quarry at the southern edge of the Strathmore Syncline provides a good opportunity to study the Lower ORS distribution in the Strathmore Syncline by short range refraction lines, or to record long profiles across the Highland Boundary Fault. The abundance of rock exposures in the Grampian Highlands allows a more reliable data to be collected and an extension of the range of detectable head-waves. But the infrequency of this quarry should be considered before planning any such project.

Using the same quarry, the reversal of line 1 can be extended to the south giving data on the nature of the basement to be correlated with that obtained by the MAVIS and such data can be integrated with the already acquired data (Dentith, 1987) for the Lothian Oil-Shale Fields south of the Firth of Forth. Carefully located rock sites are essential for such a project due to the high noise levels in the south Fife region, which caused great difficulties in this project.

[5] Poisson's ratio can be used as a technique by which subsurface lithologies are identified. Good quality second arrivals were acquired during this work, but due to a lack of time no attempt was made to interpret them.

[6] This project and Dentith (1987) suggest basement topography in the Strathmore Syncline area which could be investigated to discover any relation to this major sedimentary feature.

[7] Gravity and magnetic modelling can support/test the results obtained in this project.

REFERENCES

AFTALION, M. et al. 1984. Age Constraints on Basement of the Midland Valley of Scotland. Trans. R. Soc. Edin., v 75, pp 53-64 .

AL-MANSOURI, D. 1986. Seismological Studies of Upper Crustal Structure in the Vicinity of the Girvan-Ballantrae Area, SW Scotland. Ph.D. thesis (unpubl), University of Glasgow.

ALOMARI, M. I. 1980. Geological Interpretation of the Gravity Field of the Western Midland Valley of Scotland. Ph. D. thesis (unpubl), University of Glasgow.

ASSUMPCAO, M. and BAMFORD D. 1978, LISPB - V, Studies of Crustal Shear Waves. Geophys. J. R. Astr. Soc. v 54, pp 61-73.

ARMSTRONG, M. and PATERSON, I. B. 1970. The Lower Old Red Sandstone of the Strathmore Region. Rep. Inst. Geol. Sci. No. 70/12.

BAMFORD, D. 1979. Seismic Constraints on the Deep Geology Of The Caledonides Of Northern Britain. In: HARRIS, A. L., HOLLAND, C. H. and LEAKE, B. E., (Eds), . The Caledonides of the British Isles - Reviewed. Spec. Publ. Geol. Soc. Lond. v 8 pp 323-337.

BAMFORD, D., FABER, S., JACOB, B., KAMINSKI, W., NUNN, K., PRODEHL, C., FUCHS, K., KING, R. and WILLMORE, P. 1976. A Lithospheric Seismic Profile in Britain - I. Preliminary Results. Geophys. J. R. Astr. Soc. v 44, pp 145-160.

BAMFORD, D., NUNN, K., PRODEHL, C. and JACOB, B. 1977. LISPB - III. Upper Crustal Structure of Northern Britain. J. Geol. Soc. Lond. v 133, pp 481-488.

BAMFORD, D., NUNN, K., PRODEHL, C. and JACOB, B. 1978. LISPB - IV. Crustal Structure of Northern Britain. Geophys. J. R. Astr. Soc. v 54, pp 43-60.

BARRETT, T. J., JENKYNS, H. C., LEGGETT, J. K., ROBERTSON, A. H. F. 1982. Comment and Reply on 'Age and Origin of the Ballantrae Ophiolite and its Significance to the Caledonian Orogeny and the Ordovician Time Scale'. Geology, v 9, pp 331-333.

BLUCK, B. J. 1978. Sedimentation in a Late Orogenic Basin: The Old Red Sandstone of the Midland Valley. In: Bowes, D. R., LEAKE, B. E. (Eds). Crustal Evolution in Northwestern Britain and Adjacent Regions. Geol. J. Spec. Issue, v 10, pp 249-278.

BLUCK, B. J. 1980. Evolution of a Strike-Slip Fault Controlled Basin, Upper Old Red Sandstone, Scotland. In: BALLANCE, P. F. and READING, H. G. (Ed). Sedimentation in an Oblique Slip Mobile Zones. Spec. Publ. Int. Ass. Sedim. v 4, pp 7-26.

BLUCK, B. J. 1983. Role of the Midland Valley of Scotland in the Caledonian Orogeny. Trans. R. Soc. Edin. (Earth Sciences), v 74, pp 119-136.

BLUCK, B. J. 1984. Pre-Carboniferous History of the Midland Valley Of Scotland. Trans. R. Soc. Edin. (Earth Sciences), v 75, pp 275-295.

BLUCK, B. J. 1985. The Scottish Paratectonic Caledonides. Scott. J. Geol. v 21, pp 437-464.

BLUCK, B. J. & HALLIDAY, A. N. 1982. Comment and reply 'Age and Origin of Ballantrae Ophiolite and its Significance to the Caledonian Orogeny and Ordovcian Time Scale. Geology , v 9, pp 331-333.

BREWER, J. A., MATTHEWS, D. H., WARNER, M. R., HALL, J. and SMYTHE, D. K. 1983. BIRPS Deep Seismic Reflection Studies of the British Caledonides. Nature v 305, pp 206-210.

BROWNE, M. A. E. 1980. The Upper Devonian and Lower Carboniferous (Dinantian) of the Firth of Tay, Scotland. Inst. Geol. Sci., Report 80/9.

BROWNE, M. A. E., HARGREAVES, R. L. and SMITH, I. F. 1985. Investigation of the Geothermal Potential of the U.K., the Upper Palaeozoic Basins of the Midland Valley of Scotland. British Geological Survey.

CAMERON, I. B., STEPHENSON, D. 1985. The Midland Valley of Scotland. 3rd Ed. Mem. Geol. Sur.

CERVENY, V. and PSENCIK, I. 1983. 2-D Seismic Package. Research Report, Institute of Geophysics, Charles University, Prague.

CHISHOLM, J. I. and DEAN, J. M. 1974. The Upper Old Red Sandstone of Fife and Kinross: A Fluviatile Sequence with Evidence of Marine Incursion. Scott. J. Geol., v 10, pp 1-29.

CONWAY, A., DENTITH, M. C., DOODY, J. J. and HALL, J. 1987. Preliminary Interpretation of Upper Crustal Structure Across the Midland Valley of Scotland from Two East- West Seismic

Refraction Profiles. J. Geol. Soc. Lond. v 144, pp 865-870.

CRAMPIN, S., JACOB, A. W. B., MILLER, A. & NEILSON, A. 1970. The LOWNET Radio-linked Seismometer Network in Scotland. Geophys. J. R. Astr. Soc., v 21, pp 207-216.

DANIEL, S. 1967. The Digital Processing of Seismic Data. Geophysics, v 32, No. 6. pp 988-1002.

DAVIDSON, K. A. S. 1986. Seismological Studies of Upper Crustal Structure of the Southern Midland Valley of Scotland. Ph.D. thesis (unpubl). University of Glasgow.

DAVIDSON, K. A. S., SOLA, M. A., POWELL, D. W. and HALL, J. 1984. A Geophysical Model for the Midland Valley of Scotland. Trans. R. Soc. Edin. Earth Sci. v 75, pp 175-181.

DENTITH, M. C. 1987. Geophysical Constraints on Upper Crustal Structure in the Midland Valley of Scotland. Ph.D thesis (unpubl), University of Glasgow.

DEWEY, J. F. 1971. A Model for the Lower Palaeozoic Evolution of the Southern Margin of the Southern Caledonides of Scotland and Ireland. Scott. J. Geol. v 7, pp 219-240.

DEWEY, J. F. 1982. Plate Tectonics and the Evolution of the British Isles. J. Geol. Soc. Lond. v 139, pp 371-414.

DOBRIN, M. B. 1960. Geophysical Prospecting. 2nd Ed. McGraw-Hill.

EYLES, V. A., SIMPSON, J. B. & MacGREGOR, A. G. 1949. The Geology of Central Ayrshire. Mem. Geol. Surv., U.K., (sheet 14).

FRANCIS, E. H. 1983a. Carboniferous. In: CRAIG, G. Y. (Ed). Geology of Scotland, pp 253-296. Scottish Academic Press.

FRANCIS, E. H. 1983b. Carboniferous-Permian Igneous Rocks. In: CRAIG, G. Y. (Ed). Geology of Scotland, pp 297-324. Scottish Academic Press.

GEIKIE, A. 1900. The Geology of Central and Western Fife and Kinross. Mem. Geol. Surv. G.B.

GEORGE, T. N. 1960. The Stratigraphical Evolution of the Midland Valley. Trans. Geol. Soc. Glasgow, v 24, pp 32-107.

GRAHAM, A. M. and UPTON, B. G. J. 1978. Gneisses in Diatremes, Scottish Midland Valley: Petrology and Tectonic Implications. J. Geol. Soc. Lond. v 135, pp 219-228.

GRANT, F. S. and WEST, G. F. 1965. Interpretation Theory in Applied Geophysics. McGraw-Hill.

HAGEDOORN, J. G. 1959. The Plus-Minus Method of Interpreting Seismic Refraction Sections. Geophy. Prosp. v 7, pp 158-183.

HALL, J. 1971. A Preliminary Seismic Survey Adjacent to the Rashiehill Borehole Near Slamannan, Stirlingshire. Scott. Geol. , v 7, pp 170-174.

HALL, J. 1974. A Seismic Reflection Survey of the Clyde Plateau Lavas in North Ayrshire and Renfrewshire. Scott. J. Geol. v 9, pp 254-279.

HALL. J., BREWER, J. A., MATTHEWS, D. H. and WARNER, M. R. 1984. Crustal Structure Across the Caledonides from the "WINCH" Seismic Reflection Profile: Influences on the Evolution of the Midland Valley of Scotland. Trans. R. Soc. Edin., (Earth Sci). v 75, pp 97-109.

HALL, J., POWELL, D. W., WARNER, M. R., EL-ISA, Z. H. M., ADESANYA, O. and BLUCK, B. J. 1983. Seismological Evidence for Shallow Crystalline Basement in the Southern Uplands of Scotland. Nature, v 305, pp 418-420.

HATTON, L. , WORTHINGTON, M. H. and MAKIN, J. 1986. Seismic Data Processing Theory and Practice. Blackwell Scientific Publications.

HIPKIN, R. G. and HUSSAIN, A. 1983. Regional Gravity Anomalies, 1. Northern Britain. Rep. Inst. Geol. Sci. 82/10.

HOSSAIN, M. M. A. 1976. Analysis of the Major Gravity and Magnetic Anomalies Centred Around Bathgate, Central Scotland. M.Sc Thesis (unpubl), University of Glasgow.

HUTTON D. H. W. 1987. Strike-Slip Terranes and a Model for the Evolution of the British and Irish Caledonides. Geol. Mag. v 124, pp 405-425.

KAMINSKI, W., BAMFORD, D., FABER, S., JACOB, B., NUNN, K. and PRODEHL, C. 1976. A Lithospheric Seismic Profile in Britain - II. Preliminary Report on the Recording of a Local Earthquake. J. Geophys. v 42, pp 103-110.

KEAREY, P. and BROOKS, M. 1984. An Introduction to Geophysical Exploration. Blackwell Scientific Publications.

KENNEDY, W. Q. 1958. Tectonic Evolution of the Midland Valley of Scotland. Trans. Geol. Soc. Glasgow, v 23, pp 107-133.

KLEMPERER, S. L. and MATTHEWS, D. H. 1987. Iapetus Suture Located Beneath the North Sea by BIRPS Deep Reflection Profiling. Geology v 15, pp 195-198.

LAMBERT, R. St. J. & McKERROW, W. S. 1976. The Grampian Orogeny. Scott. J. Geol. v 12, pp 271-292.

LEEDER, M. R. 1982. Upper Palaeozoic Basins of the British Isles-Caledonide Inheritance Versus Hercynian Plate Margin Processes. J. Geol. Soc. London, v 139, pp 479-491.

LEGGETT, J. K. 1980. The Sedimentological Evolution of a Lower Palaeozoic Accretionary Fore-arc in the Southern Uplands of Scotland. Sedimentology, v 27, pp 401-417.

MacGREGOR, A. R. 1968. Fife and Angus Geology - An Excursion Guide. Blackwood & Sons Ltd.

McLEAN, A. C. 1966. A Gravity Survey in Ayrshire and its Geological Interpretation. Trans. R. Soc. Edin. Earth. Sci. v 66, pp 239-265.

McLEAN, A. C. & DEEGAN, C. E. 1978. The Solid Geology of the Clyde Sheet. Rep. Inst. Geol. Sci. 78/9.

MITCHELL, A. H. G. and McKERROW, W. S. 1975. Analogous Evolution of the Burma Orogen and the Scottish Caledonides. Bull. Geol. Soc. Amer. v 86, pp 305-315.

MYKURA, W. 1983. Old Red Sandstone. In: CRAIG, G. Y. (Ed), Geology of Scotland, pp 205-251. Scottish Academic Press.

POWELL, D. W. 1978. Gravity and magnetic anomalies Attributable to Basement Sources Under Northern Britain. In: BOWES, D. R. and LEAKE, B. E. (Eds), Crustal Evolution in North-Western Britain and Adjacent Regions. Geol. J. Spec. Issue, v 10, pp 107-114.

QURESHI, I. R. 1970. A Gravity Survey of a Region of the Highland Boundary Fault Scotland. J. Geol. Soc. Lond. v 125, pp 481-502.

ROBINSON, E. A. and TREITEL, S. 1964. Principles of Digital filtering. Geophysics, v 29, pp 395-404.

ROBINSON, E. A. and TREITEL, S. 1980. Geophysical Signal Analysis. Prentice-Hall.

ROLFE, W. D. I. 1961. The Geology of the Hagshaw Hills Sulurian Inlier, Lanarkshire. Trans. Edin. Geol. Soc. v 18, pp 240-269.

SOLA, M. A. 1985. The Seismic Structure Under the Central Midland Valley from Refraction Measurements. Ph.D. thesis, (unpubl), University of Glasgow.

UPTON, B. G. J., 1971, Carboniferous vanic Rocks of the Midland Valley of Scotland. Grant Institute of Geology, Edinburgh University.

UPTON, B. G. J., ASPEN, P. and CHAPMAN, N. A. 1983. The Upper Mantle and Deep Crust Beneath the British Isles: Evidence from Inclusion Suites in volcanic Rocks. J. Geol. Soc. Lond. v 140, pp 105-122.

UPTON, B. G. J., ASPEN, P. GRAHAM, A. M., CHAPMAN, N. A. 1976. Pre-Palaeozoic Basement of the Scottish Midland Valley. Nature v 260, pp 517-518.

WEATHERBY, B. B ,BORN, W. T. and HARDING, R. L. 1934. Granite and Limestone Velocity Determinations in Arbuckle Mountains, Oklahoma. Bull. A.A.P.G. v 18, pp 106-118.

YARDLEY, B. W. D., VINE, F. J. and BALDWIN, C. T. 1982. The Plate Tectonic Setting of NW Britain and Ireland in Late Cambrian and Early Ordovcian Time. J. Geol. Soc. Lond. v 139, pp 455-465.

APPENDIX 1. SEISMIC RECORDER SPECIFICATIONS

GLASGOW FM MARK 2 SEISMIC RECORDER

SPECIFICATIONS

Detector: Mark Products L15B 4.5 Hz geophones with 600 coil, or alternative.

Amplifier Gain: adjustable 88-118 dB in 6 dB steps; second output at 18 dB lower than first; clipped 10 V p-p (less for better linearity). Input resistance of 4.7 k for 0.65 of critical damping of L15B geophones.

Modulator: central frequency is 2 kHz; frequency deviation for 10 V p-p input is +/- 100%: current output is 250 A.

Recording: saturation.

Demodulator: produces 2 V output for maximum modulator input (10 V); 14 dB loss reduces overall system gain to the range 56-104 dB (including both gain output).

Playback filters: Kemo VBF/3.

Oscillograph: Bryans 40000 6-channel.

System frequency response: direct connection of modulator to modulator; 3 dB down points give approximate pass-band of 2-60 Hz.

Noise and distortion: system noise limits dynamic range to 46 dB at maximum gain. Distortion is less than 1% at 70% of clipping level.

Wow and flutter: less than 0.25% .

Power Requirements: Amplifier-modulator 20 MA; 18V. Recorder (during recording) 115 mA; 18V.

Cassette recorder: Tape speed 4.74 cm/s

APPENDIX 2. RECORDING SITE DETAILS AND OBSERVED TRAVEL TIMES

LINE 1 ABERDOUR QUARRY

Quarry: National Grid Reference: Easting 317.48 Northing 686.79

Rock: Quartz dolerite sill.

SITE NUMBER	SITE NAME	EASTING	NORTHING	GEOPHONE COUPLING
ac01	Easter Bucklyrie farm	317.32	688.62	Drift
ac02b	Caledonian Works	317.89	689.89	Drift
ac03b	Cowdenbeath	317.55	691.39	Drift
ac04	Lumphinnans farm	317.95	692.74	Drift
ac05	Carahore farm	317.82	694.25	Drift
ac06b	Inchgall farm	318.45	695.79	Drift
ac07	Capledrae farm	318.31	697.39	Drift
ac08	Kirkness farm	318.32	698.70	Drift
ac09	Lochend farm	318.25	700.19	Drift
ac10	Scotlandwell	318.65	701.62	Drift
ac11	Kinnesswood	317.80	703.10	Rock
ac12	Wester Balgedie farm	318.50	704.70	Drift
ac13	Lappiemoss farm	318.23	705.73	Drift
ac14	Upper Urquhart farm	319.12	708.30	Drift
ac15	Houses on A91	319.13	708.67	Drift
ac16	Wellfield farm	319.24	710.74	Drift
ac17	Glentarkie farm	319.15	712.32	Drift
ac18	Dumbarrow Forest	319.57	713.79	Rock
ac19	Gattaway farm	319.31	716.00	Drift
ac20	Rosebank House	319.75	716.70	Drift
ac21	James field farm	319.75	718.10	Drift
ac22	Nether Mains farm	320.26	719.80	Drift
ac23b	Chapelhill Street	320.21	721.18	Drift
ac24	Glendoick House	320.54	723.09	Drift
ac25	Over Drudie farm	320.35	724.44	Drift
ac26	Evelick farm	320.50	725.66	Rock
ac27	Shamny farm	320.52	727.70	Rock
ac28	Whitemyre farm	320.94	728.95	Rock
ac29	Southtown farm	320.95	730.14	Rock
ac30	Hoolmyre farm	321.64	731.49	Rock
ac31	Fairygreen farm	321.05	733.37	Drift
ac32	Over Buttergask farm	321.46	734.58	Drift
ac33	Kinnochtry farm	321.20	736.05	Drift
ac34	Coltward Holdings	321.45	737.73	Drift
ac30A	Quarry on B953	322.40	731.7	Rock
ac31A	Balloleys farm	323.36	732.51	Rock
ac32A	South Ballo farm	324.98	734.65	Rock

OBSERVED TRAVEL TIMES

SITE NUMBER	RANGE (km)	GAIN	TRAVEL TIME (s)	RED TIME (s)
ac01	1.84	1	0.29	-0.02
ac02b	3.13	1	0.74	0.22
ac03b	4.60	2	1.20	0.44
ac04	5.84	2	1.51	0.54
ac05	7.47	2	1.82	0.57
ac06b	9.05	2	2.15	0.64
ac07	10.63	2	2.51	0.73
ac08	11.94	1	2.71	0.72
ac09	13.42	1	3.01	0.77
ac10	14.88	1	3.26	0.78
ac11	16.31	4	3.44	0.72
ac12	17.94	4	3.84	0.85
ac13	18.95	4	4.02	0.86
ac14	21.57	3	4.46	0.86
ac15	22.72	2	4.66	0.87
ac16	24.01	4	4.83	0.83
ac17	25.58	3	5.06	0.80
ac18	27.08	4	5.36	0.85
ac19	29.27	4	5.65	0.78
ac20	29.99	3	5.86	0.86
ac21	31.39	1	6.14	0.91
ac22	33.07	2	6.44	0.92
ac23b	34.50	3	6.65	0.90
ac24	36.42	3	7.00	0.92
ac25	37.76	3	7.23	0.93
ac26	38.99	3	7.42	0.92
ac27	41.02	3	7.76	0.92
ac28	42.30	6	7.96	0.91
ac29	43.49	5	8.16	0.91
ac30	44.81	5	8.38	0.91
ac31	46.71	6	8.63	0.84
ac32	47.95	5	8.84	0.84
ac33	49.40	5	9.09	0.86
ac34	51.09	4	9.36	0.84
ac30A	45.18	5	8.43	0.90
ac31A	46.10	5	8.51	0.83
ac32A	48.44	4	8.69	0.62

LINE 1 COLLACE QUARRY

Quarry: National Grid Reference: Easting 320.84 Northing 731.60

Rock: Andesite (Lower Devonian lava).

SITE NUMBER	SITE NAME	EASTING	NORTHING	GEOPHONE COUPLING
co29	Southtown farm	320.88	730.21	Drift
co28	Whitemyre farm	320.30	728.42	Rock
co27	Sharnny farm	320.52	727.70	Rock
co26	Evelick farm	320.49	725.78	Rock
co25	Over Drudie farm	320.28	724.59	Drift
co24	Glendoick House	320.54	723.09	Drift
co23	Chapelhill Street	320.21	721.18	Drift
co22	Nether Mains farm	320.26	719.80	Drift
co21	James field farm	319.75	718.10	Drift
co20	Rose bank House	319.75	716.70	Drift
co19	Gattaway farm	319.31	716.00	Drift
co18	Dumbarrow Forest	319.57	713.79	Rock
co17	Glentarkie farm	319.15	712.32	Drift
co16	Wellfield farm	319.24	710.74	Drift
co15	Upper Urquhrt farm	319.12	708.65	Drift
co14	Upper Urquhrt farm	319.16	707.68	Drift
co13	Lappiemoss farm	318.20	705.75	Drift
co12	Wester Balgedie farm	318.05	704.70	Drift
co11	Kinnesswood	317.80	703.10	Rock
co08	Kirkness farm	318.60	698.45	Drift
co05	Carahore farm	317.70	694.18	Drift
co04	Lumphinnans farm	317.60	693.17	Drift
co01	Easter Bucklyrie farm	317.42	688.55	Drift
co00	Aberdour quarry	317.60	687.08	Drift

OBSERVED TRAVEL TIMES

SITE NUMBER	RANGE (km)	GAIN	TRAVEL TIME (s)	RED TIME (s)
co29	1.34	1	0.37	0.10
co28	3.23	4	0.76	0.23
co27	3.91	3	0.89	0.24
co26	5.83	3	1.33	0.36
co25	7.03	3	1.59	0.42
co24	8.51	1	1.85	0.43
co23	10.44	2	2.29	0.55
co22	12.27	2	2.58	0.54
co21	13.52	2	2.98	0.73
co20	14.94	2	3.17	0.68
co19	15.67	4	3.36	0.74
co18	17.85	5	3.72	0.74
co17	19.35	4	3.98	0.76
co16	20.92	3	4.21	0.72
co15	23.01	4	4.62	0.78
co14	23.98	3	4.86	0.87
co13	25.98	4	5.19	0.86
co12	27.04	4	5.40	0.89
co11	28.66	4	5.65	0.87
co08	33.23	4	6.41	0.87
co05	37.55	3	7.15	0.89
co04	38.57	3	7.38	0.95
co01	43.19	3	8.07	0.87
co00	44.64	3	8.36	0.92

LINE 1 NEWBURGH QUARRY (NORTH-SOUTH)

Quarry: National Grid Reference: Easting 324.43 Northing 717.76

Rock: Andesite (Lower Devonian lava).

SITE NUMBER	SITE NAME	EASTING	NORTHING	GEOPHONE COUPLING
nn32	Over Buttergask farm	321.47	734.58	Drift
nn31	Damside farm	320.90	733.70	Drift
nn30	Balmalcolm farm	321.00	732.65	Drift
nn29	Southtown farm	320.95	730.14	Rock
nn28	Whitemyre farm	320.94	728.95	Rock
nn27	Shanry farm	320.52	727.70	Rock
nn26	Evelick farm	320.50	725.66	Rock
nn25	Over Durdie farm	320.35	724.44	Drift
nn24	Glendoick farm	320.48	723.09	Drift
nn23	Chapelhill Street	320.21	721.18	Drift
nn22	Nether Mains farm	320.33	719.74	Drift
ns20	Rose bank House	319.75	716.70	Drift
ns19	Gattaway farm	319.31	716.00	Drift
ns18	Dumbarrow Hill	319.57	713.79	Rock
ns17	Glentarkie farm	319.15	712.32	Drift
ns16	Wellfield Steading farm	319.24	710.74	Drift
ns15b	House on A91	319.25	709.49	Drift
ns14	Upper Urquhrt farm	319.15	707.99	Drift
ns13b	Lappiemoss farm	317.86	707.55	Drift
ns12b	Wester Balgedie farm	317.09	704.28	Drift
ns11	Kinnesswood Town	317.80	703.10	Rock
ns10	Scotland Well	318.25	701.62	Drift

OBSERVED TRAVEL TIMES

SITE NUMBER	RANGE (km)	GAIN	TRAVEL TIME (s)	RED TIME (s)
nn32	17.08	5	3.61	0.76
nn31	16.33	4	3.37	0.65
nn30	15.28	5	3.18	0.64
nn29	12.86	5	2.75	0.61
nn28	11.38	6	2.52	0.62
nn27	10.68	4	2.37	0.58
nn26	8.82	4	1.99	0.52
nn25	7.83	3	1.75	0.44
nn24	6.63	1	1.52	0.42
nn23	5.43	2	1.22	0.31
nn22	4.55	2	1.05	0.29
ns20	4.80	1	0.93	0.13
ns19	5.41	2	1.11	0.20
ns18	6.27	6	1.33	0.28
ns17	7.58	2	1.61	0.36
ns16	8.73	3	1.84	0.39
ns15b	9.76	2	1.94	0.32
ns14	11.10	4	2.45	0.60
ns13b	12.14	3	2.53	0.51
ns12b	15.35	2	3.18	0.62
ns11	16.09	4	3.34	0.66
ns10	17.28	3	3.55	0.67

LINE 2 ABERDOUR QUARRY

Quarry: National Grid Reference: Easting 317.48 Northing 686.79

Rock: Quartz dolerite sill.

SITE NUMBER	SITE NAME	EASTING	NORTHING	GEOPHONE COUPLING
aa01	Broomside farm	316.01	686.95	Drift
aa02	Woodlee farm	314.50	687.60	Drift
aa03	Halbeath Town	312.94	688.12	Drift
aa04	Dunfermline	311.69	688.61	Drift
aa05	Town Hill Town	310.23	689.20	Drift
aa06	Colton farm	308.95	689.59	Drift
aa07	Rosebank farm	307.35	690.45	Drift
aa08	Craigluscar farm	305.94	690.80	Drift
aa09	Rhynd House	304.46	691.22	Drift
aa10	Golf Course	303.20	691.82	Drift
aa11	Craig House farm	301.85	692.43	Drift
aa12	Muirmealing farm	299.93	692.96	Drift
aa13	West Saline farm	298.54	693.14	Rock
aa14	Piperpool farm	297.28	693.13	Drift
aa15	Meadowhill farm	295.45	694.25	Drift
aa16	Aberdona House	294.84	695.00	Drift
aa17	Gatenkeir farm	293.31	695.28	Drift
aa18	Gartmorn farm	291.57	695.89	Drift
aa19	Marchglen farm	290.03	696.02	Drift
aa20	Rhodders farm	288.83	697.65	Rock
aa21	Houses Alva	287.15	697.49	Rock
aa22	Myretoun House	285.74	697.30	Drift
aa25	Pendreich farm	281.84	699.33	Drift
aa26	Kiltane farm	279.98	699.86	Drift
aa27	Kippenross farm	279.10	700.00	Drift
aa28	Wanderwrang House	277.61	700.20	Drift
aa31	Westerton farm	275.50	702.10	Drift

OBSERVED TRAVEL TIMES

SITE NUMBER	RANGE (km)	GAIN	TRAVEL TIME (s)	RED TIME (s)
aa01	1.48	3	0.50	0.25
aa02	3.09	2	0.91	0.40
aa03	4.73	1	1.39	0.60
aa04	6.07	2	1.63	0.62
aa05	7.64	1	2.03	0.76
aa06	8.98	2	2.40	0.91
aa07	10.77	2	2.75	0.98
aa08	12.22	3	2.94	0.90
aa09	13.75	2	3.28	0.98
aa10	15.14	1	3.61	1.09
aa11	16.62	2	3.83	1.06
aa12	18.60	4	4.24	1.14
aa13	19.98	3	4.42	1.09
aa14	21.17	2	4.71	1.18
ac15	23.26	3	5.13	1.26
aa16	24.08	3	5.21	1.20
aa17	25.62	3	5.47	1.20
aa18	27.46	3	5.86	1.28
aa19	28.96	4	6.09	1.26
aa20	30.64	4	6.06	0.95
aa21	32.16	5	6.35	0.99
aa22	33.43	3	6.51	0.93
aa25	37.78	4	7.32	1.03
aa26	39.71	4	7.62	1.00
aa27	40.59	4	7.78	1.01
aa28	42.06	4	8.02	1.01
aa31	44.68	4	8.49	1.04

LINE 2 TILLICOULTRY QUARRY

Quarry: National Grid Reference: Easting 291.18 Northing 697.69

Rock: Basalt (Lower Devonian lava).

SITE NUMBER	SITE NAME	EASTING	NORTHING	GEOPHONE COUPLING
ta18	Gartmorn farm	291.57	695.89	Drift
ta17	Gatenkeir farm	293.31	695.28	Drift
ta16	Aberdona House	294.84	695.00	Drift
ta15	Meadowhill farm	295.45	694.25	Drift
ta14	Piperpool farm	297.28	693.13	Drift
ta13	West Saline farm	298.54	693.14	Rock
ta12	Muirmealing farm	299.93	692.96	Drift

OBSERVED TRAVEL TIMES

SITE NUMBER	RANGE (km)	GAIN	TRAVEL TIME (s)	RED TIME (s)
ta18	1.84	1	0.60	0.29
ta17	3.22	1	0.94	0.41
ta16	4.54	1	1.23	0.48
ta15	5.48	2	1.46	0.55
ta14	7.62	2	1.96	0.69
ta13	8.65	3	2.40	0.96
ta12	9.95	2	2.41	0.76

LINE 3 TILLICOULTRY QUARRY

Quarry: National Grid Reference: Easting 291.18 Northing 697.69

Rock: Basalt (Lower Devonian lava).

SITE NUMBER	SITE NAME	EASTING	NORTHING	GEOPHONE COUPLING
tl01	Cunninghar farm	292.46	697.85	Drift
tl02	Harviestonn farm	294.20	698.18	Drift
tl03	Dollarbank farm	295.60	698.42	Drift
tl04	Forestry Commission	297.19	699.43	Drift
tl05	Castleton farm	298.13	700.06	Drift
tl06	Middlehall farm	299.42	700.69	Drift
tl07	Naemoor farm	300.80	701.34	Drift
tl08	Claysike farm	302.60	701.79	Drift
tl09	Easter Fossoway farm	304.20	702.95	Drift
tl11	Tillyochie farm	307.03	703.11	Drift
tl12	Piggery farm	308.27	703.67	Drift
tl13	Thomanean farm	309.38	704.22	Drift

OBSERVED TRAVEL TIMES

SITE NUMBER	RANGE (km)	GAIN	TRAVEL TIME (s)	RED TIME (s)
tl01	1.29	1	0.30	0.09
tl02	3.06	2	0.68	0.17
tl03	4.48	2	0.97	0.23
tl04	6.26	3	1.23	0.19
tl05	7.34	2	1.44	0.22
tl06	8.77	2	1.76	0.29
tl07	10.29	3	2.10	0.38
tl08	12.13	3	2.45	0.42
tl09	14.04	3	2.79	0.45
tl11	16.75	2	3.33	0.54
tl12	18.11	3	3.66	0.64
tl13	19.37	3	4.01	0.79

LINE 4 NEWBURGH QUARRY (WEST)

Quarry: National Grid Reference: Easting 324.43 Northing 717.76

Rock: Andesite (Lower Devonian lava).

SITE NUMBER	SITE NAME	EASTING	NORTHING	GEOPHONE COUPLING
nw01	Ninewells farm	322.71	717.36	Drift
nw02	Wesrer Clunie farm	321.18	717.11	Drift
nw03	Wester Greenside farm	319.75	716.70	Drift
nw04	Cordon farm	318.76	716.70	Drift
nw05	Broadwell farm	317.13	716.46	Drift
nw06	Gowile farm	316.15	716.35	Drift
nw07	Brich hall farm	314.11	715.89	Drift
nw08	West Dron farm	312.62	715.76	Drift

OBSERVED TRAVEL TIMES

SITE NUMBER	RANGE (km)	GAIN	TRAVEL TIME (s)	RED TIME (s)
nw01	1.72	1	0.32	0.03
nw02	3.31	4	0.64	0.09
nw03	4.80	3	0.90	0.10
nw04	5.77	3	1.42	0.45
nw05	7.41	3	1.62	0.39
nw06	8.40	1	2.01	0.61
nw07	10.49	4	2.20	0.45
nw08	11.98	4	2.59	0.60

APPENDIX 3. PLUS-MINUS ANALYSIS

LINE 1 ABERDOUR-COLLACE

SITE NO.	DISTANCE	T - (s)	T + (s)	DEPTH in km[2]	DEPTH in km[3]
4	5.84	-	0.54	2.17	2.10
5	7.47	-	0.51	2.05	1.99
8	11.94	-	3.70	0.47	1.83
11	16.31	-	2.21	0.44	1.72
12	17.94	-	1.56	0.59	2.30
13	18.95	-	1.17	0.56	2.20
14	21.57	-	0.73	0.67	2.63
15	22.72	0.05	0.63	2.45	2.53
16	24.01	0.06	0.39	1.65	1.62
17	25.58	1.08	0.40	1.67	1.64
18	27.08	1.64	0.43	1.80	1.78
19	29.27	2.30	0.37	1.53	1.50
20	29.99	2.68	0.38	1.60	1.58
21	31.39	3.16	0.48	1.98	1.95
22	33.07	-	0.51	1.84	2.11
23	34.50	-	0.68	2.45	2.82
24	36.42	-	0.50	1.80	2.07
25	37.76	-	0.50	1.80	2.07

1 Distances are from Aberdour quarry in km.

2 Depths are calculated using average velocity for layer 1 (4.65 km/s).

3 Depths at stations 4-15 are calculated using layer 1 velocity (4.6 km/s) while depths at stations 16-25 are calculated using layer 2 velocity (4.7 km/s).

APPENDIX 4. RAYTRACING RESULTS

This appendix compares times computed by raytracing with the observed values. A (+) value indicates a computed time that is later than the observed.

Times are arranged by line and then shotpoint. Ray codes show the type of first arrival and the causal layer: C - layer 1 (Carboniferous and Upper ORS); D - layer 2 (LOWER ORS and ? Lower Palaeozoic); B - layer 3 (? Precambrian crystalline basement).

An agreement of the times to within 0.03 s is considered "good".

LINE 1 (ABERDOUR SHOT)

Station number	Code	Discrepancy (s)
ac01	Direct C	+ 0.10
ac02	Direct C	+ 0.01
ac03	Direct C	+ 0.09
ac04	Direct C	- 0.10
ac05	Direct C	- 0.02
ac06	Direct C	- 0.01
ac07	Direct C	- 0.05
ac08	Direct C	+ 0.02
ac09	Headwave D	- 0.10
ac10	Headwave D	0.00
ac11	Headwave D	+ 0.09
ac12	Headwave D	- 0.03
ac13	Headwave D	- 0.03
ac14	Headwave D	0.00
ac15	Headwave D	- 0.01
ac16	Headwave D	+ 0.05
ac17	Headwave D	+ 0.06
ac18	Headwave D	+ 0.02
ac19	Headwave D	+ 0.10
ac20	Headwave D	+ 0.04
ac21	Headwave D	+ 0.01
ac22	Headwave D	+ 0.02
ac23	Headwave D	+ 0.04
ac24	Headwave D	+ 0.02
ac25	Headwave B	- 0.06
ac26	Headwave B	- 0.03
ac27	Headwave B	- 0.03
ac28	Headwave B	- 0.02
ac29	Headwave B	- 0.02
ac30	Headwave B	- 0.02
ac31	Headwave B	+ 0.04
ac32	Headwave B	+ 0.02
ac33	Headwave B	+ 0.01
ac34	Headwave B	+ 0.01

LINE 1 (COLLACE SHOT)

Station number	Code	Discrepancy (s)
co29	Direct D	- 0.05
co28	Direct D	- 0.05
co27	Direct D	- 0.04
co26	Direct D	- 0.04
co25	Direct D	- 0.03
co24	Direct D	- 0.04
co23	Direct D	- 0.03
co22	Direct D	- 0.03
co21	Direct D	- 0.03
co20	Direct D	- 0.03
co19	Direct D	- 0.04
co18	Direct D	- 0.05
co17	Direct D	- 0.05
co16	Direct D	- 0.03
co15	Headwave D	- 0.03
co14	Headwave D	- 0.03
co13	Headwave D	- 0.03
co11	Headwave D	- 0.02
co08	Headwave D	- 0.02
co05	Headwave D	+ 0.02
co04	Headwave D	- 0.01
co02	Headwave D	+ 0.04

LINE 2 (ABERDOUR SHOT)

Station number	Code	Discrepancy (s)
aa01	Direct C	- 0.07
aa02	Direct C	- 0.03
aa03	Direct C	- 0.07
aa04	Direct C	+ 0.03
aa05	Direct C	+ 0.02
aa06	Direct C	- 0.03
aa07	Direct C	+ 0.01
aa09	Headwave D	0.00
aa10	Headwave D	- 0.08
aa12	Headwave D	- 0.07
aa13	Headwave D	- 0.01
aa15	Headwave D	- 0.05
aa16	Headwave D	- 0.03
aa18	Headwave D	- 0.05
aa19	Headwave D	- 0.03